UNIVERSITÉ DU QUÉBEC À RIMOUSKI

CHANGEMENTS CLIMATIQUES ET VARIATIONS DU CHAMP MAGNÉTIQUE TERRESTRE DANS LE SUD DE LA PATAGONIE (ARGENTINE) DEPUIS 51 200 ANS RECONSTITUÉS À PARTIR DES PROPRIÉTÉS MAGNÉTIQUES DES SÉDIMENTS DU LAC *LAGUNA POTROK AIKE*

Thèse présentée

dans le cadre du programme de doctorat en océanographie

en vue de l'obtention du grade de PhD

PAR

© Agathe Lisé-Pronovost

Janvier 2014

Composition du jury :

Jean-Carlos Montero-Serrano, président du jury, Université du Québec à Rimouski

Guillaume St-Onge, directeur de recherche, Université du Québec à Rimouski

Claudia Gogorza, codirectrice de recherche, Universidad nacional del centro de la provincia de Buenos Aires

Annick Chauvin, examinateure externe, Université de Rennes

Dépôt initial le 19 novembre 2013 Dépôt final le 24 janvier 2014

À ma famille.

This was a discovery - the look of it. (...) The sky was clear blue. A puff of cloud, white as a quince flower, carried a small shadow from town, or from the South Pole. I saw it approach. It rippled across the bushes and passed over me, a brief chill, and then it went rucking east. There were no voices here. There was this, what I saw; and though beyond it were mountains and glaciers and albatrosses and Indians, there was nothing here to speak of, nothing to delay me further. Only the Patagonian paradox: tiny blossoms in vast space; to be here, it helped to be a miniaturist, or else interested in enormous empty spaces. There was no intermediate zone of study. Either the enormity of the desert or the sight of a tiny flower. In patagonia you had to choose between the tiny or the vast.

From "Patagonia revisited" by Bruce Chatwin and Paul Theroux

REMERCIEMENTS

Évidemment un doctorat ça ne se fait pas tout seul –du moins je ne souhaite à personne de le faire seul!-. La collaboration et la multidisciplinarité sont joyeusement nécessaires à la science et j'ai le plaisir de remercier ici les nombreuses personnes qui m'ont aidé tout au long de mes travaux de doctorat.

Cher Guillaume, merci pour ton amour contagieux de la science, ton attitude toujours positive et ton support dans tous mes projets, allant des nombreux congrès scientifiques et réunions de toutes sortes aux écoles d'été, formations diverses, missions en mer et projets de recherche en parallèle.

Merci à l'équipe internationale PASADO et particulièrement à Claudia Gogorza pour avoir accepté de co-superviser mes travaux de doctorat et à Bernd Zolitschka pour avoir imaginé et orchestré le forage scientifique du lac *Laguna Potrok Aike*. Merci à Pierre Francus, notre sympathique responsable de PASADO-Canada, et à Torsten Haberzettl, Christian Ohlendorf, Catalina Gehbardt, David Fortin, Guillaume Jouve, Laurence Nuttin, Pierre Kliem, Annette Hahn, Stephanie Kastner, Aurèle Vuillemin et Cristina Recasens pour les discussions passionnées et les nombreuses collaborations scientifiques depuis 2008. Je tiens aussi à souligner la contribution de Stefanie Brachfeld et de Joseph Stoner qui ne sont pas impliqués directement dans le projet PASADO mais qui ont gentiment accepté de répondre à mes questions en plus de réviser certains de mes manuscrits.

Plusieurs personnes m'ont grandement aidé lors de mes analyses de laboratoire, incluant Claude Belzile (microscope à balayage électronique, ISMER), Michel Preda (diffractomètre à rayons X, UQAM), Michael Jackson (anisotropie de la susceptibilité magnétique, IRM), Christian Ohlendorf (échantillonnages supplémentaires et logistique,

UBremen), Juan José Sagliotti et Daniela María Echazú (échantillonnage de cubes, UBremen). Merci de tout coeur!

J'ai eut la chance de travailler avec Jacques Labrie aux laboratoires de magnétisme sédimentaire de l'ISMER, sans qui toute une génération d'étudiants gradués auraient eut la vie tellement plus dure sans « boutons Jacques ». Merci à tous les étudiants et postdocs que j'ai cotoyé et avec qui je me suis lié d'amitié aux labos à Rimouski, à Québec et à Montréal, et en particulier (d'est en ouest –parce que ça me change des vents d'ouest!) à Francesco Barletta, Marie-Pier St-Onge, Ursule Boyer-Villemaire, Torsten Haberzettl, David Fortin, Hervé Guyard, Guillaume Jouve, Quentin Simon, Laurence Nuttin, Stelly Lefort. Merci les amis pour les innombrables moments partagés devant cafés et bières!

Je remercie le Conseil de recherches en sciences naturelles et en génie du Canada (CRSNG) et la Société canadienne de météorologie et d'océanographie (SCMO) d'avoir soutenu mon projet de doctorat.

Mon doctorat est aussi une histoire de famille, surtout vers la fin. Merci Ariane d'être une source inépuisable de bonheurs, de rires et de câlins. Il n'y a rien de mieux pour recharger mes batteries. Merci évidemment à ma famille : Ginette, Denis, Marilou, Thérèse, Serge, Isabelle, Alexis, Tristan, Vincent, Diego, Camilo, Véronique, Marie-France, Pierre-Olivier, Raphaël, Éloise, Josué, Doryane, Saori, Noé. Vous m'avez tous et chacun encouragé et supporté tellement plus que vous le croyez. Merci Ismael et Alice pour votre amitié et votre intérêt insoupçonné pour mes histoires de grains! Finalement, je remercie tendrement et immensément, colossalement, *the last and the beast*, mon mari. Merci Milan d'être là, depuis le début, et de croire en moi.

RÉSUMÉ

Le magnétisme des sédiments est influencé à la fois par le climat et par le champ magnétique de la Terre. L'objectif de cette thèse est d'utiliser les propriétés magnétiques de la longue séquence sédimentaire du lac *Laguna Potrok Aike* (106 m, 51200 cal BP) pour fournir un enregistrement paléomagnétique et un enregistrement paléoclimatique dans une région clé de l'hémisphère Sud pourtant peu documentée. Le lac *Laguna Potrok Aike* (52°S, 70°W) est situé dans le sud-est de la Patagonie (Argentine) et se retrouve ainsi sous l'influence des forts vents d'ouest de l'hémisphère Sud et dans la région source des poussières déposées sur les glaces du continent Antarctique durant les périodes glaciaires. La position géographique du lac est donc idéale pour reconstituer l'activité éolienne ainsi que les changements climatiques survenus en Patagonie au cours du Quaternaire. Il s'agit aussi d'un endroit clé pour reconstituer la variabilité du champ magnétique terrestre, puisque l'hémisphère Sud est significativement sous-documenté par rapport à l'hémisphère Nord. De plus, la proximité de l'anomalie magnétique de l'Atlantique Sud (SAA) ainsi que des régions à fort flux géomagnétique (lobes) dans l'hémisphère Sud pourrait potentiellement permettre de mettre en évidence des différences entre l'évolution du champ au cours du temps dans la région du sud de l'Amérique du Sud et celle, mieux connue, de l'hémisphère Nord. Pour son grand potentiel à fournir un enregistrement climatique, éolien et paléomagnétique à haute résolution et au-delà la dernière transition climatique, le lac de maar *Laguna Potrok Aike* a été foré dans le cadre du Programme international de forage scientifique continental (*International scientific Continental Drilling Program*, ICDP) pour le projet *Potrok Aike maar lake Sediment Archive Drilling prOject* (PASADO). Dans cette thèse, les propriétés magnétiques et physiques de cette longue séquence sédimentaire ont été utilisées à haute résolution pour reconstituer les enregistrements paléomagnétique et paléoclimatique dans la région la plus au sud de l'Amérique du Sud.

Dans le premier chapitre, le vecteur paléomagnétique complet (inclinaison, déclinaison et paléointensité relative) a été reconstitué. Une influence de la taille des grains sur le signal de paléointensité relative (NRM/ARM) a été corrigée en utilisant le champ médian destructif de l'aimantation rémanente naturelle (MDF_{NRM}). La comparaison du nouvel enregistrement paléomagnétique avec d'autres enregistrements dans le sud de l'Amérique du Sud, ailleurs dans l'hémisphère Sud ainsi qu'avec des modèles du champ dipolaire révèle une variabilité millénaire similaire. L'excursion géomagnétique Laschamp et possiblement aussi Mono Lake et Hilina Pali sont documentés et témoignent de la nature globale de ces événements. La comparaison du vecteur paléomagnétique complet avec les enregistrements des lacs Baikal et Biwa situés de l'autre côté du globe en Sibérie et au

Japon révèle une différence apparemment régionale et d'origine non-dipolaire à ca. 46000 cal BP.

Dans le deuxième chapitre, nous présentons des indicateurs magnétiques de l'activité éolienne depuis 51200 cal BP. La combinaison des propriétés magnétiques et des données granulométriques a permis d'établir que le champ destructif médian de l'aimantation rémanente isothermale (MDF_{IRM}) reflète la magnétite dans une taille comprise entre les silts moyens à grossiers. Ces grains sont typiquement transportés par le vent en suspension sur de courtes distances. MDF_{IRM} présente une variabilité comparable à d'autres indicateurs de l'intensité des vents dérivés de sédiments marins, lacustres, de tourbière et de modelés quartziques en Patagonie depuis la dernière transition climatique et dans l'hémisphère Sud depuis 51200 cal BP. De plus, l'estimation du flux de magnétite au lac, l'influence de la taille des grains sur le signal de susceptibilité magnétique ainsi qu'une comparaison avec des enregistrements de poussières venant de la Patagonie et déposées dans l'océan Austral ainsi qu'en Antarctique révèlent que la susceptibilité magnétique est un indicateur des poussières de Patagonie à l'échelle multi-millénaire.

Dans le troisième chapitre nous présentons des indicateurs magnétiques d'évènements d'inondation liés à des précipitations intenses et à la fonte du pergélisol depuis 51200 cal BP. Les évènements d'inondation sont d'abord identifiés par la présence de minéraux magnétiques à haute coercivité (hématite et/ou goethite), puis l'origine pédogénique des grains est révélée par un ensemble d'évidences géologiques, limnologiques, stratigraphiques et climatiques. Ces dix évènements d'inondation sont associés à des couches de sédiments redéposés généralement lors de périodes plus productives dans le lac *Laguna Potrok Aike* et plus chaudes en Antarctique. De plus, nous démontrons que la formation authigène de greigite est limitée à des couches de sables et de cendres volcaniques remobilisées qui fournissent les conditions suboxiques et le sulfate dissous requis.

Dans l'ensemble, l'étude du magnétisme des sédiments du lac *Laguna Potrok Aike* fournit un enregistrement paléomagnétique de qualité ainsi que des indicateurs magnétiques des changements climatiques dans le sud-est de la Patagonie et associés au climat en Antarctique.

Mots clés : [magnétisme sédimentaire, paléomagnétisme, paléoclimatologie, Laguna Potrok Aike, Patagonie, hémisphère Sud, variabilité millénaire à séculaire, dernière période glaciaire, Holocène, intensité des vents]

ABSTRACT

Rock magnetism is influenced by climate and by the Earth's magnetic field. The goal of this thesis is to use the rock magnetic properties of the long sedimentary sequence from the lake *Laguna Potrok Aike* (106 m, 51200 cal BP) to derive paleomagnetic and paleoclimatic records in a key area of the Southern Hemisphere that is poorly documented. *Laguna Potrok Aike* (52°S, 70°W) is located in southeastern Patagonia (Argentina) in the path of the strong Southern Hemisphere westerly winds and in the source area of the dust deposited in Antarctica during Glacial periods. The lake geographical location is therefore ideal to reconstruct past changes in aeolian activity and climate changes in Patagonia. It is also a key location to reconstruct past changes of the geomagnetic field because the Southern Hemisphere is significantly under-documented relative to the Northern Hemisphere. In addition, the proximity of the South Atlantic Anomaly (SAA) as well as the Southern Hemisphere high flux lobes could allow identifying differences in the paleomagnetic field evolution in southern South America relative to the much more documented Northern Hemisphere. For his strong potential to provide high-resolution climatic, aeolian and paleomagnetic records beyond the last climatic transition, the maar lake *Laguna Potrok Aike* was drilled in the framework of the International scientific Continental Drilling Program (ICDP) for the Potrok Aike maar lake Sediment Archive Drilling prOject (PASADO). In this thesis, high-resolution rock-magnetic and physical properties are used in order to reconstruct paleoclimate and paleomagnetic records from the southernmost part of South America.

In the first chapter, the full-vector paleomagnetic record (inclination, declination and relative paleointensity) derived from the sediments of *Laguna Potrok Aike*. A grain size influence on the relative paleointensity record (NRM/ARM) was corrected using the median destructive field of the natural remanent magnetisation (MDF_{NRM}). Full-vector comparison of the new paleomagnetic record with other records from southern South America, elsewhere in the Southern Hemisphere, as well as dipole field models and compilations reveal similar millennial-scale variability. The Laschamp geomagnetic excursion and possibly the Mono Lake as well as the Hilina Pali excursions are recorded and suggest the global nature of these events. Nevertheless comparison with the Lake Baikal and Biwa records located on the opposite side of the globe in Siberia and Japan respectively reveals a different behaviour at ca. 46000 cal BP in *Laguna Potrok Aike* and in southern South America, hinting at a non-dipolar origin.

In the second chapter, rock-magnetic proxies of dust and wind intensity since 51200 cal BP are constructed. The combined use of rock magnetism and grain size data allowed identifying the median destructive field of the isothermal remanent magnetisation

(MDF_{IRM}) as best reflecting silt-sized magnetite typically transported by wind in suspension over short distances. The MDF_{IRM} displays similar variability than other wind intensity proxies derived from marine and lacustrine sediments, peat bug and speleothem records from Patagonia since the last climatic transition and from the Southern Hemisphere since 51200 cal BP. In addition, estimation of the flux of magnetite to the lake, investigation of the grain size influence on magnetic susceptibility and comparison with distal Patagonian dust records from the Southern Ocean and Antarctica indicate that the magnetic susceptibility signal from *Laguna Potrok Aike* is a dust record at the multi-millennial scale.

In the third chapter, rock-magnetic proxies of runoff events associated with extreme precipitation and permafrost melt since 51200 cal BP are presented. The runoff events are identified by the presence of high coercivity magnetic mineral (such as hematite and goethite) which its pedogenic origin is inferred from geological, limnological, stratigraphic and climatic evidence. The runoff events are generally associated with mass movement deposits during time of enhanced lake productivity in *Laguna Potrok Aike* and are also coeval within the limit of the chronology to warm atmospheric conditions recorded in Antarctica. In addition, we show that the authigenic formation of iron sulfide such as greigite is strictly associated to reworked sands and tephra layers providing the required suboxic conditions and dissolved sulfate.

As a whole, rock magnetism of the sediment from *Laguna Potrok Aike* provides a high quality full-vector paleomagnetic record as well as rock-magnetic proxies of past climate changes in southeastern Patagonia that are also associated with climate changes in Antarctica.

Keywords: [Paleomagnetism, sediment magnetism, paleoclimatology, *Laguna Potrok Aike*, Patagonia, Southern Hemisphere, millennial- to centennial-scale variability, last Glacial period, Holocene, wind intensity]

TABLE DES MATIÈRES

LISTE DES TABLEAUX

LISTE DES FIGURES

INTRODUCTION GENERALE

CHAPITRE 1

LISTE DES ABRÉVIATIONS, DES SIGLES ET DES ACRONYMES

AF : *alternating field*, champ alternatif

AIM : *Antarctic isotopic maxima*, maximums isotopiques dans les glaces de l'Antarctique

AMS : *anisotropy of magnetic susceptibility*, anisotropie de la susceptibilité magnétique

ARM : *anhysteretic remanent magnetisation*, aimantation rémanente anhystérétique

CAIR : Centre d'appui à l'innovation par la recherche

CC : *core catcher*, système de fermeture de carottier en forme d'ogive

ChRM : *characteristic remanent magnetisation*, magnétisation caractéristique rémanente

CP : *composite profile*, séquence composite

DC : *direct current*, courant direct

DOSECC : *Consortium for Drilling, Observation and Sampling of the Earth's Continental Crust*

DRM : *detrital remanent magnetisation*, aimantation rémanente détritique

EPICA : *European Project for Ice Coring in Antarctica*

FORC : *first-order reversal curve*

GAD : *geocentric axial dipole*, dipole axial géocentré

GRM : *gyroremanent magnetisation,* aimantation gyrorémanente

Hc : *coercive force*, coercivité

Hcr : *remanent coercive force*, coercivité rémanente

ICDD : *International Center for Diffraction Data*, Centre international des données de diffraction

ICDP : *International Continental scientific Driling Program,* Programme international de forage scientifique continental

IRM : *isothermal remanent magnetisation*, aimantation rémanente isothermale

IRM : *Institute for Rock Magnetism*

kARM : *susceptibility of the anhysteretic remanent magnetisation*, susceptibilité de l'aimantation rémanente anhystérétique

k_{FD} : *frequency-dependant magnetic susceptibility*, susceptibilité magnétique en fonction de la fréquence

k_{HF} : *high field magnetic susceptibility*, susceptibilité magnétique dans un champ fort

k_{LF} : *low field magnetic susceptibility*, susceptibilité magnétique dans un champ faible

k_T : *temperature-dependence of magnetic susceptibility*, susceptibilité magnétique en fonction de la température

LPA : *Laguna Potrok Aike*

MAD : *maximum angular deviation*, déviaton angulaire maximum

MD : *multidomain*, domaines multiples

MDF : *median destructive field*, champ médian destructif

MIS : *marine isotopic stage*, stage isotopique marin

MMD : *mass movement deposit*, dépôt par mouvement de masse

Mr : *saturation remanence*, rémanence à saturation

Ms : *saturation magnetisation*, aimantation à saturation

MSCL : *multi-sensor core logger*, banc de mesures

NRM : *natural remanent magnetisation*, aimantation naturelle rémanente

ODP : *Ocean Drilling Program*

PASADO : *Potrok Aike maar lake Sediment Archive Drilling project*

PDRM : *post-depositional remanent magnetisation*, aimantation rémanente post-déposition

PSD : *pseudo-single domain,* domaine pseudo-simple

RPI : *relative paleointensity,* paléointensité relative

SAA : South *Atlantic Anomaly*, Anomalie magnétique de l'Atlantique Sud

SALSA : *South Argentinean Lake Sediment Archives and modelling*

SAPIS : *South Atlantic paleointensity stack*

SEM : *scanning electron microscope*, microscope à balayage électronique

SD : *single domain*, domaine unique

SIRM : *saturation isothermal remanent magnetisation*, aimantation rémanente isothermale à saturation

SHW and **SWW** : *Southern Hemisphere Westerly Winds*

SP: *superparamagnetic*, superparamagnétique

TOC : *total organic carbon*, carbone organique total

UQAM : Université du Québec à Montréal

UQAR : Université du Québec à Rimouski

VADM : *virtual axial dipole moment*, moment dipolaire axial virtuel

INTRODUCTION GÉNÉRALE

Paléomagnétisme

Des mesures directes du champ magnétique à la surface de la Terre sont disponibles depuis environ 400 ans grâce aux carnets de bord de navigation (Jackson et al., 2000; Jonkers et al., 2003) et aujourd'hui des réseaux d'observatoires et de satellites acquièrent des mesures magnétiques en continu. Ces données historiques ont récemment contribué à mettre en évidence les récents changements rapides du champ magnétique de la Terre aux hautes latitudes (Korte and Mandea, 2008; St-Onge and Stoner, 2011) et dans la région de l'océan Atlantique Sud (Hulot et al., 2002; Korte et al., 2009). Les changements rapides du champ magnétique suscitent un grand intérêt, à la fois pour la société technologique que pour la recherche fondamentale. Par exemple, les régions où l'intensité géomagnétique est très faible représentent un risque pour la sécurité des missions spatiales près de la Terre. C'est le cas aujourd'hui dans la région de l'anomalie magnétique de l'Atlantique sud (*South Atlantic Anomaly*, SAA), où les radiations causent des dommages (Heirtzler, 2002). Sur Terre, les changements récents représentent un risque accru de perturbations aux systèmes de transmission électriques, aux pipelines de pétroles et de gaz naturel, aux câbles de télécommunications et aux chemins de fer, comme documenté aux hautes latitudes Nord où les lignes de force du champ dipolaire permettent la pénétration de particules chargées plus qu'ailleurs (e.g., Pirjola et al., 2000; Eroshenko et al., 2010). De plus, la possibilité d'une inversion géomagnétique imminente en lien avec la migration rapide du pôle Nord magnétique (Korte and Mandea, 2008) et la rapide diminution du champ dipolaire depuis ca. 1800 AD (-5% par siècle; Gubbins et al., 2006) a été abordée (Constable and Korte, 2006; DeSantis, 2007). Afin de mieux comprendre les mécanismes de la géodynamique interne à l'origine des changements présents et futurs, une meilleure connaissance de la

variabilité du champ magnétique passée à haute résolution et dans des régions encore peu documentées est impérative.

L'étude de l'aimantation rémanente du matériel géologique et archéologique tels les sédiments lacustres (e.g., Creer, 1985; Negrini et al., 1988; Peck et al., 1996; Hayashida et al., 2007; Yang et al., 2009; Haltia-Hovi et al., 2010) et marins (e.g., Lund et al., 2006; Sager et al, 2006), les laves volcaniques et les argiles chauffées (e.g., Hervé et al., 2013a; b; Korhonen et al., 2008; Yang et al., 2000) ainsi que les modelés karstiques (Lascu and Feinberg, 2011) constitue le seul moyen de reconstituer la variabilité du champ magnétique au-delà des derniers siècles pour lesquels des mesures directes sont disponibles. Les laves volcaniques et le matériel archéologique permettent d'obtenir des valeurs absolues, toutefois de manière discontinue et avec une plus grande abondance de données lors des périodes de volcanisme intense et d'anciennes civilisations. En contraste, les archives sédimentaires permettent de reconstituer la variabilité relative de manière continue et offrent la possibilité d'atteindre les plus hautes résolutions temporelles.

Dans certaines régions du globe comme les hautes latitudes nord et l'hémisphère Sud il y a très peu d'enregistrements paléomagnétiques disponibles. Dans les dernières années, un effort de recherche en paléomagnétisme sédimentaire aux hautes latitudes nord (e.g., Stoner et al., 2007; Barletta et al., 2008; Lisé-Pronovost et al., 2009; Simon et al., 2012; St-Onge et Stoner, 2011) a récemment permis une meilleure calibration de la nouvelle génération de modèles géomagnétiques (cals3k.4 et cals10k.1b; Korte and Constable, 2011; Korte et al., 2011) et une meilleure compréhension de la variabilité holocène dans cette région. Par exemple, Stoner et al. (2013) rapportent de larges changements de directions paléomagnétiques dans l'Atlantique nord depuis 8000 cal BP qui indiqueraient les positions préférentielles des zones à forte concentration de flux magnétique (lobes) au cours du temps. Leur interprétation supporte l'idée que les lobes de flux sont effectivement une structure récurrente dynamique du champ aux hautes latitudes nord durant l'Holocène, comme le suggèrent aussi différents modèles géomagnétiques (Bloxham, 2002; Korte and Holme, 2010). Les travaux de modélisation de Korte and Holme (2010) révèlent que les

lobes de flux situés dans l'hémisphère Sud sont aussi des structures récurrentes, mais qui semblent toutefois beaucoup moins dynamiques que celles de l'hémisphère Nord. Les auteurs concluent néanmoins qu'il n'est pas clair si cette différence est réellement géomagnétique ou induite par la rareté des enregistrements paléomagnétiques dans l'hémisphère Sud. En effet, le plus important biais dans la distribution géographique des enregistrements paléomagnétiques sur le globe est la sous-représentation de l'hémisphère Sud. Par conséquent, les modèles géomagnétiques (e.g., Korte and Constable, 2011) et les courbes de références globales (e.g., Guyodo and Valet, 1996; Laj et al., 2004) reflètent en réalité davantage la variabilité de l'hémisphère Nord. Pourtant il existe bel et bien des différences entre les deux hémisphères, tel qu'illustré par un déplacement indépendant des pôles magnétiques Nord et Sud à la surface de la Terre (Korte and Mandea, 2008) ou encore l'asymétrie interhémisphérique des anomalies magnétiques, dont l'une des plus importante aujourd'hui est la SAA dans l'océan Atlantique sud (Gubbins et al., 2006; Hartmann and Pacca, 2009). Les différences interhémisphériques sont d'autant plus remarquables quand le champ dipolaire diminue et elles représentent une possible limitation à la magnétostratigraphie à l'échelle globale. Les excursions géomagnétiques sont majoritairement documentées à partir d'enregistrements situés dans l'hémisphère Nord (Laj and Channell 2007; Roberts, 2008; Singer, sous presse) et certaines excursions ne sont pas encore documentées dans l'hémisphère Sud (e.g., l'excursion Hilina Pali qui est enregistrée en détail dans les laves volcaniques à Hawaii; Teanby et al., 2002). Afin de vérifier le caractère global de marqueurs magnétostratigraphiques comme les excursions géomagnétiques et de documenter l'asymétrie interhémisphérique dans le passé, des enregistrements à haute résolution de l'évolution du champ dans l'hémisphère Sud sont donc nécessaires.

Magnétisme environnemental

Le magnétisme des sédiments est un outil robuste et reconnu pour reconstituer la variabilité environnementale et climatique, souvent utilisé en combinaison avec d'autres indicateurs paleolimnologiques ou paléocéanographiques. Les applications

(paléo)environnementales du magnétisme sédimentaire sont nombreuses et incluent entre autres la source des sédiments (e.g., Thouveny et al., 2000; Blanchet et al., 2009; Venuti et al 2011; Hu et al., 2013), la circulation océanique (e.g., Mazaud et al., 2007; Parés et al., 2007; Kissel et al., 2008) et atmosphérique (e.g., Peck et al., 2004), le niveau des lacs (e.g., Negrini et al., 2000; Marshall et al 2011) et le régime de précipitation (e.g., Thompson and Maher, 1995; Williamson et al., 1998; Maher et al 2003; Kodama et al., 2013), la glace de mer (e.g., Sagnotti et al., 2001; Brachfeld et al., 2009) et les évènements de remobilisation liés à des tremblements de terre (e.g., St-Onge et al., 2004; 2012) ou à des inondations (e.g., Blanchet et al., 2009).

Les propriétés magnétiques des sédiments sont des indicateurs sensibles de l'environnement hautement spécifiques au site de dépôt. En effet, bien que la minéralogie, la taille et la concentration des grains magnétiques soient les trois seules variables qui définissent un assemblage magnétique, aucune n'a d'interprétation unique. Au contraire, des interprétations différentes et même opposées sont fréquentes puisque les propriétés magnétiques dépendent de la roche source, du transport, du climat et du lieu de dépôt (e.g., Verosub and Roberts, 1995; Dekkers, 1997; Evans and Heller, 2003; Maher and Thompson, 1999; Liu et al., 2012).

Un exemple bien connu pour illustrer des interprétations contraires associées à un paramètre magnétique est la susceptibilité magnétique des dépôts de lœss/paléosols durant les cycles glaciaires/interglaciaires du Quaternaire. Alors que les périodes interglaciaires sont caractérisées par une augmentation de la susceptibilité magnétique dans la fameuse séquence de loess/paléosol de Chine ainsi qu'au Tajikistan, en République Tchèque et aux États-Unis, exactement l'inverse est observé en Alaska, en Sibérie et en Argentine (e.g., Maher, 1998; Evans and Heller, 2001). De manière générale aux basses à moyennes latitudes, la susceptibilité magnétique plus élevée du paléosol par rapport au lœss est due à la formation de magnétite pédogénique ultrafine pendant les plus chaudes et humides périodes interglaciaires (e.g., Hunt et al., 1995). Les grains ultrafins de magnétite (ca., 0,4-0,001 um; Maher, 1998) sont un indicateur sensible puisque c'est la seule fraction

granulométrique de ce minéral qui a une influence connue sur la susceptibilité magnétique (Dearing, 1999; Heider et al., 1996). À l'inverse, aux moyennes à hautes latitudes les paléosols ont généralement une susceptibilité magnétique plus faible que le lœss, relativement à la dissolution de la magnétite dans un sol gorgé d'eau en conditions réductrices (gléification) (en Alaska et en Sibérie : e.g., Evans and Heller, 2001; Begét et al., 2001; Liu et al., 1999) ou de l'oxydation de la magnétite détritique en hematite/goethite (en Argentine : e.g., Orgeira et al., 1998; Carter-Stiglitz et al 2006). En outre, la susceptibilité magnétique plus élevée du lœss pendant les périodes glaciaires en Alaska, Sibérie et Argentine serait attribuée à une plus grande concentration de minéraux ferrimagnétiques d'origine éolienne (Vlag et al., 1999; Begét, 1990). La susceptibilité magnétique est une propriété magnétique complexe à interpréter puisque c'est une mesure qui peut être influencée à la fois par la concentration, la minéralogie et la taille des grains ferrimagnétiques, en plus de la composition du sédiment (matériel antiferro- dia-, para- et superparamagnétique) puisque la mesure se fait dans un champ faible sur le sédiment total (Dearing, 1999). Il est donc primordial d'investiguer l'assemblage magnétique en détail si l'on veut interpréter la signification environnementale de la susceptibilité magnétique et comparer différents enregistrements, que ce soit pour des séquences de lœss/paléosols (Maher, 1998; Orgeira and Compagnucci, 2006; Kravchinksy et al., 2008) ou de sédiments marins et lacustres (Verosub and Roberts, 1995).

Un autre exemple illustrant la variété d'interprétations pour un paramètre magnétique est le ratio des magnétisations rémanentes anhystérétique et isothermale (ARM/IRM) induites en laboratoire. Le ratio interparamétrique ARM/IRM (ou kARM/IRM, en normalisant ARM par le champ de polarisation à courant continu) est couramment utilisé en magnétisme environnemental comme indicateur de la taille des grains en milieu marin (e.g., Franke et al., 2007; Mazaud et al., 2007) et lacustre (e.g., Egli, 2004; Lascu et al., 2012; Kodama et al., 2013). La réponse disproportionnée des petits grains de magnétite (ca. < 1 μm) à une ARM (Maher, 1988) et la plus grande contribution des grains > 10 μm à une IRM qu'à une ARM (Brachfeld, 1999) sont à l'origine de l'utilisation du ratio ARM/IRM comme indicateur de la taille des grains. Ainsi ce ratio est particulièrement sensible à la

magnétite biogénique (e.g., Moskowitz et al., 1993; Snowball et al., 2002; Egli, 2004), ainsi qu'à la magnétite pédogénique et extracellulaire ultrafines (e.g., Özdemir and Banerjee, 1982; Maher and Taylor, 1988; Moskovitz et al., 1993; Frankel and Bazylinski, 2003; Maher et al., 2003; Egli, 2004) qui ont typiquement un domaine unique (*single domain*; SD). Toutefois, lorsqu'il y a interaction magnétostatique entre des particules fines, l'acquisition de la ARM est plus faible (Yamazaki et al., 2008; Paterson et al., 2013). Dès lors, un agrégat de petits grains de magnétite pédogénique ultrafine ou de fragments de magnétosomes pourraient diminuer le ratio ARM/IRM alors que la taille des grains reste inchangée. Finalement, puisque les minéraux magnétiques à forte coercivité tels l'hématite et la goethite résistent à l'aimantation pour être saturés seulement dans de très forts champs (> 57 T; Rochette et al., 2005) et acquièrent proportionnellement plus de IRM que de ARM à l'inverse des minéraux à faible coercivité comme la magnétite (e.g., Maher and Thompson, 1999), le ratio ARM/IRM pourrait vraisemblablement être aussi influencé par la minéralogie magnétique lorsque la concentration de magnétite est faible.

Ces exemples illustrent bien d'une part la grande variété d'interprétations et d'applications en magnétisme environnemental et souligne d'autre part l'importance primordiale de définir avec soin l'assemblage magnétique. En outre, chaque site d'étude permet potentiellement la définition d'outils magnétiques novateurs.

Le lac *Laguna Potrok Aike* et le projet PASADO

Le lac *Laguna Potrok Aike* (51°57,337'S, 70°22.688'W) dans le sud de Argentine est un lac de cratère phréatomagmatique situé dans le champ volcanique Pali Aike (Figure 1). De forme quasi-circulaire, le lac a un diamètre de 3,5 km, de fortes pentes (jusqu'à 20°; Anselmetti et al., 2009) et un bassin atteignant 100 m de profondeur (Zolitschka et al., 2006). Des sondages sismiques permettent d'estimer l'épaisseur des sédiments lacustres à 370 m (Gebhardt et al., 2011) et des études géomorphologiques indiquent que la région était libre de glaciers durant la dernière période glaciaire (Zolitschka et al., 2006; Coronato et al., 2013). Le lac est hydrologiquement fermé et par conséquent il est très sensible au ratio précipitation/évaporation (Ohlendorf et al., 2013), comme en témoignent les

nombreuses paléo-terrasses submergées et immergées (Haberzettl et al., 2005, 2008; Anselmetti et al., 2009). En Patagonie, les forts vents d'ouest sont un facteur climatique dominant qui crée un gradient climatique extrême de part et d'autre de la cordillère des Andes, avec un climat hyperhumide à l'ouest (Chili) et semi-aride à l'est (Argentine) (e.g., Garreaud et al., 2013). Du côté sous le vent en Argentine, le climat semi-aride est caractérisé par une température annuelle moyenne de 7,4°C, de faibles précipitations annuelles < 200 mm/an (Zolitschka et al., 2006), des vents moyens de ca. 10 m/s pendant l'été et une végétation de type steppe qui résiste à la sécheresse (Schabitz et al., 2013). Le substrat géologique régional est dominé par des dépôts non-consolidés d'origine fluviale et fluvioglaciaire et des basaltes Pliocène à Pléistocène du champ volcanique Pali Aike (Zolitschka et al., 2006; Ross et al., 2011; Coronato et al., 2013). Les dépôts non-consolidés incluent notamment les sédiments d'origine fluviale (Formation Santa Cruz) associés au soulèvement tectonique de la cordillère des Andes durant le Miocène et qui atteignent plus de 1000 m d'épaisseur, et les sédiments d'origine fluvioglaciaire du Pliocène et Pléistocène (Zolitschka et al., 2006). Majoritairement l'action éolienne, mais aussi l'action périglaciaire et de mineures incisions fluviales surtout en périodes interglaciaires ont agi sur le paysage du sud-est de la Patagonie depuis le Pléistocène Moyen. Toutefois, les modifications au paysage sont seulement légères, ce qui confère à la Patagonie Argentine un aspect de « paysage fossilisé » (Coronato et al., 2013).

Figure 1. Vue sur le le lac *Laguna Potrok Aike*, dans le sud-est de la Patagonie.

Dans l'ensemble, le contexte géologique et la géomorphologie du lac *Laguna Potrok Aike* sont optimaux pour une étude paléomagnétique. En effet, la géologie régionale représente une source abondante de magnétite détritique et la stabilité géologique du paysage ainsi que l'isolement hydrologique du lac suggèrent une constance de l'apport détritique. De plus, les sédiments du lac *Laguna Potrok Aike* constituent une archive paléoenvironnementale clé pour faire le lien entre l'Antarctique et les latitudes moyennes de l'hémisphère Sud, puisque la poussière déposée dans les glaces du continent Antarctique proviennent précisément du sud de la Patagonie (Basile et al., 1997; Sudgen et al., 2009). La Patagonie est la seule masse continentale entre 38°S et le continent Antarctique, et le lac *Laguna Potrok Aike* est situé à la frontière entre les vents d'ouest de l'hémisphère sud et le front polaire Antarctique. Le précédent projet SALSA (*South Argentinean Lake Sediment Archives and modelling*) a révélé des vitesses de sédimentation élevées, de l'ordre de 100 cm/ka depuis au moins 16000 ans (Haberzettl et al., 2007), dans une région où les

enregistrements paléoenvironnementaux sont souvent discontinus et généralement limités à la période Holocène ainsi qu'à la dernière transition climatique (Kilian and Lamy, 2012). Pour son grand potentiel à fournir un enregistrement climatique, hydrologique, éolien et paléomagnétique à haute résolution en Patagonie continentale, le lac *Laguna Potrok Aike* a été foré dans le cadre de l'*International Continental scientific Driling Program* (ICDP) pour le projet *Potrok Aike maar lake Sediment Archive Drilling prOject* (PASADO) (Zolitschka et al., 2009).

Les opérations de forage scientifique pour le projet PASADO ont été réalisées au printemps austral 2008 (septembre à novembre) à partir de la plateforme GLAD800 (Figure 2A), opérée par le *Consortium for Drilling, Observation and Sampling of the Earth's Continental Crust* (DOSECC). L'objectif de forage initial qui était de récupérer la séquence sédimentaire complète ainsi que les dépôts volcaniclastiques sous-jacents n'a pas été atteint à causes de défis techniques et logistiques, en plus de conditions climatiques inhabituelles pour la saison (Zolitschka et al., 2009). En particulier, l'absence de quai sur le lac et l'impossibilité d'approcher une grue de la rive a compliqué l'assemblage de la plateforme et retardé le début des opérations de forage. De plus, chacun des sites a du être abandonné en urgence à cause de vents d'ouest extrêmement forts (Figure 2B). Un total de 533 mètres de sédiments a néanmoins été prélevé à deux sites du bassin central par carottage à piston hydraulique. Le site 1 a été foré en quadruplicata et le site 2 en triplicata. La séquence sédimentaire composite du site 2 a été sélectionnée (106,09 m; Figure 3) pour les analyses multi-proxy de l'équipe PASADO pour son haut taux de récupération (98.8%) et une moindre proportion de sables qu'au site 1.

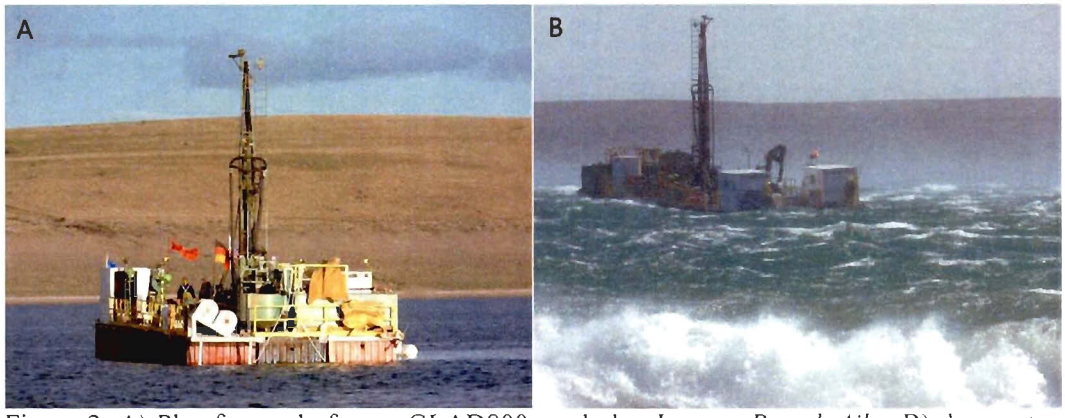

Figure 2. A) Plateforme de forage GLAD800 sur le lac *Laguna Potrok Aike*. B) des vents extrêmement forts pour la saison ont forcé l'abandon des sites de forage. (Crédit photo Bernd Zolitschka).

Objectifs de recherche

Les objectifs de recherche sont les suivants :

1° Reconstituer la variabilité du champ magnétique terrestre à haute résolution dans le sud de l'Amérique du Sud, à partir des sédiments du lac *Laguna Potrok Aike*.

En particulier, est-ce que les changements de paléointensité relative et de paléodirection (inclinaison et déclinaison) sont semblables aux enregistrements paléomagnétiques les plus proches dans le sud de l'Amérique du Sud, aux courbes de références pour l'hémisphère Nord et aux modèles du champ dipolaire à l'échelle globale? Est-ce que les excursions géomagnétiques connues sont enregistrées? Est-ce qu'il y a des différences? Est-ce que l'anomalie magnétique du sud de l'Atlantique (*South Atlantic Anomaly*, SAA) est une structure récurrente du champ?

2° Établir des indicateurs magnétiques de changements climatiques à partir des sédiments du lac *Laguna Potrok Aike*.

En particulier, est-ce que l'assemblage magnétique (concentration, minéralogie et taille des grains magnétiques) révèle des changements climatiques dans la région source des poussières atmosphériques déposées en Antarctique durant la dernière période glaciaire?

Est-ce que le climat de la dernière période glaciaire dans le sud-est de la Patagonie est comparable à la variabilité climatique documentée en Antarctique? Comment les vents à 52°S en Patagonie ont-ils variés depuis la dernière période glaciaire?

Méthode

Afin de répondre aux objectifs de recherche, des propriétés magnétiques et physiques de la séquence sédimentaire composite PASADO (106,09 m; Figure 3) ont été mesurées à haute résolution au laboratoire de paléomagnétisme sédimentaire de l'Institut des sciences de la mer de Rimouski (ISMER) à l'Université du Québec à Rimouski (UQAR). Le tableau 1 présente l'ensemble des analyses effectuées et leurs résolutions. Les analyses au diffractomètre à rayons X ont été complétées à l'Université du Québec à Montréal (UQAM), le microscope électronique à balayage a été utilisé au Centre d'appui à l'innovation par la recherche (CAIR) de l'Université du Québec à Rimouski (UQAR) et l'anisotropie de la susceptibilité magnétique a été mesurée à l'*Institute for Rock Magnetism* (IRM) de l'Université du Minnesota à Minneapolis. La méthodologie spécifique aux trois articles scientifiques au cœur de cette thèse sera détaillée dans chacun des chapitres de cette thèse.

J'ai eu la chance de participer aux opérations de forage scientifique du lac *Laguna Potrok Aike* en octobre et novembre 2008. Sur le terrain, des échantillons *core catchers* (CC) des deux sites de forage ont été divisés pour analyses multi-proxy aux différents laboratoires de recherche, incluant les propriétés magnétiques. Les résultats ont été publiés dans la revue The Holocene (Recasens et al., 2012). Le groupe canadien de l'équipe PASADO incluant P. Francus, G. St-Onge, T. Haberzettl, G. Jouve et moi-même avons effectué l'échantillonnage des u-channels et des échantillons ponctuels lors du *sampling party* PASADO en juin 2009 à l'Université de Brême (Allemagne). En août 2010 j'ai demandé des échantillons supplémentaires pour analyses magnétiques et les cubes ont été prélevés par J. J. Sagliotti, D. M. Echazú et C. Ohlendorf à l'Université de Brême, puis expédiés à l'ISMER.

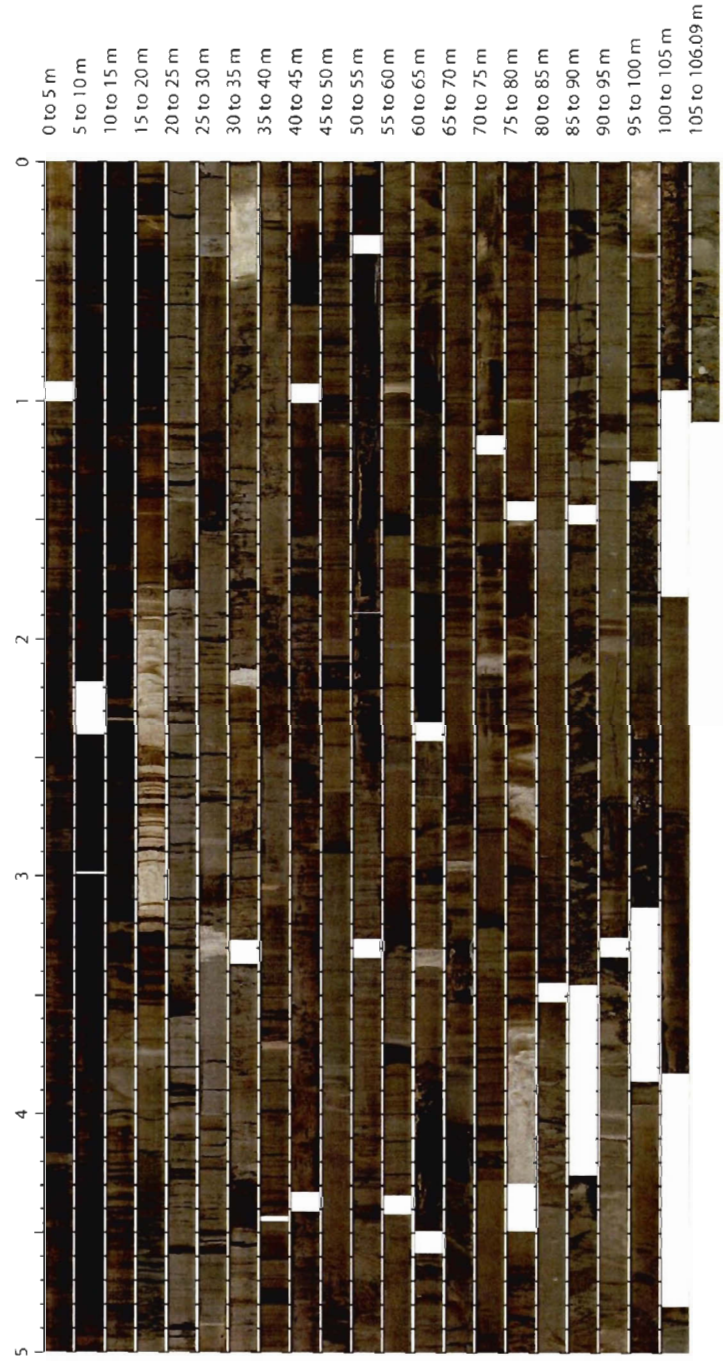

Figure 3. Photographie de la séquence sédimentaire composite PASADO-ICDP.

Tableau 1. Analyses de laboratoire effectuées dans le cadre de ce projet de doctorat

Instruments	Échantillon (nbre)	Résolution (cm)	Paramètres mesurés
Magnétomètre cryogénique pour u-channel -2G Enterprises			
	u-channels[a] (98)	1	NRM et directions paléomagnétiques
	u-channels[a] (98)	1	ARM (champ alternatif max.100 mT et ch direct 0,05 mT)
	u-channels[a] (98)	1	IRM 300 mT et 950 mT
Susceptibilité magnétique volumique dans un champ faible -Bartington MS2E			
	u-channels[a] (98)	1	k_{LF}
Spectrophotomètre -Konica Minolta 2600d			
	u-channels[a] (98)	1	L, a*, b*
Système d'imagerie digitale Geoscan IV			
	u-channels[a] (98)	25 µm	Image numérique
Magnétomètre à gradient alternatif -Princeton Measurements Corp. MicroMag 2900			
	ponctuel[b] (243); CC[c] (60)	~ 40	Ms, Mrs, Hc, Hcr, susceptibilité à 300 mT
	ponctuel[b] (43); CC[c] (26)	~150	courbe d'acquisition de l'IRM
	ponctuel[b] (36)	~300	*First-order reversal curve* (FORC)
Susceptibilité magnétique, basse (0.46 Hz) et haute (4.6 kHz) fréquences -Bartington MS2B			
	cubes[d] (59)	~ 200	k_{FD}
"Roly-Poly" pour l'anisotropie de la susceptibilité magnétique			
	cubes[d] (59)	~ 200	Anisotropie de la susceptibilité magnétiqu
Susceptibilité magnétique, haute température (0-700 °C) -Bartington MS2 k/T			
	CC[c] (34)	~300	k_T
Microscope électronique à balayage et spectroscopie rayons X à dispersion d'énergie (SEM-EDS) -JEOL 6460LV			
	ponctuel[b] (13); CC[c] (3)	-[e]	Image et composition élémentaire semi-quantitative de grains
Diffractomètre à rayons X -Siemens D5000			
	ponctuel[b] (13); CCc (3)	-[e]	Minéralogie d'extraits magnétiques

[a]Dimension maximale: 2x2x150 cm; [b]ca. 2-3 g; [c]CC: *core catchers* aux sites 1D et 2A; [d]Dimension: 2x2x2 cm; [e]Les échantillons discrets disponibles aux profondeurs d'intérêt pour le manuscrit "*Rock-magnetic signature of precipitation and extreme runoff events in southeastern Patagonia since 51,200 cal BP from the sediment of Laguna Potrok Aike*" (chapitre 3).

Organisation de la thèse

La présente thèse par articles est organisée en trois chapitres. Le premier chapitre présente la reconstitution du champ magnétique terrestre à partir des sédiments du lac *Laguna Potrok Aike* depuis 51200 cal BP. L'article est publié dans la revue *Quaternary Science Reviews*.

Lisé-Pronovost, A., St-Onge, G., Gogorza, C., Haberzettl, T., Preda, M., Kliem, P., Francus, P., Zolitschka, B. **2013**. High-resolution paleomagnetic secular variations and relative paleointensity since the Late Pleistocene in southern South America, *Quaternary Science Reviews* 71, 91-108.

Le deuxième chapitre présente des indicateurs magnétiques de l'intensité des vents et de la poussière à 52°S en Patagonie depuis 51200 cal BP. Le manuscrit sera soumis prochainement à la revue *Earth and Planetary Science Letters*.

Lisé-Pronovost, A., St-Onge, G., Gogorza, C., Haberzettl, T., Jouve, G., Francus, P., Stoner, J., Ohlendorf, C., Gebhardt, C., Zolitschka, B., sera soumis prochainement. Rock-magnetic proxies of wind intensity and dust since 51200 cal BP from the sediments of *Laguna Potrok Aike* in southern Patagonia

Le troisième chapitre présente la signature magnétique d'évènements de précipitation et d'inondation extrêmes dans le sud-est de la Patagonie durant la dernière période glaciaire, la déglaciation et l'Holocène. Le manuscrit sera soumis prochainement à la revue *Quaternary Science Reviews*.

Lisé-Pronovost, A., St-Onge, G., Gogorza, C., Jouve, G., Francus, P., Zolitschka, B., sera soumis prochainement. Rock-magnetic signature of precipitation and extreme runoff events in southeastern Patagonia since 51,200 cal BP from the sediment of Laguna Potrok Aike.

Finalement, une discussion générale pour l'ensemble des thèmes abordés en paléomagnétisme et en paléoclimatologie, ainsi que les conclusions générales et implications scientifiques de la présente thèse de doctorat suit les trois chapitres.

Contributions et collaborations

Ma contribution aux trois chapitres de cette thèse est l'analyse des résultats et la rédaction en tant que première auteure avec la supervision de mon directeur de thèse G. St-Onge. L'équipe scientifique internationale PASADO a adopté une approche multi-proxy à haute résolution sur une longue séquence sédimentaire composite (Figure 3). Ainsi, il existe une étroite collaboration entre les différents laboratoires de recherche en Allemagne, Suisse, Suède, Argentine et au Canada, où les propriétés physiques, magnétiques, sédimentologique, minéralogiques, géochimiques, géo-microbiologiques et paléobiologiques ont été analysées. Les trois chapitres de cette thèse ont bénéficié de la collaboration de plusieurs co-auteurs. Chaque co-auteur a révisé une ou plusieurs versions des manuscrits et la majorité a aussi participé au travail de terrain et/ou de laboratoire. En particulier, les trois chapitres de cette thèse incluent le travail chronostratigraphique de P. Kliem et B. Zolitschka. De plus, le premier chapitre inclus le travail de laboratoire et d'analyse minéralogique de M. Preda et le deuxième chapitre inclus les données granulométriques mesurées par C. Ohlendorf et C. Gebhardt.

Mes travaux de recherche dans le cadre de ce projet de recherche et en tant que membre de l'équipe scientifique PASADO m'ont permis de collaborer en tant que co-auteure à quatre publications scientifiques et à plusieurs présentations lors de congrès (voir section Publications ci-dessous). J'ai contribué à la publication présentant l'enregistrement paléomagnétique des sédiments de *Laguna Potrok Aike* depuis 16 ka cal BP à partir de la séquence sédimentaire prélevée lors du projet SALSA en 2003 (Gogorza et al., 2012) et les premiers résultats de magnétisme sédimentaire PASADO ont été publiés en relation avec d'autres indicateurs limnologiques (Recasens et al., 2012). De plus, mes travaux de magnétostratigraphie ont permis d'identifier la chronologie la plus probable entre deux scénarios possibles basés sur les datations radiocarbones dans la partie la plus ancienne de

la séquence sédimentaire PASADO (avant 25000 cal BP; Kliem et al., 2013). Finalement, mon travail de stratigraphie à haute résolution entre la séquence des 98 u-channels et la séquence sédimentaire initiale a été utile à une étude comparative des méthodes de détermination de la densité des sédiments (Fortin et al., 2013).

Publications réalisées dans le cadre de ma thèse de doctorat

Articles scientifiques avec comité de lecture

Articles en préparation

Lisé-Pronovost, A., St-Onge, G., Gogorza, C., Haberzettl, T., Jouve, G., Francus, P., Stoner, J., Zolitschka, B. and the PASADO science team, En préparation pour la revue *Earth and Planetary Science Letters*. Rock-magnetic proxies of wind intensity and dust since 51200 cal BP from the sediments of *Laguna Potrok Aike* in southern Patagonia.

Lisé-Pronovost, A., St-Onge, G., Gogorza, C., Jouve, G., Francus, P., Zolitschka, B. and the PASADO science team, En préparation pour *Quaternary Science Reviews*. Rock-magnetic signature of precipitation and extreme runoff events in southeastern Patagonia since 51200 cal BP from the sediment of Laguna Potrok Aike.

Articles publiés

Lisé-Pronovost, A., St-Onge, G., Gogorza, C., Haberzettl, T., Preda, M., Kliem, P., Francus, P. Zolitschka, B. and the PASADO science team, 2013. High-resolution paleomagnetic secular variation and relative paleointensity since the Late Pleistocene in Southern South America. Quaternary Science Reviews 71, 91-108. doi:10.1016/j.quascirev.2012.05.012

Fortin, D., Francus, P., Gebhardt, C., Hanh, A., Kliem, P., **Lisé-Pronovost, A.**, Royshowdury, R., Labrie, J., St-Onge, G., PASADO science team, 2013. Destructive and non-destructive density determination: method comparison and evaluation from the Laguna

Potrok Aike sedimentary record. Quaternary Science Reviews 71, 147-153. doi:10.1016/j.quascirev.2012.08.024

Kliem, P., Enters, D., Ohlendorf, C., **Lisé-Pronovost, A.**, St-Onge, G., Wastergard, S., Zolitschka, B. and the PASADO science team, in press. Lithology, radiocarbon dating and sedimentological interpretation of the 51 ka BP lacustrine record from Laguna Potrok Aike, southern Patagonia. Quaternary Science Reviews 71, 54-69. doi:10.1016/j.quascirev.2012.07.019

Gogorza, C.S.G., Irurzun, M.A., Sinito, A.M., **Lisé-Pronovost, A.**, St-Onge, G., Haberzettl, T., Ohlendorf, C., Kastner, S., Zolitschka, B., 2012. High-resolution paleomagnetic records from Laguna Potrok Aike (Patagonia, Argentina) for the last 16,000 years. Geochemistry, Geophysics, Geosystems 13, Q12Z37. doi:10.1029/2011GC003900

Recasens, C., Ariztegui, D., Gebhardt, C., Gogorza, C.S.G, Haberzettl, T., Hahn, A., Kliem, P., **Lisé-Pronovost, A.**, Lücke, A., Maidana, N.I., Mayr, C., Ohlendorf, C., Schäbitz, F., St-Onge, G., Wille, M., Zolitschka, B., the PASADO ScienceTeam, 2012. New insights into paleoenvironmental changes in Laguna Potrok Aike, Southern Patagonia, since the Late Pleistocene: the PASADO multiproxy record. The Holocene 22, 1323-1335. doi:10.1177/0959683611429833

Actes de conférences

Lisé-Pronovost, A, St-Onge, G., Gogorza, C., Haberzettl, T., Zolitschka, B. and the PASADO science team, 2012. Rock-magnetic proxies of environmental changes since 51.2 ka cal BP from Laguna Potrok Aike, southern Patagonia. 4th International PASADO Workshop, Terra Nostra 2012/2.

Lisé-Pronovost, A., St-Onge, G., Gogorza, C., Kliem, P., Ohlendorf, C., Zolitschka, B. and the PASADO science team, 2011. High-resolution magnetostratigraphy in southern South America: results from the long sedimentary sequence of the maar lake Laguna Potrok Aike (ICDP-PASADO), GEOHYDRO conference proceeding.

Présentations lors de congrès

Lisé-Pronovost, A., St-Onge, G., Gogorza, C., Haberzettl, T., Kliem, P. Francus, P., Zolitschka, B. and the PASADO Science Team, 2012. High-resolution paleomagnetic secular variations and relative paleointensity since the Late Pleistocene in southern South America. Présentation orale lors du congrès AGU, 3-7 décembre 2012, San Francisco, California, USA.

St-Onge, G., **Lisé-Pronovost, A.**, Gogorza, C., Haberzettl, H., Kliem, P., Francus, P., Zolitschka, B. and the PASADO science team, 2012. High-resolution paleomagnetic secular variations and relative paleointensity from Southern Patagonia since the Late Pleistocene. Présentation orale lors du congrès *International Paleolimnology Symposium*, 21-24 août 2012, Glasgow, Scotland.

Lisé-Pronovost, A., St-Onge. G., Gogorza, C., Kliem, P., Ohlendorf, C., Zolitschka, B. and the PASADO science team, 2011. High-resolution magnetostratigraphy in southern South America : results from the long sedimentary sequence of the maar lake Laguna Potrok Aike (ICDP-PASADO). Présentation orale lors du congrès GEOHYDRO meeting, 28-31 août 2011, Québec (QC) Canada.

Lisé-Pronovost, A., Recasens, C., St-Onge, G., Gogorza, C., Haberzettl, T., Zolitschka, B. and the PASADO science team, 2011. Étude multidisciplinaire de la longue séquence sédimentaire du lac de cratère Laguna Potrok Aike (sud de l'Argentine) : résultats préliminaires de l'équipe scientifique PASADO-ICDP. Présentation orale lors du congrès annuel des étudiants du GEOTOP, 24-26 janvier 2011, Orford (QC) Canada.

Lisé-Pronovost, A., St-Onge, G., Gogorza, C., Haberzettl, T. and the PASADO science team, 2010. Rock magnetic study and paleomagnetic reconstruction for the maar lake Laguna Potrok Aike, southern Argentina : preliminary results from the PASADO-ICDP record. Affiche au congrès AGU, 13-17 décembre 2010, San Francisco (CA) USA.

Lisé-Pronovost, A., St-Onge, G., Haberzettl, T. and the PASADO science team, 2010. High-resolution Late Pleistocene paleomagnetic secular variation record from Laguna Potrok Aike, Southern Patagonia (Argentina): preliminary results from the ICDP-PASADO drilling. Affiche au congrès EGU, 2-7 mai 2010, Vienne, Autriche.

Lisé-Pronovost, A., St-Onge, G., Haberzettl, T. et l'équipe scientifique PASADO, 2010. Paléomagnétisme sédimentaire au sud de la Patagonie : variabilité millénaire à séculaire de l'inclinaison et de la déclinaison depuis 16 000 ans à partir de sédiments du lac de cratère Laguna Potrok Aike (ICDP-PASADO). Présentation orale lors du congrès annuel des étudiants du GEOTOP, 24-26 février 2010, Montréal (QC) Canada.

Lisé-Pronovost A., Haberzettl, T., St-Onge, G., Brown, L., Gebhardt, C.A., and the PASADO science team, 2009. Magnetostratigraphy and environmental magnetism of Laguna Potrok Aike : Preliminary results from the ICDP project PASADO. Affiche au congrès AGU, 24-27 mai 2009, Toronto (ON) Canada.

Haberzettl, T., Anselmetti, F.S., Bowen, S.W., Gebhardt, C., Hahn, A., Kliem, P., **Lisé-Pronovost A.**, Ohlendorf, C., St-Onge, G., Zolitschka, B., Laguna Potrok Aike, Southern Patagonia, Argentina : Achievements and resulting potential for the ICDP project PASADO. Présentation orale lors du congrès AGU, 24-27 mai 2009, Toronto (ON) Canada.

Références

Anselmetti, F.S., Ariztegui, D., De Batist, M., Catalina Gebhardt, A., Haberzettl, T., Niessen, F., Ohlendorf, C., Zolitschka, B., 2009. Environmental history of southern Patagonia unravelled by the seismic stratigraphy of Laguna Potrok Aike. Sedimentology 56, 873–892.

Barletta, F., St-Onge, G., Channell, J.E.T., Rochon, A., Polyak, L., Darby, D.A., 2008. High-resolution paleomagnetic secular variation and relative paleointensity records

from the western Canadian Arctic: implication for Holocene stratigraphy and geomagnetic field behaviour. Can. J. Earth Sci. 45, 1265-1281.

Basile, I., Grousset, F.E., Revel, M., Petit, J.R., Biscaye, P.E., Barkov, N.I., 1997. Patagonian origin of glacial dust deposited in East Antarctica (Vostok andDome C) during glacial stages 2, 4 and 6, Eart and Planet. Sci. Lett. 146, 573-589.

Begét, J.E., Stone, D.B., Hawkins D.B., 1990. Paleoclimatic forcing of magnetic susceptibility variations in Alaskan loess during the late Quaternary, Geology. 18. 40-43.

Begét, J.E., 2001. Continuous Late Quaternary proxy climate records from loess in Beringia. Quat. Sci. Rev. 20, 499–507.

Blanchet, C.L., Thouveny, N., Vidal, L., 2009. Formation and preservation of greigite (Fe_3S_4) in sediments from the Santa Barbara Basin: Implications for paleoenvironmental changes during the past 35 ka: GREIGITE IN SANTA BARBARA BASIN. Paleoceanography 24, PA2224.

Bloxham, J., 2002. Time-independent and time-dependent behaviour of high-latitude flux bundles at the core-mantle boundary, Geophys Res. Lett., 29(18).

Brachfeld, S., Barletta, F., St-Onge, G., Darby, D., Ortiz, J.D., 2009. Impact of diagenesis on the environmental magnetic record from a Holocene sedimentary sequence from the Chukchi–Alaskan margin, Arctic Ocean. Glob. Planet. Change 68, 100–114.

Brachfeld, S.A., 1999. Separation of geomagnetic paleointensity and paleoclimate signals in sediments: examples from North America and Antarctica. PhD thesis, University of Minnesota.

Carter-Stiglitz, B., Banerjee, S.K., Gourlan, A., Oches, E., 2006. A multi-proxy study of Argentina loess: Marine oxygen isotope stage 4 and 5 environmental record from pedogenic hematite. Palaeogeogr. Palaeoclim. Palaeoecol. 239, 45–62.

Constable, C., Korte, M., 2006. Is Earth's magnetic field reversing? Earth Planet. Sci. Lett. 246, 1–16.

Coronato, A., Ercolano, B., Corbella, H., Tiberi, P., 2013. Glacial, fluvial and volcanic landscape evolution in the Laguna Potrok Aike maar area, Southern Patagonia, Argentina. Quat. Sci. Rev. 71, 13–26.

Creer, K.M., 1985. Review of lake sediment palaeomagnetic data (Part 1). Geophysical Surveys 7, 125-160.

De Santis, A., 2007. How persistent is the present trend of the geomagnetic field to decay and, possibly, to reverse? Phys. Earth Planet. Inter. 162, 217–226.

Dearing, J.A., 1999. Environmental magnetic susceptibility: using the Bartington MS2 system. Chi Pub., Kenilworth.

Dekkers, M.J., 1997. Environmental magnetism: an introduction. Geol. En Mijnb. 76, 163–182.

Egli, R., 2004. Characterization of individual rock magnetic components by analysis of remanence curves. Phys. Chem. Earth Parts ABC 29, 851–867.

Eroshenko, E.A., Belov, A.V., Boteler, D., Gaidash, S.P., Lobkov, S.L., Pirjola, R., Trichtchenko, L., 2010. Effects of strong geomagnetic storms on Northern railways in Russia. Adv. Space Res. 46, 1102–1110.

Evans, M.E., Heller, F., 2001. Magnetism of loess/palaeosol sequences: recent developments. Earth-Sci. Rev. 54, 129–144.

Evans, M.E. and Heller, F., 2003. Environmental magnetism: Principles and applications of enviromagnetics, international geophysics series vol. 86, Academic press, 299p.

Fortin, D., Francus, P., Gebhardt, A. C., Hahn, A., Kliem, P., Lisé-Pronovost, A., St-Onge, G. **2013.** Destructive and non-destructive density determination: Method comparison and evaluation from the laguna potrok aike sedimentary record. *Quaternary Science Reviews* 71, 147-153.

Franke, C., von Dobeneck, T., Drury, M.R., Meeldijk, J.D., Dekkers, M.J., 2007. Magnetic petrology of equatorial Atlantic sediments: Electron microscopy results and their implications for environmental magnetic interpretation. Paleoceanography 22, PA4207.

Frankel, R.B., Bazylinski D.A., 2003. Biologically induced mineralization by bacteria. Rev Mineral Geochem 54, 95-114.

Garreaud, R., P. Lopez, M. Minvielle, M. Rojas, 2013. Large Scale Control on the Patagonia Climate. J. of Climate 26, 215-230.

Gebhardt, A.C., De Batist, M., Niessen, F., Anselmetti, F.S., Ariztegui, D., Haberzettl, T., Kopsch, C., Ohlendorf, C., Zolitschka, B., 2011. Deciphering lake and maar geometries from seismic refraction and reflection surveys in Laguna Potrok Aike (southern Patagonia, Argentina). J. Volcanol. Geotherm. Res. 201, 357–363.

Gogorza, C.S.G., Irurzun, M.A., Sinito, A.M., Lisé-Pronovost, A., St-Onge, G., Haberzettl, T., Ohlendorf, C., Kastner, S., Zolitschka, B. **2012.** High-resolution paleomagnetic records from Laguna Potrok Aike (Patagonia, Argentina) for the last 16,000 years. *Geochemistry, Geophysics, Geosystems* 13, Q12Z37.

Gubbins, D., Jones, A.L., Finlay, C.C., 2006. Fall in Earth's Magnetic Field Is Erratic, Science 312 (5775), 900-902.

Guyodo, Y., Valet, J.-P., 1996. Relative variations in geomagnetic intensity from sedimentary records: the past 200 thousand years. Earth Planet. Sci. Lett. 143 (1-4), 23-36.

Haberzettl, T., Corbella, H., Fey, M., Janssen, S., Lucke, A., Mayr, C., Ohlendorf, C., Schabitz, F., Schleser, G.H., Wille, M., Wulf, S., Zolitschka, B., 2007. Lateglacial and Holocene wet--dry cycles in southern Patagonia: chronology, sedimentology and geochemistry of a lacustrine record from Laguna Potrok Aike, Argentina. The Holocene 17, 297–310.

Haberzettl, T., Fey, M., Lücke, A., Maidana, N., Mayr, C., Ohlendorf, C., Schäbitz, F., Schleser, G.H., Wille, M., Zolitschka, B., 2005. Climatically induced lake level changes during the last two millennia as reflected in sediments of Laguna Potrok Aike, southern Patagonia (Santa Cruz, Argentina). J. Paleolimnol. 33, 283–302.

Haberzettl, T., Kück, B., Wulf, S., Anselmetti, F., Ariztegui, D., Corbella, H., Fey, M., Janssen, S., Lücke, A., Mayr, C., Ohlendorf, C., Schäbitz, F., Schleser, G.H., Wille, M., Zolitschka, B., 2008. Hydrological variability in southeastern Patagonia and explosive volcanic activity in the southern Andean Cordillera during Oxygen Isotope Stage 3 and the Holocene inferred from lake sediments of Laguna Potrok Aike, Argentina. Palaeogeogr. Palaeoclim. Palaeoecol. 259, 213–229.

Haltia-Hovi, E., Nowaczyk, N., Saarinen, T., 2010. Holocene palaeomagnetic secular variation recorded in multiple lake sediment cores from eastern Finland. Geophys. J. Int. 180, 609–622.

Hartmann, G.A., Pacca, I.G., 2009. Time evolution of the South Atlantic magnetic anomaly. An. Acad. Bras. Ciênc. 81, 243–255.

Hayashida, A., Ali, M., Kuniko, Y., Kitagawa, H., Torii, M., Takemura, K., 2007. Environmental magnetic record and paleosecular variation data for the last 40 kyrs from the Lake Biwa sediments, Central Japan. Earth Planets Space 59, 807–814.

Heider, F., A. Zitelsberger, K. Fabian, 1996. Magnetic susceptibility and remanence coercive force in grown magnetite crystals from 0.1 mm to 6 mm, Physics of the Earth and Planet. Int. 93, 239-256.

Heirtzler, J.R., 2002. The future of the South Atlantic anomaly and implications for radiation damage in space. J. Atmospheric Sol.-Terr. Phys. 64, 1701–1708.

Hervé, G., Chauvin, A., Lanos, P., 2013a. Geomagnetic field variations in Western Europe from 1500BC to 200AD. Part I: Directional secular variation curve. Phys. Earth Planet. Inter. 218, 1–13.

Hervé, G., Chauvin, A., Lanos, P., 2013b. Geomagnetic field variations in Western Europe from 1500BC to 200AD. Part II: New intensity secular variation curve. Phys. Earth Planet. Inter. 218, 51–65.

Hu, P., Liu, Q., Torrent, J., Barrón, V., Jin, C., 2013. Characterizing and quantifying iron oxides in Chinese loess/paleosols: Implications for pedogenesis. Earth Planet. Sci. Lett. 369-370, 271–283.

Hulot, G., Eymin, C., Langlais, B., Mandea, M., Olson, N., 2002. Small-scale structure of the geodynamo inferred from Ørsted and Magsat satellite data. Nature 416, 620-623.

Hunt, C.P., Banerjee, S.K., Han, J., Solheid, P.A., Oches, E., Sun, W., Liu, T., 1995. Rock-magnetic proxies of climate change in the loess-palaeosol sequences of the western Loess Plateau of China. Geophys. J. Int. 123, 232–244.

Jackson, A., Jonkers, A.R.T, Walker, M.R., 2000. Four centuries of geomagnetic secular variation from historical records, Phil. Trans. R. Soc. Lond. A. 358, 957-990.

Jonkers, A.R.T., 2003. Four centuries of geomagnetic data from historical records. Rev. Geophys. 41.

Kilian, R., Lamy, F., 2012. A review of Glacial and Holocene paleoclimate records from southernmost Patagonia (49–55°S). Quat. Sci. Rev. 53, 1–23.

Kissel, C., Laj, C., Piotrowski, A.M., Goldstein, S.L., Hemming, S.R., 2008. Millennial-scale propagation of Atlantic deep waters to the glacial Southern Ocean. Paleoceanography 23, PA2102.

Kliem, P., Enters, D., Hahn, A., Ohlendorf, C., Lisé-Pronovost, A., St-Onge, G., Wastegård, S., Zolitschka, B. **2013**. Lithology, radiocarbon chronology and sedimentological interpretation of the lacustrine record from Laguna Potrok Aike, southern Patagonia, *Quaternary Science Reviews* 71, 54-69.

Kodama, K.P., Moeller, R.E., Bazylinski, D.A., Kopp, R.E., Chen, A.P., 2013. The mineral magnetic record of magnetofossils in recent lake sediments of Lake Ely, PA. Glob. Planet. Change. Disponible en ligne le 20 avril 2013, http://dx.doi.org/10.1016/j.gloplacha.2013.03.012.

Korhonen, K., Donadini, F., Riisager, P., Pesonen, L.J., 2008. GEOMAGIA50: An archeointensity database with PHP and MySQL: GEOMAGIA50 ARCHEOINTENSITY DATABASE. Geochem. Geophys. Geosystems 9(4) Q04029.

Korte, M., Constable, C., 2011. Improving geomagnetic field reconstructions for 0–3ka. Phys. Earth Planet. Inter. 188, 247–259.

Korte, M., Constable, C., Donadini, F., Holme, R., 2011. Reconstructing the Holocene geomagnetic field. Earth Planet. Sci. Lett. 312, 497–505.

Korte, M., Holme, R., 2010. On the persistence of geomagnetic flux lobes in global Holocene field models. Phys. Earth Planet. Inter. 182, 179–186.

Korte, M., Mandea, M., Linthe, H.J., Hemshorn, A., Kotzé, P., Ricaldi, E., 2009. New geomagnetic field observations in the South Atlantic Anomaly region. Ann Geophys 52, 65–82.

Korte, M., Mandea, M., 2008. Magnetic poles and dipole tilt variation over the past decades to millennia. Earth Planets Space EPS 60, 937.

Kravchinsky, V.A., Zykina, V.S., Zykin, V.S., 2008. Magnetic indicator of global paleoclimate cycles in Siberian loess–paleosol sequences. Earth Planet. Sci. Lett. 265, 498–514.

Laj, C., Kissel, C., Beer, J., 2004. High resolution global paleointensity stack since 75 kyrs (GLOPIS-75) calibrated to absolute values. In: Channell, J.E.T., Kent, D.V., Lowrie, W., Meert, J.G. (Eds.), Timescales of the Paleomagnetic Field. AGU Geophysical Monograph, vol. 145.

Laj, C., Channell, J.E.T., 2007. Geomagnetic excursions. In: Kono, M. (Ed.), Treatise on Geophysics. Geomagnetism, vol. 5. Elsevier, Amsterdam, pp. 373-416.

Lascu, I., Feinberg, J.M., 2011. Speleothem magnetism. Quat. Sci. Rev. 30, 3306–3320.

Lascu, I., McLauchlan, K.K., Myrbo, A., Leavitt, P.R., Banerjee, S.K., 2012. Sediment-magnetic evidence for last millennium drought conditions at the prairie–forest ecotone of northern United States. Palaeogeogr. Palaeoclim. Palaeoecol. 337-338, 99–107.

Lisé-Pronovost, A., St-Onge, G., Brachfeld, S., Barletta, F., Darby, D., 2009. Paleomagnetic constraints on the Holocene stratigraphy of the Arctic Alaskan margin. Glob. Planet. Change 68, 85–99.

Liu, X.M., Hesse, P., Rolph, T., Béget, J.E., 1999. Properties of magnetic mineralogy of Alaskan loess : evidence for pedogenesis. Quat. Int. 62, 93-102.

Liu, Q., Roberts, A.P., Larrasoaña, J.C., Banerjee, S.K., Guyodo, Y., Tauxe, L., Oldfield, F., 2012. Environmental magnetism: Principles and applications. Rev. Geophys. 50.

Lund, S., Stoner, J.S., Channell, J.E.T., Acton, G., 2006. A summary of Brunhes paleomagnetic field variability recorded in Ocean Drilling Program cores. Phys. Earth Planet. Inter. 156, 194–204.

Maher, B. A. 1988. Magnetic properties of some synthetic submicron magnetites. Geophysical Journal 94, 83-96.

Maher, B.A. and Taylor, R.M., 1988. Formation of ultrafine-grained magnetite in soils, Nature 336 (6197), 368-370.

Maher, B.A, 1998. Magnetic properties of modern soils and Quaternary loessic paleosols: paleoclimatic implications. Palaeogeo. Palaeoclim. Palaeoeco. 137, 25-54.

Maher, B.A., Alekseev, A., Alekseeva, T., 2003. Magnetic mineralogy of soils across the Russian Steppe: climatic dependence of pedogenic magnetite formation. Palaeogeogr. Palaeoclim. Palaeoecol. 201, 321–341.

Maher, B.A., Thompson, R., 1999. Quaternary climates, environments, and magnetism. Cambridge University Press, Cambridge, UK; New York.

Marshall, M.H., Lamb, H.F., Huws, D., Davies, S.J., Bates, R., Bloemendal, J., Boyle, J., Leng, M.J., Umer, M., Bryant, C., 2011. Late Pleistocene and Holocene drought events at Lake Tana, the source of the Blue Nile. Glob. Planet. Change 78, 147–161.

Mazaud, A., Kissel, C., Laj, C., Sicre, M.A., Michel, E., Turon, J.L., 2007. Variations of the ACC-CDW during MIS3 traced by magnetic grain deposition in midlatitude South Indian Ocean cores: Connections with the northern hemisphere and with central Antarctica. Geochem. Geophys. Geosystems 8, Q05012.

Moskowitz, B.M., Frankel, R.B., Bazylinski, D.A., 1993. Rock magnetic criteria for the detection of biogenic magnetite. Earth Planet. Sci. Lett. 120, 283–300.

Negrini, R.N., Verosub, K.L., Davis, J.O., 1988. The middle to late Pleistocene geomagnetic field recorded in fine-grained sediments from Summer Lake, Oregon, and Double Hot Springs, Nevada, U.S.A. Earth Planet. Sci. Lett. 87, 173-192.

Negrini, R.N., Erbes, D., Faber, K., Herrera, A., Roberts, A., Cohen, A., Wigand, P., Foit, F., 2000. A paleoclimate record for the past 250,000 years from Summer Lake, Oregon, USA. 1. chronology and magnetic proxies for lake level. J. Paleolimnol. 24, 125–149.

Ohlendorf, C., Fey, M., Gebhardt, C., Haberzettl, T., Lücke, A., Mayr, C., Schäbitz, F., Wille, M., Zolitschka, B., 2013. Mechanisms of lake-level change at Laguna Potrok Aike (Argentina) – insights from hydrological balance calculations. Quat. Sci. Rev. 71, 27–45.

Orgeira, M.J., Compagnucci, R.H., 2006. Correlation between paleosol-soil magnetic signal and climate. Earth Planets Space 58, 1373–1380.

Orgeira, M.J., Walther, A.M., Vásquez, C.A., Tommaso, I.D., Alonso, S., Sherwood, G., Yuguan, H., Vilas, J.F.A., 1998. Mineral magnetic record of paleoclimate variation in loess and paleosol from the Buenos Aires formation (Buenos Aires, Argentina). J. South Am. Earth Sci. 11, 561–570.

Özdemir, Ö., and S.K. Banerjee, 1982. A preliminary magnetic study of soil samples from West-Central Minnesota. Earth Planet. Sci. Lett., 59, 393-403.

Parés, J.M., Hassold, N.J.C., Rea, D.K., van der Pluijm, B.A., 2007. Paleocurrent directions from paleomagnetic reorientation of magnetic fabrics in deep-sea sediments at the Antarctic Peninsula Pacific margin (ODP Sites 1095, 1101). Mar. Geol. 242, 261–269.

Paterson, G.A., Wang, Y., Pan, Y., 2013. The fidelity of paleomagnetic records carried by magnetosome chains. Earth Planet. Sci. Lett. 383, 82–91.

Peck, J.A., King, J.W., Colman, S.M., Kravchinsky, V.A., 1996. An 84-kyr paleomagnetic record from the sediments of Lake Baikal Siberia. J. Geophys. Res. 101 (B5), 11365-11385.

Peck, J.A., Green, R.R., Shanahan, T., King, J.W., Overpeck, J.T., Scholz, C.A., 2004. A magnetic mineral record of Late Quaternary tropical climate variability from Lake Bosumtwi, Ghana. Palaeogeogr. Palaeoclim. Palaeoecol. 215, 37–57.

Pirjola, R., Viljanen, A., Pulkkinen, A., Amm, O., 2000. Space weather risk in power systems and pipelines. Phys. Chem. Earth Part C Sol. Terr. Planet. Sci. 25, 333–337.

Recasens, C., Ariztegui, D., Gebhardt, C., Gogorza, C., Haberzettl, T., Hahn, A., Kliem, P., Lisé-Pronovost, A., Lücke, A., Maidana, N., Mayr, C., Ohlendorf, C., Schäbitz, F., St-Onge, G., Wille, M., Zolitschka, B. **2012**. New insights into paleoenvironmental changes in Laguna Potrok Aike, southern Patagonia, since the Late Pleistocene: The PASADO multiproxy record, *Holocene* 22 (11), 1323-1335.

Roberts, A.P., 2008. Geomagnetic excursions: Knowns and unknowns. Geophys. Res. Lett. 35.

Rochette, P., Mathé, P.-E., Esteban, L., Rakoto, H., Bouchez, J.-L., Liu, Q., Torrent, J., 2005. Non-saturation of the defect moment of goethite and fine-grained hematite up to 57 Teslas. Geophys. Res. Lett. 32.

Ross, P.-S., Delpit, S., Haller, M.J., Németh, K., Corbella, H., 2011. Influence of the substrate on maar–diatreme volcanoes — An example of a mixed setting from the Pali Aike volcanic field, Argentina. J. Volcanol. Geotherm. Res. 201, 253–271.

Sager, W.W., Acton, G.D., Clement, B.M., Fuller, M., 2006. Paleomagnetism in the ocean drilling program. Phys. Earth Planet. Inter. 156, 159–161.

Sagnotti, L., Macri, P., Camerlenghi, A., Rebesco, M., 2001.Environmental magnetism of Antarctic Late Pleistocene sediments and interhemispheric correlation of climatic events, Earth Planet. Sci. Let. 192, 65-80.

Schäbitz, F., Wille, M., Francois, J.-P., Haberzettl, T., Quintana, F., Mayr, C., Lücke, A., Ohlendorf, C., Mancini, V., Paez, M.M., Prieto, A.R., Zolitschka, B., 2013. Reconstruction of palaeoprecipitation based on pollen transfer functions – the record of the last 16 ka from Laguna Potrok Aike, southern Patagonia. Quat. Sci. Rev. 71, 175–190.

Singer, B.S., sous presse. A Quaternary Geomagnetic Instability Time Scale. Quat. Geochronol.

Snowball, I., Zillén, L., Sandgren, P., 2002. Bacterial magnetite in Swedish varved lake-sediments: a potential bio-marker of environmental change, Quat. Int. 88, 13-19.

Stoner, J.S., Jennings, A., Kristjánsdóttir, G.B., Dunhill, G., Andrews, J.T., Hardardóttir, J., 2007. A paleomagnetic approach toward refining Holocene radiocarbon-based chronologies: Paleoceanographic records from the north Iceland (MD99-2269) and east Greenland (MD99-2322) margins. Paleoceanography 22, PA1209.

Stoner, J.S., Channell, J.E.T., Mazaud, A., Strano, S.E., Xuan, C., 2013. The influence of high-latitude flux lobes on the Holocene paleomagnetic record of IODP Site U1305 and the northern North Atlantic: Paleomagnetic Record of the N. Atlantic. Geochem. Geophys. Geosystems 14.

St-Onge, G., Chapron, E., Mulsow, S., Salas, M., Viel, M., Debret, M., Foucher, A., Mulder, T., Winiarski, T., Desmet, M., Costa, P.J.M., Ghaleb, B., Jaouen, A., Locat, J., 2012. Comparison of earthquake-triggered turbidites from the Saguenay (Eastern Canada) and Reloncavi (Chilean margin) Fjords: Implications for paleoseismicity and sedimentology. Sediment. Geol. 243-244, 89–107.

St-Onge, G., and J.S. Stoner. 2011. Paleomagnetism near the North Magnetic Pole: A unique vantage point for understanding the dynamics of the geomagnetic field and its secular variations. Oceanography 24(3):42–50.

St-Onge, G., Mulder, T., Piper, D.J.W., Hillaire-Marcel, C., Stoner, J.S., 2004. Earthquake and flood-induced turbidites in the Saguenay Fjord (Québec): a Holocene paleoseismicity record. Quat. Sci. Rev. 23, 283–294.

Sugden, D.E., McCulloch, R.D., Bory, A.J.-M., Hein, A.S., 2009. Influence of Patagonian glaciers on Antarctic dust deposition during the last glacial period. Nat. Geosci. 2, 281–285.

Teanby, N., Laj, C., Gubbins, D., Pringle, M., 2002. A detailed palaeointensity and inclination record from drill core SOH1 on Hawaii. Phys. Earth Planet. Inter. 131, 101–140.

Thompson, R. and Maher, B.A., 1995. Age models, sediment fluxes and palaeoclimatic reconstructions for the Chinese loess and paleosol sequences, Geophys. J. Int. 123, 611-622.

Thouveny, N., Moreno, E., Delanghe, D., Candon, L., Lancelot, Y., Shackleton, N.J., 2000. Rock magnetic detection of distal ice-rafted debries: clue for the identification of Heinrich layers on the Portuguese margin. Earth Planet. Sci. Lett. 180, 61–75.

Venuti, A., Florindo, F., Caburlotto, A., Hounslow, M.W., Hillenbrand, C.-D., Strada, E., Talarico, F.M., Cavallo, A., 2011. Late Quaternary sediments from deep-sea sediment drifts on the Antarctic Peninsula Pacific margin: Climatic control on provenance of minerals. J. Geophys. Res. 116.

Verosub, K. L. and A. P. Roberts, 1995. Environmental magnetism: Past, present, and future, J. Geophys. Res. 100 (B2), 2175–2192.

Vlag, P.A., Oches, E.A., Banerjee, S.K., Solheid, P.A., 1999. The paleoenvironmental-magnetic record of the Gold Hill Steps loess section in central Alaska, Phys. Chem. Earth (A) 24 (9), 779-783.

Williamson, D., Jelinowska, A., Kissel, C., Tucholka, P., Gibert, E., Gasse, F., Massault, M., Taieb, M., Van Campo, E., Wieckowski, K., 1998. Mineral-magnetic proxies of erosion/oxidation cycles in tropical maar-lake sediments (Lake Tritrivakely, Madagascar): paleoenvironmental implications, Earth Planet. Sci. Lett. 155, 205-219.

Yamazaki, T., 2008. Magnetostatic interactions in deep-sea sediments inferred from first-order reversal curve diagrams: Implications for relative paleointensity normalization: MAGNETOSTATIC INTERACTIONS IN DEEP-SEA SEDIMENTS. Geochem. Geophys. Geosystems 9, Q02005.

Yang, X., Heller, F., Yang, J., Su, Z., 2009. Paleosecular variations since ~9000 yr BP as recorded by sediments from maar lake Shuangchiling, Hainan, South China. Earth Planet. Sci. Lett. 288, 1–9.

Yang, S., Odah, H., Shaw, J., 2000. Variations in the geomagnetic dipole moment over the last 12000 years. Geophys. J. Int. 140, 158-162.

Zolitschka, B., Anselmetti, F., Ariztegui, D., Corbella, H., Francus, P., Ohlendorf, C., Schäbitz, the P.S.D.T., 2009. The Laguna Potrok Aike Scinetific Drilling Project PASADO (ICDP Expedition 5022). Sci. Drill.

Zolitschka, B., Schäbitz, F., Lücke, A., Corbella, H., Ercolano, B., Fey, M., Haberzettl, T., Janssen, S., Maidana, N., Mayr, C., Ohlendorf, C., Oliva, G., Paez, M.M., Schleser, G.H., Soto, J., Tiberi, P., Wille, M., 2006. Crater lakes of the Pali Aike Volcanic Field as key sites for paleoclimatic and paleoecological reconstructions in southern Patagonia, Argentina. J. South Am. Earth Sci. 21, 294–309.

CHAPITRE 1
ENREGISTREMENT PALÉOMAGNÉTIQUE À HAUTE RÉSOLUTION DES DIRECTIONS ET DE LA PALÉOINTENSITÉ RELATIVE DEPUIS LE PLÉISTOCENE SUPÉRIEUR DANS LE SUD DE L'AMÉRIQUE DU SUD

RÉSUMÉ

Les directions paléomagnétiques (inclinaison et déclinaison) et la paléointensité relative ont été reconstituées à partir des sédiments du lac *Laguna Potrok Aike* dans le cadre du *International Continental scientific Drilling Program* (ICDP) *Potrok Aike maar lake Sediment Archive Drilling prOject* (PASADO). Le vecteur magnétique complet est reconstitué à haute résolution depuis 51200 cal BP à partir d'échantillons u-channels. La paléointensité relative (RPI) est obtenue en normalisant l'aimantation naturelle rémanente avec l'aimantation anhystérétique rémanente. Le ratio moyen sur 4 étapes de démagnétisation ($NRM/ARM_{10\text{-}40\ mT}$) faisant partie de la magnétisation rémanente caractéristique est utilisé. Une influence de la taille des grains magnétiques sur la RPI a été soustraite en appliquant une correction basée sur la relation linéaire entre la RPI et le champ destructeur médian de l'aimantation naturelle rémanente (MDF_{NRM}). Le nouvel enregistrement paléomagnétique est comparé avec d'autres enregistrements lacustres et marins ainsi qu'avec des courbes de références des moyennes à hautes latitudes de l'hémisphère Sud et révèle une variabilité millénaire similaire. L'excursion géomagnétique Laschamp et possiblement Mono Lake sont documentées, en plus d'un large et brusque changement de direction possiblement associé à l'excursion Hilina Pali à 20000 cal BP. Finalement, une comparaison à l'échelle du globe avec d'autres enregistrements à haute résolution situés de l'autre côté de la Terre ainsi qu'avec des courbes de références du

champ dipolaire indiquent une variabilité différente du champ dans le sud de l'Amérique du Sud il y a 46000 cal BP.

HIGH-RESOLUTION PALEOMAGNETIC SECULAR VARIATIONS AND RELATIVE PALEOINTENSITY SINCE THE LATE PLEISTOCENE IN SOUTHERN SOUTH AMERICA

Agathe Lisé-Pronovost[1,2], Guillaume St-Onge[1,2], Claudia Gogorza[3], Torsten Haberzettl[4], Michel Preda[5], Pierre Kliem[6], Pierre Francus[7,2], Bernd Zolitschka[6] and the PASADO science team[8]

[1] Canada Research Chair in Marine Geology, Institut des sciences de la mer de Rimouski (ISMER), Université du Québec à Rimouski (UQAR), Rimouski, Canada

[2] GEOTOP research center, Canada

[3] Instituto de Física Arroyo Seco, Universidad Nacional del Centro de la Provincia de Buenos Aires, Tandil, Argentina

[4] Institute of Geography, Friedrich-Schiller-University Jena, Jena, Germany

[5] Département des sciences de la Terre et de l'atmosphère, Université du Québec à Montréal (UQAM), Montréal, Canada

[6] Geomorphology and Polar Research (GEOPOLAR), Institute of Geography, University of Bremen, Bremen, Germany

[7] Institut national de la recherche scientifique, centre Eau, Terre, Environnement (INRS-ÉTÉ), Québec, Canada

[8] http://www.icdp-online.org/front_content.php?idcat=1494

Abstract

Paleomagnetic inclination, declination and relative paleointensity were reconstructed from the sediments of Laguna Potrok Aike in the framework of the International Continental scientific Drilling Program (ICDP) Potrok Aike maar lake Sediment Archive Drilling prOject (PASADO). Here we present the u-channel-based full vector paleomagnetic field reconstruction since 51.2 ka cal BP. The relative paleointensity proxy (RPI) was built by normalising the natural remanent magnetisation with the anhysteretic remanent magnetisation using the average ratio at 4 demagnetisation steps part of the ChRM interval ($NRM/ARM_{10\text{-}40\ mT}$). A grain size influence on the RPI was removed using a correction based on the linear relationship between the RPI and the median destructive field of the natural remanent magnetisation (MDF_{NRM}). The new record is compared with other lacustrine and marine records and stacks from the mid- to high-latitudes of the Southern Hemisphere, revealing consistent millennial-scale variability, the identification of the Laschamp and possibly the Mono Lake geomagnetic excursions, and a direction swing possibly associated to the Hilina Pali excursion at 20 ka cal BP. Nonetheless, a global-scale comparison with other high-resolution records located on the opposite side of the Earth and with various dipole field references hint at a different behaviour of the geomagnetic field around southern South America at 46 ka cal BP.

Keywords

ICDP-project PASADO, Laguna Potrok Aike, paleomagnetism, relative paleointensity, secular variation, Southern Hemisphere

1. Introduction

Geological archives such as marine and lacustrine sediments are the only way to reconstruct the past millennial- to centennial-scale variability of the geomagnetic field beyond historical time; however the uneven distribution of the records on Earth does not allow addressing the possible global nature of its variability. The reason for this geographical bias is that high-resolution paleomagnetic records from the Southern Hemisphere are rare. As a consequence, global stacks are truly derived from a majority of records located in the Northern Hemisphere (e.g., GLOPIS-75, Laj et al., 2004; SINT-200, Guyodo and Valet, 1996) and geomagnetic field models lack calibration data from the Southern Hemisphere in order to better understand the core geodynamics (e.g., Korte et al., 2005; Roberts, 2008; Korte and Constable, 2011). A major limit to the collection of high-resolution records from the Southern Hemisphere is the scarcity of adequately high sedimentation rate basins and their accessibility. In particular, the mid-latitudes of the Southern Hemisphere are dominated by the open ocean realm with its typically low accumulation rates (e.g., Lund et al., 2006a) and south of 48°S, the South American continent is the only land mass beside islands in the Southern Ocean and the ice-covered Antarctica.

Despite technical and logistical difficulties and in order to better understand the geomagnetic field variability, a series of paleomagnetic records from the mid- to high-latitudes of the Southern Hemisphere (from 30°S to Antarctica) emerged in the last decade. The available high-resolution paleomagnetic records are often limited to the Holocene and deglacial period and include sediment drifts near Antarctica (Brachfeld et al., 2000; Willmott et al., 2006) and lacustrine sediments from Argentina (e.g., Gogorza et al., 2002; 2004; 2006; Irurzun et al., 2006). In addition, a very high resolution record from offshore Chile covers the last 70 ka cal BP (Kaiser et al., 2005; Lund et al., 2006b). Other records from the Southern Hemisphere extending back to the last glacial period are however at lower temporal resolutions (e.g., Atlantic sector of the Southern Ocean, Stoner et al., 2002; 2003; Indian sector of the southern Ocean, Mazaud et al., 2002; near Antarctica: Macri et

al., 2005; 2010; Scotia Sea, Collins et al., 2012; Lake Pupuke in New Zealand, Nillson et al., 2011).

In southern Argentina, the absence of a continental glacier over the Pali Aike Volcanic Field during the last glaciation (Coronato et al., this issue; Zolitschka et al., 2006) suggests a continuous accumulation of sediment in the maar lake Laguna Potrok Aike, and previous studies indicate high sedimentation rates of ca. 100 cm/ka since 16 ka cal BP (Haberzettl et al., 2007). Therefore Laguna Potrok Aike is a key site for high-resolution paleomagnetic reconstruction in the mid-latitudes of the Southern Hemisphere. Previous paleomagnetic studies from the sediments of Laguna Potrok Aike include a series of short cores covering the last 0.7 ka cal BP (Gogorza et al., 2011) and the full vector paleomagnetic record for the last 16 ka cal BP was reconstructed as part of the South Argentinean Lake Sediment Archives and modelling (SALSA) project (Gogorza et al., 2012). A low resolution rock-magnetic study from that lake recently revealed that no major change in the magnetic mineral assemblage occurred since the last glacial period (Recasens et al., in press). Here we present a high-resolution rock-magnetic study of the lacustrine sediments and a continuous full-vector paleomagnetic record since 51.2 ka cal BP from a continental archive in the mid-latitudes of the Southern Hemisphere in order to document the variability of the geomagnetic field in an area of the world where observations are scarce.

2. Geological setting

Laguna Potrok Aike (51°58'S, 70°22'W) is a maar lake within the Pali Aike Volcanic Field in the province of Santa Cruz in southern Argentina. The Pali Aike volcanic field is a series of phreatomagmatic craters formed by back-arc volcanism since the Pliocene to the Pleistocene (Corbella, 2002; Zolitschka et al., 2006; Coronato et al., this issue). Laguna Potrok Aike is today a perennial lake in the Patagonian steppe, with a maximum water depth of 100 m and a maximum diameter of 3.5 km. The lake is fed by groundwater with no inflow or outflow at present (Mayr et al., 2007); however, gullies (visible in Fig. 1) indicate episodic inflow most likely related to snowmelt events. In addition, lake level

terraces above and below the present lake level document the sensitivity of the lake system to hydrological changes (Haberzettl et al., 2008; Anselmetti et al., 2009; Gebhardt et al., 2012). Laguna Potrok Aike is influenced by the strong Southern Hemisphere westerly winds (SHW) and as a result the water column is not stratified or well-oxygenated from top to bottom (Zolitschka et al., 2006). The lake is located at ca. 100 km from the Atlantic coast and ca. 200 km on the lee-side of the Andes, where the annual precipitation is less than 300 mm/yr (Zolitschka et al., 2006). These geomorphological and geographical settings suggest that the terrigenous sediment enters the lake by eolian input and periodic runoff. The sources of the detrital sediment deposited in Laguna Potrok Aike are 1) the Andean Cordillera and the derived fluvioglacial sediments, tills and moraines deposited in the catchment area before the Late Pleistocene, and 2) the basaltic lavas and volcanic structures such as maars, tuff-rings, scoria and spatter cones in the Pali Aike Volcanic Field (D'Orazio et al., 2000; Zolitschka et al., 2006; Ross et al., 2011; Coronato et al., this issue).

Figure 1 1. A) Aerial photograph and bathymetry of the maar lake Laguna Potrok Aike in the Patagonian steppe of southern Argentina. The position of the PASADO-ICDP sites 1 and 2, the holes at site 2 and the SALSA records discussed in the text are indicated. B) Location of the paleomagnetic records discussed in the text. From west to east, LFH: Lava flow stack from Hawaii (Teanby et al., 2002), ODP-1233: Ocean Drilling Program core 1233 offshore Chile (Lund et al., 2006b), LEs & LEt: Lake Escondido and Lake El Trébol (Gogorza et al., 2002; 2004; 2006; Irurzun et al., 2006), LPA: Laguna Potrok Aike (Gogorza et al., submitted; this work), WBB: Western Bansfeld Basin (Willmott et al., 2006), PD: Palmer Deep (Brachfeld et al., 2000), SS: Scotia Sea stack (Collins et al., 2012), ODP-1089 & SAPIS: Ocean Drilling Program core 1089 (Stoner et al., 2003) and stack of the sub-Antarctic South Atlantic Ocean (Stoner et al., 2002), WEGA: Wilkes Land Basin stack (Macri et al., 2005), LBa: Lake Baikal (Peck et al., 1996), LBi: Lake Biwa (Hayasaki et al., 2007), LPu: Lake Pupuke (Nilsson et al., 2011).

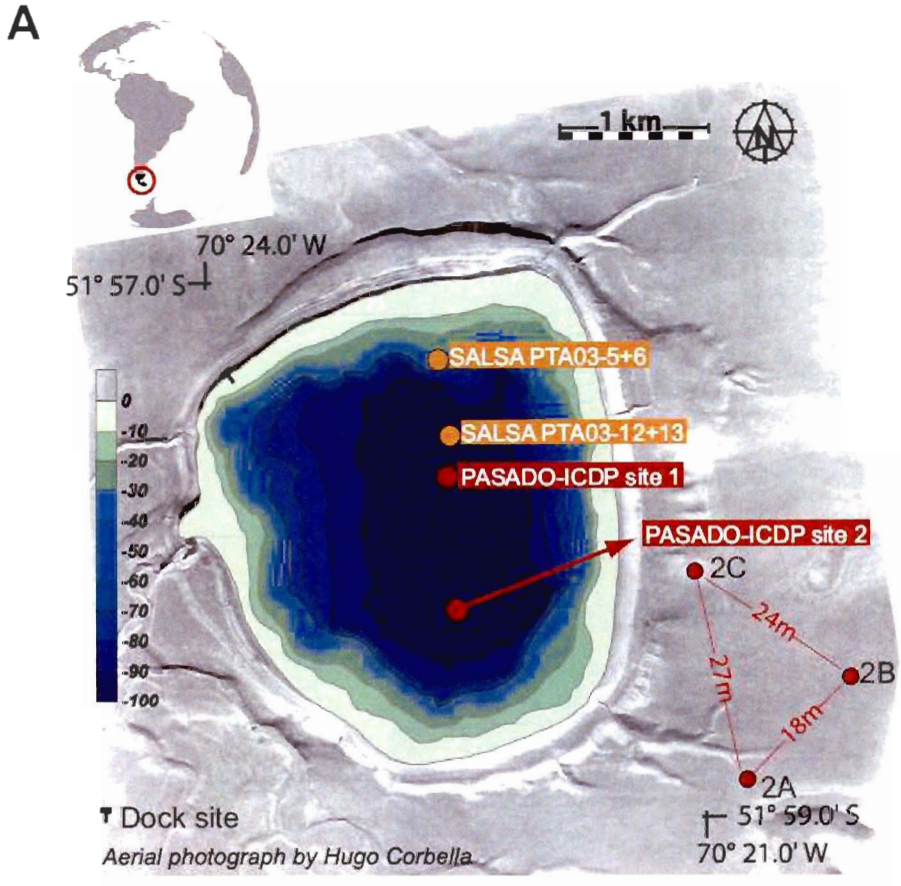
A
1 km
N
70° 24.0' W
51° 57.0' S
SALSA PTA03-5+6
SALSA PTA03-12+13
PASADO-ICDP site 1
PASADO-ICDP site 2
2C
24m
27m
18m
2B
2A
0
-10
-20
-30
-40
-50
-60
-70
-80
-90
-100
Dock site
51° 59.0' S
70° 21.0' W
Aerial photograph by Hugo Corbella

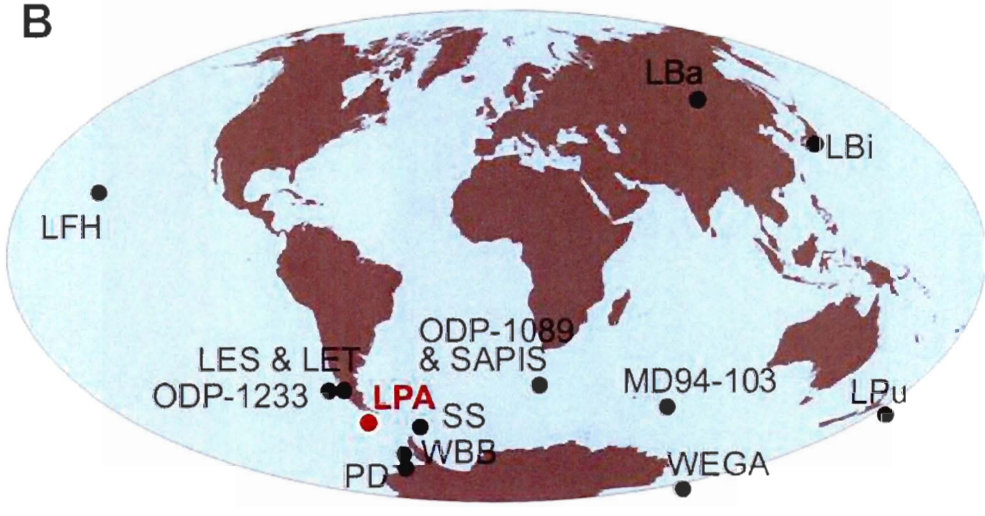
B
LBa
LBi
LFH
ODP-1089
& SAPIS
LES & LET
ODP-1233
LPA
SS
WBB
PD
MD94-103
LPu
WEGA

3. Methods

3.1 Coring and sampling

The PASADO-ICDP scientific drilling operations at Laguna Potrok Aike were completed during the austral spring 2008 (September to November). The PASADO science team recovered 533 m of azimuthally unoriented sediment cores from 2 sites using a piston coring system supported by a barge (GLAD800) and operated by the Consortium for Drilling, Observation and Sampling of the Earth's Continental Crust (DOSECC) (Zolitschka et al., 2009). Site 2 was selected for high-resolution multi-proxy analyses because of its higher recovery rate (98.8%) and its apparent lower proportion of sands compared to site 1. The composite profile of site 2 (2CP; 106.09 m composite depth (cd)) was constructed by correlating the lithology of parallel cores from three holes (Fig. 1) (Kliem et al., this issue). The 2CP was continuously sampled with u-channels (2x2 cm section plastic liner) following the method of Stoner and St-Onge (2007) at the University of Bremen in June 2009. A total of 98 u-channels (maximum length of 1.5 m) were sampled, with the exception of section 85 which contained gravel (2A-30H-2; from 8813 to 8896 cm cd). Here we present the results of the pelagic sediments, which represent 43% (45.8 m) of the 2CP. The remaining 57% (60.29 m) was identified as reworked material from mass movement deposits (Kliem et al., this issue; see section 3.5 Lithology below). Finally, the core catcher samples from hole A at site 2 (position on Fig. 1) as well as discrete samples (ca. 2-3 g) collected at ca 40 cm-interval along the 2CP were used for rock-magnetic investigation.

3.2 Continuous magnetic measurements

The magnetic measurements of the 2CP u-channel samples were performed at 1 cm-interval at the *Institut des sciences de la mer de Rimouski* (ISMER). The low-field volumetric magnetic susceptibility (k_{LF}) was measured using a point sensor mounted on a multi sensor core logger (MSCL) and the natural remanent magnetisation (NRM) was measured using a 2G cryogenic magnetometer for u-channels. Because of the edge effect

associated with the response function of the cryogenic magnetometer pick-up coils (Weeks et al., 1993), 4-cm of data were not used on both sides of intersections and stratigraphic gaps. Likewise, unreliable points linked to incompletely filled u-channels, disturbed sediment and outlier values were not considered for the paleomagnetic reconstruction. A minimum of 13 demagnetisation steps (0, 5, 10, 15, 20, 25, 30, 35, 40, 45, 50, 60, 70 mT) were used to progressively demagnetise the initial NRM to less than 20%. The paleomagnetic inclination and declination as well as the associated maximum angular deviation (MAD) values were calculated from the characteristic remanent magnetisation (ChRM) interval using principal component analysis (Kirschvink, 1980) in the Excel spreadsheet developed by Mazaud (2005). The cores were not azimuthally oriented and hence the declination values were "un-rotated" to obtain a continuous record and each section was centered to zero. An anhysteretic remanent magnetisation (ARM) was imparted with a peak alternating field (AF) of 100 mT and a direct current (DC) biasing field of 0.05 mT, then demagnetised and measured in a minimum of 8 steps (0, 10, 20, 30, 40, 50, 60, 70 mT). Afterward two isothermal remanent magnetisations (IRM_{300mT} and IRM_{950mT}) were induced using a 2G pulse magnetometer and step-wise demagnetised using the same method as for the ARM. The $IRM_{950\ mT}$ is used as the saturation isothermal remanent magnetisation (SIRM). The susceptibility of the ARM (kARM) is calculated by dividing the ARM with the biasing DC field applied and is commonly used to establish a magnetic grain size indicator such as kARM/SIRM (e.g., Stoner and St-Onge, 2007) or kARM/k (e.g., Banerjee et al., 1981; King et al., 1982). The median destructive field (MDF) of the remanent magnetisations (e.g., MDF_{NRM}, MDF_{ARM} and MDF_{IRM}) were calculated in order to determine the required applied field to remove half of the initial remanence. It is a measure of the coercivity of the remanence carriers and hence depends on the magnetic mineralogy and grain size. When the magnetic mineralogy is uniform, the MDF informs on the magnetic grain size of the magnetic recording assemblage.

3.3 Discrete magnetic measurements

A total of 103 discrete pelagic sediment samples were measured using a Princeton Measurement Corporation alternating gradient force magnetometer (model MicroMag 2900 AGM) in order to obtain the hysteresis curves and derived properties, including the bulk coercive force (Hc), the remanent coercive force (Hcr), the saturation magnetisation (Ms) and the saturation remanence (Mr). The isothermal remanent magnetisation (IRM) acquisition curve was also acquired for 43 samples using the same instrument. The coercivity (Hcr/Hc) and the remanence (Mr/Ms) ratios are commonly used as magnetic grain size indicators (Day et al., 1977; Dunlop, 2002) and the hysteresis properties, together with the IRM acquisition curve, inform on the coercivity of the remanence carriers (Dunlop and Özdemir, 1997; 2007). In order to further investigate the magnetic mineralogy, the temperature-dependence of magnetic susceptibility (k_T) was measured for all core catcher samples of hole A site 2 using a Bartington MS2 κ/T system with the ceramic crucible filled at full capacity (ca. 3 g). Recasens et al. (in press) showed that 4 core catcher samples from hole A site 2 are dominated by reworked tephra (samples 21, 22 and 27CC) or organic-rich (sample 6CC) material and were readily identifiable by rock-magnetic properties. The present study focuses on the pelagic sedimentation and therefore the remaining core catcher samples from hole A site 2 were considered. Mineralogical analysis of typical core catcher samples (samples 10, 12 and 28CC) was conducted using a Siemens D5000 X-Ray diffractometer at the X-ray diffraction laboratory of UQAM. The bulk sediment was sieved to isolate the grain size fractions < 38 μm and between 38 and 106 μm. For each size fraction a magnetic extract was obtained using a rare earth neodymium hand magnet. This method is rapid, but less efficient in collecting the smaller magnetic grains and it is therefore not quantitative (Hounslow and Maher, 1999). The semi-quantitative mineralogical identification was conducted by diffraction peak analysis (based on Bragg's law) using the International Center for Diffraction Data (ICDD) database as a reference.

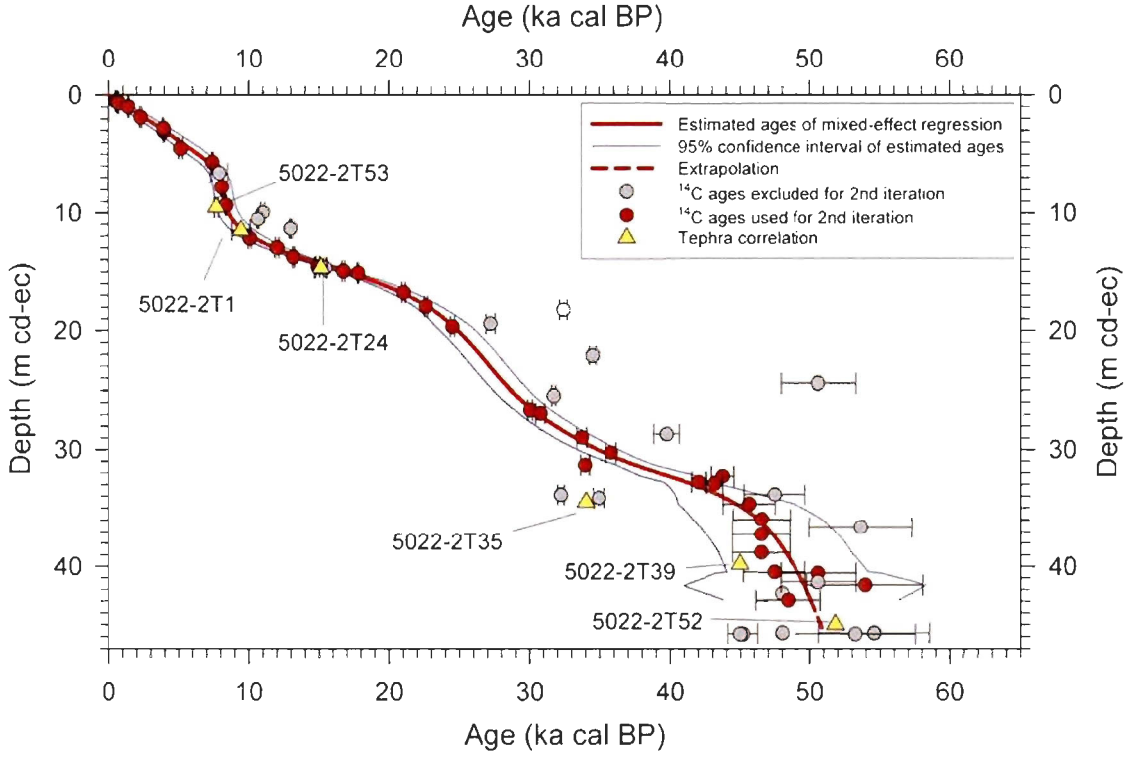

Figure 1 2. Radiocarbon-based age model for the PASADO-ICDP site 2 sedimentary record (modified from Kliem et al., this issue). The composite depth event-corrected (cd-ec) corresponds to the depth after removal of mass movement deposits and it represents the pelagic sediment sequence. The red line is the estimated age after two iteration of the mixed-effect regression using the constant-variance function (for more details, see Kliem et al., this issue).

Table 1 1. AMS radiocarbon ages for the PASADO-ICDP site 2 sedimentary record from Laguna Potrok Aike (modified from Kliem et al., this issue). The ages are calibrated with CalPal applying the CalPal_2007_HULU calibration curve. Ages from reworked sediment sections are printed in bold.

Laboratory no.	Sample description	Sediment depth (m cd)	Event corrected sediment depth (m cd–eg)	^{14}C Age (BP)	Error (1σ)	Calibrated age (cal BP)	Error (1σ)
Poz-834[a]	Stems of aquatic moss	0.51	0.51	440	30	510	30
Poz-897[a]	Bulk sediment	0.56	0.55	655	25	630	50
Poz-3570[a]	Calcite fraction of bulk sample	0.67	0.67	735	35	690	20
Poz-896[a]	Stems of aquatic moss	0.92–1.04	0.92–1.04	1470	40	1370	40
Poz-5182[b]	Twig of Berberis	1.96	1.95	2300	30	2290	70
Poz-8549[b]	Calcite fraction of bulk sample	2.88	2.87	3600	35	3910	50
Poz-8390[b]	Stems of aquatic moss	3.10–3.15	3.10–3.15	3625	35	3940	50
Poz-8398[b]	Stems of aquatic moss	4.83	4.53	4465	50	5130	120
Poz-8550[b]	Calcite fraction of bulk sample	6.09	5.71	6440	70	7360	80
Poz-8391[b]	**Stems of aquatic moss**	6.91	6.63	7025	50	7870	60
Poz-8548[b]	Calcite fraction of bulk sample	8.12	7.83	7200	50	8090	60
Poz-8392[b]	Stems of aquatic moss	9.69	9.37	7980	50	8790	40
Poz-8393[b]	**Stems of aquatic moss**	10.44	9.97	9640	60	11000	140
Poz-8547[b]	**Calcite fraction of bulk sample**	11.00–11.08	10.53–10.61	9410	50	10640	60
Poz-8394[b]	**Stems of aquatic moss**	12.00	11.37	11090	60	12980	80
Poz-5985[b]	Bone of Tuco Tuco	13.04	12.22	8930	90	10060	110
Poz-8548[b]	Calcite fraction of bulk sample	14.78	13.90	10240	60	11970	130
Poz-8396[b]	Stems of aquatic moss	15.53	13.78	11200	60	13130	80
Poz-8397[b]	Stems of aquatic moss	16.40	14.61	12490	70	14960	140
Poz-5072[b]	**Stems of aquatic moss**	16.78–18.20	14.70	12850	70	15420	90
Poz-5073[b]	Stems of aquatic moss	18.48–18.54	14.93–14.99	13450	70	16710	100
Poz-37017[c]	Stems of aquatic moss	18.69	15.13	14640	70	17760	90
Poz-37022[c]	Stems of aquatic moss	22.09	16.74	17460	80	20970	120
Poz-37007[c]	Stems of aquatic moss	23.25	17.90	18700	120	22570	170
Poz-32491[c]	**Stems of aquatic moss**	23.90	18.23	27910	240	32420	280
Poz-34233[c]	**Stems of aquatic moss**	26.85	19.42	22450	140	27230	320
Poz-37020[c]	Stems of aquatic moss	27.20	19.69	20490	120	24540	190
Poz-37008[c]	**Stems of aquatic moss**	31.01	22.14	30300	300	34500	240
Poz-37010[c]	**Organic macro remains**	33.45	24.46	47000	2000	50590	2670
Poz-34235[c]	**Stems of aquatic moss**	35.10	25.49	26930	210	31720	140
Poz-34236[c]	Stems of aquatic moss	36.38	26.67	25110	180	30030	150
Poz-34237[c]	Stems of aquatic moss	36.66	26.95	25820	190	30950	320
Poz-32492[c]	**Stems of aquatic moss**	39.77	28.69	34500	500	39770	910
Poz-37011[c]	Stems of aquatic moss	40.09	28.98	29300	300	33700	350
Poz-37012[c]	Organic macro remains	45.81	30.30	31900	300	35780	380
Poz-37002[c]	Stems of aquatic moss	47.34	31.34	29600	300	33930	360
Poz-37013[c]	Stems of aquatic moss	48.58	32.32	40000	1000	43730	810
Poz-34238[c]	Stems of aquatic moss	52.98	32.82	37300	800	42040	500
Poz-37003[c]	Stems of aquatic moss	53.12	32.96	39200	700	43140	570
Poz-32493[c]	**Stems of aquatic moss**	54.23	33.88	27650	230	32230	230
Poz-37014[c]	**Stems of aquatic moss**	54.23	33.88	44000	2000	47450	2260
Poz-37075[c]	Stems of aquatic moss	55.59	34.15	39000	400	34920	380
Poz-34239[c]	Stems of aquatic moss	56.66	34.71	42000	2000	45610	1870
Poz-34240[c]	Stems of aquatic moss	58.94	36.60	43000	2000	46540	2040
Poz-34241[c]	Stems of aquatic moss	63.18	36.70	50000	3000	53610	3600
Poz-37018[c]	Organic macro remains	65.11	37.33	43000	2000	46510	2040
Poz-32494[c]	Stems of aquatic moss	67.13	38.87	43000	2000	46510	1040
Poz-34242[c]	Stems of aquatic moss	72.80	40.56	44000	2000	47450	1200
Poz-37004[c]	Stems of aquatic moss	73.32	40.66	47000	2000	50590	2670
Poz-34243[c]	**Stems of aquatic moss**	75.18	41.40	47000	2000	50590	2670
Poz-37006[c]	Stems of aquatic moss	75.68	41.67	51000	4000	55910	4130
Poz-37021[c]	Organic macro remains	78.43	42.39	>48000			
Poz-32495[c]	Stems of aquatic moss	80.60	42.97	45000	2000	48430	2320
Poz-34245[c]	Stems of aquatic moss	96.21	45.71	>48000			
Poz-37015[c]	Organic macro remains	96.21	45.71	52000	4000	54580	3940
Poz-37016[c]	Organic macro remains	98.95	45.79	42000	1000	45200	1040
Poz-34246[c]	**Stems of aquatic moss**	99.89	45.80	50000	4000	53220	4250
Poz-32496[c]	**Stems of aquatic moss**	102.96	45.80	>45000			

[a] Haberzettl et al. 2005.
[b] Haberzettl et al. 2007.
[c] Kliem et al., this issue.

3.4 Chronology

The chronology of the event-corrected PASADO 2CP pelagic sediment sequence (45.80 m cd-ev) is based on 36 radiocarbon dates and supported with 6 tephra layers (see Kliem et al., this issue for details; Table 1; Figure 2). It is also supported by lithological and tephra correlation with previously studied cores from Laguna Potrok Aike, including a core located nearby in the lake center and covering the last 16 ka cal BP (PTA03/12+13; location on Fig. 1; Haberzettl et al., 2007) and a low-resolution core from a lake level terrace covering a similar time span (PTA03/5+6; location on Fig. 1; Haberzettl et al., 2009).

3.5. Lithology

Kliem et al (this issue) described five lithological units for the sediment of Laguna Potrok Aike since 51.2 ka cal BP. The units are based on the type of pelagic sediment and the frequency of mass movement deposits (MMD) and include (A) pelagic laminated silts, (B) pelagic laminated silts intercalated with thin fine sand and coarse silt layers, (C-1, C-2 and C-3) alternation of A and B with an increase in the frequency and thickness of MMD from C-1 to C-3. The present work concerns exclusively the pelagic sediment from these different units (see the log on Figs. 4 and 7).

4. Results

4.1 Magnetic mineralogy

The isothermal remanent magnetisation (IRM) acquisition curves of the 43 pelagic sediment samples (Fig. 3A; position on Fig. 4) reach saturation below ca 200 mT, indicating a magnetic assemblage dominated by low coercivity minerals. The median destructive field of the natural remanent magnetisation (MDF_{NRM}; Fig. 4) and the coercive force (Hc; not shown) vary around average values of 16 mT and 7.2 mT, respectively. Along with the typical shape of the hysteresis loop (Fig. 3C) (Tauxe et al., 1996), these results are characteristic of magnetite. Furthermore, zero magnetic susceptibility is reached

during heating at or near the Curie temperature of magnetite (580°C; Dunlop and Özdemir, 1997; 2007) for the 22 core catcher samples of site 2 hole A (Fig. 3B). A drop in magnetic susceptibility slightly before 580°C suggests the presence of Ti-poor titanomagnetite (Dearing, 1999). However, the diffractogram of the magnetic extracts further identifies magnetite as the dominant magnetic mineral both in the grain size fraction 106-38 μm and < 38μm (Fig. 3C). Altogether these results support the previous magnetic mineral analyses for the last 16 ka cal BP (Gogorza et al., 2011; Gogorza et al., 2012) as well as the low-resolution analyses of the PASADO-ICDP core catcher samples (Recasens et al., in press) and reveal that magnetite is the dominant remanence carrier at Laguna Potrok Aike since 51.2 ka cal BP.

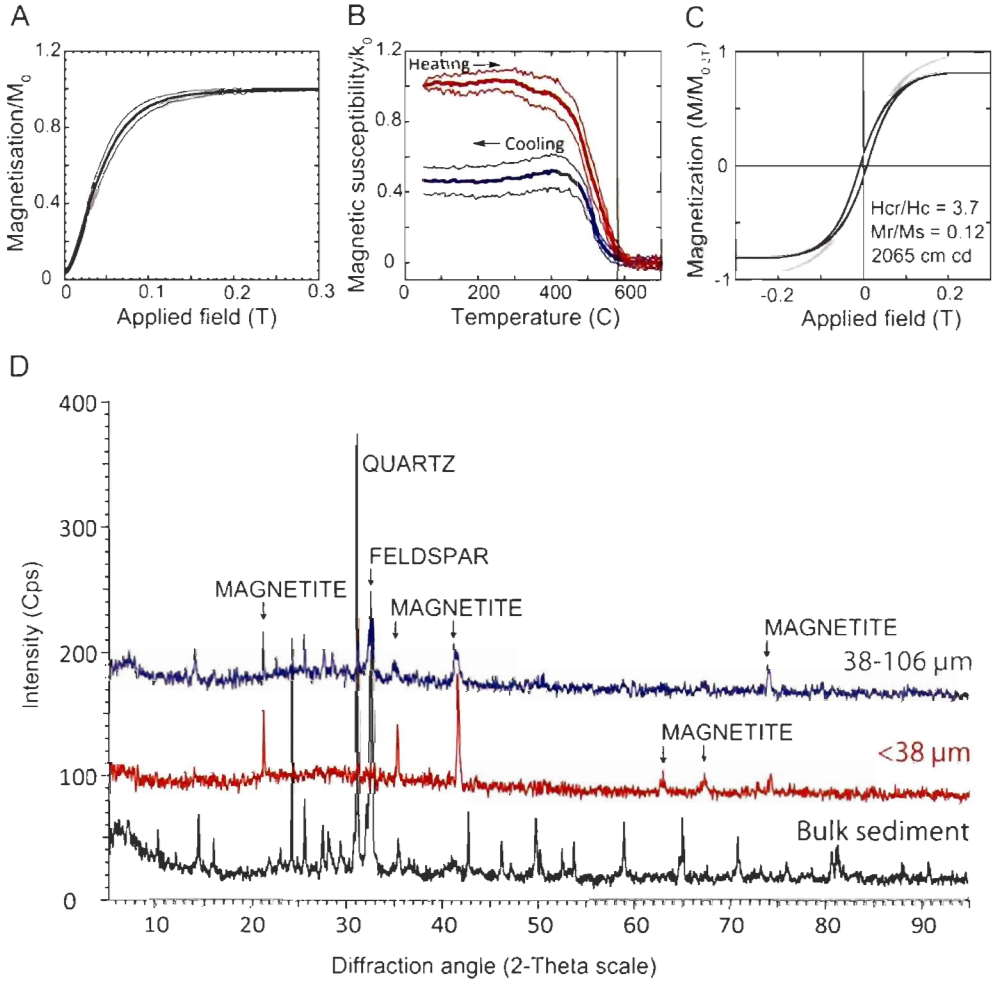

Figure 1 3. A) Average isothermal remanent magnetisation (IRM) acquisition curves of 43 pelagic samples from the composite profile at site 2. The IRM is normalized with the value in an applied field of 0.3 T. B) Average heating (red) and cooling (blue) curves of the magnetic susceptibility for 22 core catcher samples at site 2 hole A. The magnetic susceptibility is normalized with the initial value (at 50°C). The standard deviation (thin lines) are shown for A and B. C) Hysteresis curve for a typical sample. The raw (grey) and high-field slope corrected (black) magnetisation are illustrated. D) Typical X-ray diffraction spectrum for the bulk sediment and for magnetic extracts (sample 2A-12CC). The curves for the magnetic extracts (38-106 µm and < 38 µm) were shifted vertically for clarity. The rock-magnetic and mineralogical analyses indicate that magnetite dominates the magnetic mineral assemblage at Laguna Potrok Aike.

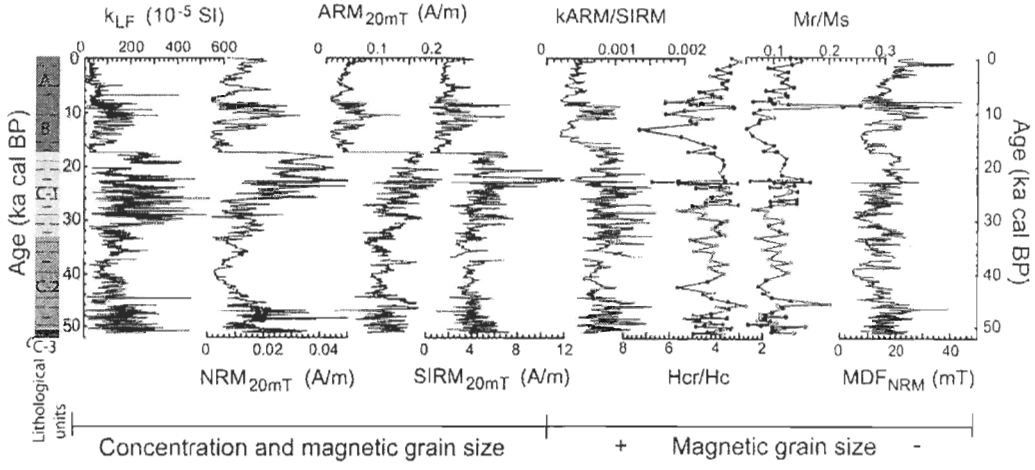

Figure 1. 4. Rock-magnetic properties of the pelagic sediments at Laguna Potrok Aike since 51.2 ka cal BP. A) The low field magnetic susceptibility (k_{LF}), the natural remanent magnetisation (NRM_{20mT}) and the anhysteretic and isothermal remanent magnetisations after 20 mT demagnetisation (ARM_{20mT}, IRM_{20mT}) are influenced by the concentration and the grain size of the magnetic minerals; kARM/SIRM, Hcr/Hc, Mr/Ms and MDF_{NRM} reflect grain size changes for a magnetic assemblage dominated by magnetite. Samples analyzed for IRM acquisition curves are indicated by a grey symbol. The lithological units from Kliem et al. (this issue) are located on the left hand side. The log represents the pelagic sediments only, after removal of the mass movement deposits._**Unit A**: Pelagic laminated silts prevail; almost no mass movement deposits. **Unit B**: Dominance of pelagic laminated silts intercalated with thin fine sand and coarse silt layers; normal graded units and ball and pillow structures occur; high content of plant macro remains and gastropods. **Unit C-1**: Dominance of pelagic laminated silts intercalated with thin fine sand and coarse silt layers; normal graded units and ball and pillow structures occur. **Unit C-2:** Dominance of normal graded units and ball and pillow structures among pelagic laminated silts intercalated with thin fine sand and coarse silt layers. **Unit C-3**:Dominance of normal graded units, ball and pillow structures, sand and gravel layers; a few pelagic laminated silts intercalated with thin fine sand and coarse silt layers occur.

4.2 Magnetic concentration

The natural remanent magnetisation (NRM) of sediments is influenced by the intensity of the Earth's magnetic field at the moment of deposition and by lithological factors such as the mineralogy, the concentration and the grain size of the magnetic carriers (Tauxe, 1993). Figure 4 presents the NRM after 20 mT demagnetisation along with the magnetic grain size and concentration proxies since 51.2 ka cal BP. While the magnetic susceptibility and the remanent magnetisations (NRM, ARM, IRM) depend on both the concentration and the magnetic grain size, the ratio kARM/SIRM, Hcr/Hc and Mr/Ms, as well as MDF_{NRM}, reflect changes in grain size (e.g., Stoner and St-Onge, 2007; Dunlop and Özdemir, 1997 and references herein). The similarity of the curves clearly illustrates the influence of the magnetic concentration and grain size on the NRM, as expected for a magnetic mineralogy dominated by magnetite.

The more notable rock-magnetic change is a sharp diminution in the concentration of magnetic minerals at 17.3 ka cal BP, and is observed in all concentration-dependant parameters (k_{LF}, NRM, ARM, IRM) (Fig. 4). The concentration change at 17.3 ka cal BP is coeval with a sharp increase of the total organic carbon (TOC) (Recasens et al., in press; Hahn et al., this issue; Zhu et al., this issue) and it represents the limit between the lithological units C-1 and B (Fig. 4), where plant macro remains and gastropods become abundant (Kliem et al., this issue). Hence the diminution in the magnetic concentration proxies most likely reflects the dilution of magnetic minerals by increased organic sediments. This transition corresponds to the onset of the last deglaciation in the Southern Hemisphere (Schaefer et al., 2006). The maximum change in the concentration of magnetic minerals for the PASADO-ICDP 2CP record is of approximately one order of magnitude (see the concentration-dependant parameters in Fig. 4), which is commonly considered as a maximal range for a high quality paleomagnetic study (Tauxe, 1993).

4.3 Magnetic grain size

The grain size proxies vary with similar amplitudes throughout the record (Fig. 4). Nonetheless, there is a gradual coarsening trend from 18 to 12 ka cal BP followed by a slight trend towards finer magnetic grains during the Holocene. These results suggest that no drastic change occurred in the grain size of the remanence carriers since 51.2 ka cal BP. This is supported with the coercivity and remanence ratios (Hcr/Hc and Mr/Ms) used in a "Day plot" to estimate the domain state of the magnetic grains (Day et al., 1977) (Fig. 5). All 103 samples fall in and to the right of the region indicative of pseudo-single domain (PSD) magnetite and also align parallel to the theoretical single and multi domain (SD+MD) mixing line for magnetite (Dunlop, 2002). The samples in which sand, tephra and/or vegetal debris were visually identified (20 samples) plot to the right of the cluster (Fig. 5). This suggests that these particular and easily identifiable samples contain a higher proportion of MD magnetite grains or a contribution of other magnetic minerals. On the other hand, the rest of the samples are dominated by PSD magnetite, which is optimal for paleomagnetic recording (King et al., 1983; Tauxe, 1993; Stoner and St-Onge, 2007).

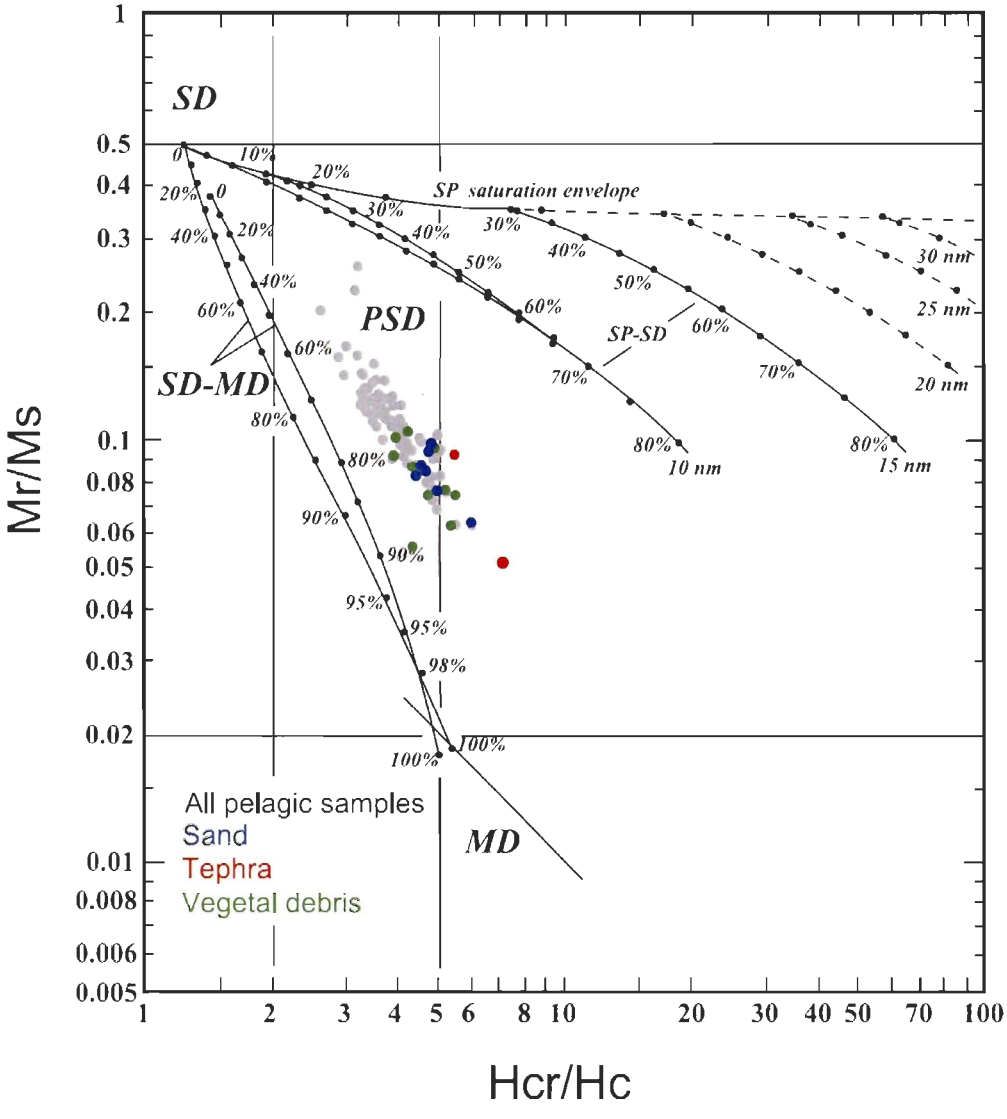

Figure 1. 5. Day plot (Day et al., 1977) for the pelagic sediment samples of Laguna Potrok Aike since 51.2 ka cal BP. The mixing reference lines for single and multi-domain (SD and MD) are from Dunlop (2002).

4.4 Paleomagnetic directions

A strong and stable single-component magnetisation is isolated from 10 mT to 40 mT (7 demagnetisation steps) and is identified as the characteristic remanent magnetisation (ChRM) (Fig. 6). A viscous magnetisation, if present, is easily removed after 5 or 10 mT demagnetisation. The NRM at the demagnetisation steps 10, 20, 30 and 40 mT only are presented in Figure 7 for clarity. The ChRM MAD values are generally $\leq 5°$ (81% of the data), indicating a well-defined component magnetisation for Quaternary sediments (Stoner and St-Onge, 2007). The data associated with MAD values between 10° and 5° (17%) and >10° (2%) generally correspond to intervals with relatively low NRM and MDF, most likely indicating coarser PSD magnetic grains and/or a lower concentration of magnetic minerals. However, these intervals are still relatively well-defined with MAD values generally < 15° (Butler, 1992; Opdyke and Channell, 1996) and they are not systematically associated to inclination values departing significantly from the theoretical value considering a geocentric axial dipole (GAD; -68°, indicated with a vertical line on Fig. 7). The average inclination value is -67° for the last 17.3 ka cal BP and -55° for the period from 51.2 to 17.3 ka cal BP. The average inclination value during the last Glacial period is lower than the GAD value and results from of a series of intervals with lower inclinations (I-1 to I-6; Fig. 7). There is no systematic inclination shallowing that would be attributed to geological recording (Tauxe, 2005). The inclination lows I-1, I-3 and I-6 depart up to approximately 20° from the GAD value (vertical dashed line in Fig. 7), whereas I-2, I-4 and I-5 depart more than 20° from the GAD. Flattening by post-depositional compaction induced by frequent mass movement deposits (MMD) at Laguna Potrok Aike could account for low inclinations (Anson and Kodama, 1987; Tauxe, 2005) and a greater effect of compaction on the inclination record would be expected with depth, where the number and thickness of the MMD are higher (Kliem et al., this issue). This is not the case and for example, the deepest pelagic sediment recovered within the stratigraphic unit characterised by thick and numerous MMD (C-3; Kliem et al., this issue) recorded an average inclination of -64°, which is near the GAD value.

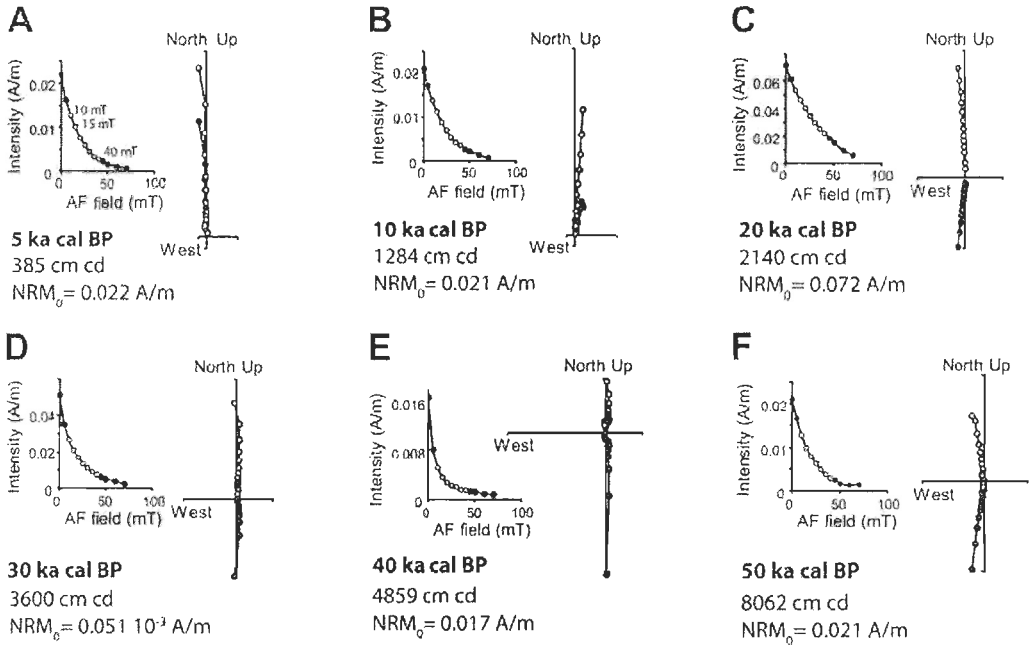

Figure 1. 6. Typical demagnetisation curves and orthogonal projections for the pelagic sediment from Laguna Potrok Aike at A) 5 ka cal BP, B) 10 ka cal BP, C) 20 ka cal BP, D) 30 ka cal BP, E) 40 ka cal BP, F) 50 ka cal BP. The characteristic remanent magnetisation (ChRM) interval (from 10 to 40 mT demagnetisation steps) is represented with light grey symbols. The open (closed) symbols in the vector end-point orthogonal diagram represent the projection in the vertical (horizontal) plane.

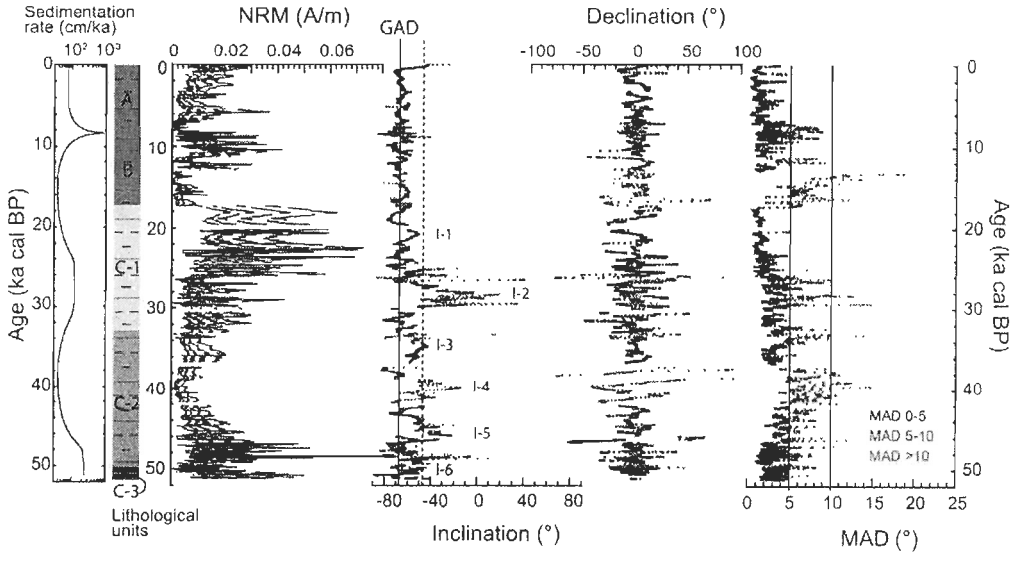

Figure 1. 7. Paleomagnetic directions recorded at Laguna Potrok Aike since 51.2 ka cal BP. From left to right: the natural remanent magnetisation (NRM) at the demagnetisation steps 10, 20, 30 and 40 mT, the paleomagnetic inclination, declination and the maximum angular deviation (MAD) values calculated for the characteristic remanent magnetisation (ChRM) interval from 10 to 40 mT (7 steps). The continuous vertical line on the inclination graph is the geocentric axial dipole (GAD) value at the coring site. Intervals of low inclinations are indicated (I-1 to I-6; see text for details) and the dashed line represent a departure of 20° from the GAD. The sedimentation rates and the lithological units from Kliem et al. (this issue) are located on the left hand side. For the description of the lithological units A, B, C-1, C-2 and C-3, the reader is referred to Fig.4.

I-2 is the interval displaying the lowest inclination values. It is found from 30 to 27 ka cal BP and positive inclination values are reached. The inclination abruptly shifts to low values at 30 ka cal BP and progressively returns to the GAD value at ca. 27 ka cal BP. This large feature represents 4 m of pelagic sediments and corresponds to a period of high sedimentation rates (Fig. 7; Kliem et al., this issue) with an average of 133 cm/ka. This interval corresponds to a period of extended land exposure associated with an absence of terminal lakes in Patagonia (Sugden et al., 2009) and may correspond to a period of low lake level during which a major unconformity was formed on the lake shoulder (Gebhardt et al., 2012). Even though an environmental influence might appear likely, the magnetic

grain size indicators in this interval reveal only a mild increase that does not differ from the average values (Fig. 4) and altogether the rock-magnetic results support a genuine geomagnetic recording. A flattening of the inclinations by compaction during a period of high sedimentation rates could induce low inclinations. However, no relation is found between the sedimentation rates and the inclination values at Laguna Potrok Aike (Fig. 7) and similar high-sedimentation rates previously allowed the recording of excellent paleomagnetic records (>100 cm/ka; St-Onge et al., 2003; Stoner et al., 2007; Lisé-Pronovost et al., 2009). In addition, the two periods with the highest sedimentation rates (from 51.2 to 46.3 and from 9.4 to 6.6 ka cal BP) display inclination values around the GAD value, further supporting a genuine geomagnetic signal. An alternative explanation for the low inclinations of the interval 30-27 ka cal BP is linked to the observation that this sedimentary interval was difficult to correlate between the two overlapping holes (A and C). For example, one tephra layer was present in one hole (part of the composite depth) but absent in the other. Therefore although a stable and well-defined ChRM associated with MAD values lower than 10 (average of 8.3°) and carried by PSD magnetite suggest a genuine geomagnetic origin of the paleomagnetic direction, the possibility of a large and undetected synsedimentary deformation (e.g., Channell and Stoner, 2002) cannot be excluded. There are no sedimentary structures suggesting deformation (for more detail see Kliem et al., this issue) and without additional evidence, the interval 30-27 ka cal BP is considered pelagic; however the paleomagnetic record in this interval should be regarded with caution.

The two other intervals with inclinations deviating more than 20° from the GAD are I-4 and I-5. I-4 represents the interval from 41.5 to 38.7 ka cal BP with a minimum inclination recorded at 39.8 ka cal BP (-14°). This interval represents 1.03 m of sediment and the sedimentation rates are lower (37 cm/ka) relative to the average since 51.2 ka cal BP at Laguna Potrok Aike. Sharp and large amplitude declination changes are associated with this interval, as well as distinctively low NRM values (Fig. 4), while the other concentration-dependant parameters do not present such a minimum. In addition, this interval is characterized by relatively low MDF_{NRM} (< 10 mT; Fig. 4) and MAD values >5°

(Fig. 7), thus suggesting the presence of coarser PSD magnetic grains, also illustrated by a rapid decrease of the NRM during step-wise demagnetisation (Fig. 6E). Coarse MD magnetite grains are generally poor recorder of the geomagnetic field (Tauxe, 1993). However the rock-magnetic result still indicate PSD domain state and as other intervals with similar rock-magnetic properties (NRM, MDF, and MAD) display inclinations values around the GAD value (e.g., ca. 17-11 and 9-7 ka cal BP), directions in this interval are considered reliable.

I-5 is the interval from 46.7 to 43.5 ka cal BP and is characterised by a sharp shallowing of the inclination to values around -50°, followed by a sharp return around the GAD value at 43.5 ka cal BP. Large amplitude changes in declination are also observed from 47 to 46 ka cal BP. It represents ca. 2.08 m of sediment deposited with a mean sedimentation rate of 65 cm/ka. Like all the other intervals departing from the GAD value during the last Glacial period, the rock-magnetic results support a genuine geomagnetic origin of the signal.

4.5 Relative paleointensity

The natural remanent magnetisation (NRM) carried by sediments is a detrital remanent magnetisation (DRM). In order to build a relative paleointensity proxy (RPI), it is assumed that the DRM is proportional to the paleo field (Tauxe, 1993). However, changes in the concentration, grain size and mineralogy of the magnetic grains can additionally affect the natural remanence. Therefore the NRM is commonly normalised using a rock-magnetic parameter, typically ARM, IRM or k_{LF}. Because k_{LF} is measured in the presence of an applied field, it is not only influenced by concentration and grain size changes, but also by grains that do not contribute to the DRM, including coarse MD grains, diamagnetic and paramagnetic material. For this reason k_{LF} should be used with caution and here we use ARM and IRM.

The relative paleointensity estimates using ARM and IRM as normalisers of the NRM yield similar results. In order to identify the appropriate normaliser, two different

normalisation methods were compared for each paleointensity estimate using UINT (Xuan et al., 2009) (Fig. 8A and B). The average ratio method is widely used (e.g., Stoner et al., 2003; Barletta et al., 2008; Lisé-Pronovost et al., 2009) and is built by averaging the normalized NRM at different demagnetisation steps. Here we use four demagnetisation steps (10, 20, 30 and 40 mT) of the characteristic remanent magnetisation interval (ChRM). The pseudo Thellier method or the slope method (Tauxe et al., 1995; Channell et al., 2002; Snowball and Sandgren, 2004; Xuan and Channell, 2009) uses the slope of the NRM versus the normaliser at different demagnetisation steps, here at 10, 20, 30 and 40 mT. The two methods give similar results for $NRM/ARM_{10\text{-}40mT}$ and the correlation coefficient (R) calculated from the slope method are high (average R=0.997; dotted line in Fig. 8A), suggesting a close resemblance of the NRM and ARM coercivity spectrum. In contrast, the two methods of paleointensity estimate using IRM as a normaliser ($NRM/IRM_{10\text{-}40mT}$; Fig. 8B) are different for several intervals, notably for the last 4000 cal BP. In addition, the correlation coefficients are systematically lower for $NRM/IRM_{10\text{-}40mT}$ and present more scatter and sharp minima (Fig. 8B). Furthermore, the MDF_{NRM} is best correlated with the MDF_{ARM} (R=0.42) than with the MDF_{IRM} (R=0.07), indicating that the grains acquiring the ARM more closely match the coercivity of the grains carrying the natural remanence (Levi and Banerjee, 1976). This is also illustrated by looking at the demagnetisation behaviour of NRM, ARM and IRM for the entire pelagic sediment record, where ARM better matches the behaviour of the NRM than IRM (Fig. 8C). This figure illustrates in a continuous way the remaining magnetisation after each demagnetisation steps 10, 20, 30 and 40 mT. The demagnetisation behaviour is clearly more variable for the IRM than for the NRM and ARM.

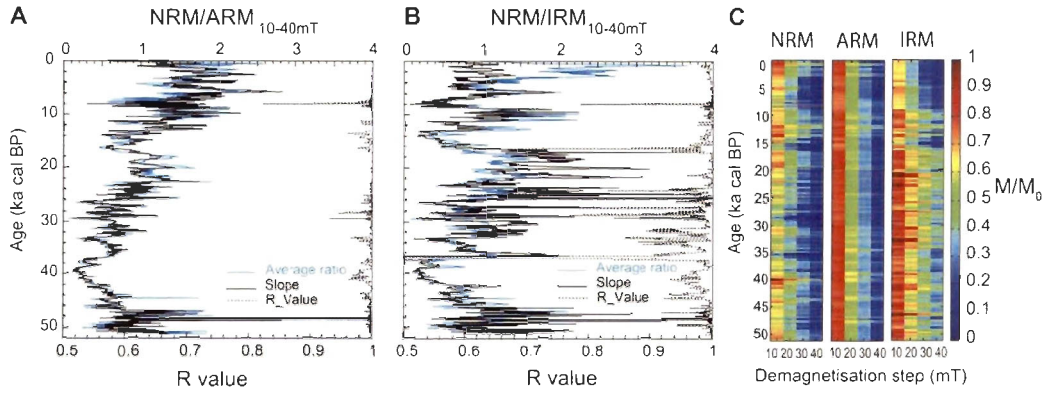

Figure 1. 8. Comparison of the relative paleointensity estimates A) $NRM/ARM_{10\text{-}40mT}$ and B) $NRM/IRM_{10\text{-}40mT}$ using the average ratio and the slope methods. C) Demagnetisation behaviour of the NRM, ARM and IRM at 10, 20, 30 and 40 mT demagnetisation steps. The color scale represents the magnetic remanence (M) normalized by the value before step-wise demagnetisation (M_0).

Coherence tests of the best relative paleointensity estimate ($NRM/ARM_{10\text{-}40mT}$) with its normaliser were achieved for the average ratio and slope methods following the Tauxe and Wu (1990) method and using the software Analyseries (Paillard et al., 1996) (Fig. 9A). The relative paleointensity estimates $NRM/ARM_{10\text{-}40mT}$ using the ratio and slope methods are superimposed and there is coherence at some frequencies (Fig. 9A), hinting at a possible environmental overprint. Most of the periods where coherence is observed are from 100 to 200 years, illustrating high-frequency secular variations possibly not normalized adequately and thus lithological in origin. However, only very few periods (> 300 yr) are coherent at the secular to millennial and millennial timescales, suggesting that both RPI estimates are geomagnetic in origin at these timescales. In addition, these few frequencies are not significant in the power spectrum of neither the RPI estimates, or for the normalisers (Fig. 9A). Nevertheless, the source of the high-frequency environmental overprint was investigated, identified and is illustrated in Figure 9B where a good correspondence of the RPI estimates with MDF_{NRM} is observed. Correlation coefficients (R) of 0.58 and 0.41 for the ratio and slope methods, respectively, suggest a grain size

influence on the RPI estimates. In order to correct for that grain size influence and to obtain the best possible RPI proxy, a secondary normalisation was applied to both RPI estimates by using a correction factor used previously by Brachfeld and Banerjee (2000) to remove the grain size influence on the RPI estimate of Holocene sediments from Lake Pepin (Minnesota, USA). Brachfeld and Banerjee (2000) revealed that this simple correction can be used effectively to correct a paleomagnetic signal overprinted by grain size changes. The correction is based on the linear relationship between the paleointensity estimate (RPI) and MDF_{NRM} using the equation:

$$RPI' = RPI \times MDF_{NRM\text{-}CM}/MDF_{NRM}$$

where $MDF_{NRM\text{-}CM}$ is the center of mass of the MDF_{NRM}, which is determined from the RPI vs. MDF_{NRM} scatter plot (median value of 15.8 mT; Fig. 9B). The correction simply adjusts the amplitude of the RPI variations to account for the non-geomagnetic effect of coercivity changes on the RPI. Therefore, intervals of greater difference between the RPI and RPI' (corrected intervals) correspond to the minimum and maximum values of the MDF_{NRM}. Considering that the MDF_{NRM} is a grain size proxy for the sediments of Laguna Potrok Aike (Fig. 4), coarser (finer) magnetite grains underestimate (overestimate) the relative paleointensity. The greater corrections are found for the intervals 41-38, 30-28, 16-13, 11-8 and 3-0 ka cal BP (Fig. 9B). Finally, the correlation of the RPI' with the magnetic grain size proxy MDF_{NRM} is significantly reduced for both RPI estimates (average ratio and slope; Fig. 9B), and especially for the average ratio method ($R = 0.06$). Therefore, the preferred RPI proxy for the PASADO-ICDP record is $NRM/ARM_{10\text{-}40mT}$ calculated using the average ratio method.

The RPI proxy presented here fulfils the required criteria for high quality record from sediments (King et al., 1983; Tauxe, 1993; Stoner and St-Onge, 2007), including 1) a single, strong and well-defined ChRM (Fig. 6) carried by PSD magnetite (Figs. 3, 4 and 5), 2) no inclination error (Fig. 7), 3) the variation in the concentration of magnetic minerals is limited to approximately one order of magnitude (Fig. 4), 4) similar RPI estimates are obtained from different normalization methods (Fig. 8), 5) the RPI proxy is independent of

bulk rock magnetic parameters after a secondary normalization using MDF_{NRM} (Fig. 9), 6) there is a good agreement of the paleomagnetic record with the closest available records (Fig. 11; see below).

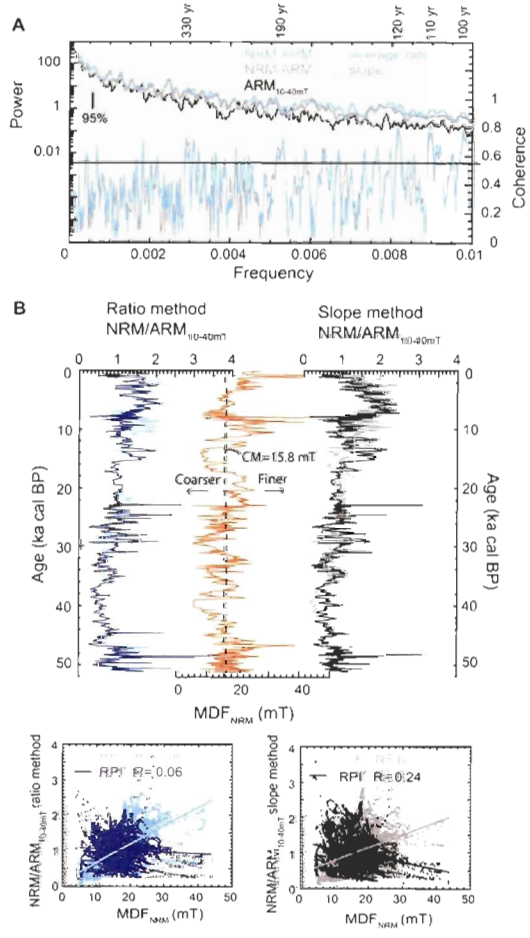

Figure 1. 9. A) Coherence tests of the relative paleointensity estimate $NRM/ARM_{10\text{-}40mT}$ with its normaliser using the Blackman-Tukey method with a Bartlett window. The solid horizontal line represents the level above which the coherence is significant at the 95% confidence. B) Relative paleointensity estimates using the average ratio and the slope methods before (RPI) and after (RPI') the secondary normalisation using MDF_{NRM} to account for magnetic grain size influence on DRM (see text for details). CM is the center of mass and represents the median MDF_{NRM} value. The scatter plots in inset reveal that the correlation is significantly reduced for both methods and the $NRM/ARM_{10\text{-}40mT}$ average ratio is not correlated with the MDF_{NRM}.

5. Discussion

5.1 Geomagnetic secular variations and excursions

Changes of the virtual geomagnetic pole by less than 40-45° are commonly referred to as geomagnetic secular variation and greater changes, also associated to low geomagnetic intensity, are considered as geomagnetic excursions (e.g., Merrill and McFadden, 1994; Laj and Channell, 2007; Roberts, 2008). In the last 52 ka cal BP, the Laschamp (40.7 +/-1 ka cal BP; Singer et al., 2009) and Mono Lake (32.4 +/- 0.3 ka cal BP, Singer, 2007) geomagnetic excursions are the only two recognized geomagnetic excursion and they are believed to occur globally (Laj and Channell, 2007). They are however not always recorded because of their short durations, which are estimated from the cosmogenic isotope records from Greenland to 1.2 and 2.5 kyr, for the Mono Lake and Laschamp geomagnetic excursion, respectively (Wagner et al., 2000). Therefore, the capability of recording geomagnetic excursions depends on the sedimentation rate, the lock-in depth and the associated post-depositional remanent magnetisation (PDRM) smoothing (Roberts and Winklhofer, 2004). In the Southern Hemisphere, excursional geomagnetic directions associated with the Laschamp geomagnetic excursion were recorded from sedimentary archives in the Indian sector of the Southern Ocean (MD94-103; Mazaud et al., 2002) and offshore Chile with an unprecedented resolution (Ocean Drilling Program (ODP) site 1233; Table 2) (Lund et al., 2006a). At Laguna Potrok Aike, a large directional swing (I-4 and D-2; Fig. 10A and B) associated with the lowest relative paleointensity value recorded since 51.2 ka cal BP (Fig. 10C) is associated with the Laschamp geomagnetic excursion. The Mono Lake geomagnetic excursion was reported in southern South America at 35 ka cal BP in core ODP-1233 (Lund et al., 2006b), and elsewhere in the Southern Hemisphere at 31.6 ± 1.8 ka in lava flow of the Aukland volcanic field in New Zealand (Cassata et al., 2008). A low in inclination (I-3; Fig. 10A) and a minimum in RPI (Fig. 10C) at 34 ka cal BP could be associated with the Mono Lake excursion in the LPA record.

The major inclination low during the period 30-27 ka cal BP (I-2) is from pelagic sediment (Kliem et al., this issue) and the paleomagnetic results indicate excursional

geomagnetic inclinations (Fig. 10A). Coeval sharp changes in inclination are observed in the ODP-1233 marine record from offshore Chile (Lund et al., 2006b), however with lower amplitude (Fig. 10A). An inclination low centered at ca. 26 ka cal BP in the ODP-1089 marine record (Stoner et al., 2003) and the WEGA marine stack (Macri et al., 2005) could further correspond to I-2 (Fig. 10A). Recently, Hodgson et al. (2009) reported a geomagnetic excursion at 26.8 +/- 0.4 ka cal BP from the former subglacial Lake Hodgson in Antarctica (72°00'S, 68°29'W; 2200 km distance from LPA) and tentatively linked it to the Mono Lake excursion. If I-2 corresponds to the Mono Lake excursion (32.4 +/- 0.3 ka cal BP, Singer et al., 2007), it would imply that "too young" ages are attributed to the sediment of Laguna Potrok Aike in this interval. This is unlikely for a radiocarbon-based chronology; however we note that no radiocarbon ages contribute to the age model in this specific interval (from 30.03 to 27.23 ka cal BP; Kliem et al., this issue). The strongest argument against the interpretation of I-2 being the Mono Lake excursion, however, is the absence of a coeval declination swing (Fig. 10B) and of a relative paleointensity minimum (Fig. 10C), as would be expected during a geomagnetic excursion. Instead, the large inclination swing I-2 at Laguna Potrok Aike is associated with the intensity maxima R-4. Hence I-2 is interpreted either as 1) a regional feature of the field, or 2) associated with an undetected synsedimentary deformation.

Table 1 2. Position, resolution and chronology of the paleomagnetic records presented in figures 10, 11 and 12.

Record[a]	Distance from LPA (km)	Latitude	Longitude	Time period (kyr)	Sedimentation rate[b] (cm/ka)	Chronology	Reference[c]
Dipole moment							
VADM from ^{10}Be, Greenland				60–0		–	1
GEOMAGIA model			–	50–0		-	2
GLOPIS-75 (24 cores)			–	75–10	5–34.5	-	3
Lava flow							
LFH	11,330	19°29'N	154°54'W	45–0			4
Lacustrine records							
LPA-PASADO		51°37'S	69°10'W	51.2–0	89	36 ^{14}C	5
LPA-SALSA		51°37'S	69°10'W	16–0	84	16 ^{14}C, 1 tephra	6
LEs	1210	41°03'S	71°34'W	18.8–1.8	40	13 ^{14}C	7,8
LEt	1210	41°04'S	71°29'W	23.8–0.2	40	3 ^{14}C, magnetostratigraphy (inc and dec) with LEs	9,10
LBa	19,840	52°52'N	107°21'E	84–0.3	12	26 ^{14}C, 3 climatic tie-points	11
LBi	17,230	35°15'N	136°03'E	40–0	40	5 ^{14}C, 5 tephra	12
LPu	8320	36°47'S	174°46'E	50–25	20	22 ^{14}C	13
Marine records and stacks							
ODP-1233	1260	41°00'S	74°24'W	70–0	170	24 ^{14}C, oxygen isotope stratigraphy	14
PD	1340	64°52'S	64°13'W	8.6–0.6	250	38 ^{14}C	15
WBB	1480	63°08'S	61°55'W	8.5–0.8	100	Magnetostratigraphy (RPI)	16
SS (2 cores)	1780	57°S	44°W	45–15.8	10	Magnetostratigraphy (RPI), diatom abondance stratigraphy	17
SAPIS (5 cores)	5970	41–47°S	6–10°E	80–0	15–25	ODP-1089 chronology	18
ODP-1089	5970	40°56'S	9°54'E	578–0.5	19	Oxygen isotope stratigraphy	19
MD94-103	8970	45°35'S	86°31'E	60–3.3	23	Magnetostratigraphy (RPI)	20
WEGA (6 cores)	6700	65°S	144°E	300–0	0.6–19	Magnetostratigraphy (RPI)	21

[a] The reader is referred to Fig. 1B for the complete name of the records and their position on the globe.

[b] The sedimentation rate is the average since 52 ka cal BP or for the complete record if it is younger.

[c] (1) Muscheler et al., 2005 (2) Knudsen et al., 2008 (3) Laj et al., 2004 (4) Teanby et al., 2002 (5) Kliem et al., in this issue (6) Haberzettl et al., 2007 (7) Gogorza et al., 2002 (8) Gogorza et al., 2004 (9) Irurzun et al., 2006 (10) Gogorza et al., 2006 (11) Peck et al., 1996 (12) Hayashida et al., 2007 (13) Nilsson et al., 2011 (14) Kaiser et al., 2005 (15) Brachfeld et al., 2000 (16) Willmott et al., 2006 (17) Collins et al., 2012 (18) Stoner et al., 2002 (19) Stoner et al., 2003 (20) Mazaud et al., 2002 (21) Macrì et al., 2005.

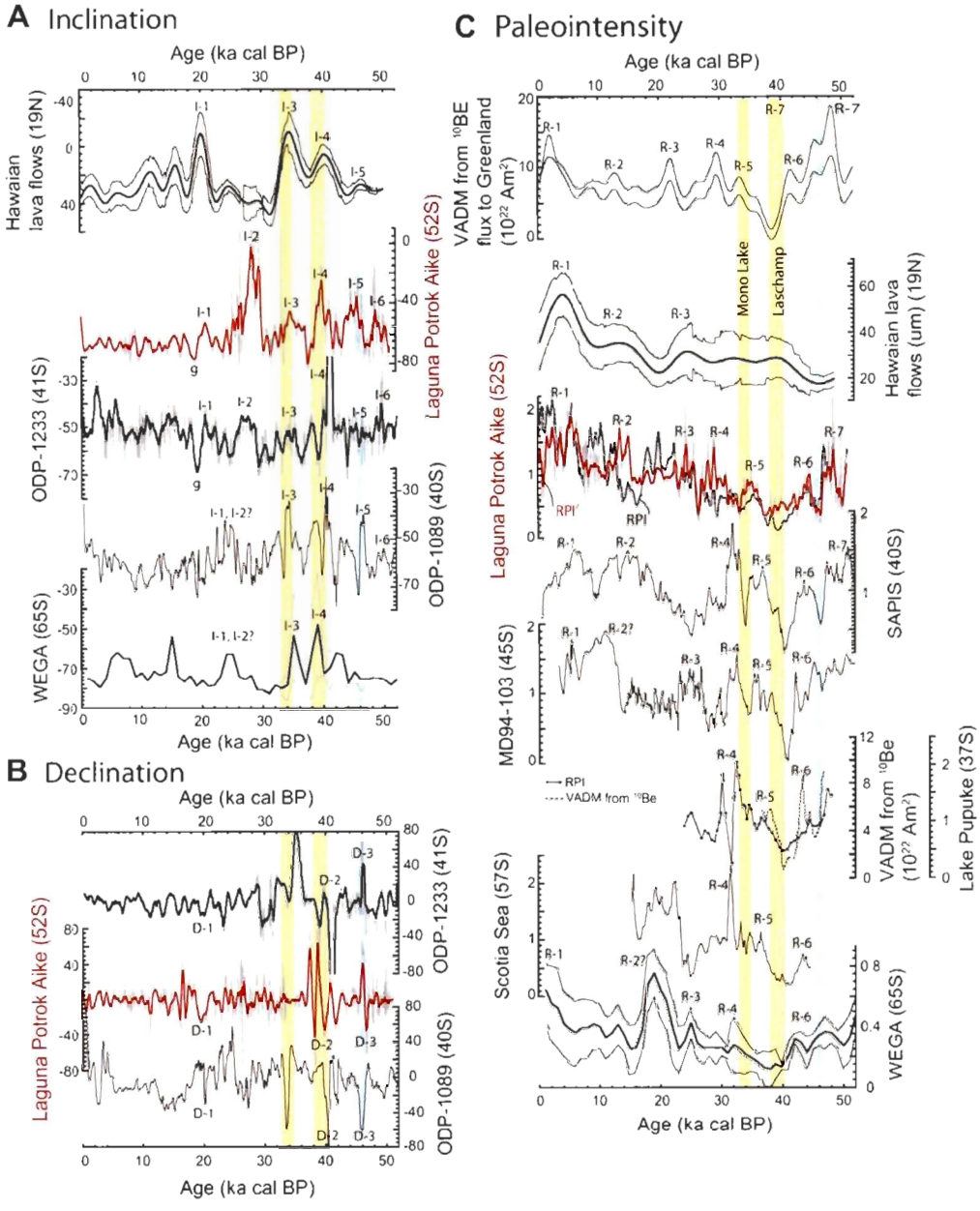
A Inclination
Age (ka cal BP)
Hawaian lava flows (19N)
Laguna Potrok Aike (52S)
ODP-1233 (41S)
ODP-1089 (40S)
WEGA (65S)
B Declination
Age (ka cal BP)
Laguna Potrok Aike (52S)
ODP-1233 (41S)
ODP-1089 (40S)
C Paleointensity
Age (ka cal BP)
VADM from 10BE flux to Greenland (10^22 Am^2)
Mono Lake
Laschamp
Hawaian lava flows (um) (19N)
Laguna Potrok Aike (52S)
RPI
SAPIS (40S)
MD94-103 (45S)
RPI
VADM from 10Be
VADM from 10Be (10^22 Am^2)
Lake Pupuke (37S)
Scotia Sea (57S)
WEGA (65S)
Age (ka cal BP)

Figure 1. 10. Comparison of paleomagnetic A) inclination, B) declination and C) relative paleointensity records from the mid-to high-latitudes (37°-65°S) of the Southern Hemisphere since 52 ka cal BP. The virtual axial dipole moment (VADM) derived from the ^{10}Be flux to Summit, Greenland (Muscheler et al., 2005) and a lava flow compilation from Hawaii (Teanby et al., 2002) are also presented for comparison. The records include Laguna Potrok Aike in Patagonia (this study), the marine ODP-1233 core offshore Chile (Lund et al., 2006b), the marine ODP-1089 core (Stoner et al., 2003) and the SAPIS stack (Stoner et al., 2002) from the Atlantic sector of the Southern Ocean, the Scotia Sea stack (Collins et al., 2012), Lake Pupuke in New Zealand (RPI and VADM from ^{10}Be; Nillson et al., 2011), the marine core MD93-104 from the Indian sector of the Southern Ocean (Mazaud et al., 2002), and the WEGA marine stack from the Wilkes Land Basin near Antarctica (Macri et al., 2005). The thick lines represent the millennial variability of the high resolution records (Laguna Potrok Aike and ODP-1233). The millennial-scale variability of the uncorrected (RPI) and corrected (RPI') relative paleointensity from Laguna Potrok Aike are also presented. Notable features of the paleomagnetic inclination (I-1 to I-6), declination (D-1 to D-3) and intensity (R-1 to R-7) are indicated. Note the reverse inclination axis for the Hawaiian lava flow compilation record located in the Northern Hemisphere. The Laschamp and Mono Lake geomagnetic excursions are underlined in yellow and the event at ca. 46 ka cal BP in blue (see text for details). For the location of the records, please see Figure 1B and Table 2.

A directional swing at ca. 20 ka cal BP is recorded around southern South America (LPA, ODP-1233 and ODP-1089) and identified as I-1 and D-1 (Fig. 10A and B). This feature is associated with a local low in paleointensity from Laguna Potrok Aike (Fig. 10C), as well as from global dipole estimates such as the GEOMAGIA dipole model (Knudsen et al., 2008) and the marine stack GLOPIS-75 (Laj et al., 2004) (Fig. 12C). Interestingly, this feature could correspond to the Hilina Pali geomagnetic excursion, recorded with details during times of intense volcanic activity in Hawaii at ca. 20 ka cal BP (Teanby et al., 2002; Laj et al., 2002). Excursional directions at 18-22 cal BP were also reported from Eastern Arctic cores (Nowaczyk and Knies, 2000; Nowaczyk et al., 2003), Lake Baikal in Siberia (Peck et al., 1996) and lava flows from Amsterdam Island, southeastern Indian Ocean (Carvallo et al., 2003). However, the age for this feature is often poorly constrained and Xuan and Channell (2010) recently argued that the paleomagnetic inclination signal of Arctic sediments might be altered by diagenetic processes. To date, the geomagnetic excursion at 20 ka cal BP was only confidently dated in Hawaii. Nonetheless,

a direction swing is recorded in southern South America at 20 ka cal BP and if it is associated to the geomagnetic excursion recorded 11,300 km away in Hawaii, it suggests a dominant feature of the field.

5.2 Geomagnetic field variability in the Southern Hemisphere and in southern South America

Several directional features can be correlated among the records from the mid- to high-latitudes of the Southern Hemisphere, including most of the inclination lows (I-1, I-2, I-3, I-4, I-5, I-6) and the sharp declination swings (D-1, D-2, D-3) recorded at Laguna Potrok Aike (Fig. 10A and B). Similarly, a series of intensity high (R-1 to R-7) following the virtual axial dipole moment (VADM) record from the ^{10}Be flux to Greenland (Muscheler et al., 2005) can be identified in the records from the Southern Hemisphere (Fig. 10C). Some differences are also observed in the relative paleointensity records. All the records generally agree from 52 to 35 ka cal BP (R-7, R-6 and R-5; see also Figure 11 of Kliem et al., this issue), however R-4 appears younger in LPA and in the VADM from Greenland. While the record from Laguna Potrok Aike is comparable to MD94-103 for the interval from ca. 25 to 15 ka cal BP (including R-3, which is absent from SAPIS), it more closely resembles SAPIS since 15 ka cal BP (Fig. 10C).

The next step is to compare the new high-resolution full vector paleomagnetic record from Laguna Potrok Aike (LPA) to the available marine and lacustrine records around southern South America since 20 ka cal BP (Fig. 11), where more high-resolution paleomagnetic records are available. The LPA-PASADO (this study) u-channel-based paleomagnetic record is in good agreement with the LPA-SALSA discrete samples-based record (Gogorza et al., submitted). Common directional paleomagnetic features are marked among the records from the southern South America region (<1500 km distance from LPA) (Fig. 11A and B). Some temporal shifts are observed and could be linked to the uncertainties of the respective chronologies (Table 2). Differences in the amplitude of variations could in turn be related to different sedimentation rates and lock-in depths of the different records, as well as non-dipolar local features. A particularly good millennial-scale

comparison is found between the paleomagnetic inclination (Fig. 11A) and declination (Fig. 11B) records of LPA-PASADO with the high-resolution marine record ODP-1233 from offshore Chile (Lund et al., 2006b). The majority of peaks and troughs can be readily correlated, including a large inclination swing preceding I-1 at ca. 18 ka cal BP (from f to g), also visible in the records from Lake El Trébol (Irurzun et al., 2006) (Fig. 11A). Large declination swings, such as the features C, D, E, F and G (Fig. 11B), are also present in all the records from southern South America. All relative paleointensity records from the region (Fig. 11C) display relatively high values in the intervals 15-11 ka cal BP, followed by a decrease to lower values in the intervals 11-8 ka cal BP and 3-0 ka cal BP. However, the millennial-scale comparison is not straightforward, probably because of the variable quality of the available records. The highest resolution record (WBB; Willmott et al., 2006) is limited to 9 ka cal BP and the SAPIS stack should be treated with caution in the interval 20-0 ka cal BP because of a different magnetic assemblage (Stoner et al., 2002). The intervals 16-13, 11-8 and 3-0 ka cal BP were the most affected by the correction using MDF_{NRM} (Fig. 9B). Both the uncorrected and corrected RPI are presented in Figure 11C and the better general fit of the corrected LPA-PASADO RPI record with the available regional records supports the use of this correction. In particular, a magnetic grain size influence on the RPI was successfully corrected in the interval 11-8 cal BP, where relatively smaller magnetite grains were inducing a peak (Fig. 9) that is not present in the other regional records (Fig. 11C). Overall, the full-vector paleomagnetic variability of the records from around southern South America is generally comparable at the millennial-scale since 20 ka cal BP.

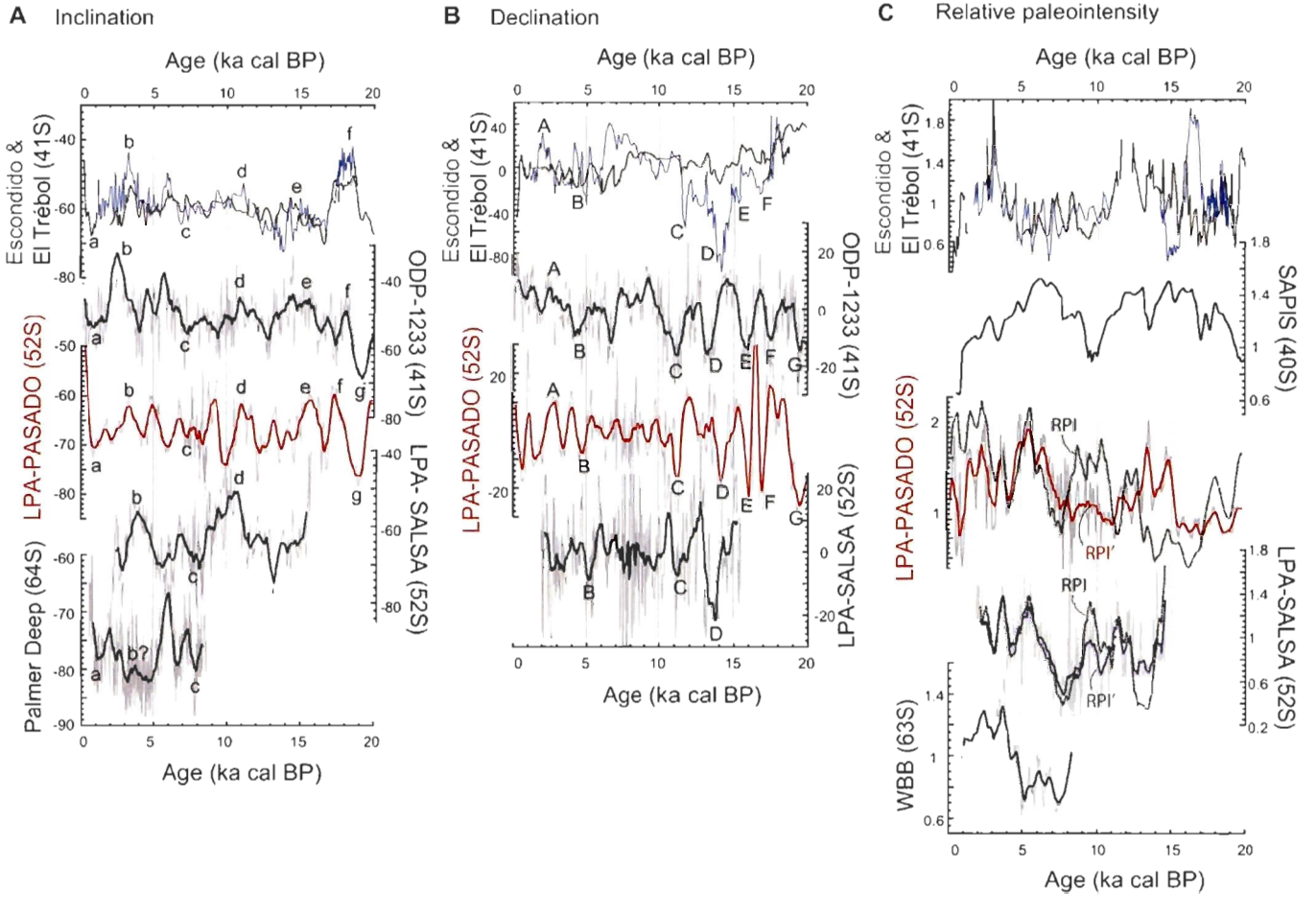
A Inclination
Age (ka cal BP)
Escondido & El Trébol (41S)
LPA-PASADO (52S)
Palmer Deep (64S)
ODP-1233 (41S)
LPA- SALSA (52S)
B Declination
Age (ka cal BP)
Escondido & El Trébol (41S)
LPA-PASADO (52S)
ODP-1233 (41S)
LPA-SALSA (52S)
C Relative paleointensity
Age (ka cal BP)
Escondido & El Trébol (41S)
SAPIS (40S)
LPA-PASADO (52S)
RPI
RPI'
LPA-SALSA (52S)
WBB (63S)

Figure 1. 11. Paleomagnetic A) inclination, B) declination, and C) relative paleointensity around Southern South America since 20 ka cal BP. The records are located from 40° to 64°S and include lake Escondido (Gogorza et al., 2002; 2004), lake El Trébol (Irurzun et al., 2006; Gogorza et al., 2006) and Laguna Potrok Aike (SALSA and PASADO projects, Gogorza et al., submitted and this work) in Argentina, as well as marine records from offshore Chile (ODP-1233, Lund et al., 2006b), offshore the Antarctic Peninsula (WBB, Willmott et al., 2006; Palmer Deep, Brachfeld et al., 2000) and a stack from the sub-Antarctic South Atlantic (SAPIS; Stoner et al., 2002). The thick curves represent the millennial-scale variability of the high-resolution records (> 80 cm/ka; Table 2). The millennial-variability of the uncorrected (RPI) and corrected (RPI') relative paleointensity from Laguna Potrok Aike are also presented. A set of correlative features for the inclination (a to g) and the declination (A to G) are indicated. Lake El Trébol is presented on the same graph as Lake Escondido because its chronology was established by magnetostratigraphy to Lake Escondido located less than 10 km away. The SAPIS stack is presented with the average data. All the records are presented on their own chronology and the PTA-SALSA record is plotted on the updated SALSA chronology from Kliem et al. (this issue). For the location of the records, please see Figure 1B and Table 2.

5.3 Global-scale paleomagnetic intensity and direction comparison

The relative paleointensity record from Laguna Potrok Aike is compared with widely used dipole moment estimates since 52 ka cal BP from different types of archives (Fig. 12C). These records include the VADM derived from the ^{10}Be flux to Summit in Greenland (Muscheler et al., 2005), the marine stack GLOPIS-75 (Laj et al., 2004) and a dipole model based on archeomagnetic and volcanic data (GEOMAGIA dipole model; Knudsen et al., 2008). The records are generally consistent and most peak values of the dipole moment (R-1 to R-7) can be correlated among the records. Nonetheless, the global comparison reveals a marked difference at ca. 46 ka cal BP. The inclination low event I-5 in Laguna Potrok Aike (Fig. 10A) is associated with the sharp declination swing D-3 (Fig. 10B) and a marked intensity low (Fig. 10C). Similar direction swing and intensity low are observed in the closest records (ODP-1233, Lund et al., 2006b; ODP-1089, Stoner et al., 2003) and the intensity low is observed at different degrees in numerous records from the Southern Hemisphere, including the Scotia Sea (Collins et al., 2012), the Sulu Sea (Schneider and Mello, 1996), the Indian and Atlantic sectors of the Southern Ocean (MD94-103; Mazaud et al., 2002, and SAPIS; Stoner et al., 2002), the western Equatorial Pacific (Blanchet et al.,

2006), Lake Pupuke in New Zealand (Nilsson et al., 2011), and the WEGA stack near Antarctica (Macri et al., 2005). This minimum in intensity is often absent or subdued in records from the Northern Hemisphere. For example, it represents a major difference between the NAPIS and SAPIS stacks in the interval 52 to 20 ka cal BP (Stoner et al., 2002). In addition, the records part of GLOPIS-75 and located in the Southern Hemisphere display this feature, but it was removed in the stack procedure, as most of the records were from the Northern Hemisphere (Laj et al., 2004). Therefore, the intensity low at 46 ka cal BP could represent an important Southern Hemisphere geomagnetic feature such as a possible analogue to the actual South Atlantic Anomaly, associated with a reverse flux patch at the core mantle boundary (e.g., Gubbins and Bloxham, 1985; Hulot et al., 2002). The South Atlantic anomaly (SAA) is an distinctive feature of the present field characterized at the surface of the Earth by a growing area of decreasing geomagnetic intensity since ca. 400 years and currently located over South America (Hartmann and Pacca, 2009). The CALS10k.1b spherical harmonic model supports the recent character of the SAA, with Laguna Potrok Aike located within one of the two Southern Hemisphere high-flux patches when averaged over the last 10 ka (Korte et al., 2011).

Laguna Potrok Aike in the Southern Hemisphere (51°37'S, 69°10'W) is diametrically opposite to Lake Baikal in the Northern Hemisphere (52°51'N, 107°22'E). The geographical location of the two records on opposite sides of the Earth (Fig. 1B) is therefore ideal to investigate the dipolar geomagnetic field since 51.2 ka cal BP. A full vector paleomagnetic comparison, including the LPA record, Lake Baikal (Peck et al., 1996) and a high-resolution record from Lake Biwa in Japan (Hayashida et al., 2007) is presented in Fig. 12. The comparison reveals a striking correlation of the inclination lows I-1, I-2, I-3, I-4, I-6, (with however different amplitudes for I-2 (Fig. 12A) and the declination swings D-1 and D-2 (Fig. 12B). As discussed previously, the directional feature (I-5 and D-3) associated with the intensity low at ca. 46 ka cal BP (R-5) from LPA and other Southern Hemisphere records is absent from the Lake Baikal record in the Northern Hemisphere. All other relative paleointensity features are readily identified from the three records; however R-2 is missing from the Lake Baikal record, where there is a gap in the

data. Furthermore, distinct peaks within each intensity maxima can be correlated between the high-resolution records from LPA and Lake Biwa, supporting the dipolar geomagnetic origin of these features for both records.

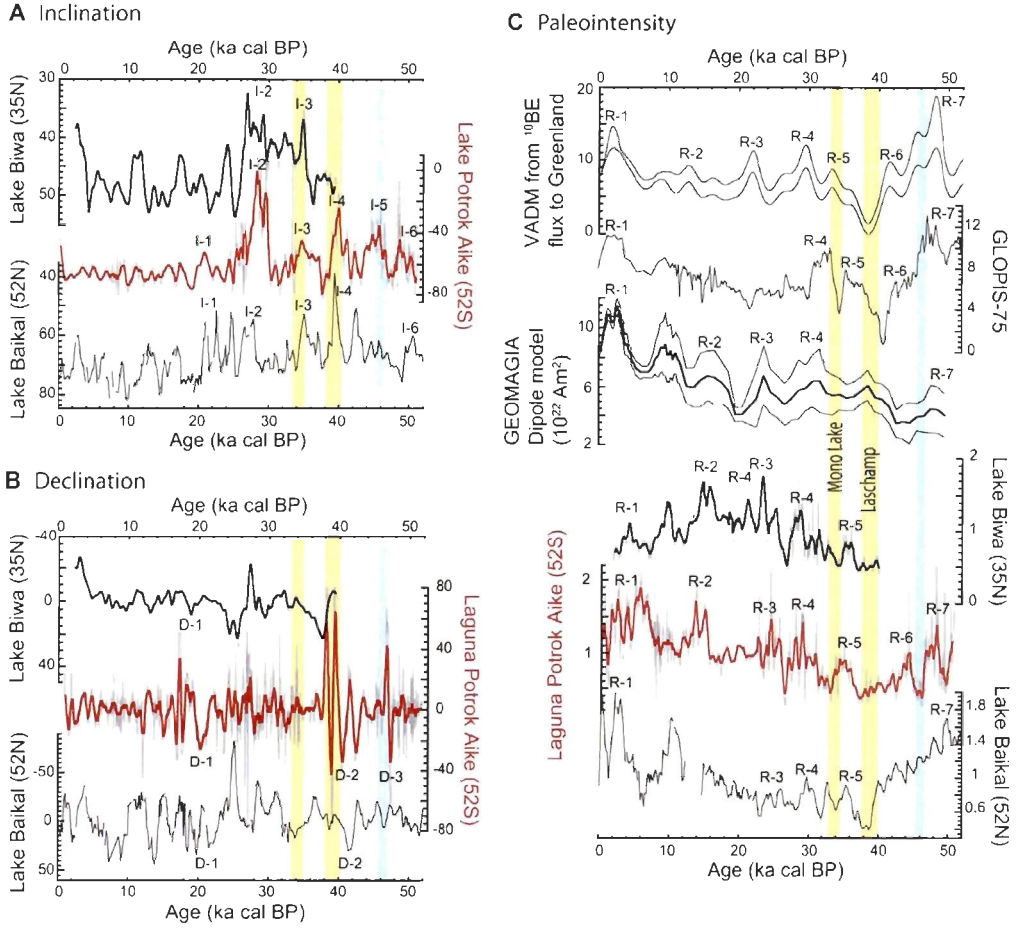

Figure 1. 12. Global-scale comparison of paleomagnetic A) inclination, B) declination and C) geomagnetic field intensity since 52 ka cal BP. The record from Laguna Potrok Aike (this study) is compared with the records from Lake Baikal in Siberia (Peck et al., 1996) and Lake Biwa in Japan (Hayashida et al., 2007). In addition, high-quality records of the dipole moment variability are presented and include the virtual axial dipole moment (VADM) derived from the ^{10}Be flux to Summit, Greenland (Muscheler et al., 2005), the marine stack GLOPIS-75 (Laj et al., 2004) and a model of the geomagnetic dipole based on absolute paleointensity data (Knudsen et al., 2008). The minimum and maximum VADM values from the ^{10}Be flux to Greenland are presented, the stack

GLOPIS-75 with the average value and the GEOMAGIA dipole model with the average and error. Notable features of the paleomagnetic inclination (I-1 to I-6), declination (D-1 to D-3) and intensity (R-1 to R-7) are indicated. The Laschamp and Mono Lake geomagnetic excursions are underlined in yellow and the event at ca. 46 ka cal BP in blue (see text for details). Note the reverse axis for the paleomagnetic directions of the records from the Northern Hemisphere. All the records are presented on their own chronology. For the location of the records, please see Figure 1.

6. Conclusions

A new high-resolution rock-magnetic and paleomagnetic record was constructed from the long sedimentary archive of Laguna Potrok Aike (PASADO-ICDP) covering the last 51.2 ka cal BP. While the magnetic assemblage is dominated by PSD magnetite and remains stable from the last Glacial period to the present interglacial, a marked decrease in the concentration of magnetic minerals at 17.3 ka cal BP is associated to the onset of the last deglaciation in Southern South America. A full vector paleomagnetic comparison of the Laguna Potrok Aike record with marine and lacustrine records from southern South America, other records from the mid- to high-latitudes of the Southern Hemisphere, and records located on the opposite side of the Earth as well as with global dipole moment reference curves 1) supports a genuine geomagnetic signal of the LPA-PASADO record, 2) generally supports the radiocarbon-based chronology (Kliem et al., this issue) at the millennial-scale, 3) verifies the global nature of the Laschamp and probably the Mono Lake geomagnetic excursion and 4) document distinct secular variations in southern South America at ca. 20 and 46 ka cal BP, possibly reflecting important features of the past geomagnetic field. In particular, the directional swing and sharp minimum in intensity at 46 ka cal BP seem to be mainly observed in the Southern Hemisphere and could likely be used as a new regional chronostratigraphic marker. Finally, these new paleomagnetic results reveal magnetostratigraphy as a promising tool to better constrain the PASADO-ICDP chronology at least at the millennial-scale in specific intervals where geomagnetic changes are either global or regional.

7. Acknowledgements

We thank F. Barletta, J. Labrie, D. Veres, M.-P. St-Onge and A. Leclerc for their help in the laboratory at ISMER. We are grateful to L.G. Collins, A. Hayashida, P. Macri, A. Mazaud, R. Muscheler, A. Nillson, J. Peck, J. Stoner and N. Teanby for kindly sharing their data. This research is supported by the International Continental Scientific Drilling Program (ICDP) in the framework of the "Potrok Aike Maar Lake Sediment Archive Drilling Project" (PASADO). Funding for drilling was provided by the ICDP, the German

Science Foundation (DFG), the Swiss National Funds (SNF), the Natural Sciences and Engineering Research Council of Canada (NSERC), the Swedish Vetenskapsradet (VR) and the University of Bremen. For their invaluable help in field logistics and drilling, we thank the staff of INTA Santa Cruz and Rio Dulce Catering as well as the Moreteau family and the DOSECC crew. This research was made possible through an NSERC Special Research Opportunity and Discovery grants to P. Francus and G. St-Onge. We also acknowledge the Canadian Foundation for Innovation (CFI) for the acquisition and operation of the u-channel cryogenic magnetometer. C. Gogorza thanks the *Comisión Nacional de Investigaciones Científicas y Técnicas de la República Argentina* (CONICET), the *Agencia Nacional de Promoción Científica y Tecnológica* (ANCyT) and the *Universidad Nacional del Centro de la Provincia de Buenos Aires* (UNCPBA). Finally, we acknowledge the support of NSERC and the Canadian Meteorological and Oceanographical Society (CMOS) for graduate scholarships to A. Lisé-Pronovost, and the *Fonds de recherche du Québec -Nature et technologies* (FQRNT) for a postdoctoral fellowship to T. Haberzettl.

8. References

Anselmetti, F.S., Ariztegui, D., De Batist, M., Gebhardt, C., Haberzettl, T., Niessen, F., Ohlendorf, C. and Zolitschka, B., 2009. Environmental history of southern Patagonia unravelled by the seismic stratigraphy of Laguna Potrok Aike. Sedimentology 56, 873–892.

Anson, G. L. and Kodama, K. P., 1987. Compaction-induced inclination shallowing of the post-depositional remanent magnetisation in a synthetic sediment. Geophys. J. Roy. Astr. Soc. 88, 673–692.

Banerjee, S.K., King, J., Marvin, J., 1981. A rapid method for magnetic granulometry with applications to environmental studies, Geophys. Res. Lett. 8, 333-336.

Barletta, F., St-Onge, G., Channell, J.E.T., Rochon, A., Polyak, L., Darby, D.A., 2008. High-resolution paleomagnetic secular variation and relative paleointensity records from the western Canadian Arctic: implication for Holocene stratigraphy and geomagnetic field behaviour. Can. J. Earth Sci. 45, 1265-1281.

Blanchet, C.L., Thouveny, N., de Garidel-Thoron, T., 2006. Evidence for multiple paleomagnetic intensity lows between 30 and 50 ka BP from a western Equatorial Pacific sedimentary sequence . Quat. Sci. Rev. 25, 1039-1052.

Brachfeld, S. and Banerjee, S.K., 2000. A new high-resolution geomagnetic paleointensity record for the North American Holocene: A comparison of sedimentary and absolute intensity data. J. Geophys. Res. 105(B1), 821-834.

Brachfeld, S., Acton, G.D., Guyodo, Y., and Banerjee, S.K., 2000. High-resolution paleomagnetic records from the Palmer Deep, western Antarctic Peninsula. Earth Planet. Sci. Lett. 181, 429-441.

Butler, R.F., 1992. Paleomagnetism: Magnetic domains to geologic terranes. Oxford: Blackwell.

Carvallo, C., Camps, P., Ruffet, G., Henry, B., Poidras, T., 2003. Mono Lake or Laschamp geomagnetic event recorded from lava flows in Amsterdam Island (southeastern Indian Ocean). Geophys. J. Int. 154, 767–782.

Cassata, W.S., Singer B.S., Cassidy, J., 2008. Laschamp and Mono Lake geomagnetic excursions recorded in New Zealand, Earth Planet. Sci. Lett. 268, 76-88.

Channell, J.E.T. and Stoner J.S., 2002. Plio-Pleistocene magnetic polarity stratigraphies and diagenetic magnetite dissolution at ODP Leg 177 Sites (1089, 1091, 1093 and 1094). Mar. Micropaleontol. 45, 269-290.

Channell, J.E.T., Mazaud, A., Sullivan, P., Turner, S., Raymo, M.E., 2002. Geomagnetic excursions and paleointensities in the 0.9-2.15 Ma interval of the Matuyama Chron at ODP Site 983 and 984 (Iceland Basin). J. Geophys. Res. 107(B6), 1-11.

Collins, L.G., Hounslow, M.W., Allen, C.S., Hodgson, D.A., Pike, J., Karloukovski, V.V., 2012. Palaeomagnetic and biostratigraphic dating of marine sediments from the Scotia Sea, Antarctica: First identification of the Laschamp excursion in the Southern Ocean, Quat. Geochronol. 7, 67-75.

Corbella, H., 2002. El campo volcano-tecto´nico de Pali Aike. In: Haller, M.J., Geologı´a y Recursos Naturales de Santa Cruz Relatorio del XV Congreso Geolo´gico Argentino, El Calafate. Buenos Aires. pp. 287–303.

Coronato, A., Ercolano, B., Corbella, H. , Tiberi, P., this issue. Glacial, fluvial and volcanic landscape evolution in the Laguna Potrok Aike Maar area, Argentina. Quat. Sci. Rev.

Day, R., Fuller, M., Schmidt, V.A., 1977. Hysteresis properties of titano-magnetite: grain size and compositional dependence. Phys. Earth Planet. Int. 13, 260–267.

D'Orazio, M., Agostini, S., Mazzarini, F., Innocenti, F., Manetti, P., Haller , M.J., Lahsen, A.A., 2000. The Pali Aike Volcanic Field, Patagonia: slab-window magmatism near the tip of South America. Tectonophysics 321, 407-427.

Dunlop, D.J., 2002. Theory and application of the Day plot (Mrs/Ms versus Hcr/Hc) 1.Theoretical curves and tests using titanomagnetite data. J. Geophys. Res. 107(B3), 1-22.

Dunlop, D. J., Özdemir, O., 2007. Magnetizations in rocks and minerals. In: Geomagnetism, Treatise on Geophysics vol.5, Schubert, G. (ed.), Elsevier, 277-336.

Dunlop, D.J., Özdemir, Ö, 1997. Rock Magnetism: Fundamentals and Frontiers. Cambridge University Press, Cambridge, New York.

Gebhardt, A.C., Ohlendorf, C., Niessen, F., De Batist, M., Anselmetti, F.S., Ariztegui, D., Kliem, P., Wastegård, S., Zolitschka, B., 2012. Seismic evidence of up to 200 m lake-level change in Southern Patagonia since MIS 4, Sedimentology 59, 1087-1100.

Gogorza, C.S.G., Sinito, A.M., Lirio, J.M., Nuñez, H., Chaparro, M., Vilas, J.F., 2002. Paleosecular variations 0–19,000 years recorded by sediments from Escondido Lake (Argentina). Phys. Earth Planet. Int. 133, 35–55.

Gogorza, C.S.G., Lirio, J.M., Nuñez, H., Chaparro, M.A.E., Bertorello, H.R., Sinito, A.M., 2004. Paleointensity studies on Holocene-Pleistocene sediments from lake Escondido, Argentina, Phys. Earth Planet. Int. 145, 219-238.

Gogorza, C.S.G., Irurzun, M.A., Chaparro, M.A.E., Lirio, J.M., Nuñez, H., Bercoff, P.G., Sinito, A.M., 2006. Relative paleointensity of the geomagnetic field over the last 21,000 years BP from sediment cores, Lake El Trébol (Patagonia, Argentina), Earth Planets Space 58, 1323-1332.

Gogorza, C.S.G., Sinito, A.M., Ohlendorf, C., Kastner, S., Zolitschka, B., 2011. Paleosecular variation and paleointensity records for the last millennium from southern South America (Laguna Potrok Aike, Santa Cruz, Argentina), Phys. Earth Planet. Int. 184, 41-50.

Gogorza, C.S.G., Irurzun, M.A., Sinito, A.M., Lisé-Pronovost, A., St-Onge, G., Haberzettl, T., Ohlendorf, C., Kastner, S., Zolitschka, B. 2012. High-resolution paleomagnetic records from Laguna Potrok Aike (Patagonia, Argentina) for the last 16,000 years. Geochem. Geophys. Geosyst (13) 12.

Gubbins, D. and Bloxham, J., 1985. Geomagnetic field analysis—III. Magnetic fields on the core-mantle boundary. Geophys. J. R. Astron. Soc. 80, 695–713.

Guyodo Y. and Valet J.-P., 1996. Relative variations in geomagnetic intensity from sedimentary records: the past 200 thousand years, Earth Planet. Sci. Lett. 143(1-4), 23-36.

Haberzettl, T., Corbella, H., Fey, M., Janssen, S., Lücke, A., Mayr, C., Ohlendorf, C., Schäbitz, F., Schleser, G.H., Wille, M., Wulf, S., Zolischka, B., 2007. Lateglacial and Holocene wet-dry cycles in southern Patagonia: chronology, sedimentology and geochemistry of a lacustrine record from Laguna Potrok Aike, Argentina. The Holocene 17(3), 297-310.

Haberzettl, T., Kück, B., Wulf, S., Anselmetti, F., Ariztegui, D., Corbella, H., Fey, M., Janssen, S., Lücke, A., Mayr, C., Ohlendorf, C., Schäbitz, F., Schleser, G.H., Wille, M., Zolitschka, B., 2008. Hydrological variability in southeastern Patagonia and explosive volcanic activity in the southern Andean Cordillera during Oxygen Isotope Stage 3 and the Holocene inferred from lake sediments of Laguna Potrok Aike, Argentina. Palaeogeogr., Palaeoclimatol., Palaeoecol. 259, 213–229.

Haberzettl, T., Anselmetti, F.S., Bowen, S.W., Fey, M., Mayr, C., Zolitschka, B., Ariztegui, D., Mauz, B., Ohlendorf, C., Kastner, S., Lücke, A., Schäbitz, F., Wille, M., 2009. Late Pleistocene dust deposition in the Patagonian steppe – extending and refining the paleoenvironmental and tephrochronological record from Laguna Potrok Aike back to 55 ka, Quat. Sci. Rev. 28, 2927-2939.

Hahn, A., Kliem, P., Ohlendorf, C., Zolitschka, B., Rosen, P. and the PASADO science team, this issue. Climate induced changes in the content of carbonaceous and organic matter of sediments from Laguna Potrok Aike (Argentina) during the past 50 ka inferred from infrared spectroscopy, Quat. Sci. Rev.

Hartmann G.A., Pacca I.G., 2009. Time evolution of the South Atlantic Magnetic Anomaly. An. Acad. Bras. Ciênc. 81(2), 243-255.

Hayashida, A., Ali, M., Kuniko, Y., Kitagawa H., Torii, M., Takemura, K., 2007. Environmental magnetic record and paleosecular variation data for the last 40 kyrs from the Lake Biwa sediments, Central Japan. Earth Planets Space 59, 807–814.

Hodgson, D.A., Roberts, S.J., Bentley, M.J., Carmichael, E.L., Smith, J.A., Verleyen, E., Vyverman, W., Geissler, P., Leng, M.J., Sanderson, D.C.W., 2009. Exploring former subglacial Hodgson Lake. Paper II: Palaeolimnology. Quat. Sci. Rev. 28, 2310–2325.

Hounslow, M.W. and Maher, B.A., 1999. Laboratory procedures for quantitative extraction and analysis of magnetic minerals from sediments, In: Walden, J., Oldfield, F., Smith, J. (eds.) Environmental Magnetism, a practical guide. Quaternary Research Association, Technical Guide No. 6., pp.139-164.

Hulot, G., Eymin, C., Langlais, B., Mandea, M., Olson, N., 2002. Small-scale structure of the geodynamo inferred from Ørsted and Magsat satellite data. Nature 416, 620–623.

Irurzun, M.A., Gogorza, C.S.G., Sinito, A.M., Lirio, J.M., Nuñez, H., Chaparro, M.A.E., 2006. Paleosecular variations recorded by sediments from Lake El Trébol, Argentina. Phys. Earth Planet. Int. 154, 1–17.

Kaiser, J., Lamy, F., Hebbeln, D., 2005. A 70-kyr sea surface temperature record off southern Chile (Ocean Drilling Program Site 1233). Paleoceanography 20, PA4009.

King, J.W., Banerjee, S.K., Marvin, J.A., Özdemir, Ö., 1982. A comparison of different magnetic methods for determining the relative grain size of magnetite in natural materials: some results from lake sediments, Earth Planet. Sci. Lett. 59, 404-419.

King, J.W., Benerjee, S.K., Marvin, J., 1983. A new rock-magnetic approach to selecting sediments for geomagnetic paleointensity studies: application to paleointensity for the last 4000 years, J. Geophys. Res. 88(B7), 5911-5921.

Kirschvink, J.L.,1980. The least-squares line and plane and the analysis of paleomagnetic data. Geophys. J. Roy. Astr. Soc. 62, 699–718.

Kliem, P., Enters, D., Hahn, A., Ohlendorf, C., Lisé-Pronovost, A., St-Onge, G., Wastegård, S., Zolitschka, B. and the PASADO science team, this issue. Lithology, radiocarbon dating and sedimentological interpretation of the 51 ka BP lacustrine record from Laguna Potrok Aike, southern Patagonia, Quat. Sci. Rev.

Knudsen, M.F., Riisager, P., Donadini, F., Snowball, I., Muscheler, R., Korhonen, K., Pesonen, L.J., 2008. Variations in the geomagnetic dipole moment during the Holocene and the past 50 kyr, Earth Planet. Sci. Lett. 272(1-2), 319-329.

Korte, M., Constable, C., 2011. Improving geomagnetic field reconstructions for 0–3 ka, Phys. Earth Planet. Int. 188(3-4), 247-259.

Korte, M., Constable, C., Donadini, F., Holme, R., 2011. Reconstructing the Holocene geomagnetic field, Earth Planet. Sci. Lett. 312, 497-505.

Korte, M., Genevey, A., Constable, C.G., Frank, U., Schnepp, E., 2005. Continuous geomagnetic field models for the past 7 millennia: 1. A new global data compilation, Geochem. Geophys. Geosyst., 6, Q02H15.

Laj, C., and Channell, J.E.T., 2007. Geomagnetic excursions, In: Kono, M. (Eds.), Treatise on Geophysics, vol. 5, Geomagnetism, Elsevier, Amsterdam, pp. 373–416.

Laj, C., Kissel, C., Scao, V., Beer, J., Muscheler, R., Wagner, G., 2002. Geomagnetic intensity variations at Hawaii for the past 98 kyr from core SOH4 (Big Island): new results. Phys. Earth Planet. Int. 129, 205–243.

Laj, C., Kissel, C., Beer, J., 2004. High resolution global paleointensity stack since 75 kyrs (GLOPIS-75) calibrated to absolute values. In: Channell, J.E.T., Kent, D.V., Lowrie, W., Meert, J.G. (Eds.), Timescales of the Paleomagnetic Field, AGU Geophysical Monograph, 145.

Levi, S., and Banerjee, S.K., 1976. On the possibility of obtaining relative paleointensities from lake sediments. Earth Planet. Sci. Lett. 29, 219-226.

Lisé-Pronovost, A. St-Onge, G., Brachfeld, S., Barletta, F., Darby, D. 2009. Paleomagnetic constraints on the Holocene stratigraphy of the Arctic Alaskan margin. Global and Planet. Change 68, 85-99.

Lund, S.P., Stoner, J.S., Channell, J.E.T., Acton, G., 2006a. A summary of Bruhnes paleomagnetic field variability recorded in Ocean Drilling Program cores. Phys. Earth Planet. Int. 156(3-4), 194-204.

Lund, S.P., Stoner, J., Lamy, F., 2006b. Late Quaternary paleomagnetic secular variation and chronostratigraphy from ODP sites 1233 and 1234, In: Tiedemann, R., Mix, A.C., Richter, C., Ruddiman, W.F. (Eds.) Proceedings of the Ocean Drilling Program, Scientific Results Volume 202.

Macrì, P., Sagnotti, L., Dinares-Turell, J., Caburlotto, A., 2005. A composite record of Late Pleistocene relative geomagnetic paleointensity from the Wilkes Land Basin (Antarctica). Phys. Earth Planet. Int. 151, 223–242.

Macrì, P.,Sagnotti, L., Dinarès-Turell, J., Caburlotto, A., 2010. Relative geomagnetic paleointensity of the Brunhes Chron and the Matuyama–Brunhes precursor as recorded in sediment core from Wilkes Land Basin (Antarctica), Phys. Earth Planet. Int. 179, 72-86.

Mayr, C., Wille, M., Haberzettl, T., Fey, M., Janssen, S., Lücke, A., Ohlendorf, C., Oliva, G., Schäbitz, F., Schleser, G.H., Zolitschka, B., 2007. Holocene variability of the Southern Hemisphere westerlies in Argentinean Patagonia (52°S). Quat. Sci. Rev. 26, 579–584.

Mazaud, A., Sicre, M.A., Ezat, U., Pichon, J.J., Duprat, J., Laj, C., Kissel, C., Beaufort, L., Michel, E., Turon, J.L., 2002. Geomagnetic-assisted stratigraphy and sea surface temperature changes in core MD94-103 (Southern Indian Ocean): possible implications for North–South climatic relationships around H4, Earth Planet. Sci. Lett. 201(1) 15, 159-170.

Mazaud A., 2005. User-friendly software for vector analysis of the magnetisation of long sediment cores, Geochem. Geophys. Geosyst., 6, 1-5.

Merrill, R. T. and McFadden, P. L., 1994. Geomagnetic field stability; reversal events and excursions. Earth Planet. Sci. Lett. 121, 57–69.

Muscheler, R., Beer, J., Kubik, P.W., Synal, H.-A., 2005. Geomagnetic field intensity during the last 60,000 years based on ^{10}Be and ^{36}Cl from the Summit ice cores and ^{14}C. Quat. Sci. Rev. 24, 1849-1860.

Nilsson, A., Muscheler, R., Snowball, I., Aldahan, A., Possnert, G., Augustinus, P., Atkin, D., Stephens, T., 2011. Multi-proxy identification of the Laschamp geomagnetic field excursion in Lake Pupuke, New Zealand, Earth Planet. Sci. Lett. 311(1-2), 155-164.

Nowaczyk, N. R. and Knies, J., 2000. Magnetostratigraphic results from the eastern Arctic Ocean: AMS ^{14}C ages and relative palaeointensity data of the Mono Lake and Laschamp geomagnetic reversal excursions. Geophys. J. Int. 140(1), 185-197.

Nowaczyk, N. R., Antonow, M., Knies, J., Spielhagen, R. F., 2003. Further rock magnetic and chronostratigraphic results on reversal excursions during the last 50 ka as derived from northern high latitudes and discrepancies in precise AMS ^{14}C dating, Geophys. J. Int. 155(5), 1065-1080.

Opdyke, N.D., Channell, J.E.T. 1996. Magnetic stratigraphy. San Diego, CA: Academic Press.

Paillard, D., Labeyrie, L., Yiou, P., 1996. Macintosh program performs time-series analysis. Eos Trans. AGU 77, 379.

Peck, J.A., King, J.W., Colman, S.M., Kravchinsky, V.A., 1996. An 84-kyr paleomagnetic record from the sediments of Lake Baikal Siberia. J. Geophys. Res. 101 (B5), 11365–11385.

Recasens, C., Ariztegui, D., Gebhardt, C., Gogorza, C., Haberzettl, T., Hahn, A., Kliem, P., Lisé-Pronovost, A., Lücke, A., Maidana, N.I., Mayr, C., Ohlendorf, C., Schäbitz, F., St-Onge, G., Wille, M., Zolitschka, B. and the PASADO Science Team, in press. New insights into paleoenvironmental changes in Laguna Potrok Aike, Southern Patagonia, since the Late Pleistocene: the PASADO multiproxy record. The Holocene.

Roberts, AP., 2008. Geomagnetic excursions: Knowns and unknowns, Geophys. Res. Lett., 35, L17307.

Roberts, A. P., and M. Winklhofer, 2004. Why are geomagnetic excursions not always recorded in sediments? Constraints from post-depositional remanent magnetisation lock-in modelling, Earth Planet. Sci. Lett. 227(3-4), 345-35.

Ross, P.-S., Delpit, S., Haller, M.J., Németh, K. et Corbella, H., 2011 Influence of the substrate on maar-diatreme volcanoes – an example of a mixed setting from the Pali Aike volcanic field, Argentina. Journal of Volcanology and Geothermal Research 201(1), 253-272.

Schaefer, J.M., Denton, G.H., Barrell, D.J.A., Ivy-Ochs, S., Kubik, P.W., Andersen, B.G., Phillips, F.M., Lowell, T.V., Schluchter, C., 2006. Near-synchronous interhemispheric termination of the last glacial maximum in mid-latitudes. Science 312, 1510-1513.

Schneider, D.A. and Mello, G.A., 1996. A high-resolution marine sedimentary record of geomagnetic intensity during the Brunhes Chron, Earth Planet. Sci. Lett. 144(1-2), 297-314.

Singer, B.S., 2007. Polarity transitions: radioisotopic dating. In: Bervera, E.H., Gubbins, D. (Eds.), Encyclopedia of Geomagnetism and Paleomagnetism. Springer-Verlag, pp. 834–839.

Singer, B.S., Guillou, H., Jicha, B.R., Laj, C., Kissel, C., Beard, B.L., Johnson, C.M., 2009. $^{40}Ar/^{39}Ar$, K–Ar and $^{230}Th–^{238}U$ dating of the Laschamp excursion: A radioisotopic tie-point for ice core and climate chronologies. Earth Planet. Sci. Lett. 286(1-2), 80-88.

Snowball, I. and Sandgren, P, 2004. Geomagnetic field intensity changes in Sweden between 9000 and 450 cal BP: extending the record of "archeomagnetic jerks" by means of lake sediments and the pseudo-Thellier technique, Earth Planet. Sci. Lett. 227, 361-376.

Stoner, S. J. and St-Onge, G., 2007. Magnetic stratigraphy in paleooceanography: reversal, excursion, paleointensity and secular variation. In: Proxies in Late Cenozoic Paleoceanography, Hillaire-Marcel, C. and de Vernal, A. (Eds.), Elsevier, pp.99-138.

Stoner, J.S., Laj, C., Channell, J.E.T., Kissel, C., 2002. South Atlantic and North Atlantic geomagnetic paleointensity stacks (0-80 ka): implications for inter-hemispheric correlation, Quat. Sci. Rev. 21, 1141-1151.

Stoner, J.S., Channell, J.E.T., Hodell, D.A., Charles, C.D., 2003. A 580 kyr paleomagnetic record from the sub-Antarctic South Atlantic (Ocean Drilling Program Site 1089), J. Geophys. Res. 108(B5), 2244.

Stoner, J.S., Jennings, A., Kristjánsdóttir, G.B., Dunhill, G., Andrews, J.T., Hardardóttir, J., 2007. A paleomagnetic approach toward refining Holocene radiocarbon-based chronologies: paleoceanographic records from the north Iceland (MD99-2269) and east Greenland (MD99-2322) margins. Paleoceanography 22, PA1209.

St-Onge, G., Stoner, J.S.,Hillaire-Marcel, C., 2003. Holocene paleomagnetic records fromthe St. Lawrence Estuary, eastern Canada: centennial- to millennial-scale geomagnetic modulation of cosmogenic isotopes. Earth Planet. Sci. Lett. 209, 113–130.

Sugden, D.A., McCulloch, R.D., Bory, A.J.-M., Hein, A.S., 2009. Influence of Patagonian glaciers on Antarctic dust deposition during the last glacial period, Nature geosciences 2, 281-285.

Tauxe, L., 1993. Sedimentary records of relative paleointensity of the geomagnetic field: theory and practice, Rev. Geophys. 31(3), 319-354.

Tauxe, L., 2005. Inclination flattening and the geocentric axial dipole hypothesis. Earth Planet. Sci. Lett. 233(3-4), 247-261.

Tauxe, L. and G. Wu, 1990. Normalized remanence in sediments of the Western Equatorial Pacific: relative paleointensity of the geomagnetic field? J. Geophys. Res. 95(B8), 12337-12350.

Tauxe, L., Pick, T., Kok, Y.S., 1995. Relative paleointensity in sediments: a pseudo-Thellier approach, Geophys. Res. Lett. 22, 2885– 2888.

Tauxe, L., Mullender, T.A.T., Pick, T., 1996. Potbellies, wasp-waists, and superparamagnetism in magnetic hysteresis, J. Geophys. Res. 101(B1), 571-583.

Teanby, N., Laj, C., Gubbins, D., Pringle, M., 2002. A detailed palaeointensity and inclination record from drill core SOH1 on Hawaii. Phys. Earth Planet. Int. 131, 101-140.

Wagner, G., Beer, J., Laj, C., Kissel, C., Masarik, J., Muscheler, R., Synal, H.-A., 2000. Chlorine-36 evidence for the Mono Lake event in the summit GRIP ice core, Earth Planet. Sci. Lett. 181, 1–6.

Weeks, R., Laj, C., Endigoux, L., Fuller,M., Roberts, A., Manganne, R., Blanchard, E., Goree,W., 1993. Improvements in long-core measurements techniques: applications in paleomagnetism and paleoceanography. Geophys. J. Int. 114, 651–662.

Willmott, V., Domack, E.W., Canals, M., Brachfeld, S., 2006. A high resolution paleointensity record from the Gerlache-Boyd paloe-ice stream region, northern Antarctic Peninsula, Quat. Res. 66, 1-11.

Xuan, C., and Channell, J.E.T., 2009. UPmag: MATLAB software for viewing and processing u-channel or other pass-through paleomagnetic data. Geochem. Geophys. Geosyst. 10, Q10Y07.

Xuan, C., and Channell, J.E.T., 2010. Origin of apparent magnetic excursions in deep-sea sediments from Mendeleev-Alpha Ridge, Arctic Ocean. Geochem. Geophys. Geosyst. 11, Q02003.

Zolitschka, B., Schäbitz, F., Lücke, A., Corbella, H., Ercolano, B., Fey, M., Haberzettl, T., Janssen, S., Maidana, N., Mayr, C., Ohlendorf, C., Oliva, G., M.Paez, M., Schleser, G.H., Soto, J., Tiberi, P., Wille, M., 2006. Crater lakes of the Pali Aike Volcanic Field as key sites for paleoclimatic and paleocological reconstructions in southern Patagonia, Argentina. J. South Am. Earth Sci. 21, 294-309.

Zolitschka, B., Anselmetti, F., Ariztegui, D., Corbella, H., Francus, P., Ohlendorf, C., Schäbitz, F and the PASADO Scientific Drilling team, 2009. The Laguna Potrok Aike Scientific Drilling Project PASADO (ICDP Expedition 5022). Scientific Drilling 8, 29-34.

Zhu, J., Lücke, A., Wissel, H., Mayr, C., Ohlendorf, C., Zolitschka, B., this issue. Environmental instability at the last Glacial-Interglacial transition in Patagonia, Argentina: the stable isotope record of bulk sedimentary organic matter from Laguna Potrok Aike. Quat. Sci. Rev.

CHAPITRE 2

INDICATEURS MAGNÉTIQUES DE L'INTENSITÉ DES VENTS ET DE LA POUSSIÈRE DANS LE SUD-EST DE LA PATAGONIE DEPUIS 51200 CAL BP À PARTIR DES SÉDIMENTS DU LAC LAGUNA POTROK AIKE

RÉSUMÉ

L'archive sédimentaire du lac *Laguna Potrok Aike* est unique dans le sud de l'Amérique du Sud puisque c'est le seul enregistrement paléoclimatique en continu depuis la dernière période glaciaire. Situé dans la zone d'influence des forts vents d'ouest de l'hémisphère Sud et dans la région source des poussières atmosphériques déposées sur les glaces Antarctiques durant les périodes glaciaires, le sud de la Patagonie constitue un endroit clé pour reconstituer l'activité éolienne. Des propriétés magnétiques et physiques ont été mesurées à haute résolution sur la longue séquence sédimentaire du projet *Potrok Aike maar lake Sediment Archive Drilling prOject* (PASADO) afin de développer des indicateurs magnétiques de l'activité éolienne dans le sud-est de la Patagonie depuis 51200 cal BP.

L'assemblage magnétique des sédiments est dominé par la magnétite détritique et le signal de susceptibilité magnétique (k_{LF}) est influencé à la fois par la concentration des minéraux ferrimagnétiques, la composition du sédiment et la taille des grains de magnétite. L'interprétation paléoenvironnementale de k_{LF} à l'échelle millénaire à séculaire est complexe à cause d'une relation inverse avec les indicateurs de la taille des grains magnétiques (e.g., kARM/IRM, MDF_{IRM}). À l'échelle multi-millénaire toutefois, la concentration des minéraux ferrimagnétiques est le principal contrôle de la k_{LF}, tel qu'indiqué par une estimation du flux de magnétite dans le lac et une comparaison avec des enregistrements de poussières venant de la Patagonie et déposées dans l'océan Austral et en

Antarctique. k_{LF} est interprété comme un indicateur de poussières dans la région source du sud de la Patagonie à l'échelle multi-millénaire.

La combinaison des propriétés magnétiques et physiques à haute résolution indique que le champ médian destructif de la magnétisation isothermale rémanente (MDF_{IRM}) reflète l'apport éolien de magnétite transporté au lac par suspension sur de courtes distances. MDF_{IRM} est donc interprété comme un indicateur de l'intensité des vents indépendant des changements hydrologiques dans le sud-est de la Patagonie. Une comparaison du nouvel indicateur éolien avec d'autres dérivés de sédiments marins, lacustres, de tourbière et de modelés karstiques disponibles dans l'hémisphère Sud durant la dernière période glaciaire et en Patagonie depuis la déglaciation révèlent une variabilité similaire jusqu'à une résolution séculaire.

ROCK-MAGNETIC PROXIES OF WIND INTENSITY AND DUST SINCE 51200 CAL BP FROM THE LACUSTRINE SEDIMENTS OF LAGUNA POTROK AIKE, SOUTHEASTERN PATAGONIA

Agathe Lisé-Pronovost[1,2], Guillaume St-Onge[1,2], Claudia Gogorza[3], Torsten Haberzettl[4], Guillaume Jouve[2,5], Pierre Francus[2,5], Joseph Stoner[6], Christian Ohlendorf[7], Catalina Gebhardt[7], Bernd Zolitschka[7] and the PASADO science team[8]

[1] Canada Research Chair in Marine Geology, Institut des sciences de la mer de Rimouski, Université du Québec à Rimouski, Rimouski, Canada

[2] GEOTOP Research Center, Montréal, Québec, Canada

[3]Instituto de Física Arroyo Seco, Universidad Nacional del Centro de la Provincia de Buenos Aires, Tandil, Argentina

[4] Institute of Geography, Friedrich-Schiller-University Jena, Jena, Germany

[5] Centre Eau, Terre et Environnement, Institut National de la Recherche Scientifique, Québec, Québec, Canada

[6]College of Ocean and Atmospheric Sciences, Oregon State University, Corvallis, United States

[7] GEOPOLAR, Institute of Geography, University of Bremen, Bremen, Germany

[8] http://www.icdp-online.org/front_content.php?idcat=1494

Abstract

The sedimentary archive from Laguna Potrok Aike is the only continuous record reaching back to the last Glacial period in continental Patagonia. Located in the path of the Southern Hemisphere westerly winds and in the source region of dust deposited in Antarctica during Glacial periods, southern Patagonia is a vantage point to reconstruct past changes in aeolian activity. Here we use a set of high-resolution rock-magnetic and sediment grain size properties measured on the Potrok Aike maar lake Sediment Archive Drilling prOject (PASADO) composite sequence (site 2) in order to build rock-magnetic proxies of aeolian activity at 52°S in southeastern Patagonia since 51,200 cal BP.

In Laguna Potrok Aike the magnetic assemblage is dominated by detrital magnetite and the magnetic susceptibility (k_{LF}) signal is influenced by ferrimagnetic mineral concentration changes, sediment composition and magnetite grain sizes. The paleoenvironmental interpretation of k_{LF} at the millennial to centennial-scale is hampered by an inverse relationship to magnetite grain size (e.g., kARM/IRM, MDF_{IRM}). At the multi millennial-scale however, the concentration of ferrimagnetic mineral dominantly controls k_{LF} as indicated by the estimated flux of magnetite to the lake and comparison with distal dust records from the Southern Ocean and Antarctica. k_{LF} is interpreted as a dust indicator in the dust source of southern Patagonia at the multi millennial-scale.

High-resolution rock-magnetic and physical grain size analyses indicate that the median destructive field of the isothermal remanent magnetisation (MDF_{IRM}) mostly reflect aeolian input of silt-sized magnetite brought to the lake by short-term suspension. MDF_{IRM} is thus interpreted as a wind intensity proxy independent of moisture changes in southeastern Patagonia. Comparison with wind intensity proxies from the Southern Hemisphere during the last Glacial period and with regional records from Patagonia since the deglaciation including marine, lacustrine and peat bog sediments as well as speleothems reveals similar variability with MDF_{IRM} up to the centennial-scale.

Keywords

Rock magnetism, Wind intensity, dust, Southern Hemisphere westerly winds, Last Glacial period, lake sediment, Laguna Potrok Aike, Patagonia, magnetic susceptibility

1. Introduction

The southern Hemisphere westerly winds (SWW) are of great importance to oceanic circulation and global climate of the last Glacial period and termination (e.g., Anderson et al., 2009; Sijp and England, 2008; Toggweiler et al., 2006). Yet the latitudinal position and intensity of the SWW in the past relative to today are unclear and remain an open question (Kohfeld et al., 2013). Patagonia is one of the five major dust producing regions of the globe (Roberts et al., 2011) and of particular interest because it is identified as the source area for dust deposited in Antarctica during the last glacial cycles (Basile et al., 1997; Delmonte et al., 2010, 2004; Gaiero, 2007; Petit et al., 1999; Sugden et al., 2009). Dust emission is believed to be related to changes in environmental conditions and possibly wind intensity (e.g., Muhs, 2013; Basile et al., 1997; Sudgen et al., 2009). Sudgen et al. (2009) argue that Patagonian glacier discharge into outwash plains or proglacial lakes acted like an on/off switch for dust deposition in Antarctica, hence providing evidence for environmental control on the sediment supply during the last Glacial. In contrast, there is to date no Glacial record of paleo-wind intensities in southern Patagonia, where the available records mainly reach back to the Holocene and deglacial periods (e.g., Villa-Martinez and Moreno, 2007; Bjork et al., 2012; Lamy et al., 2010; Mayr et al., 2007a; Moreno et al., 2012, 2009; Waldman et al., 2010). In order to fully address dust emission in southern Patagonia during the last Glacial and better constrain past changes in the SWW, paleo-wind intensity records from the source region of dust deposited in Antarctica is much needed.

Paleo-wind indicators in southern Patagonia are commonly moisture proxies (e.g., pollen, paleo-fire history, lake level, and mineralogical data) assuming a major control of wind intensity on rainfall (Kilian and Lamy, 2012; Kohfeld et al., 2013). However on the eastern side of the Andes, precipitation is only weakly correlated to westerly wind strength because the very low precipitation mostly comes from the east and south-west (Garreaud et al., 2013) and evaporation strongly influences the available moisture (Lamy et al., 2010; Moy et al., 2008; Ohlendorf et al., 2013). As a result, numerous moisture-related wind intensity proxies can be difficult to interpret (Fletcher and Moreno, 2012; Moreno et al.,

2009) and there is a need for different types of wind intensity proxies in southeastern Patagonia.

The long sedimentary archive from Laguna Potrok Aike is the only continuous paleoenvironmental archive from this region reaching back to the last Glacial period (Kilian and Lamy, 2012; Zolitschka et al., 2013). Interestingly, Haberzettl et al (2009) recently revealed that the millenial-scale variability of magnetic susceptibility measured on a short sediment core from the lake shoulder vary like the non-sea-salt calcium (a dust proxy) from the Antarctic ice core EDC (Röthlisberger et al., 2002), hence providing the first evidence of contemporaneous deposition of aeolian sediment in the dust source (southern Patagonia) and distal mineral dust in Antarctica during the last Glacial. The magnetic susceptibility is a measurement reflecting how "magnetisable" the sediment is and while it often primarily reflects changes in the concentration of ferrimagnetic minerals, it can also be significantly influenced by dia- antiferro- para- and superparamagnetic materials when the concentration of ferrimagnetic mineral is low, as well as changes in the magnetic grain sizes (e.g., Dearing, 1999; Liu et al., 2012). Hence interpreting magnetic susceptibility records is not straightforward and detailed rock-magnetic study from Laguna Potrok Aike is necessary to investigate its environmental significance, as pointed out by Haberzettl et al (2009) as well as Maher et al. (2011) reviewing the paleoclimatic significance of Quaternary aeolian dusts and sediments magnetic properties. Here we use high-resolution rock-magnetic data from the sediment deposited in the central basin of Laguna Potrok Aike in order to 1) investigate what controls the magnetic susceptibility signal, and 2) present a new proxy of wind intensity in southern Patagonia since 51,200 cal BP.

2. Geological setting

Laguna Potrok Aike (51°58'S, 70°23'W; 113 m a.s.l.) is a maar lake in the Pali Aike volcanic field of southern Argentina (Figure 1). The maximum water depth is 100 m and the maximum diameter is 3.5 km (Haberzettl et al., 2005; Zolitschka et al., 2009). The lake is located in the mid-latitudes of the Southern Hemisphere, presently at the southern limit of the strong SWW belt, where winds can reach monthly average speed about 10 ms^{-1} at the

beginning of the summer (Schäbitz et al., 2013). On the lee-side of the Andean Cordillera, the annual precipitation is low (ca. 200 mm/yr; Mayr et al., 2007b; Ohlendorf et al., 2013), the climate is semi-arid and the vegetation is characterized by a dry steppe (Schäbitz et al., 2013; Wille et al., 2007). Precipitation in this area mostly originates from moist Atlantic air masses at times of weaker SWW (Mayr et al., 2007b; Ohlendorf et al., 2013). There is currently no permanent surface inflow from the catchment area (200 km^2 in size) and no outflow (Haberzettl et al., 2005; Zolitschka et al., 2009). These particular geographical, climatic and geomorphological setting result in frequent sediment remobilisation events (Kliem et al., 2013a) and suggests that detrital sediments are brought to the lake primarily by wind and subordinated by episodic runoff.

The surface geology of the region (Figure 1B) is dominated by semi-consolidated sedimentary rocks of the Miocene Santa Cruz Formation (sandstone and siltstone) that are 660 meters thick and extensively crops out around Laguna Potrok Aike (Coronato et al., 2013). Also present are Mio-Pliocene basalts and pyroclastic sediments, and unconsolidated Quaternary deposits including tills, glaciofluvial, fluvial, lacustrine and aeolian sediments (Coronato et al., 2013; D'Orazio et al., 2000; Ross et al., 2011; Zolitschka et al., 2006). Only minor modification to the overall landscape occurred since the phreatomagmatic formation of the maar in the Middle Pleistocene (Coronato et al., 2013; Zolitschka et al., 2013).

Figure 2. 1. A) Aerial photograph and bathymetry from Laguna Potrok Aike in Southern Argentina. Position of the PASADO coring sites as well as cores from previous studies is indicated. B) Geological and geomorphological map of regional surface deposits in the Pali Aike Volcanic Field (modified from Ross et al., 2011).

A)

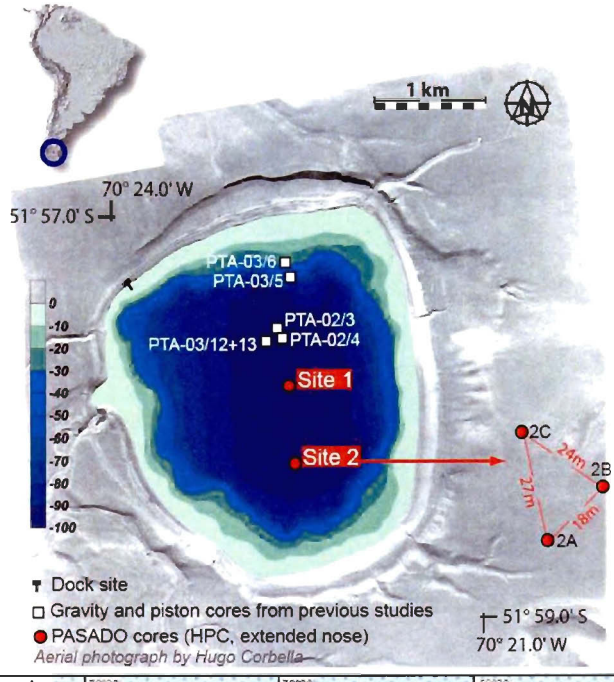
1 km
70° 24.0' W
51° 57.0' S
PTA-03/6
PTA-03/5
PTA-02/3
PTA-02/4
PTA-03/12+13
Site 1
Site 2
2C
2B
2A
24m
27m
18m
0
-10
-20
-30
-40
-50
-60
-70
-80
-90
-100
Dock site
Gravity and piston cores from previous studies
PASADO cores (HPC, extended nose)
Aerial photograph by Hugo Corbella
51° 59.0' S
70° 21.0' W

B)

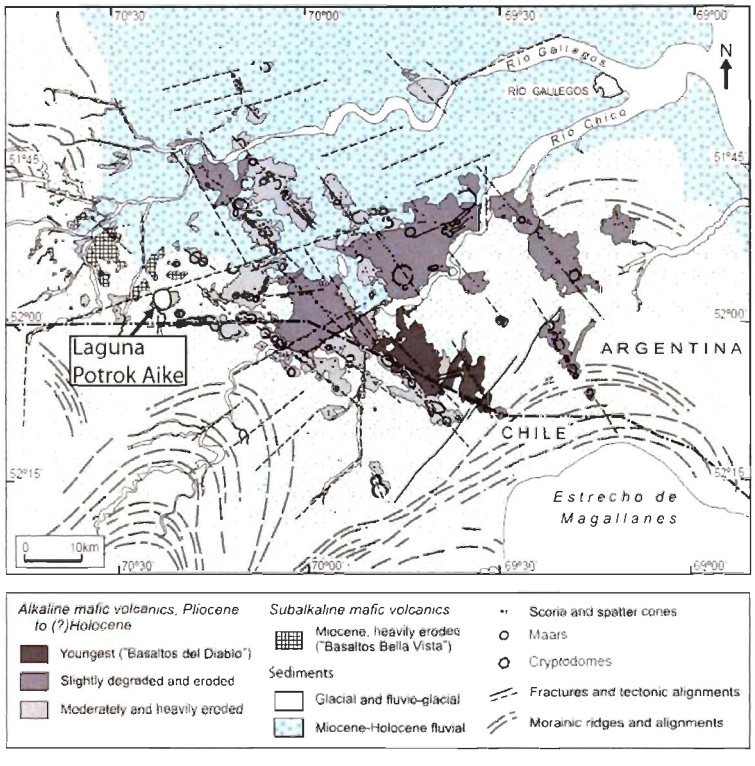
70°30
70°00
69°30
69°00
N
Río Gallegos
RIO GALLEGOS
Río Chico
51°45
52°00
52°15
Laguna
Potrok Aike
ARGENTINA
CHILE
Estrecho de
Magallanes
0
10km

Alkaline mafic volcanics, Pliocene to (?)Holocene
Youngest ("Basaltos del Diablo")
Slightly degraded and eroded
Moderately and heavily eroded
Subalkaline mafic volcanics
Miocene, heavily eroded ("Basaltos Bella Vista")
Sediments
Glacial and fluvio-glacial
Miocene-Holocene fluvial
Scoria and spatter cones
Maars
Cryptodomes
Fractures and tectonic alignments
Morainic ridges and alignments

3. Methods

3.1 Coring and sampling

The international science team of the Potrok Aike maar lake Sediment Archive Drilling prOject (PASADO) cored the sediments of Laguna Potrok Aike in the framework of the International Continental scientific Drilling Program (ICDP) during austral spring 2008. The sedimentary infill of the maar was sampled up to a depth of ca. 100 meters at two sites in the central basin using a hydraulic piston corer on the GLAD800 platform operated by DOSECC (Drilling, Observation and Sampling of the Earths Continental Crust).

Site 2 (Figure 1A) was selected as the principal record for the multi-proxy PASADO paleoenvironmental studies because of higher core recovery and lower apparent sand content than site 1 (Zolitschka et al., 2009). The composite sedimentary sequence was established from three holes at site 2 and is 106.09 meters long (Kliem et al., 2013a). It was continuously sampled for paleomagnetic and rock-magnetic analyses using u-channels (2x2 cm section plastic liner) at the University of Bremen in June 2009.

3.2 Rock-magnetic measurements

Rock-magnetic measurements were performed at 1-cm intervals at the *Institut des sciences de la mer de Rimouski* (ISMER). Magnetic susceptibility was measured on u-channel samples using a Bartington point sensor MS2E (Dearing, 1999) mounted on an automatic GEOTEK Multi Sensor Core Logger (e.g., Stoner and St-Onge, 2007). The anhysteretic remanent magnetisation (ARM) was induced in a peak alternative field of 100 mT in the presence of a weak direct current (DC) biasing field of 0.05 mT. The isothermal remanent magnetisation (IRM) was imparted using the pulse magnetizer in a DC field of 300 mT. Both remanent magnetisations were step-wise demagnetized and measured with a minimum of 8 steps (0, 10, 20, 30, 40, 50, 60, 70 mT) using a 2G Enterprises cryogenic magnetometer for u-channel.

ARM and IRM are primarily related to the concentration of ferrimagnetic grains and they are also influenced by the magnetic domain state. Single domain (SD) grains more easily acquire ARM than multi domain (MD) grains (e.g., Maher, 1988; Dunlop and Ozdemir 2007; Evans and Heller, 2003; King et al., 1982) and as a result, the grains acquiring an ARM are typically smaller (< 10 μm) than the grains acquiring an IRM (>10 μm and up to a few tens of μm) (Stoner et al., 1996; Peter and Dekkers, 2003). The susceptibility of anhysteretic remanent magnetisation (kARM) is calculated by dividing the ARM with the DC bias field. kARM is a measure of the magnetic concentration and grain size, commonly used as a magnetic grain size indicator as a ratio with magnetic susceptibility or IRM (e.g., kARM/k, kARM/IRM) (e.g., Egli, 2004; Maher, 1988; Evans and Heller, 2003; Stoner and St-Onge, 2007; Banerjee et al., 1981; King et al., 1982). The median destructive field (MDF) is the required field to demagnetise half of the initial remanent magnetisation of a sample. Within uniform mineralogy, MDF indicates magnetic grain size with coarser grains displaying lower values and vice-versa (e.g., Tauxe, 2010).

In the particular geological settings of Laguna Potrok Aike, detrital sediments (including magnetite) are most probably brought to the lake primarily by winds and as a result the concentration of ferrimagnetic mineral is likely to follow changes in sedimentation rates. The estimation of the magnetite flux (Fmag) to the coring site is calculated in order to evaluate the influence of concentration changes on the k_{LF} record. Based on previous magnetic mineralogy investigations from Laguna Potrok Aike including temperature-dependent magnetic susceptibility, shape of the hysteresis loop, s-ratio (IRM_{300mT}/IRM_{1200mT}), thermal demagnetisation after induction of a saturating field, and X-ray diffraction analyses (Gogorza et al., 2012; 2011; Lisé-Pronovost et al., 2013; Recasens et al., 2012), it was shown that magnetite dominates the magnetic assemblage. If the concentration of magnetite is the only control on k_{LF}, one would expect Fmag to be the same as k_{LF}. Differences between Fmag and k_{LF} would in turn indicate that changes in magnetite grain size also influence k_{LF}. Following the method previously used by Mazaud et al. (2010, 2007), Fmag is calculated with equation 1 using the volumetric low field magnetic susceptibility (k_{LF}), the sedimentation rate derived from the radiocarbon-based

chronology (sedrate; Kliem et al., 2013a) and a theoretical mass specific magnetic susceptibility value of 5.96 10^{-3} m^3 kg^{-1} for magnetite (Kmag) (Dearing, 1999).

$$Fmag = (k_{LF}/Kmag) \times sedrate \qquad \text{Equation 1}$$

3.3 Physical grain size measurement

Physical grain size measurements were conducted at ca. 8-cm intervals at the University of Bremen. Freeze-dried and homogenized samples were pre-treated with 5% NaClO over 4 days to remove organic material. The sediment was then washed with demineralized water until a pH of 7-8 was reached, and charged with calgon some 24 h before measurements were carried out in order to prevent flocculation of particles. Grain-size analyses were performed using a laser diffraction particle size analyzer (LS 200, Beckman Coulter) equipped with a variable-speed fluid module which measures particles from 0.4 to 2000 μm.

3.4 Lithology

Five lithological units were described for the composite sediment record (106.09 m cd) of Laguna Potrok Aike reaching back to 51,200 cal BP (Kliem et al., 2013a). The units are based on the type of pelagic sediment and the frequency of mass movement deposits (MMD) and include: (A) pelagic laminated silts, (B) pelagic laminated silts intercalated with thin fine sand and coarse silt layers, (C) alternation of A and B with an increase in the frequency and thickness of MMD from C-1 to C-3. MMD are classified as ball and pillow structures, normally graded beds, structureless sand and fine gravel layers, matrix supported layers and one folded sediment structure (Kliem et al., 2013a). Here we present results from the event-corrected composite depth (45.8 m cd-ec), comprising pelagic sediment deposited at an average rate of 80 cm ka^{-1} (207 cm ka^{-1} including the MMDs; Kliem et al., 2013a).

3.5 Chronology

The chronology of the PASADO site 2 pelagic sediment sequence is based on 58 radiocarbon dates and the age model was built using a mixed-effect regression procedure (Kliem et al, 2013a) (Figure 2). The age model is supported by lithological and tephra correlation with previously studied cores from Laguna Potrok Aike, including a core located nearby in the lake center and covering the last 16,000 cal. BP (PTA03/12+13; location on Figure 1A; Haberzettl et al., 2007) and a low-resolution core from a lake level terrace reaching back to the last Glacial period (PTA03/5+ 6; location on Figure 1A; Haberzettl et al., 2009). The age uncertainty is larger at the base of the record because of the increased occurrence of MMD and because the time period approaches the limit of radiocarbon dating. Nonetheless, magnetostratigraphy using the relative paleointensity record supports the chronology in this problematic interval (Kliem et al., 2013a; Lisé-Pronovost et al., 2013).

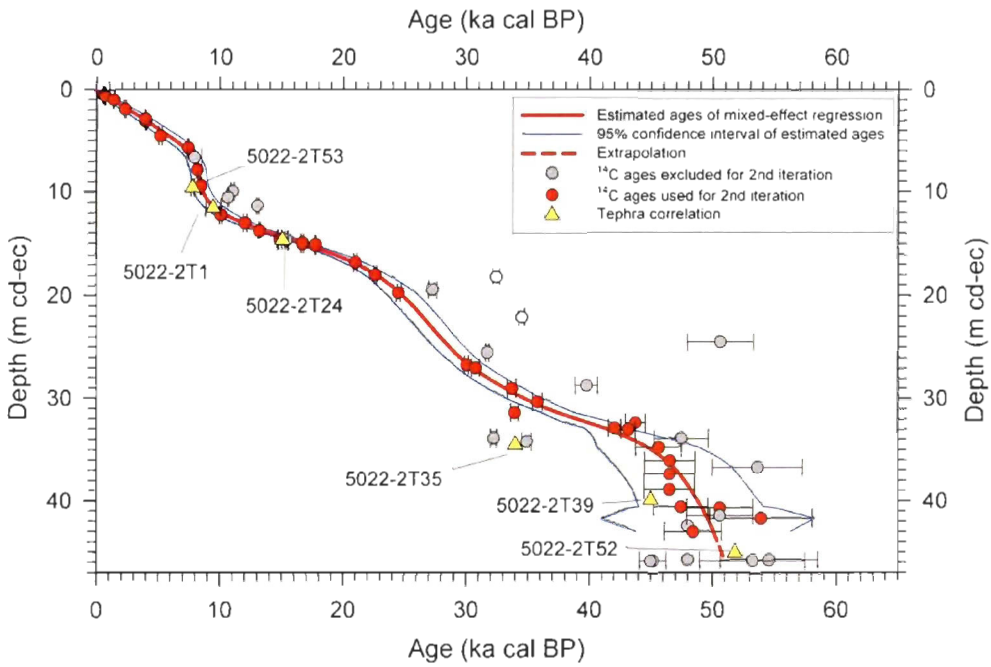

Figure 2. 2. Radiocarbon-based age model for the sedimentary record of PASADO site 2 (modified from Kliem et al., 2013). Radiocarbon dates and tephra correlation are presented along the event-corrected composite depth (cd-ec), after removal of mass movement deposits. The red line is the estimated age after two iterations of the mixed-effect regressions using the constant-variance function (for more details, see Kliem et al., 2013).

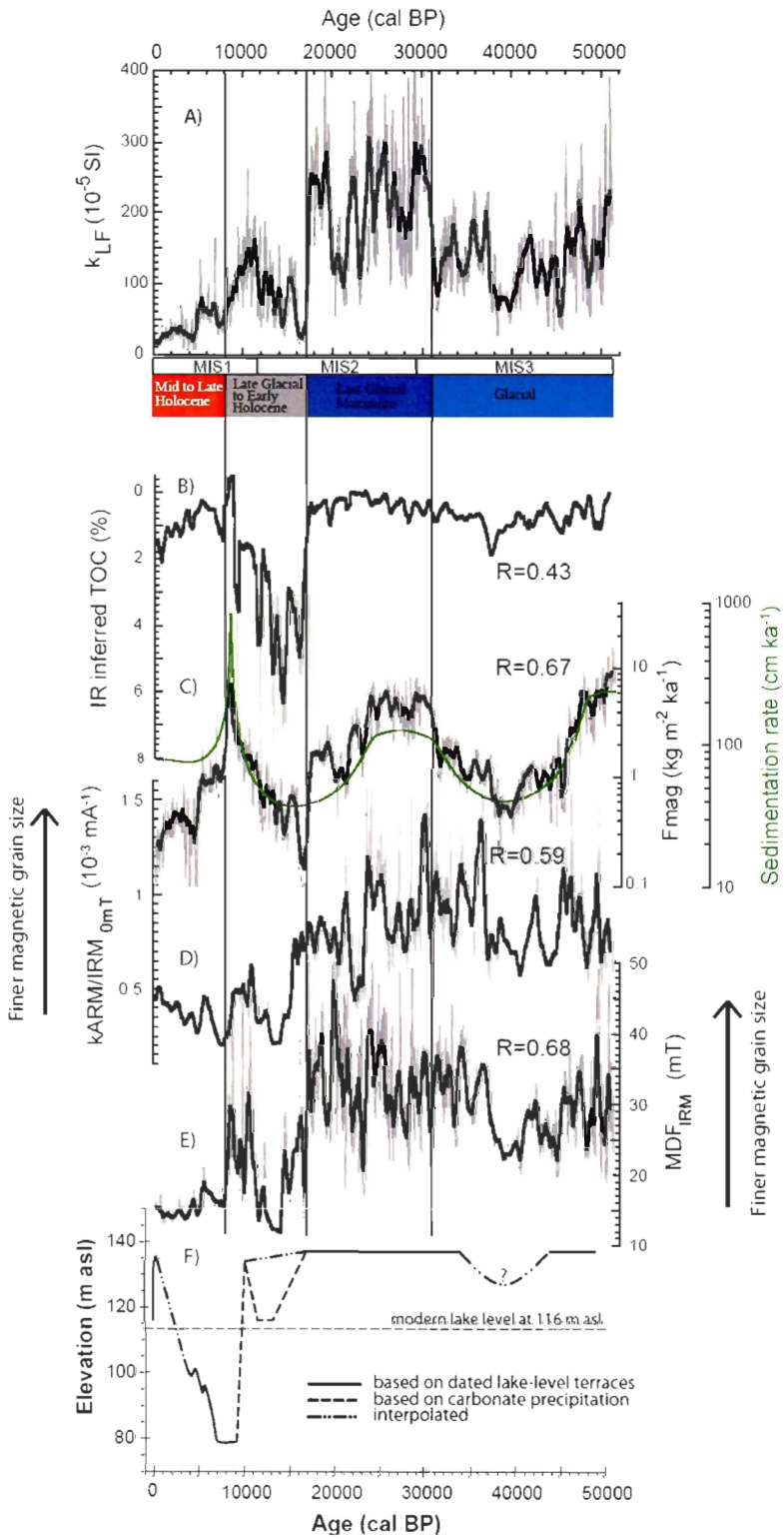
Age (cal BP)
0
10000
20000
30000
40000
50000
A)
k_{LF} (10^{-5} SI)
MIS1
MIS2
MIS3
Mid to Late Holocene
Late Glacial to Early Holocene
Glacial
B)
IR inferred TOC (%)
R=0.43
C)
R=0.67
Fmag (kg m^{-2} ka^{-1})
Sedimentation rate (cm ka^{-1})
Finer magnetic grain size
kARM/IRM$_{0mT}$ (10^{-3} mA^{-1})
R=0.59
D)
R=0.68
E)
MDF$_{IRM}$ (mT)
Finer magnetic grain size
F)
Elevation (m asl)
modern lake level at 116 m asl.
based on dated lake-level terraces
based on carbonate precipitation
interpolated
Age (cal BP)

Figure 2. 3. A) The low field volumetric magnetic susceptibility record (k_{LF}) from Laguna Potrok Aike compared with B) the infrared inferred total organic carbon (IR inferred TOC; Hanh et al., 2013), C) the calculated flux of magnetite to the lake floor (Fmag) and sedimentation rates (Kliem et al., 2013a), D) the ratio $kARM/IRM_{0mT}$, E) the median destructive field of the isothermal remanent magnetisation (MDF_{IRM}) and F) the lake level reconstruction (Zolitschka et al., 2013). Each rock-magnetic parameter was interpolated to 10 yr interval (lower than the average initial resolution of 11.34 yr; Kliem et al., 2013) and smoothed over 50 data points in order to obtain the millennial-scale variability. For each parameter the R coefficient (n= 5066) with k_{LF} is indicated. Climatic periods inferred from rock-magnetic parameters and previous sedimentological studies from Laguna Potrok Aike (Hahn et al., 2013; Kliem et al., 2013) as well as marine isotopic stages (MIS) according to Lisiecki and Raymo (2005) are indicated.

4. Results

4.1 Rock-magnetic stratigraphy

Parameters used for stratigraphic purposes are those displaying greater variability and include volumetric low field magnetic susceptibility (k_{LF}), susceptibility of the anhysteretic remanent magnetisation (kARM), median destructive field of the isothermal remanent magnetisation (MDF_{IRM}) and the magnetic interparamagnetic ratio kARM/IRM (Fig. 3). Four main units stand out: from the base of the record (51,200 cal BP) to 31,500 cal BP, 31,500-17,300 cal BP, 17,300-8100 cal BP and 8100-0 cal BP. These four rock-magnetic units are in general agreement with the lithostratigraphic units C-3/2, C-1, B and A described by Kliem et al. (2013a) (see the logs on Fig. 4) and interpreted from sedimentological analyses as the following climatic periods: the Glacial period (C-3/2), the Last Glacial Maximum (C-1), the Late Glacial to Early Holocene (B) and the mid to Late Holocene (A) (Hahn et al., 2013; Kliem et al., 2013a).

The unit from the base of the record (51,200 cal BP) to 17,300 cal BP corresponds to the Last Glacial period. It is characterized by distinctively finer magnetic grains, as indicated by the kARM/IRM ratio and MDF_{IRM} (Figs. 3 and 4). It is also characterized by relatively high amplitude changes in proxies of magnetic grain size and concentration, notably during the last Glacial Maximum (31,500-17,300 cal BP; Fig. 3). The last Glacial

Maximum period is delimited by a sharp change to higher values of k_{LF} at 31,500 cal BP and a sharp decrease at 17,300 cal BP (Fig. 3A). The Late Glacial to Early Holocene period (17,300-8100 cal BP) presents intermediate values of magnetic grain size and concentration proxies, with relatively high amplitude of change (Figs. 3 and 4). At the onset of the deglaciation in the mid-latitudes of the Southern Hemisphere (17,300 cal BP; Schaefer et al., 2006), the organic content in the sediments of Laguna Potrok Aike increases drastically (Fig. 3B; Hahn et al., 2013). This is mainly related to the high vesicularity of micropumice fragments that enrich the sediment until 11,700 cal BP (Jouve et al., 2013). Thus, this dilutes the detrital input with much less magnetic grains and the concentration-dependent parameters such as k_{LF} and the calculated Fmag decrease (Figs. 3A and C). The mid- to Late Holocene unit (since 8100 cal BP) is characterized by distinctively coarser magnetic grains acquiring an IRM (e.g., MDF_{IRM}, Figs. 3E and 4) and lower concentration of magnetic minerals (Fig. 4).

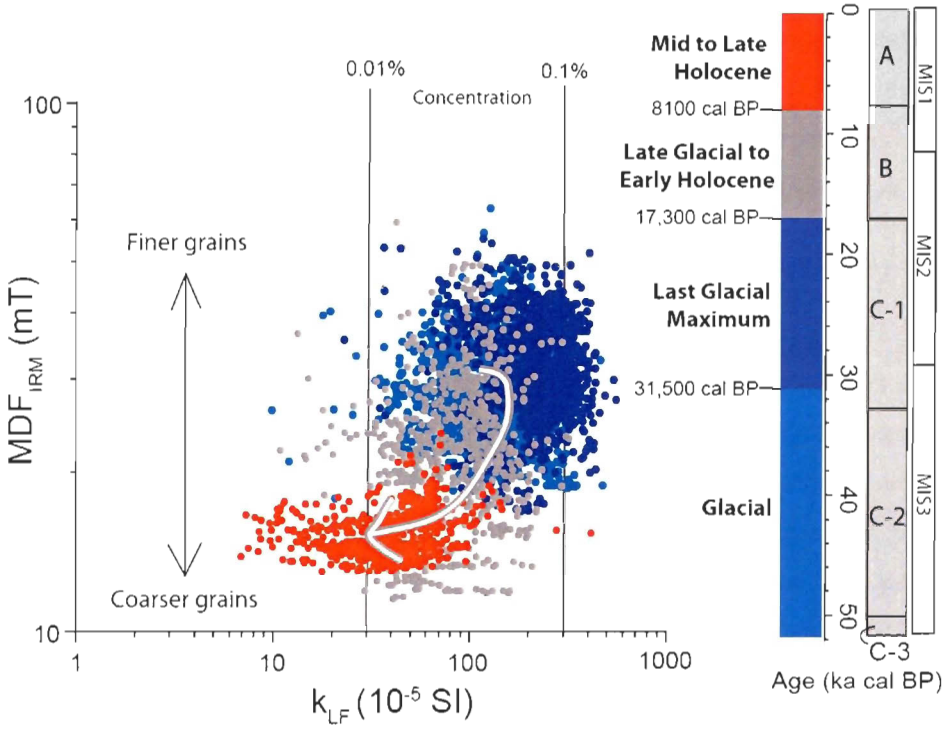

Figure 2. 4. Biplot of the low field volumetric magnetic susceptibility (k_{LF}) with the median destructive field of the isothermal remanent magnetisation (MDF_{IRM}). Data from different climatic periods are identified with colors and reported to the right. The arrow indicates the chronological change since 51,200 cal BP. The marine isotopic stage (MIS) according to Lisiecki and Raymo (2005) and the simplified lithostratigraphic log from Kliem et al. (2013) are also shown. The volumetric concentration of ferrimagnetic material is estimated from the k_{LF} values (Thompson, 1986) and indicated as vertical lines.

4.2 Control on magnetic susceptibility

The magnetic susceptibility of sediments is primarily influenced by the concentration of ferrimagnetic minerals, and also related to the sediment composition, the magnetic mineralogy and grain size (Dearing, 1999). Considering that magnetite undoubtedly dominates the magnetic assemblage of the PASADO record (Gogorza et al., 2012; Lisé-Pronovost et al., 2013; Recasens et al., 2012) and that magnetite is 3 to 4 orders of

magnitude more magnetic than antiferromagnetic minerals such as hematite, and paramagnetic compounds such as clays (Dearing, 1999; Gubbins and Herrero-Bervera, 2007), the magnetic susceptibility record from Laguna Potrok Aike is interpreted as reflecting changes in 1) the concentration and 2) the grain size of magnetite, rather than mineralogical changes.

4.2.1 Concentration of magnetite

The change in the concentration of magnetic minerals is estimated with the flux of magnetite (Fmag) to the lake (Figure 3C). The average value of Fmag at Laguna Potrok Aike using the millennial-scale variability for the Glacial period (51,200-17,300 cal BP) and for the Late Glacial and Holocene (since 17,300 cal BP) is 2.63 and 1.00 kg m^{-2} ka^{-1}, respectively. These values are in the same order of magnitude as the present-day iron flux to the Patagonian coast (Gaiero et al., 2003), iron-oxides concentration in Argentinean loess deposits (Sayago et al., 2001), as well as model output for dust deposition in Patagonia (Zender, 2003; Mahowald et al., 2006) and in the Atlantic sector of the Southern Ocean (Roberts et al., 2011), suggesting that Fmag is a realistic estimation of the magnetite flux to Laguna Potrok Aike. Figure 3A and C reveals that the sedimentation rate and Fmag on log scales follow the multi-millennial-scale trends of k_{LF} (R=0.67). The similar variability using log scales points to aeolian transport of detrital magnetite to Laguna Potrok Aike because the transport of particles by wind is an exponential function of wind velocity (e.g. Pye, 1995; Maher et al., 2010). k_{LF} and Fmag both display sharp changes at 31,500 and 17,300 cal BP (Figures 3A,C and 4), however the millennial- to centennial-scale high amplitude changes in k_{LF} are not reproduced in Fmag, notably during the Glacial period (before 17,300 cal BP; Figure 3). These observations 1) reveal that the concentration of ferrimagnetic minerals apparently controls the multi-millennial-scale trends in k_{LF} and 2) points to a significant influence of magnetite grain sizes on k_{LF} at the millennial- to centennial-scale.

4.2.2 Grain size of magnetite

Previous studies investigating the influence of the physical grain size of magnetite on magnetic susceptibility reveal mixed results and overall suggest there is no predicable relationship between these two parameters for the grain size range 0.09-6000 μm (Brachfeld, 1999 and references therein; Dearing, 1999; Tauxe, 2010; Heider et al., 1996). At Laguna Potrok Aike, the magnetic grain size indicators kARM/IRM and MDF_{IRM} (Figs. 3D and E) indicate that finer magnetic grain sizes correlates with stronger magnetic susceptibilities (see also Lisé-Pronovost et al., 2013). While the MDF_{NRM} and MDF_{ARM} do not correlate with k_{LF} (R= 0.05 and 0.03, respectively), MDF_{IRM} is the magnetic grain size indicator with the strongest correlation to k_{LF} (R= 0.68) and its millennial- to centennial-scale high amplitudes variability resemble those of k_{LF} (Figs. 3A and E). This is supported by a coherence analysis using the software Analyseries software (Paillard et al., 1996) between the two rock-magnetic parameters indicating that MDF_{IRM} and k_{LF} are coherent at periods less than 135 years, at periods centered at ca.170, 250, 500, 1000 and more than 5000 years (Fig. 5). A closer look at the correlation between magnetic susceptibility and the magnetite grain size proxy MDF_{IRM} with physical grain size intervals (Udden, 1914; Wentworth, 1922) (Table 1) reveals that the coarse to medium silt fractions hold most of the rock-magnetic grain size information in our record. This sediment fraction roughly corresponds to the first fraction moved by winds (Hjulström, 1935; Tucker, 1991). It is thus typical of some loess deposits and more specifically of short-term aeolian transport in near-surface to low suspension clouds (Vandenberghe, 2013 and references therein). Similar results linking silt-sized particles and magnetic grain size were previously observed for aeolian iron oxides in paleosols of the semi-arid Colorado Plateau (Reynolds et al., 2006) and for sediments of the northern North Atlantic region (Hatfield et al., 2013). The rock-magnetic and physical grain size data from the sediment of Laguna Potrok Aike indicate that the millennial- to centennial-scale variability of the k_{LF} signal is inversely correlated to magnetite grain size changes in the coarse to medium silt fraction.

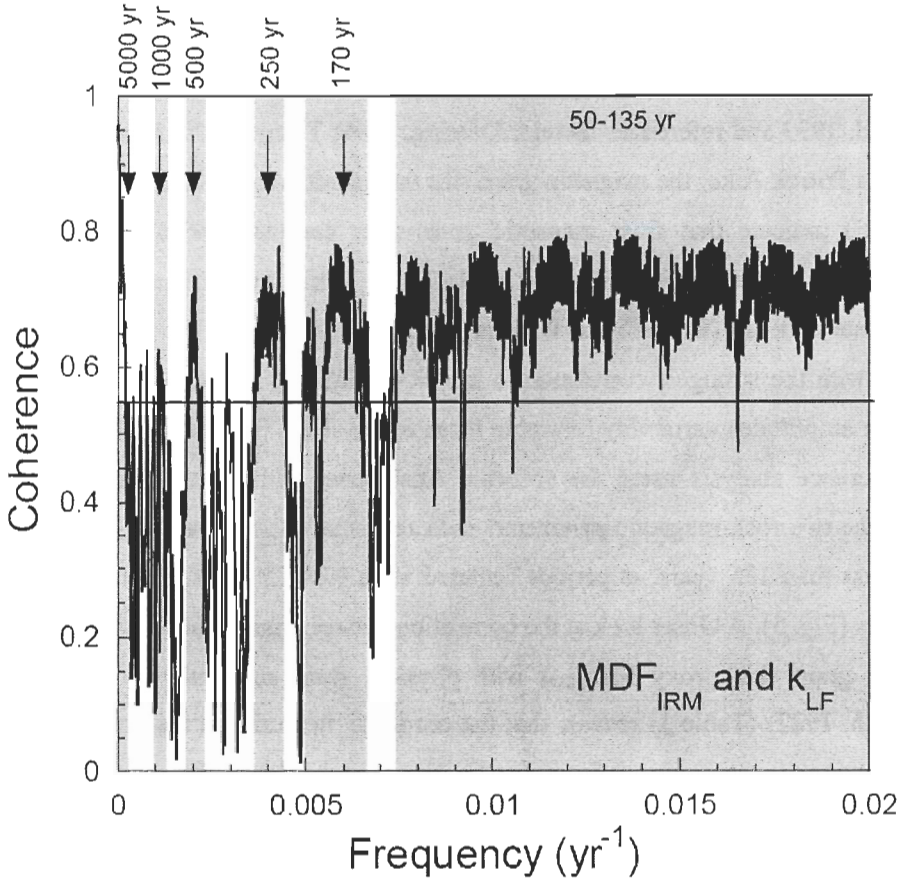

Figure 2. 5. Coherence of MDF_{IRM} and the k_{LF} signals using a Blackman-Tukey spectrum and a Bartlett window in software Analyseries (Paillard, 1996). Non-zero coherence (95%) over the horizontal line is mostly found at periods less than 135 years and around 170, 250, 500, 1000 and 5000 years, as indicated by grey intervals.

Table 2. 1. Correlation coefficient (R) of physical grain size classes with the median destructive field of the isothermal remanent magnetisation (MDF_{IRM}) and the magnetic susceptibility (k_{LF}). Data were interpolated in 10 a intervals and smoothed over 50 points in order to obtain the millennial-scale variability and calculate R coefficients on a common scale (n=5066). Both rock-magnetic parameters are best correlated to the coarse to medium silt fraction.

Physical grain size[1]		Magnetic grain size	Magnetic grain size and concentration
Class	(μm)	(MDF_{IRM})	(k_{LF})
Bulk		**0,26**	**0,36**
Fine sand	125-250	0,11	0,25
Very fine sand	63-125	0,40	0,45
Very coarse silt	31-63	0,04	0,14
Coarse silt	**16-31**	**-0,66**	**-0,59**
Medium silt	**8-16**	**-0,53**	**-0,56**
Fine silt	4-8	-0,27	-0,37
Very fine silt	2-4	-0,05	-0,18
Clay	<2	0,21	0,06

[1]The grain size intervals are from Udden (1914) and Wentworth (1922)

5. Discussion

5.1 Interpretation of magnetic susceptibility

Rock magnetic control on the magnetic susceptibility record from Laguna Potrok Aike is investigated in order to interpret its environmental signal. The results indicate that higher (lower) values of magnetic susceptibility reflect more (less) magnetite and/or smaller (coarser) grains. Higher amount of magnetite grains brought to the lake during the Last Glacial can possibly be attributed to the activation of a glacial source richer in detrital magnetite and/or a larger surface of erodible land such as outwash plains (Sugden et al., 2009), increased runoff due to permafrost (Kliem et al., 2013b), and/or enhanced gustiness

(McGee et al., 2010) capable of transporting more detrital magnetite to the lake. However the interpretation of the magnetic susceptibility signal with respect to winds is complicated by its inverse relation to magnetite grain size (Fig. 3). For example, windstorm can reasonably be expected to bring more and coarser magnetite grains to the lake, which will tend to increase and lower k_{LF}, respectively. Hence the k_{LF} signal from Laguna Potrok Aike is not straightforward because of the dual control of magnetite grains concentration and size.

Nevertheless comparison of the high-resolution k_{LF} record from Laguna Potrok Aike with the flux of dust to the Dome C ice core, Antarctica (Lambert et al., 2012) (Fig. 6A and C) reveals a similar multi-millennial variability during the last Glacial period, as was first pointed out by Haberzettl et al. (2009) using a low resolution record from a lake level terrace (core location on Fig. 1). Figure 6B also presents the magnetic susceptibility of a marine core in the Scotia Sea interpreted as a distal dust record from southern Patagonia (Weber et al., 2012). All records are smoothed to common millennial-scale variability for comparison purposes (thick lines, Fig. 6). The fluctuations from 51,200 to 17,300 cal BP can be correlated among the three records in the limit of the chronologies and common peak values are indicated with lowercase letters on figure 6A, B and C. In particular, all records display large amplitude change at 31,500 cal BP (before feature *d*) and 17,300 cal BP (after feature *a*) also observed in the estimated flux of magnetite to Laguna Potrok Aike (Fmag; Fig. 3C) but absent in the magnetic grain size indicators kARM/IRM and MDF_{IRM} (Fig. 3D and E), thus hinting at a common environmental control on dust emission at the multi-millennial-scale. However, the millennial- to centennial-scale changes of the distal records from Scotia Sea and Antarctica (Lambert et al., 2012; Weber et al., 2012) are not consistent with k_{LF} from Laguna Potrok Aike. Rock-magnetic and physical granulometry results reveal that this difference is the result of the inverse magnetite grain size influence on k_{LF} from Laguna Potrok Aike. While proximal lacustro-aeolian records such as Laguna Potrok Aike accumulates grains transported by saltation and short-term suspension (Vandenberghe, 2013), distal dust records do not reflect grain size changes because the size distribution of aerosols (grain sizes generally < 10 μm travelling long distances; Muhs,

2013; Maher et al., 2010) is independent of wind intensity (Kok, 2011) (Fig. 7). Consequently, the magnetic susceptibility signal from Laguna Potrok Aike is interpreted as a dust indicator from southern Patagonia uniquely at multi-millennial resolution, where the magnetite grain size influence is minimal (Fig. 5).

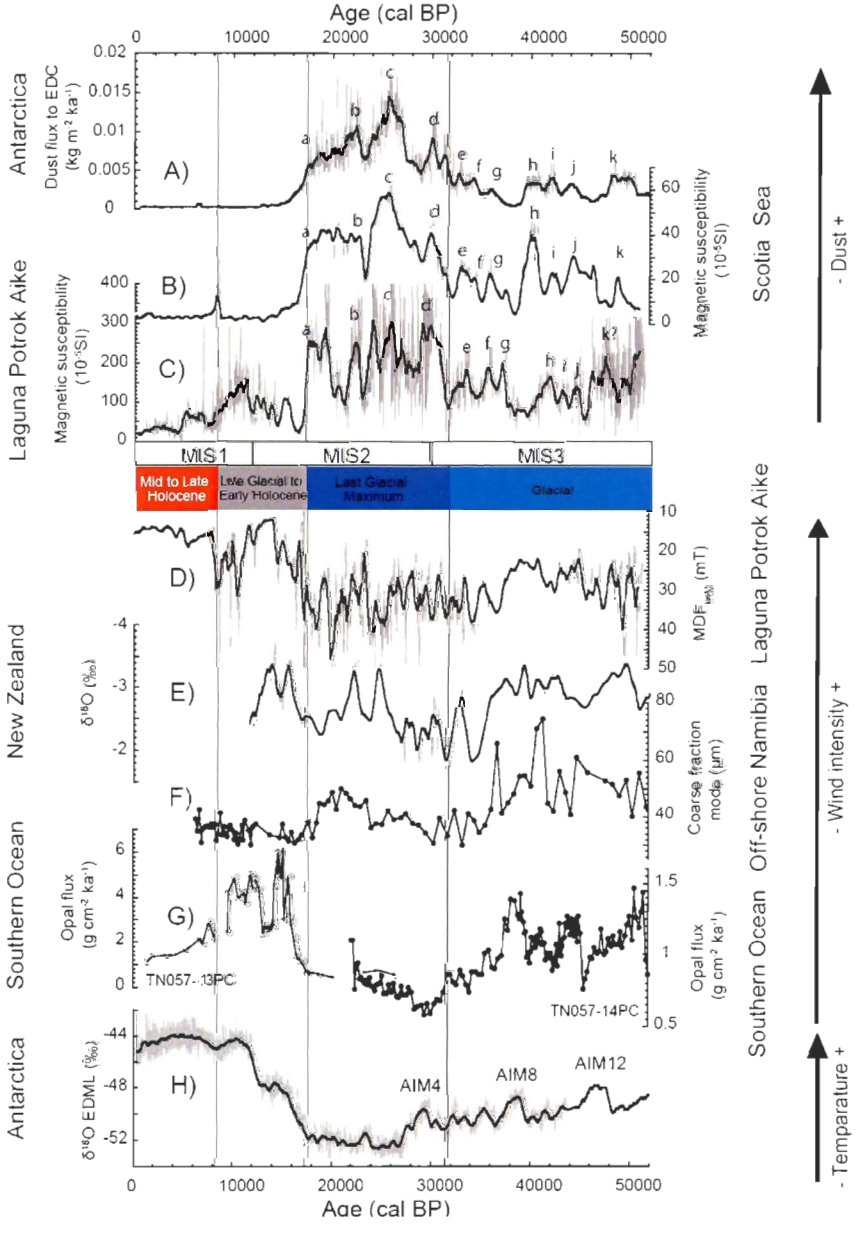

Figure 2. 6. Comparison of Southern Hemisphere dust, wind and temperature proxies since 52,000 cal BP (Table 2). From top to bottom: A) dust flux to EPICA Dome C (EDC) ice core in Antarctica (Lambert et al., 2012), B) magnetic susceptibility from the Scotia Sea (Weber et al., 2012), C) magnetic susceptibility from Laguna Potrok Aike (this study), D) Median destructive field of the isothermal remanent magnetisation (MDF_{IRM}) from Laguna Potrok Aike (this study), E) $\delta^{18}O$ record from a speleothem in New Zealand (Whittaker et al., 2011), F) upwelling intensity off-shore Namibia from coarse fraction mode of marine sediments (Pichevin et al., 2005), G) wind-driven upwelling intensity from opal flux in the Southern Ocean (Anderson et al., 2009) and H) paleo-temperature proxy $\delta^{18}O$ from Dronning Maud Land (EDML) ice core in Antarctica (EPICA community members, 2006). All records are presented on their own chronology. The thick lines represent the millennial-scale variability of the high-resolution records A, B, C, D, E and H. Lowercase letters indicate dust maxima in A, B and C. Climatic periods from the PASADO record (Figures 3 and 4; Kliem et al., 2013; Hahn et al., 2013) and marine isotopic stage (MIS) according to Lisiecki and Raymo (2005) are indicated.

Table 2. 2. Dust and wind intensity proxies from the Southern Hemisphere discussed in the text.

Proxy	Site position				Age (cal BP)		References
	Site	Distance from LPA (km)	Latitude	Longitude	min	max	
Dust							
Magnetic susceptibility (k) of marine sediments	Scotia Sea	1780	58°S	42°W	0	92,500	Weber et al., 2012
Flux of dust to ice core	EPICA Dome C, Antarctica	5870	75°06'S	123°24'E	0	62,000	Lambert et al., 2012
Wind intensity							
$\delta^{18}O$ from stalagmite (MA1)	Bahia Arevalo, southern Chile	220	52°41'S	73°23'W	0	4500	Schimpf et al., 2011
Annual precipitation reconstructed from pollen data	Lago Argentino, southern Argentina	240	50°24'S	72°42'W	0	12,400	Tonello et al., 2009
Eolian sand influx in peat bog	Isla de los Estados, Tierra del Fuego	500	54°45'S	64°30'W	0	14,000	Bjork et al., 2012
Opal flux to marine sediment cores TN057-13	Atlantic sector of the Southern Ocean	4940	52° 06'S	5° 06'E	0	27,000	Anderson et al., 2009
" TN057-14	"	4910	51°59'S	4°31'E	22,000	82,000	Anderson et al., 2009
Coarse grain size fraction mode of marine sediment	Off-shore Namibia	7450	25°06'S	13°38'E	0	190,000	Pichevin et al., 2005
$\delta^{18}O$ from stalagmite (HW3)	Hollywood cave, New Zealand	8020	41°57'S	171°28'E	11,000	73,000	Whittaker et al., 2011

5.2 Rock-magnetic proxy of wind intensity

5.2.1 Physical processes

The coercivity of magnetic grains acquiring an IRM is best correlated (R=-0.66 and R=-0.53) to coarse and medium silt fractions (31-16 μm and 8-16 μm, respectively; Table 1) corresponding to the grain-size fraction lifted by winds but unlikely to travel long distances (Muhs, 2013; Vandenberghe, 2013; Maher et al., 2010 and references therein) (Fig.7). Coronato et al. (2013) reported that silty sands deposited by winds cover the Pali Aike volcanic field region. The sources of silt-sized magnetite are numerous in the area and include the release of particles from the siltstones of the Santa Cruz Formation, aeolian abrasion of volcanic rocks under the semi-arid climate, deflation of glacial deposits accumulated in outwash plains and fans, available for wind erosion due to the scarcity of vegetation. The coarse to medium silts are typically emitted for a short-term suspension transport by the impact of sand in the saltation layer (Fig. 7). They are generally deposited within ca. 30 km from the source (Muhs, 2013) but can be transported over maximum distances of tens to hundreds of km under windstorm conditions (Pye, 1995). Therefore, the MDF_{IRM} signal from the sediments of Laguna Potrok Aike primarily reflects grain size changes of detrital magnetite brought to the lake by short-term suspension.

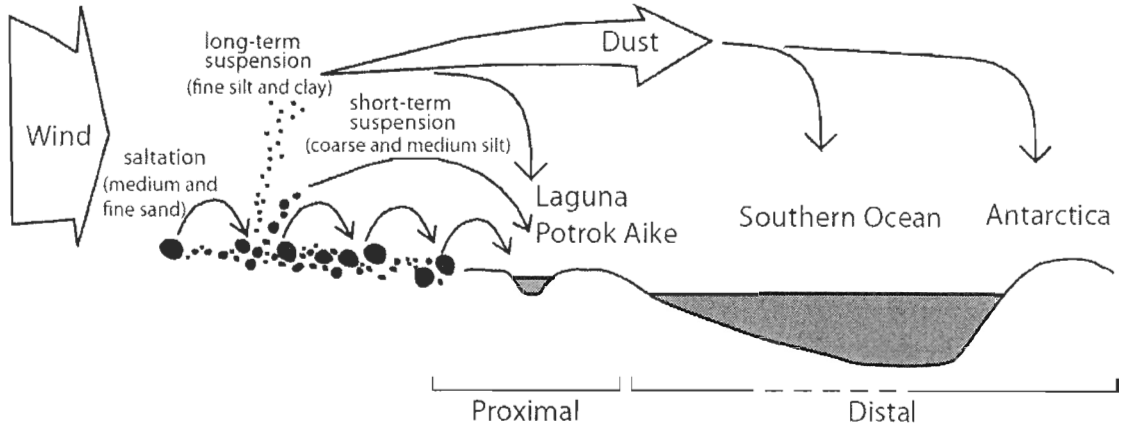

Figure 2. 7. Scheme of wind-induced transport processes for different grain sizes (modified from Pye, 1995) illustrating that while distal dust records (e.g., Southern Ocean and Antarctica) are not influenced by grain size changes, proximal records such as Laguna Potrok Aike are. Medium to fine sands are transported by saltation (cm to m distance) and the impact of saltating grains on the ground results in short-term suspension of coarse to medium silts (travelling tens to hundreds of km distance) and long-term suspension of fine silt and clay (thousands of km distance).

MDF_{IRM} is interpreted as a wind intensity proxy in the dust source area of southern Argentina, with stronger winds capable of carrying coarser silts to the lake. Stronger winds are also capable of moving coarser grains by creep and saltation. These coarser grains are unlikely to reach the central lake basin; however they can certainly settle closer to the lake shore. This interpretation is supported by coarser grain-sizes deposited on the lake level terrace during the last glacial period (mean of 51 μm; Haberzettl et al., 2008) than at PASADO site 2 in the lake center (mean of 36 μm). Interestingly, Kliem et al (2013a) reported occasional millimeter-thick layers of fine sands to coarse silts intercalated within pelagic sediment in units B and C (51,200-8100 cal BP) from Laguna Potrok Aike. These fine event layers occur at irregular frequencies of ca. 100 to 1000 years and were not removed from the event-corrected composite sediment sequence because of their low contribution to the lithostratigraphic units (Kliem et al., 2013a). Lower MDF_{IRM} values

associated with these intervals indicates coarser magnetite grains and points to enhanced gustiness/storminess conditions triggering these fine event deposits. Similar episodic wind-driven "saltation burst" events are documented today in cold and dry desert such as Taylor Valley in Antarctica (Šabacká et al., 2012).

5.2.2 Advantages

One significant advantage of MDF_{IRM} as a wind intensity proxy at Laguna Potrok Aike is its ability to target mostly the magnetite grains of a specific grain size range. The narrow grain-size target facilitates the identification of the transport process. In addition, MDF_{IRM} is not influenced by changes in the magnetic concentration (as opposed to k_{LF}) or by changes in the various sediment types and grain sizes of the bulk sediment. In particular, micropumice in the sediments of Laguna Potrok Aike was demonstrated problematic for the interpretation of elemental data during the Late Glacial and as a result, caution was raised against using some elemental ratio on the complete sequence (Hahn et al., submitted; Jouve et al., 2013). Finally, because winds in southeastern Patagonia are only weakly related to precipitation (Garreaud et al., 2013; Ohlendorf et al., 2013), MDF_{IRM} is believed to be independent of moisture changes. This is a significant advantage in southern Patagonia where the moisture-related wind intensity proxies are often difficult to interpret (Moreno et al., 2009) and particularly during times of a rearrangement of the hydrological cycle such as during deglaciation (Kohfeld et al., 2013).

5.2.3 Possible limitations

Other control than wind strength on silt-sized detrital magnetite in the sediment of Laguna Potrok Aike would impact MDF_{IRM} values and limits its use as a wind-intensity proxy. Here we discuss the possible influence including the presence of permafrost, changes in lake level and sediment remobilisation events.

Permafrost and vegetation changes in the vicinity of the lake could potentially influence the availability of grains for aeolian transport. There is some evidence of permafrost during the last Glacial period (Jouve et al., submitted; Kliem et al., 2013b)

which probably contributed via increased runoff to higher lake levels (Fig. 3F). The presence of permafrost is associated to very limited vegetation cover and unprotected soils. As a result, the upper melted soil layer forming during summer is very prone to erosion or deflation (e.g., Guglielmin, 2012). Therefore in the presence of permafrost, grains can still be easily mobilized. Under extremely cold conditions permafrost and/or snow cover would blanket the ground all-year round, aeolian transport would be inhibited and the concentration of magnetite within sediment would be significantly reduced. Similarly, sustained ice cover on the lake would stop detrital input of magnetite. However, on the contrary the concentration-dependent parameters k_{LF} (Figs. 3A and 4), ARM and IRM (Lisé-Pronovost et al., 2013) display distinctively higher values during the Glacial period than during the Holocene and Fmag is not lower (Fig. 3C), indicating no apparent change or greater magnetite grain availability during the last Glacial period. Therefore permafrost, snow and/or ice cover during the last Glacial period are unlikely to have influenced the input of detrital magnetite at the millennial to centennial-scale; however they may have acted discontinuously, on annual basis or over short periods of time, possibly contributing to the high amplitude of changes in rock-magnetic properties.

One could argue that if the lake level is lowered, the distance from the shore to the coring site is reduced and coarser grains can possibly reach the coring site. However, the steep slopes of Laguna Potrok Aike (up to 20°; Anselmetti et al., 2009) do not allow large surface area changes following lake level fluctuations. In addition, the lake diameter (maximum of 3.5 km) is one to two orders of magnitude smaller than the typical distance travelled by short-term suspension (Pye, 1995). Therefore the lake level influence on the silt grain size deposited in the lake center is believed to be small. Moreover, lake levels in Laguna Potrok Aike seem not having substantially fluctuated during the last Glacial period (51,200-17,300 cal BP) (Fig. 3F). During the mid to Late Holocene, the strong SWW are persistent over the region (Zolitschka et al., 2013 and references therein), accordingly bringing distinctively coarser magnetite grains to Laguna Potrok Aike (lower values of MDF_{IRM}; Figs. 3E and 4). Finally, the general similarity of the reconstructed lake level curve and MDF_{IRM} most probably reflects common wind control (Fig. 3E and F) and the

absence of MDF_{IRM} change during the ca. 40 m Holocene lake level transgression further supports the independence of MDF_{IRM} on lake level changes.

Finally, another possible influence on the MDF_{IRM} signal is the input of silt-sized magnetite by runoff events such as extreme precipitations (Ohlendorf et al., 2013), permafrost and snowcover melt, or remobilisation of previously deposited coarser mud induced by lake level changes. However, such events were recognized and removed from the event-corrected PASADO composite sediment sequence (Kliem et al., 2013a) used in this study, and hence do not impact the MDF_{IRM} data presented here. Altogether, the discussed environmental influence on magnetite grain size deposition is unlikely to impact MDF_{IRM} at the millennial to centennial-scale.

5.2.3 Comparison with paleoclimate records

As a final step testing the reliability of the new rock-magnetic proxy of wind intensity, MDF_{IRM} is compared with other wind-intensity records from the Southern Hemisphere. During the last Glacial period (51,200-17,300 cal BP), the wind intensity proxy from Laguna Potrok Aike indicates generally lower winds with large amplitude changes. Lower wind intensities during the last Glacial period relative to the present are similarly documented in the Australian region (Schulmeister et al., 2004; Hesse and McTainsh, 1999), in agreement with an equatorward displacement of the polar front (Iriondo, 1999; Moreno et al., 1999; Pollock and Bush, 2013; Toggweiler et al., 2006) or a weakening of the SWW (Kohfeld et al., 2013). This pattern is interrupted by two periods of enhanced wind strength and reduced amplitudes centered at ca. 44,000 and ca. 39,000 cal BP (Fig.6D). These two relatively stronger wind periods are coeval within limits of the chronology to enhanced wind-driven upwelling in the Pacific, Indian and Atlantic sectors of the Southern Ocean (Anderson et al., 2009; Fig.6G) as well as to stronger winds in the mid-latitudes of the Southern Hemisphere in New Zealand (Whittaker et al., 2011; Fig.6E) and further north offshore Namibia (Pichevin et al., 2005; Fig.6F).

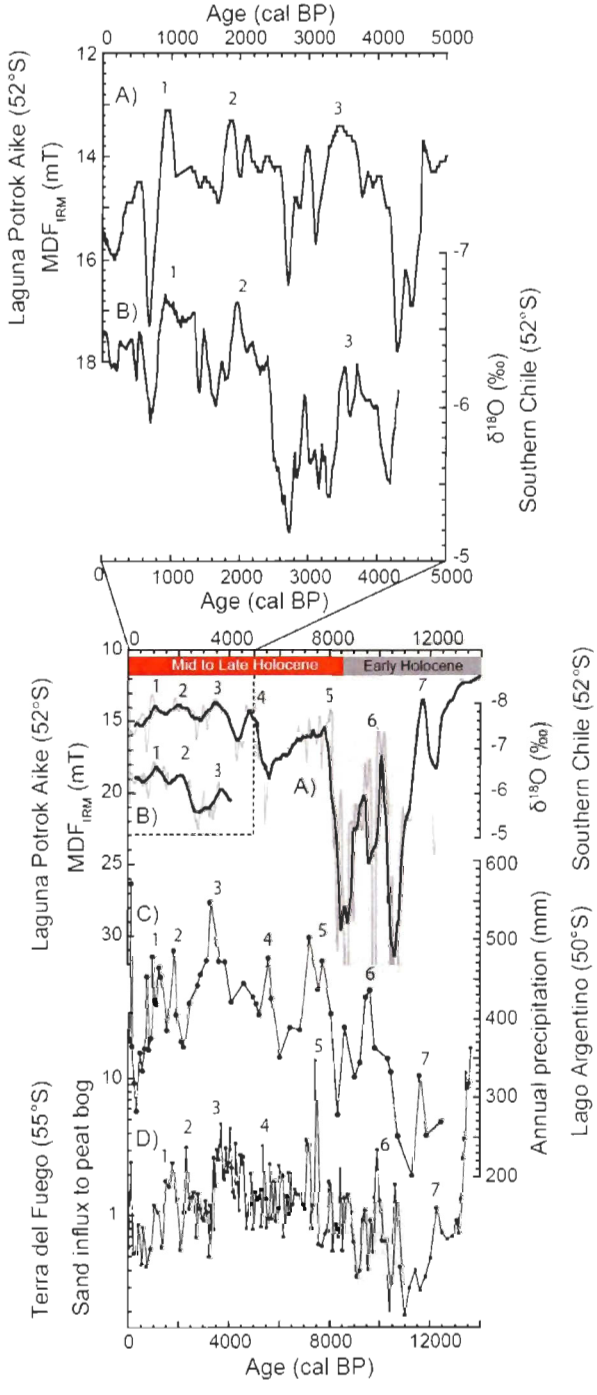
Age (cal BP)
Laguna Potrok Aike (52°S)
MDF$_{IRM}$ (mT)
A)
B)
δ^{18}O (‰)
Southern Chile (52°S)
Mid to Late Holocene
Early Holocene
C)
D)
Terra del Fuego (55°S)
Sand influx to peat bog
Annual precipitation (mm)
Lago Argentino (50°S)

Figure 2. 8. Regional comparison of wind-intensity proxies for southern South America since 14,000 cal BP (Table 2). A) Median destructive field of the isothermal remanent magnetisation (MDF_{IRM}) from the sediment of Laguna Potrok Aike (this study), B) $\delta^{18}O$ from the stalagmite MA1 in Southern Chile (Schimpf et al., 2011), C) annual precipitation reconstruction from pollen data of Lago Argentino in southern Argentina (Tonello et al., 2009) and D) sand (125-350 μm) influx to a peat bog in Terra del Fuego (Björck et al., 2012). All records are presented on their own chronology. The thick lines represent millennial-scale variability for high-resolution records A and B. Numbers (1 to 7) indicate a series of relative maximum in wind intensity in all records. Climatic periods of the PASADO record are indicated and the shaded area indicates a period of weak westerly flow in the mid-latitudes of the Southern Hemisphere according to Fletcher and Moreno (2012).

During the Late Glacial warming recorded in Antarctica (EPICA community members, 2006) (Fig.6H), MDF_{IRM} from Laguna Potrok Aike and paleowind records from the mid-latitudes of the Southern Hemisphere indicate increased intensities (Fig.6 D, E and G) (Anderson et al., 2009; Whittaker et al., 2011) while no change is observed further north offshore Namibia (Pichevin et al., 2005; Fig.6F), in agreement with a poleward shift of the SWW at the last Glacial termination. The Early Holocene period is characterized by high amplitude changes and generally weaker winds in Laguna Potrok Aike. This period corresponds to the cessation of wind-driven upwelling in the sub-polar Southern Ocean (Anderson et al., 2009; Fig 6.G) and to reduced flow across the entire zone of westerly influence from ca.11,000 to 8000 cal BP (shaded area on figure 8) as reported by Fletcher and Moreno (2012 and references therein) reviewing continuous paleoenvironmental data in the mid-latitudes of the Southern Hemisphere.

Figure 8A, C and D presents a regional comparison (within 500 km; Table 2) of MDF_{IRM} from Laguna Potrok Aike with wind intensity records in southeastern Patagonia since 14,000 cal BP (Table 2). The annual precipitation of westerly origin inferred from palynological data from Lago Argentino on the Andean piedmont (Tonello et al., 2009; Figure 8C), as well as the sand influx to peat bug in Terra del Fuego (Björck et al., 2012;

Figure 8D), display similar series of maximum wind intensities (labelled from 1 to 7), providing regional support for MDF_{IRM} as a wind intensity proxy.

The mid to Late Holocene period (8100-0 cal BP) is characterized by distinctively stronger wind intensities and low amplitude variability consistent with the present-day strong and persistent SWW over the region (e.g., Ohlendorf et al., 2013). The sharp shift to stronger winds at 8100 cal BP inferred from MDF_{IRM} likely marks the onset of the SWW influence over 52°S in southeastern Patagonia, in agreement with the zonally symmetric increase in westerly flow at ca. 8000 cal BP reported by Fletcher and Moreno (2012). This period correspond to major environmental changes in Laguna Potrok Aike including low lake levels (Anselmetti et al., 2009; Haberzettl et al., 2007; Kliem et al., 2013b), decreased precipitation as indicated by pollen assemblage (Schäbitz et al., 2013), maximum Andean forest taxa pollen (Mayr et al., 2007a; Wille et al., 2007), diminution of total diatom-valve abundance and changes in the taxonomical assemblage (Massaferro et al., 2013), as well as monohydrocalcite precipitation (Haberzettl et al., 2007; Nuttin et al., 2013). Marked landscape changes including peat growth termination by aeolian sand deposition and dunes development are also reported at that time on the West Falkland Island ca. 600 km east of Laguna Potrok Aike (Wilson et al., 2002).

Finally, the record from Laguna Potrok Aike is compared since 5000 cal BP with a high-resolution wind intensity record derived from $\delta^{18}O$ of stalagmite on the western side of the Andean cordillera (Schimpf et al., 2011) (Fig. 8A and B). The two records are located only 220 km apart at 52°S under the influence of the strong SWW. Despite contrasting climate (hyperhumid in southern Chile and dry steppe in southern Argentina), the records are in excellent agreement at the centennial-scale. Altogether the regional to hemispheric comparisons of wind intensity proxies and well-established high-resolution paleoclimate data from the Southern Hemisphere reveal that the MDF_{IRM} signal from Laguna Potrok Aike can confidently be used as a wind intensity proxy in southeastern Patagonia at least at the millennial-scale and up to the centennial-scale during the mid to Late Holocene.

6. Conclusions

High-resolution rock-magnetic study of the sediment deposited in the maar lake Laguna Potrok Aike since 51,200 cal BP revealed a lacustro-aeolian record in the dust source region of southern Patagonia. The magnetic susceptibility signal (k_{LF}) displays very clear LGM signal (from 31,500 to 17,300 cal BP), not provided by most other proxies from Laguna Potrok Aike (Zolitschka et al., 2013). There is an inverse correlation of k_{LF} with magnetite grain size indicators (e.g., kARM/IRM, MDF_{IRM}) at the millennial to centennial-scale; however the multi millennial variability of k_{LF} is primarily controlled by the concentration of ferrimagnetic mineral. Based on coherence analysis, estimation of magnetite flux to the lake and comparison with distal dust records, k_{LF} is interpreted as a dust proxy in the dust source region of southern Patagonia at the multi millennial-scale, where grain size influence is minimal.

This study establishes the MDF_{IRM} record from Laguna Potrok Aike as a wind intensity proxy at 52°S in southeastern Patagonia since 51,200 cal BP. The coercivity of the magnetite grains acquiring an isothermal remanent magnetisation (MDF_{IRM}) mostly tracks the coarse to medium silt-sized magnetite transported by short-term suspension. The new wind-intensity proxy is in good agreement with other continuous wind-intensity records derived from marine, lacustrine and peat bog sediments, as well as speleothems in southern Patagonia since the deglaciation and from the Southern Hemisphere during the last Glacial period. The new proxy of wind-intensity is independent of moisture change and based on a rapidly acquired room-temperature magnetic measurement.

Acknowledgements

We aknowledge J. Labrie, F. Barletta and M.-P. St-Onge for their help in the laboratory at ISMER. We are grateful to A. Mazaud and Q. Simon for fruitful discussion and to S. Bjork, A.Hahn, P. Kliem, L. Pichevin, D. Schimpf, M. Weber, T. Whittaker for sharing their data. This research was supported by the International Continental Scientific Drilling Program (ICDP) in the framework of the "Potrok Aike Maar Lake Sediment

Archive Drilling Project" (PASADO). Funding for drilling was provided by the ICDP, the German Science Foundation (DFG), the Swiss National Funds (SNF), the Natural Sciences and Engineering Research Council of Canada (NSERC), the Swedish Vetenskapsradet (VR) and the University of Bremen. For their invaluable help in field logistics and drilling, we thank the staff of INTA Santa Cruz and Rio Dulce Catering as well as the Moreteau family and the DOSECC crew. This research was made possible through a NSERC Special Research Opportunity and Discovery grants to G. St-Onge. We also acknowledge the Canadian Foundation for Innovation (CFI) for the acquisition and operation of the u-channel cryogenic magnetometer. Finally, we acknowledge the support of NSERC and the Canadian Meteorological and Oceanographical Society (CMOS) for graduate scholarships to A. Lisé-Pronovost, and the *Fonds de recherche du Québec - Nature et technologies* (FQRNT) for a postdoctoral fellowship to T. Haberzettl.

References

Anderson, R.F., Ali, S., Bradtmiller, L.I., Nielsen, S.H.H., Fleisher, M.Q., Anderson, B.E., Burckle, L.H., 2009. Wind-Driven Upwelling in the Southern Ocean and the Deglacial Rise in Atmospheric CO_2 , Science 323 (5920), 1443-1448.

Anselmetti, F., Ariztegui, D., De Batist, M., Gebhardt, C., Haberzettl, T., Niessen, F., Ohlendorf, C., Zolitschka, B., 2009. Environmental history of southern Patagonia unraveled by the seismic stratigraphy of Laguna Potrok Aike. Sedimentology 56, 873-892.

Basile, I., Grousset, F.E., Revel, M., Petit, J.R., Biscaye, P.E., Barkov, N.I., 1997. Patagonian origin of glacial dust deposited in East Antarctica (Vostok andDome C) during glacial stages 2, 4 and 6, Eart and Planet. Sci. Lett. 146, 573-589.

Banerjee, S.K., King, J., Marvin, J., 1981. A rapid method for magnetic granulomtery with applications to environmental studies, Geophys. Res. Lett. 8, 333–336.

Brachfeld, S.A., 1999. Separation of geomagnetic paleointensity and paleoclimate signals in sediments: examples from North America and Antarctica. PhD thesis, University of Minnesota.

Coronato, A., Ercolano, B., Corbella, H., Tiberi, P., 2013. Glacial, fluvial and volcanic landscape evolution in the Laguna Potrok Aike maar area, Southern Patagonia, Argentina. Quat. Sci. Rev. 71, 13–26.

Dearing, J.A., 1999. Environmental magnetic susceptibility: using the Bartington MS2 system. Chi Pub., Kenilworth.

Delmonte, B., Andersson, P.S., Schöberg, H., Hansson, M., Petit, J.R., Delmas, R., Gaiero, D.M., Maggi, V., Frezzotti, M., 2010. Geographic provenance of aeolian dust in East Antarctica during Pleistocene glaciations: preliminary results from Talos Dome and comparison with East Antarctic and new Andean ice core data. Quat. Sci. Rev. 29, 256–264.

Delmonte, B., Basile-Doelsch, I., Petit, J.-R., Maggi, V., Revel-Rolland, M., Michard, A., Jagoutz, E., Grousset, F., 2004. Comparing the Epica and Vostok dust records during the last 220,000 years: stratigraphical correlation and provenance in glacial periods. Earth-Sci. Rev. 66, 63–87.

D'Orazio, M., Agostini, S., Mazzarini, F., Innocenti, F., Manetti, P., Haller, M.J., Lahsen, A., 2000. The Pali Aike volcanic field, Patagonia: slab-window magmatism near the tip of South America. Tectonophysics 321, 407–427.

Dunlop, D.J. and Özdemir, Ö., 2007. Magnetizations in rocks and minerals, Vol. 5 – Geomagnetism, Treatise on Geophysics, ed. G. Schubert, Elsevier.

Egli, R., 2004. Characterization of individual rock magnetic components by analysis of remanence curves. Phys. Chem. Earth Parts Abc 29, 851–867.

EPICA community members, 2006. One-to-one coupling of glacial climate variability in Greenland and Antarctica. Nature 444, 195–198.

Evans and Heller, 2003. Environmental magnetism: Principles and applications of enviromagnetics, international geophysics series vol. 86, Academic press, 299p.

Fletcher, M.-S., Moreno, P.I., 2012. Have the Southern Westerlies changed in a zonally symmetric manner over the last 14,000 years? A hemisphere-wide take on a controversial problem. Quat. Int. 253, 32-46.

Gaiero, D.M., 2007. Dust provenance in Antarctic ice during glacial periods: From where in southern South America? Geophys. Res. Lett. 34, L17707.

Gaiero, D.M., Probst, J.L., Depetris, P.J., Bidart, S.M., Leleyter, L., 2003. Iron and other transition metals in Patagonian riverborne and windborne materials : Geochemical control and transport to the southern South Atlantic Ocean. Geochemica Et Cosmochimica Acta 67 (19), 3603-3623.

Garreaud, R., P. Lopez, M. Minvielle, M. Rojas, 2013. Large Scale Control on the Patagonia Climate. J. of Climate 26, 215-230.

Gogorza, C.S.G., Sinito, A.M., Ohlendorf, C., Kastner, S., Zolitschka, B., 2011. Paleosecular variation andpaleointensity records for the last millennium from southern South America (Laguna Potrok Aike, Santa Cruz, Argentina). Physics of the Earth and Planetary Interiors 184, 41-50.

Gogorza, C.S.G., Irurzun, M.A., Sinito, A.M., Lisé-Pronovost, A., St-Onge, G., Haberzettl, T., Ohlendorf, C., Kastner, S., Zolitschka, B., 2012. High-resolution paleomagnetic records from Laguna Potrok Aike (Patagonia, Argentina) for the last 16,000 years. Geochemistry, Geophysics, Geosystems 13.

Gubbins, D., Herrero-Bervera, E., 2007. Encyclopedia of geomagnetism and paleomagnetism. Springer, Dordrecht.

Guglielmin, M., 2012. Advances in permafrost and periglacial research in Antarctica: A review. Geomorphology 155-156, 1–6.

Haberzettl, T., Anselmetti, F.S., Bowen, S.W., Fey, M., Mayr, C., Zolitschka, B., Ariztegui, D., Mauz, B., Ohlendorf, C., Kastner, S., Lücke, A., Schäbitz, F., Wille, M., 2009. Late Pleistocene dust deposition in the Patagonian steppe - extending and refining the paleoenvironmental and tephrochronological record from Laguna Potrok Aike back to 55ka. Quat. Sci. Rev. 28, 2927–2939.

Haberzettl, T., Kück, B., Wulf, S., Anselmetti, F., Ariztegui, D., Corbella, H., Fey, M., Janssen, S., Lücke, A., Mayr, C., Ohlendorf, C., Schäbitz, F., Schleser, G.H., Wille, M., Zolitschka, B., 2008. Hydrological variability in southeastern Patagonia and explosive volcanic activity in the southern Andean Cordillera during Oxygen Isotope Stage 3 and the Holocene inferred from lake sediments of Laguna Potrok Aike, Argentina. Palaeogeogr. Palaeoclim. Palaeo. 259, 213–229.

Haberzettl, T., Corbella, H., Fey, M., Janssen, S., Lücke, A., Mayr, C., Ohlendorf, C., Schäbitz, F., Schleser, G.-H., Wessel, E., Wille, M., Wulf, S., Zolitschka, B., 2007. A continuous 16,000 year sediment record from Laguna Potrok Aike, southern Patagonia (Argentina): sedimentology, chronology, geochemistry. The Holocene 17, 297-310.

Haberzettl, T., Fey, M., Lücke, A., Maidana, N., Mayr, C., Ohlendorf, C., Schäbitz, F., Schleser, G.H., Wille, M., Zolitschka, B., 2005. Climatically induced lake level changes during the last two millennia as reflected in sediments of Laguna Potrok Aike, southern Patagonia (Santa Cruz, Argentina). J. Paleolimnol. 33, 283–302.

Hahn, A., Kliem, P., Oehlerich, M., Ohlendorf, C., Zolitschka, B. and the PASADO Science Team, submitted. Elemental composition of Laguna Potrok Aike sediment sequence reveals paleoclimate change over the past 51 ka in southern Patagonia, Argentina.

Hahn, A., Kliem, P., Ohlendorf, C., Zolitschka, B., Rosén, P., 2013. Climate induced changes as registered in inorganic and organic sediment components from Laguna Potrok Aike (Argentina) during the past 51 ka. Quat. Sci. Rev. 71, 154–166.

Hatfield, R.G., Stoner, J.S., Carlson, A.E., Reyes, A.V., Housen, B.A., 2013. Source as a controlling factor on the quality and interpretation of sediment magnetic records from the northern North Atlantic. Earth Planet. Sci. Lett. 368, 69–77.

Heider, F., A. Zitelsberger, K. Fabian, 1996. Magnetic susceptibility and remanence coercive force in grown magnetite crystals from 0.1 mm to 6 mm, Physics of the Earth and Planet. Int. 93, 239-256.

Hjulström, F. 1935: Studies of the morphological activity of rivers as illustrated by the river Fyris, University of Uppsala Geological Institute Bulletin, 25, 221–557.

Jouve, G., Francus, P., De Coninck, A.,Bouchard, F., Lamoureux, S.F. and the PASADO scvience team, submitted. microsedimentological investigations in lacustrine sediments from a maar lake: implications for paleoenvironmental reconstructions.

Jouve, G., Francus, P., Lamoureux, S., Provencher-Nolet, L., Hahn, A., Haberzettl, T., Fortin, D., Nuttin, L., 2013. Microsedimentological characterization using image analysis and μ-XRF as indicators of sedimentary processes and climate changes during Lateglacial at Laguna Potrok Aike, Santa Cruz, Argentina. Quat. Sci. Rev. 71, 191–204.

Kilian, R., Lamy, F., 2012. A review of Glacial and Holocene paleoclimate records from southernmost Patagonia (49–55°S). Quat. Sci. Rev. 53, 1–23.

King, J., Banerjee, S.K., Marvin, J., Özdemir, Ö., 1982. A comparison of different magnetic methods for determining the relative grain size of magnetite in natural materials: Some results from lake sediments. Earth and Planetary Science Letters 59, 404-419.

Kliem, P., Enters, D., Hahn, A., Ohlendorf, C., Lisé-Pronovost, A., St-Onge, G., Wastegård, S., Zolitschka, B., 2013a. Lithology, radiocarbon chronology and sedimentological interpretation of the lacustrine record from Laguna Potrok Aike, southern Patagonia. Quat. Sci. Rev. 71, 54–69.

Kliem, P., Buylaert, J.P., Hahn, A., Mayr, C., Murray, A.S., Ohlendorf, C., Veres, D., Wastegård, S., Zolitschka, B., 2013b. Magnitude, geomorphologic response and climate links of lake level oscillations at Laguna Potrok Aike, Patagonian steppe (Argentina). Quat. Sci. Rev. 71, 131–146.

Kohfeld, K.E., Graham, R.M., de Boer, A.M., Sime, L.C., Wolff, E.W., Le Quéré, C., Bopp, L., 2013. Southern Hemisphere westerly wind changes during the Last Glacial Maximum: paleo-data synthesis. Quat. Sci. Rev. 68, 76–95.

Kok, J.F., 2011. Does the size distribution of mineral dust aerosols depend on the wind speed at emission? Atmospheric Chem. Phys. 11, 10149–10156.

Lambert, F., Bigler, M., Steffensen, J.P., Hutterli, M., Fischer, H., 2012. Centennial mineral dust variability in high-resolution ice core data from Dome C, Antarctica. Clim. 8, 609–623.

Lisiecki, L.E., Raymo, M.E., 2005. A Plio-Pleistocene stack of 57 globally distributed benthic d18O records. Paleoceanography 20.

Lisé-Pronovost, A., St-Onge, G., Gogorza, C., Haberzettl, T., Preda, M., Kliem, P., Francus, P., Zolitschka, B., 2013. High-resolution paleomagnetic secular variations and relative paleointensity since the Late Pleistocene in southern South America. Quat. Sci. Rev. 71, 91–108.

Liu, Q., Roberts, A.P., Larrasoaña, J.C., Banerjee, S.K., Guyodo, Y., Tauxe, L., Oldfield, F., 2012. Environmental magnetism: Principles and applications. Rev. Geophys. 50.

Maher, B. A. 1988. Magnetic properties of some synthetic submicron magnetites. Geophysical Journal 94, 83-96.

Maher, B.A., Prospero, J.M., Mackie, D., Gaiero, D., Hesse, P.P., Balkanski, Y., 2010. Global connections between aeolian dust, climate and ocean biogeochemistry at the present day and at the last glacial maximum. Earth-Sci. Rev. 99, 61–97.

Maher, B.A., 2011. The magnetic properties of Quaternary aeolian dusts and sediments, and their palaeoclimatic significance. Aeolian Res. 3, 87–144.

Mahowald, N.M., Muhs, D.R., Levis, S., Rasch, P.J., Yoshioka, M., Zender, C.S., Luo, C., 2006. Change in atmospheric mineral aerosols in response to climate: Last glacial period, preindustrial, modern, and doubled carbon dioxide climates. J. Geophys. Res. 111.

Massaferro, J., Recasens, C., Larocque-Tobler, I., Zolitschka, B., Maidana, N.I., 2013. Major lake level fluctuations and climate changes for the past 16,000 years as reflected by diatoms and chironomids preserved in the sediment of Laguna Potrok Aike, southern Patagonia. Quat. Sci. Rev. 71, 167–174.

Mayr, C., Wille, M., Haberzettl, T., Fey, M., Janssen, S., Lücke, A., Ohlendorf, C., Oliva, G., Schäbitz, F., Schleser, G.-H., Zolitschka, B., 2007a. Holocene variability of the Southern Hemisphere westerlies in Argentinean Patagonia (52S). Quat. Sci. Rev. 26, 579-584.

Mayr, C., Lücke, A., Stichler, W., Trimborn, P., Ercolano, B., Oliva, G., Ohlendorf, C., Soto, J., Fey, M., Haberzettl, T., Janssen, S., Schäbitz, F., Schleser, G.H., Wille, M., Zolitschka, B., 2007b. Precipitation origin and evaporation of lakes in semi-arid Patagonia (Argentina) inferred from stable isotopes (d18O, d2H). Journal of Hydrology 334, 53-63.

Mazaud, A., Kissel, C., Laj, C., Sicre, M.A., Michel, E., Turon, J.L., 2007. Variations of the ACC-CDW during MIS3 traced by magnetic grain deposition in midlatitude South Indian Ocean cores: Connections with the northern hemisphere and with central Antarctica. Geochem. Geophys. Geosystems 8.

Mazaud, A., Michel, E., Dewilde, F., Turon, J.L., 2010. Variations of the Antarctic Circumpolar Current intensity during the past 500 ka. Geochem. Geophys. Geosystems 11.

McGee, D., Broecker, W.S., Winckler, G., 2010. Gustiness: The driver of glacial dustiness? Quat. Sci. Rev. 29, 2340–2350.

Moreno, P.I., François, J.P., Villa-Martínez, R.P., Moy, C.M., 2009. Millennial-scale variability in Southern Hemisphere westerly wind activity over the last 5000 years in SW Patagonia. Quat. Sci. Rev. 28, 25–38.

Muhs, D.R., 2013. The geologic records of dust in the Quaternary. Aeolian Res. 9, 3–48.

Nuttin, L., Francus, P., Preda, M., Ghaleb, B., Hillaire-Marcel, C., 2013. Authigenic, detrital and diagenetic minerals in the Laguna Potrok Aike sediment sequence. Quat. Sci. Rev. 71, 109–118.

Ohlendorf, C., Fey, M., Gebhardt, C., Haberzettl, T., Lücke, A., Mayr, C., Schäbitz, F., Wille, M., Zolitschka, B., 2013. Mechanisms of lake-level change at Laguna Potrok Aike (Argentina) – insights from hydrological balance calculations. Quat. Sci. Rev. 71, 27–45.

Paillard, D., Labeyrie, L., Yiou, P., 1996. Macintosh program performs time-series analysis. Eos Trans. AGU 77, 379.

Peters, C. and Dekkers, M.J., 2003. Selected room temperature magnetic parameters as a function of mineralogy, concentration and grain size. Phys. Chem. Earth Parts ABC 28, 659–667.

Petit, J.R., J. Jouzel, D. Raynaud, N.I. Barkov, J.-M. Barnola, I. Basile, M. Benders, J. Chappellaz, M. Davis, G. Delayque, M. Delmotte, V.M. Kotlyakov, M. Legrand, V.Y. Lipenkov, C. Lorius, L. Pépin, C. Ritz, E. Saltzman, and M. Stievenard. 1999. Climate and atmospheric history of the past 420,000 years from the Vostok ice core, Antarctica. *Nature* 399: 429-436.

Pichevin, L., Cremer, M., Giraudeau, J., Bertrand, P., 2005. A 190 ky record of lithogenic grain-size on the Namibian slope: Forging a tight link between past wind-strength and coastal upwelling dynamics. Mar. Geol. 218, 81–96.

Pye, 1995. The nature, origin and accumulation of loess, Quaternary Science Review 14, 653-667.

Recasens, C., Ariztegui, D., Gebhardt, C., Gogorza, C., Haberzettl, T., Hahn, A., Kliem, P., Lisé-Pronovost, A., Lücke, A., Maidana, N.I., Mayr, C., Ohlendorf, C., Schäbitz, F., St-Onge, G., Wille, M., Zolitschka, B., the PASADO ScienceTeam, 2012. New insights into paleoenvironmental changes in Laguna Potrok Aike, Southern Patagonia, since the Late Pleistocene: the PASADO multiproxy record. The Holocene 22, 1323-1335.

Reynolds, R.L., Reheis, M.C., Neff, J.C., Goldstein, H., Yount, J., 2006. Late Quaternary eolian dust in surficial deposits of a Colorado Plateau grassland: Controls on distribution and ecologic effects. CATENA 66, 251–266.

Roberts, A.P., Rohling, E.J., Grant, K.M., Larrasoaña, J.C., Liu, Q., 2011. Atmospheric dust variability from Arabia and China over the last 500,000 years. Quat. Sci. Rev. 30, 3537–3541.

Ross, P.-S., Delpit, S., Haller, M.J., Németh, K., Corbella, H., 2011. Influence of the substrate on maar–diatreme volcanoes: An example of a mixed setting from the Pali Aike volcanic field, Argentina. J. Volcanol. Geotherm. Res. 201, 253–271.

Röthlisberger, R., 2002. Dust and sea salt variability in central East Antarctica (Dome C) over the last 45 kyrs and its implications for southern high-latitude climate. Geophys. Res. Lett. 29.

Šabacká, M., Priscu, J.C., Basagic, H.J., Fountain, A.G., Wall, D.H., Virginia, R.A., Greenwood, M.C., 2012. Aeolian flux of biotic and abiotic material in Taylor Valley, Antarctica. Geomorphology 155-156, 102–111.

Sayago, J.M., Collantes, M.M., Karlson, A., Sanabria, J., 2001. Genesis and distribution of the Late Pleistocene and Holocene loess of Argentina: a regional approximation. Quat. Int. 76, 247–257.

Schäbitz, F., Wille, M., Francois, J.-P., Haberzettl, T., Quintana, F., Mayr, C., Lücke, A., Ohlendorf, C., Mancini, V., Paez, M.M., Prieto, A.R., Zolitschka, B., 2013. Reconstruction of palaeoprecipitation based on pollen transfer functions – the record of the last 16 ka from Laguna Potrok Aike, southern Patagonia. Quat. Sci. Rev. 71, 175–190.

Schimpf, D., Kilian, R., Kronz, A., Simon, K., Spötl, C., Wörner, G., Deininger, M., Mangini, A., 2011. The significance of chemical, isotopic, and detrital components in three coeval stalagmites from the superhumid southernmost Andes (53°S) as high-resolution palaeo-climate proxies, Quat. Sci. Rev. 30, 443-459.

Sijp, W.P., England, M.H., 2008. The effect of a northward shift in the southern hemisphere westerlies on the global ocean. Prog. Ocean. 79, 1–19.

Stoner, J.S.,Channell, J.E.T., Hillaire-Marcel, C., 1996. The magnetic signature of rapidly deposited detrital layers from the deep Labrador Sea: Relationship to North Atlantic Heinrich layers, paleoceanography 11:3, 309-325.

Stoner, J.S. and St-Onge, G., 2007. Chapter Three Magnetic Stratigraphy in Paleoceanography: Reversals, Excursions, Paleointensity, and Secular Variation, in: Developments in Marine Geology. Elsevier, pp. 99–138.

Sugden, D.E., McCulloch, R.D., Bory, A.J.-M., Hein, A.S., 2009. Influence of Patagonian glaciers on Antarctic dust deposition during the last glacial period. Nat. Geosci. 2, 281–285.

Tauxe, L., 2010. Essentials of Paleomagnetism. Berkeley, University of California Press, 489 p.

Thompson, R., 1986. Palaeomagnetic dating, in Handbook of Holocene Palaeoecology and Palaeohydrology, edited by B. E. Berglund, pp. 313–327, Wiley, Chichester, U. K.

Toggweiler, J.R., Russell, J.L., Carson, S.R., 2006. Midlatitude westerlies, atmospheric CO2, and climate change during the ice ages. Paleoceanography 21.

Tonello, M.S., Mancini, M.V., Seppa, H., 2009. Quantitative reconstruction of Holocene precipitation changes in southern Patagonia, Quaternary Research 72, 410-420.

Tucker, M.E., 1991. Sedimentary petrology: an introduction to the origin of sedimentary rocks. Blackwell Science Publications, Cambridge.

Udden, J.A., 1914. Mechanical composition of clastic sediments. Bulletin of the Geological Society of America 25, 655-744.

Vandenberghe, J., 2013. Grain size of fine-grained windblown sediment: A powerful proxy for process identification. Earth-Sci. Rev. 121, 18–30.

Waldmann, N., Ariztegui, D., Anselmetti, F., Austin, J.A., Moy, C.M., Stern, C., Recasens, C., Dunbar, R.B., 2010. Holocene climatic fluctuations and positioning of the Southern Hemisphere westerlies in Tierra del Fuego (54°S), Patagonia. J. Quat. Sci. 25 (7), 1063-1075.

Weber, M.E., Kuhn, G., Sprenk, D., Rolf, C., Ohlwein, C., Ricken, W., 2012. Dust transport from Patagonia to Antarctica – A new stratigraphic approach from the Scotia Sea and its implications for the last glacial cycle. Quat. Sci. Rev. 36, 177–188.

Wentworth, C.K., 1922. A scale of grade and class terms for clastic sediments. Journal of Geology 30, 377-392.

Whittaker, T.E., Hendy, C.H., Hellstrom, J.C., 2011. Abrupt millennial-scale changes in intensity of Southern Hemisphere westerly winds during marine isotope stages 2-4. Geology 39, 455–458.

Wille, M., Maidana, N.I., Schäbitz, F., Fey, M., Haberzettl, T., Janssen, S., Lücke, A., Mayr, C., Ohlendorf, C., Schleser, G.H., Zolitschka, B., 2007. Vegetation and climate dynamics in southern South America: The microfossil record of Laguna Potrok Aike, Santa Cruz, Argentina. Rev. Palaeobot. Palynol. 146, 234–246.

Wilson, P., Clark, R., Birnie, J., Moore, D.M., 2002. Late Pleistocene and Holocene landscape evolution and environmental change in the Lake Sulivan area, Falkland Islands, South Atlantic. Quat. Sci. Rev. 21, 1821–1840.

Zender, C.S., 2003. Mineral Dust Entrainment and Deposition (DEAD) model: Description and 1990s dust climatology. J. Geophys. Res. 108 (D14) 4416.

Zolitschka, B., Anselmetti, F., Ariztegui, D., Corbella, H., Francus, P., Lücke, A., Maidana, N.I., Ohlendorf, C., Schäbitz, F., Wastegård, S., 2013. Environment and climate of the last 51,000 years – new insights from the Potrok Aike maar lake Sediment Archive Drilling prOject (PASADO). Quat. Sci. Rev. 71, 1–12.

Zolitschka, B., Schäbitz, F., Lücke, A., Corbella, H., Ercolano, B., Fey, M., Haberzettl, T., Janssen, S., Maidana, N., Mayr, C., Ohlendorf, C., Oliva, G., Paez, M.M., Schleser, G.H., Soto, J., Tiberi, P., Wille, M., 2006. Crater lakes of the Pali Aike Volcanic Field as key sites for paleoclimatic and paleoecological reconstructions in southern Patagonia, Argentina. J. South Am. Earth Sci. 21, 294–309.

CHAPITRE 3

SIGNATURE MAGNÉTIQUE D'ÉVÈNEMENTS DE PRÉCIPITATION ET D'INONDATION EXTRÊMES DANS LE SUD-EST DE LA PATAGONIE (ARGENTINE) DEPUIS 51200 CAL BP À PARTIR DES SÉDIMENTS DU LAC LAGUNA POTROK AIKE

RÉSUMÉ

Une séquence sédimentaire de 106 mètres a été prélevée au lac *Laguna Potrok Aike* dans le cadre du Programme international de forage scientifique continental (ICDP) pour le projet *Potrok Aike maar lake Sediment Archive Drilling prOject* (PASADO). Des mouvements de masses (MMDs) représentent environ la moitié de la séquence sédimentaire qui couvre la période depuis 51200 ans. L'étude des propriétés magnétiques à haute résolution révèle deux faciès magnétiques distincts associés aux MMDs et caractérisés par deux types de magnétisation gyrorémanente (GRM) acquise lors de la démagnétisation par champ alternatif. Le premier faciès magnétique est détecté à l'intérieur de MMDs composées de sables et de cendres volcaniques remobilisés. La signature magnétique consiste en l'acquisition de GRM pendant la démagnétisation de l'aimantation naturelle rémanente et des propriétés magnétiques typiques des sulfides de fer. Ces intervalles sont associés à la formation authigène de greigite dans des conditions suboxiques à l'intérieur des MMDs. Le deuxième faciès magnétique forme une série de 10 courts intervalles caractérisés par l'acquisition de GRM pendant la démagnétisation de l'aimantation rémanente isothermale et la présence de minéraux à forte coercivité comme l'hématite et la goethite. Ce faciès est interprété comme contenant des minéraux magnétiques d'origine pédogénique transportés au lac par de rares évènements de précipitations et d'inondations extrêmes. Les particules pédogéniques ainsi mobilisées se sont déposées au-dessus de MMDs associé à l'inondation. La série d'évènement

d'inondation correspond à des périodes de productivité accrue dans le lac *Laguna Potrok Aike* et sont associées, dans les limites de la chronologie, aux périodes chaudes de la dernière glaciation en Antarctique, à la transition climatique aux latitudes moyennes de l'hémisphère Sud, et aux précipitations plus fréquentes du début de l'Holocène dans le sud-est de la Patagonie.

ROCK-MAGNETIC SIGNATURE OF PRECIPITATION AND EXTREME RUNOFF EVENTS IN SOUTH-EASTERN PATAGONIA SINCE 51,200 CAL BP FROM THE SEDIMENTS OF LAGUNA POTROK AIKE

Lisé-Pronovost, A.[1,2], St-Onge, G.[1,2], Gogorza, C.[3], Jouve, G.[2,4], Francus, P.[2,4], Zolitschka, B.[5] and the PASADO science team[6]

[1] Canada Research Chair in Marine Geology, Institut des sciences de la mer de Rimouski, Université du Québec à Rimouski, Rimouski, Canada

[2] GEOTOP Research Center, Montréal, Québec, Canada

[3]Centro de Investigaciones en Física e Ingeniería del Centro de la Provincia de Buenos Aires (CIFICEN-CONICET), Tandil, Argentina

[4]Centre Eau, Terre et Environnement, Institut National de la Recherche Scientifique, Québec, Québec, Canada

[5]GEOPOLAR, Institute of Geography, University of Bremen, Bremen, Germany

[6] http://www.icdp-online.org/front_content.php?idcat=1494

Abstract

A 106-meter long sediment sequence from the maar lake Laguna Potrok Aike in southern Patagonia was recovered in the framework of the International Continental Scientific Drilling Program (ICDP) Potrok Aike maar lake Sediment Archive Drilling prOject (PASADO). About half of the sedimentary sequence is composed of mass movement deposits (MMDs) and the event-corrected record reaches back to 51,200 cal BP. Here we present a high-resolution rock-magnetic study revealing two sedimentary facies associated with MMDs and characterized by two different types of spurious gyroremanent magnetisation (GRM) acquired during static alternating field demagnetisation. The first rock-magnetic signature is detected in MMDs composed of reworked sand and tephra material. The signature consists of GRM acquired during demagnetisation of the natural remanent magnetisation (NRM) and other rock-magnetic properties typical of iron sulfides such as greigite. We interpret these intervals as authigenic formation of iron sulfides in suboxic conditions within the MMD. The second rock-magnetic signature consists of a series of 10 short intervals located on the top of MMDs characterized by GRM acquisition during demagnetisation of the isothermal remanent magnetisation (IRM). Based on geological, limnological, stratigraphic and climatic evidence these layers are interpreted as reflecting pedogenic hematite and/or goethite brought to the lake by runoff events related to precipitation and permafrost melt. The pedogenic iron minerals mobilized from the catchment most likely settled out of suspension on top of MMDs after a rapid remobilisation event. The series of runoff events corresponds to periods of increased lacustrine productivity in Laguna Potrok Aike and are coeval within the limit of the chronology to warm periods of the last Glacial as recorded in Antarctica, the deglaciation in the mid-latitudes of the Southern Hemisphere and enhanced precipitation during the Early Holocene in southeastern Patagonia.

Keywords

Rock magnetism, Laguna Potrok Aike, lacustrine sediment, paleoenvironment, mass movement deposit, gyroremanent magnetisation

1-Introduction

Millennial-scale climate change recorded in Antarctica ice cores during the last Glacial period led changes in Greenland (e.g., EPICA community members, 2006) and possible trigger mechanisms for the last climatic transition include the impact of changing westerly winds intensity (e.g., Anderson et al., 2009) and sea-ice cover (e.g., Knorr and Lohmann, 2003) on ocean circulation. Despite its importance in the global climate system, the pre-Holocene Antarctic millennial-scale climate variability remains less documented than its Greenland counterpart (e.g., Dansgaard/Oeschger events). This limitation is partly due to the scarcity of pre-Holocene high-resolution records in the Southern Hemisphere largely dominated by the open ocean. Nevertheless, in recent years a growing number of high-resolution paleoclimate records from the Southern Hemisphere emerged and revealed in-phase climate patterns with Antarctica, including marine sediment cores from offshore Australia and New Zealand (e.g., Barrows et al., 2007; Pahnke, 2003), southern South America (e.g. Caniupán et al., 2011; Kaiser et al., 2007; Weber et al., 2012) and in the path of the Antarctic circum-polar current (Pugh et al., 2009). Continental records from Australia (Williams et al., 2009), southern Africa (Gasse et al., 2008) and southern South America (Kilian and Lamy, 2012) also document Antarctic-like climate changes during the last Glacial, however generally at low temporal resolution and often discontinuously.

The Potrok Aike maar lake Sediment Archive Drilling prOject (PASADO) in the framework of the International Continental Scientific Drilling Program (ICDP) recovered a high-resolution sedimentary archive reaching back to the last Glacial in southern South America (Zolitschka et al., 2009; 2013 and papers therein). Previous records from this region are mostly limited to the Holocene and the Late Glacial (cf. Kilian and Lamy, 2012). Located in a region identified as the source area for Glacial dust deposited in Antarctica during the last glacial periods (Basile et al., 1997), the new continental record from Laguna Potrok Aike provides a unique opportunity to document past climate changes in south-eastern Patagonia since the last Glacial period for comparison with the Antarctic climate.

Careful macroscopic sedimentological study of the long PASADO sedimentary sequence revealed that mass movement deposits (MMD) including ball and pillow structures, normally graded beds, structureless sands and fine gravel layers constitute about half of the record (Kliem et al., 2013). The presence of micropumice (Jouve et al., 2013) and fine sands to coarse silt layers disseminated throughout the record (Kliem et al., 2013) highlight the difficulty for readily identifying some MMD and for interpreting paleoclimatic signals. Recent geochemical, mineralogical and elemental studies indicate rare diagenetic remobilization linked to oxic conditions and only sparse organic and carbonate inputs (Hahn et al., submitted; Nuttin et al., 2013). Despite a relatively homogeneous clastic composition of the long sedimentary sequence, Jouve et al (submitted) documented identical geochemical signatures for different types of microfacies and as a result, Jouve et al (2013; submitted) and Hahn et al. (submitted) raised caution against the use of some elemental ratios (e.g., Fe/Mn, Fe/Ti, Mn/Ti) to infer paleoclimatic changes on the complete sequence.

Magnetic properties of the sediment appear especially suited to overcome these difficulties and build continuous paleoclimate proxies from the sediments of Laguna Potrok Aike. Magnetic properties have the advantage of targeting only magnetic mineral (primarily iron oxides, oxyhydroxides and sulfides) and they are not necessarily biased by dilution effects such as the presence of rhyolitic micropumice in Laguna Potrok Aike (Jouve et al., 2013; Wastergard et al., 2013). Mineralogy and grain size-dependent magnetic properties are not influenced by concentration changes, and concentration-dependent parameters can be normalized to avoid such influences (Verosub and Roberts, 1995; Dekkers, 1997; Maher and Thompson, 1999; Evans and Heller, 2003). Previous rock-magnetic measurements from the sediments of Laguna Potrok Aike indicate a magnetic assemblage dominated by magnetite (Gogorza et al., 2012, 2011; Lisé-Pronovost et al., 2013; submitted; Recasens et al., 2012). But evidence for other iron oxides such as maghemite and/or hematite (Gogorza et al., 2012), as well as iron sulfides (Jouve et al., 2013; Vuillemin et al., 2013) were reported. The low-resolution analyses of the PASADO core-catcher samples recently uncovered the potential to use rock magnetism to identify MMD (Recasens et al., 2012).

Here we present a high-resolution rock-magnetic study of the complete sedimentary sequence from Laguna Potrok Aike in order to investigate changes in the magnetic assemblage associated with MMDs and discuss their paleoclimatic implications.

2-Geological setting

Laguna Potrok Aike (51°58'S, 70°23'W; 113 m a.s.l.) is the only maar lake in the Pali Aike volcanic field in southern Argentina (Figure 1A), with a maximum diameter of 3.5 km and water depth of 100 m. Located on the lee-side of the Andean cordillera in south-eastern Patagonia, the region is today influenced by the strong, dry and persistent Southern Hemisphere Westerly Winds (SWW) (e.g., Garreaud et al., 2013). As a result, the annual precipitation is low (ca. 200 mm/yr ; Mayr et al., 2007; Ohlendorf et al., 2013), the climate is semi-arid and aridisols are capable of holding only sparse Patagonian steppe vegetation (Schäbitz et al., 2013; Wille et al., 2007). Winds rarely originate from other directions but easterly winds from the humid Atlantic air masses are often accompanied by extreme precipitation events (Ohlendorf et al., 2013; Schäbitz et al., 2013) (Figure 1B). The lake is polymictic; there is currently no stratification of the water column (Zolitschka et al., 2006) and a recent high-resolution geochemical study revealed that such oxic conditions have predominated since 51,200 cal yr BP (Hahn et al, submitted). Both aerial and submerged lake level terraces indicate significant lake level changes have occurred since the last glacial period (Haberzettl et al., 2008, 2005; Kliem et al., 2013; Zolitschka et al., 2013). At present there is no inflow or outflow and the clastic lacustrine sediment is primarily deposited after eolian transport, and subordinated by remobilisation of sediments during lake level changes and episodic runoff event.

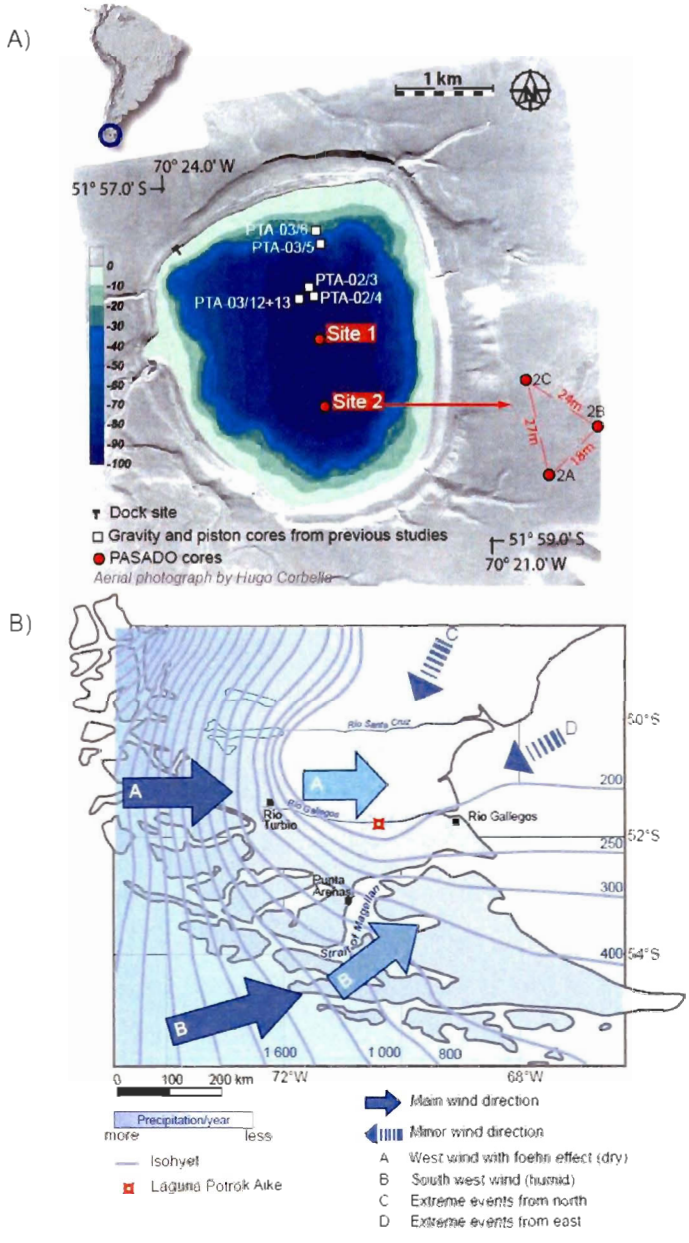

Figure 3. 1. A) Aerial photograph and bathymetry of Laguna Potrok Aike in southern South America. The PASADO coring sites 1 and 2 as well as other coring sites discussed in the text are indicated. B) Main and minor wind directions as well as annual precipitation in southern South America (modified from Schabitz et al., 2013).

The regional surface geology consists of semi-consolidated sedimentary rocks of the Miocene Santa Cruz Formation, Mio-Pliocene basalts, pyroclastic and phreatomagmatic sediments, and unconsolidated Quaternary deposits including tills, glaciofluvial, fluvial, lacustrine and aeolian sediments (D'Orazio et al., 2000; Zolitschka et al., 2006; Ross et al., 2011; Coronato et al., 2013). The unconsolidated deposits provide abundant silt to sand size detrital magnetite (Coronato et al., 2013; Lisé-Pronovost et al., 2013; submitted).

3-Methods

3.1 Field work

A total of 533 m of sediment were retrieved in 2008 at two sites in the deep basin of Lake Laguna Potrok Aike (position on Figure 1) in the framework of the ICDP. Cores were collected using the GLAD800 drilling platform operated by the consortium for Drilling, Observation and Sampling of the Earth's Continental Crust (DOSECC). Site 2 was selected for multi-proxy high-resolution analyses by the PASADO science team because of higher core recovery (98.8%) and lower apparent sand content (Zolitschka et al., 2009). The sedimentary sequence at site 2 was built from 3 holes (Figure 1; Kliem et al., 2013) and has a composite length of 106.09 m.

3.2-Discrete samples

A series of 59 pilot cube samples (2x2x2 cm) were recovered from parallel cores (holes A, B and C at site 2; Figure 1) at depths readily correlated to the composite profile using high-resolution core images. The cube samples were first used to measure the frequency dependence of magnetic susceptibility at room-temperature using Bartington dual frequency (0.46 and 4.6 kHz) MS2B meter. Difference in the susceptibility measured at low and high frequency is diagnostic of ultrafine (<0.03 μm) superparamagnetic and ferrimagnetic particles (Dearing, 1999). Afterward the anisotropy of magnetic susceptibility (AMS) was measured in 600 directions using the magnetic anisotropy susceptibility bridge "Roly-Poly" at the Institute for Rock Magnetism (IRM) of the University of Minnesota in

Minneapolis. The best-fit AMS tensor was obtained by least-squares and the degree of AMS was calculated by dividing the maximum by minimum susceptibility.

The composite profile at site 2 was sampled at ca. 40 cm intervals (total of 243 samples) for the measurement of hysteresis loops and derived properties including saturation remanence (Mr), saturation magnetisation (Ms), bulk coercive force (Hc) as well as remanent coercive force (Hcr) using a Princeton Corp. alternating gradient force magnetometer (model MicroMag 2900 AGM). The magnetic properties Mr, Ms, Hc and Hcr depend on coercivity and the domain state of the magnetic assemblage. The ratios Mr/Ms and Hcr/Hc are commonly used as a magnetic grain size indicator (Day et al., 1977; Dunlop, 2002; Tauxe, 2010). The high-field magnetic susceptibility (k_{HF}) is the high-field slope of magnetisation on the hysteresis curve. It reflects the contribution of non-ferrimagnetic material (diamagnetic and paramagnetic minerals), unsaturated antiferromagnetic minerals and unsaturated ultrafine superparamagnetic particles (e.g., Brachfeld, 2006). The proportion of high-field susceptibility for each sample was calculated by normalizing the hysteresis curve slope correction in a field of 0.3T (k_{HF}) with Ms. As low coercivity minerals (magnetite and maghemite) are saturated in fields < 0.3 T and higher coercivity minerals such as hematite and goethite are not (Dunlop and Özdemir, 2007), the proportion of high-field susceptibility reflect the hardness of the sediment in the absence of dia-, para- and superparamagnetic change. In order to further investigate the grain size distribution, 36 samples were selected for first-order reversal curve (FORC; Roberts et al., 2000) analyses in a saturating field of 1.2 T using the same instrument. Five of the discrete samples are associated to rock-magnetic facies 1 and were used for additional analysis. Unfortunately, no samples from facies 2 were left available. Magnetic extracts (using a neodymium hand-magnet) from rock-magnetic facies 1-*B*, *D*, *E*, *C* and *G* were analyzed using JEOL 6460LV scanning electron microscope equipped with an Energy Dispersive X-ray Spectrometer (SEM-EDS) in order to identify the iron minerals.

3.3-Continuous u-channel samples

The continuous u-channel samples from the composite sediment sequence at site 2 (99 sections; 106.09 m) were measured at 1-cm resolution. The natural, anhysteretic and isothermal remanent magnetisations (NRM, ARM, IRM) were measured using a minimum of 8 alternating field (AF) demagnetisation steps (0, 10, 20, 30, 40, 50, 60 and 70 mT) using a 2G cryogenic magnetometer for u-channels. ARM was imparted with a peak AF of 0.1 T and a direct current (DC) bias field of 0.05 T. Susceptibility of anhysteretic remanent magnetisation (kARM) was obtained by normalizing ARM by the DC field applied. Two IRMs at 0.3 T and 0.95 T were successively induced using a 2G pulse magnetizer and then stepwise AF demagnetised. The low field magnetic susceptibility (k_{LF}) using a point sensor and the diffuse spectral reflectance (L*, a*, b* color space) using a Minolta in-line spectrophotometer were measured on a GEOTEK Multi-Sensor Core Logger (MSCL) at 1 cm intervals at ISMER.

We use a set of rock-magnetic ratios and indicators to effectively discriminate between different magnetic minerals and magnetic grain sizes (e.g., Stoner and St-Onge, 2007; Maher et al., 1999). This approach is particularly useful when working with large datasets such as high-resolution measurements on continuous u-channel samples of long sediment cores. The median destructive field (MDF) is the field required to remove half of the initial remanence, whether natural or induced. The MDF is influenced by magnetic grain size and mineralogy; hence MDF is a measure of the coercivity of a magnetic recording assemblage. Similarly, the remanence ratios permit isolation of a coercivity population between two demagnetisation steps of a natural, anhysteretic or isothermal remanent magnetisation (NRM, ARM or IRM). The ratio of ARM (or kARM) normalised by IRM is often referred to as the ARM ratio (e.g., Egli, 2004a; Lascu and Plank, in press). It is commonly used as a magnetic grain size indicator for a magnetic assemblage dominated by magnetite because small single domain (SD) grains display disproportionately high ARM values (Maher et al., 1988). As a result, the ARM ratio responds to small SD biogenic magnetite (Moskowitz et al., 1993; Snowball et al., 2002;

Egli, 2004a) as well as to ultrafine magnetite near the superparamagnetic (SP) / stable singe domain (SSD) boundary, to SD extracellular or pedogenic magnetite particles (Özdemir and Banerjee, 1982; Maher and Taylor, 1988; Moskovitz et al., 1993; Frankel and Bazylinski, 2003; Maher et al., 2003; Egli, 2004a). The ratio of saturation isothermal remanent magnetisation (SIRM) and magnetic susceptibility (k_{LF}) is also a magnetic grain size indicator for a mineralogy dominated by magnetite, but can be influenced by paramagnetic and superparamagnetic contributions k_{LF} (e.g., Thompson and Oldfield, 1986; Stoner et al., 1996). For a magnetic mineralogy containing iron sulfides (greigite and pyrrhotite), high values of SIRM/k_{LF} are caused by typically low k_{LF} (Snowball and Thompson, 1990; Fu et al., 2008; Roberts, 1995). Higher values of SIRM/k_{LF} are associated with high coercivity minerals such as hematite and goethite because their strong resistance to magnetisation results in relatively low IRM acquired in a given field than other magnetic minerals and exceptionally low k_{LF}, which is measured in a weak applied field (Maher, 2011). Finally, the ratio IRM/SIRM reflects the degree of magnetic "hardness" i.e., the proportion of high coercivity minerals relative to low coercivity minerals (e.g., Stoner and St-Onge, 2007; Maher, 2011).

The sediment from Laguna Potrok Aike overall displays very high values of IRM in direct current (DC) fields of 0.3 T and 0.95 T (average value of all data > 6 Am^{-1}; Table 1). The intensity of $IRM_0$0.95 T is sometimes lower than $IRM_0$0.3 T. This result is due to the inability of the cryogenic magnetometer system to accurately detect magnetisation > ca. 1 Am^{-1} in samples with high concentration of magnetic mineral (Roberts, 2006) such as the sediment from Laguna Potrok Aike (2-9 wt % of Fe2O3; Hahn et al., submitted). This instrumental limitation obviously prevents us from using the IRM/SIRM ratio to continuously track the relative contribution of high coercivity minerals in a continuous way; however the arithmetic average values for the different sediment types are included in Table 1. In this study, we use the remanence ratios, kARM/$IRM_0$0.3 T (herein referred to the ARM ratio), $IRM_0$0.95 T/k_{LF} (herein referred to SIRM/k_{LF}) and $IRM_0$0.3 T/$IRM_0$0.95 T (herein referred to IRM/SIRM) from continuous u-channel samples data to identify different rock-magnetic facies.

3.3-Lithology and chronology

Kliem et al. (2013) described five lithological units for the composite sediment sequence from Laguna Potrok Aike based on the type of pelagic sediment and the frequency of MMDs. The simplified lithostratigraphic log as well as the radiocarbon-based chronology is presented in Figure 2. The three lowermost units (10609-8153cm, 8153-4023cm and 4023-1872 cm) correspond to the last Glacial period and are characterized by progressive decrease in the percentage, frequency and thickness of MMD. From 1872 to 882 cm (Early Holocene, Late Glacial and ending last Glacial) there is a dominance of pelagic laminated silts intercalated with thin fine sand and coarse silt layers, high content of plant macro remains and gastropods, few carbonate crystals and the occurrence of normally graded beds and pillow structures. The uppermost sediment type (882-0cm) corresponds to the Holocene and consists of pelagic laminated silts with relatively high amounts of carbonates, in agreement with Nuttin et al (2013). The chronology of the event-corrected composite depth (cd-ec) of the pelagic sediment sequence (4580 cm cd-ec) is based on a mixed-effect regression model of 58 radiocarbon dates and supported by 6 known tephra layers as well as by a global-scale magnetostratigraphy using relative paleointensity (Kliem et al., 2013; Lisé-Pronovost et al., 2013). Lithological and tephra correlation with previously studied cores from Laguna Potrok Aike further supports the radiocarbon-based chronology, including a core located nearby in the lake center covering the last 16,000 cal BP (PTA03/12-13; location on Figure 1; Haberzettl et al., 2007) and a low-resolution core from a lake level terrace covering a similar time span (PTA03/5-6; location on Figure 1; Haberzettl et al., 2009).

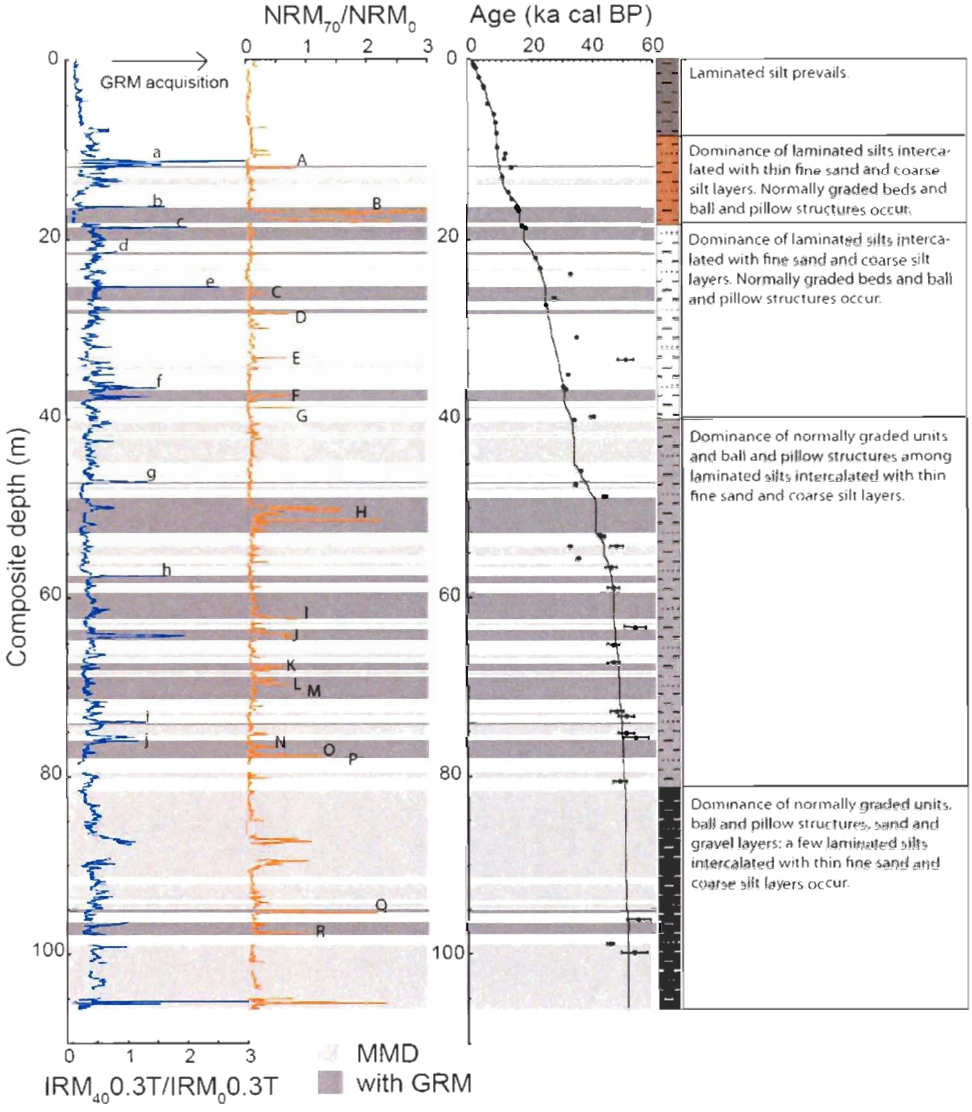

Figure 3. 2. Acquisition of gyroremanent magnetisation (GRM) during static alternating field (AF) demagnetisation of the sediment of Laguna Potrok Aike is observed within and over mass movement deposits (MMD; in light grey, those with GRM in dark grey). Rock-magnetic ratios $IRM_{40}0.3$ T /$IRM_0 0.3$ T and NRM_{70}/NRM_0 indicate GRM acquired during AF demagnetisation of isothermal and natural remanent magnetisation, respectively. The lowercase and capital lettered features indicate the position of rock-magnetic facies 1 (from *A* to *R*) and rock-magnetic facies 2 (from *a* to *j*) discussed in the text. The radiocarbon-based chronology, lithological units and description from Kliem et al. (2013) are presented on the right.

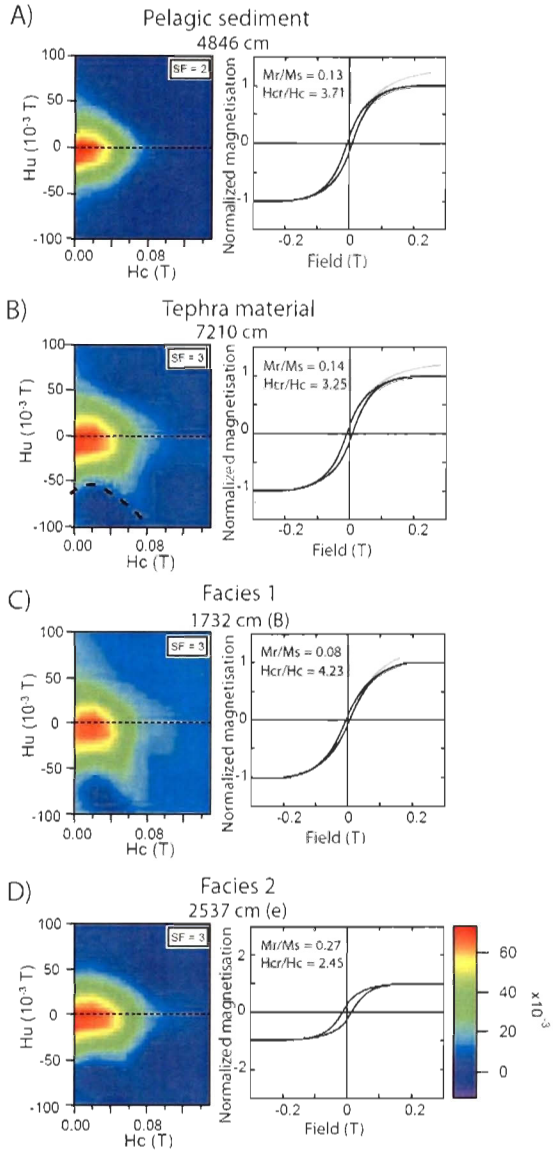

Figure 3. 3. First-order reversal curve (FORC) diagrams and hysteresis curves depicting the coercivity distribution of a typical pelagic sediment (A) and a tephra layer sample (B) from Laguna Potrok Aike, compared with samples from facies 1-*B* and 2-*e* (C and D*)*. The raw (grey) and high-field slope corrected (black) magnetisation are illustrated. The "kidney" shape indicated by a broken line on tephra's is reported for iron sulfides (Wehland et al., 2005; Roberts, 2011).

4-Results

4.1-Magnetic assemblage

4.1.1-Discrete samples

The rock-magnetic analysis of cube samples reveals that 1) the degree of anisotropy is weak (less than 1.15), which indicates that the magnetic assemblage is not dominated by minerals with strong magnetocrystalline or shape anisotropy, and 2) the frequency-dependant magnetic susceptibility is generally lower than 2%, which indicates that there is no detectable superparamagnetic (SP) contribution (Dearing, 1999) in the general magnetic assemblage. Similar frequency-dependant results were obtained for the sediments of Laguna Potrok Aike for the last 16,000 cal BP (Gogorza et al., 2011; 2012) however we note that SP in low abundances are difficult to detect in the absence of low temperature measurements. The typical hysteresis curve for the pelagic sediment has a narrow loop and the shape is typical of pseudo single domain (PSD) magnetite (Figure 4A) (Tauxe, 1996). The associated first-order reversal curve (FORC) diagram also indicates PSD magnetite with closed peak structures and coercivity spectra centered at ca. 20 mT (Figure 4A). The enlargement of the contours near the applied field axe (Hu) additionally indicates a possible contribution of MD or SP magnetite (Muxworthy and Roberts, 2007). The typical FORC diagram of tephra material displays a "kidney" shape towards higher coercivities (Figure 4B). This shape is reported for iron sulfides greigite and pyrrhotite (Larrasoaña et al., 2007; Roberts et al., 2011, 2006; Wehland et al., 2005). The "kidney" shape is frequent in FORC diagrams of tephra material, in agreement with previous observation of iron sulfide framboids in the micropumice vesicles of reworked tephra from Laguna Potrok Aike (Jouve et al., 2013; Vuillemin et al., 2013). The "kidney" shape is also observed in different degrees in pelagic and MMD samples throughout the record, suggesting a small contribution of iron sulfides in addition to magnetite. Together, cube and discrete sample analyses further support PSD magnetite as the dominant magnetic mineral in the sediment of Laguna Potrok Aike since 51,200 cal BP (Gogorza et al., 2011; 2012; Recasens et al., 2012; Lisé-Pronovost et al., 2013; submitted).

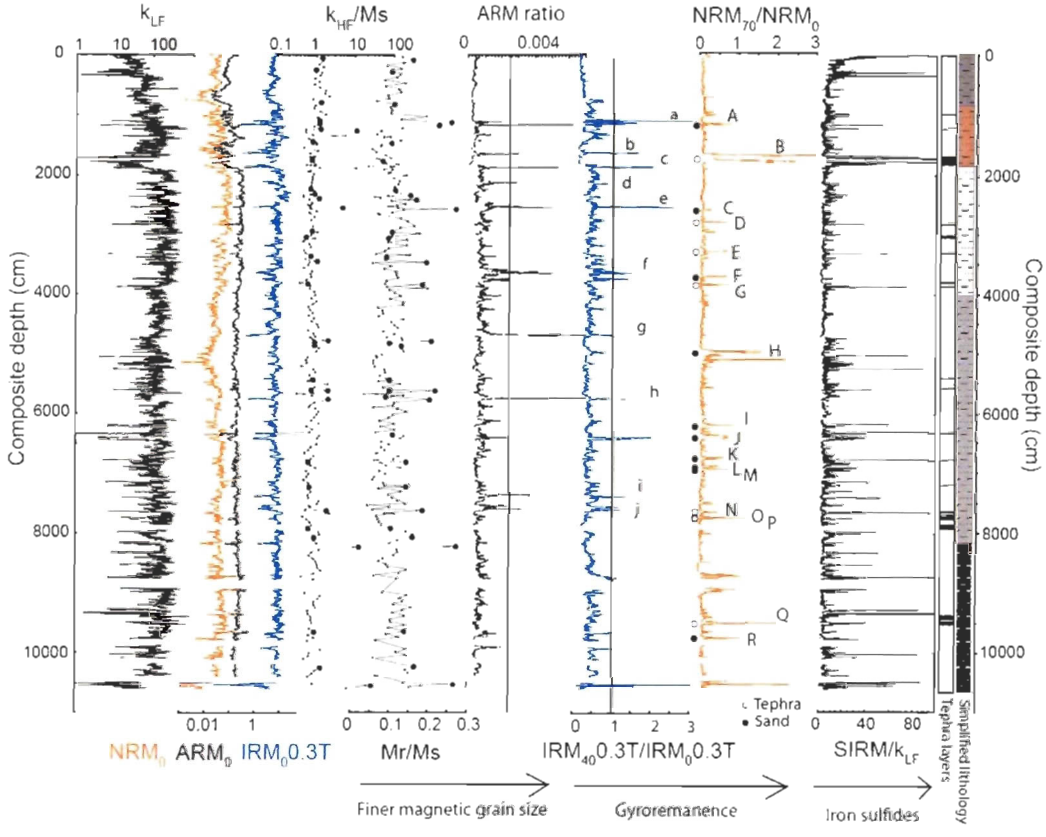

Figure 3. 4. Rock-magnetic properties of the composite sedimentary sequence at site 2 from Laguna Potrok Aike. From left to right: low field magnetic susceptibility (k_{LF}), natural (NRM_0), anhysteretic (ARM_0) and isothermal ($IRM_0$0.3 T) remanent magnetisations before alternating field (AF) demagnetisation, and the proportion of high-field susceptibility normalized by saturation magnetization (k_{HF}/Ms) are presented on a log scale. The grain size indicators Mr/Ms and the ARM ratio (kARM/$IRM_0$0.3 T) are presented. Selected samples for FORC analyses are shown with larger symbols on k_{HF}/Ms and Mr/Ms curves. High values of the remanence ratio IRM_{40}0.3 T/$IRM_0$0.3T within facies 2 that indicate the acquisition of gyroremanence during AF demagnetisation of IRM and the rock-magnetic facies 2 is labelled from *a* to *j*. High values of the remanence ratio NRM_{70}/NRM_0 that indicate gyroremanence acquisition during AF demagnetisation of NRM within rock-magnetic facies 1 is labelled from *A* to *R*. Symbols (open or closed) represent the associated sediment type (tephra or sand, respectively.) of type 1 intervals. Peak values of SIRM/k_{LF} ($IRM_0$0.95 T/k_{LF}) are indicative of iron sulfides (Maher et al., 1999). The position of tephra layers and lithological units from Kliem et al. (2013) are presented on the right panel.

4.1.2-Continuous u-channel samples

Figure 4 presents a set of u-channel-based high-resolution magnetic properties for the PASADO sedimentary sequence (106.06 m). The average values of selected parameters are listed in Table 1. There is an overall low amplitude variability within the rock-magnetic parameters that is interrupted by peaks in the ARM ratio, SIRM/k_{LF}, Mr/Ms and k_{HF}/Ms. The peaks fall within or over MMD and represent two particular rock-magnetic signatures associated with two distinct types of gyroremanence best represented by remanence ratios NRM_{70}/NRM_0 (features *A* to *R*) and $IRM_{40}0.3$ T/$IRM_0$0.3 T (features *a* to *j*) associated to MMD (Figure 2). These intervals are discussed in more detail.

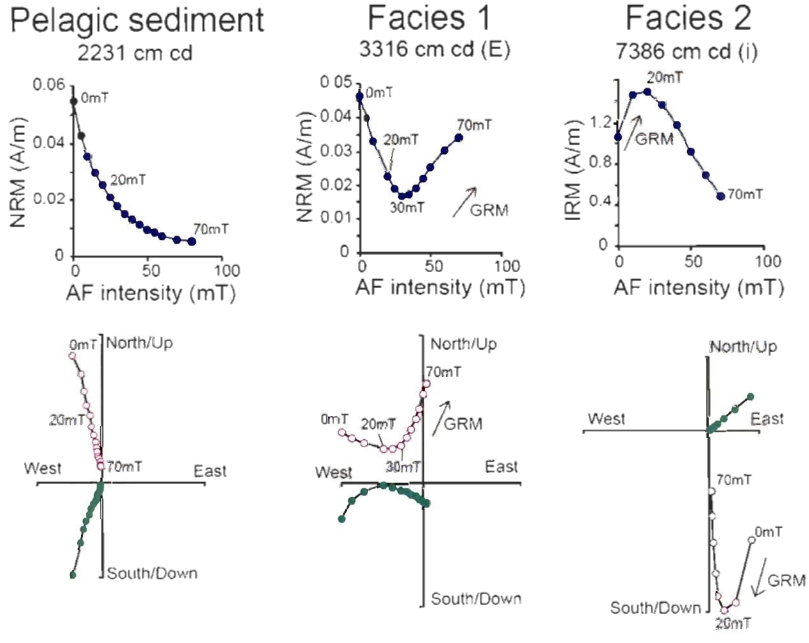

Figure 3. 5. Demagnetisation plots and orthogonal projection diagrams illustrating the typical behavior of pelagic sediment from Laguna Potrok Aike, facies 1 and 2. Arrows indicate the spurious gyroremanent magnetisation (GRM) acquired during AF demagnetisation of NRM (facies 1) and IRM (facies 2). Open (closed) symbols in the vector end-point orthogonal diagram represent projection in the vertical (horizontal) plane.

Table 3. 1. Average values of selected parameters for rock-magnetic facies 1 and 2 compared to all data from Laguna Potrok Aike. The high values of SIRM/k_{LF} ($IRM_0$0.95 T/k_{LF}) in facies 1 is linked to low k_{LF} values. High values of ARM ratio (kARM/$IRM_{0.3T}$) in facies 2 is linked to low $IRM_{0.3T}$ values.

	k_{LF} (10^{-5}SI)	NRM_0 (Am^{-1})	ARM_0 (Am^{-1})	IRM_0 0.3T (Am^{-1})	IRM_0 0.9T (Am^{-1})	IRM/SIRM	ARM ratio (mmA^{-1})	SIRM/k_{LF} (kAm^{-1})
All data	137	0,033	0,18	6,5	6,2	1,08	0,78	7,4
Facies 1	86	0,027	0,14	6,3	5,9	1,07	0,65	**23,1**
Facies 2	117	0,025	0,17	**1,3**	1,5	0,88	**4,10**	2,6

4.2-Rock-magnetic facies

4.2.1- Facies 1

Rock -magnetic facies 1 represents a total of 4.60 m or 4.3% of the total sediment record and is characterized by gyroremanence acquisition during AF demagnetisation of NRM, as indicated by high values of the remanence ratio NRM_{70}/NRM_0 (features *A* to *R*; Figures 2 and 4). The spurious remanence is acquired perpendicular to the AF direction (Figure 5) from 20-55 mT in sandy sediment and from 30-45 mT in tephra material. The example shown in figure 5 (facies 1E at 3316 cm) is composed of tephra material. Facies 1 is generally characterized by low and unstable NRM, low k_{LF} values, and peak values of SIRM/k_{LF} (Table1; Figure 2). The discrete sample at 1732 cm depth is part of a reworked tephra displaying the facies 1 rock-magnetic properties (feature *B*; Figure 2). Its FORC diagram displays coercivity spectra centered at ca. 20 mT and a "kidney" shape towards higher coercivities. The paleomagnetic directions display large amplitude changes in rock-magnetic facies 1, and in particular the paleomagnetic inclination sharply departs from the theoretical geocentric axial dipole (GAD) value for the site latitude (Figure 6). Together the shape of the FORC diagram, the acquisition of gyroremanent magnetisation during AF demagnetisation of the NRM and peak values of SIRM/k_{LF} are diagnostic of iron sulfides such as greigite and pyrrhotite in facies 1 (Snowball, 1991; Maher et al., 1999; Roberts,

1995; Roberts et al., 2011; Sagnotti and Winkler, 1999). This is further supported by SEM-EDS identification of framboidal iron sulfides (Fe and S) in the facies 1 sample (Figure 7). In addition, abundant iron oxide (Fe and O) coatings are observed on all types of grains in facies 1, including detrital quartz, magnetite and micropumice (Figure 7). The iron coatings were also observed in tephra layers using SEM-EDS analysis of thin slices (Jouve et al., submitted).

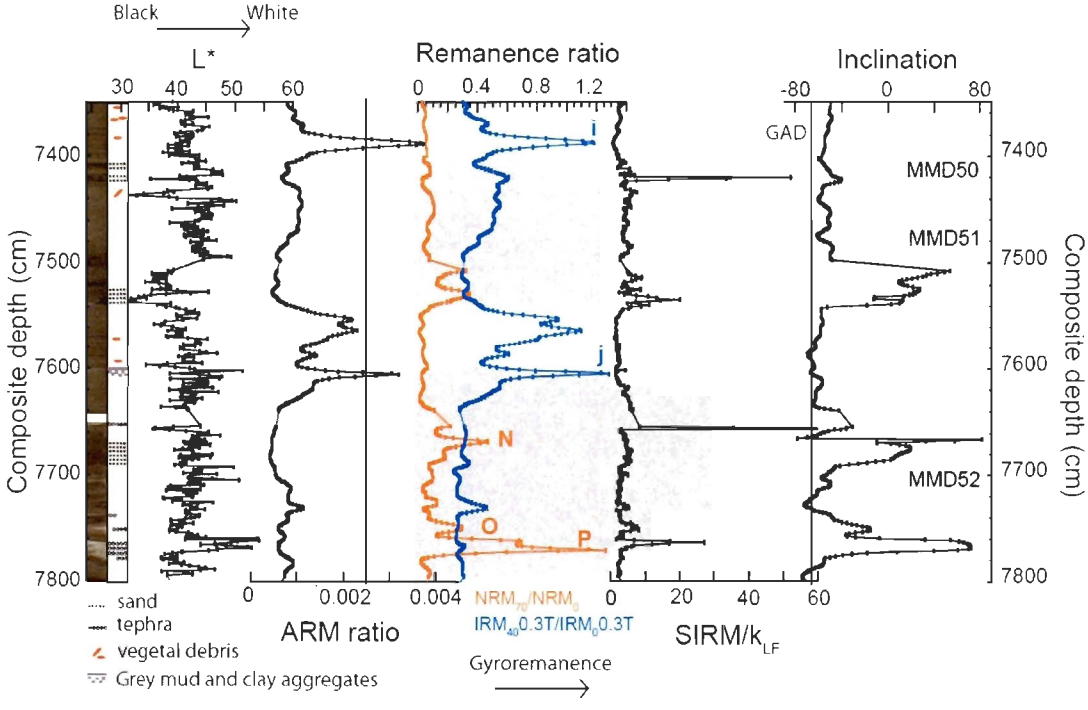

Figure 3. 6. Stratigraphy of facies 1 and 2 with mass movement deposits (MMDs) in the interval 73-78 m blf. From left to right: core photograph, and simplified lithostratigraphic log, L*, ARM ratio (ARM/$IRM_0$0. 3 T), remanence ratios IRM_{40}0.3 T/$IRM_0$0.3 T and NRM_{70}/NRM_0, SIRM/k_{LF} and paleomagnetic inclination. The vertical line on the inclination plot indicates the theoretical value for a geocentric axial dipole (GAD) at the latitude of the coring site. The MMDs are underlined in grey and the features *N*, *O*, *P* (facies 1) as well as *i*, *j* (facies 2) are indicated.

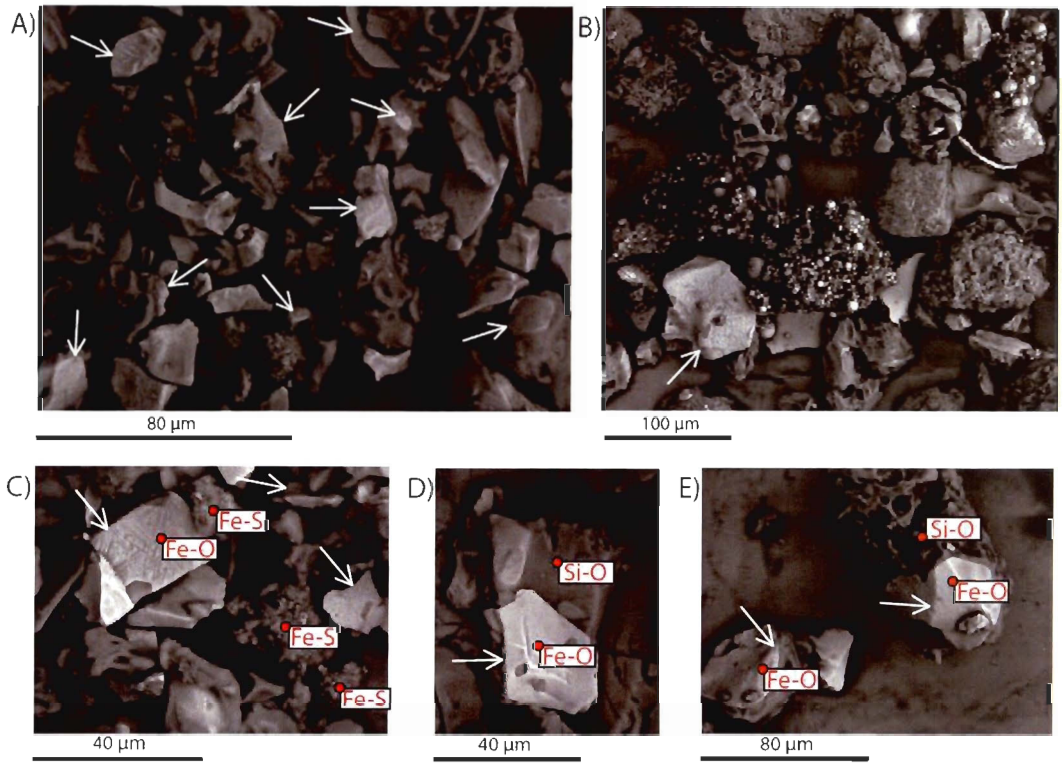

Figure 3. 7. Scanning electron microscopic (SEM) images and X-ray identification of framboidal iron sulfides and iron oxide coatings in facies 1. Red circles indicate spots for X-ray element analyses and white arrows indicate iron oxide coatings precipitated on detrital grains. A) General view of iron oxide coatings on various types of detrital grains in facies1-*G*, B) aggregates of framboidal iron sulfides and iron coating in facies 1-*B* and C) in facies 1-*D*, close-up of D) iron oxide coating on a detrital grains in facies 1-*E* and E) on micropumice in facies 1-*G*.

4.2.2- Facies 2

Rock-magnetic facies 2 represents a total of 0.99 m or 0.93% of the total sediment record and is characterized by maximum peak values of the ARM ratio (>2.5 mmA^{-1}), relatively lower $IRM_0$0.3 T values (Table 1; Figure 4) and acquisition of gyroremanence during AF demagnetisation of IRM. The latter is best represented by the remanence ratio

IRM_{40}0.3 T/$IRM_0$0.3 T (Figure 4). Acquisition of the spurious remanence begins between 5-15 mT and continues up to 15-35 mT, and then the sample is progressively demagnetized (Figure 5). The GRM is acquired between perpendicular and antiparallel to the alternating field (Figure 5). Paleomagnetic directions are stable and consistent with the GAD inclination for the coring site (Figure 6) and the magnetic assemblage is sometimes characterized by single domain-like (SD) magnetic properties, as indicated by a higher Mr/Ms ratios (features *a*, *e*, *h*, *j*; Figure 4) as well as MDF_{ARM}/MDF_{IRM} values greater than 1 (*a*, *c*, *e*, *f*; not shown). The occasional SD-like properties and high values of the ARM ratio (average of 4.1 mmA^{-1}; Table 1) point to finer magnetic particles such as magnetosomes, authigenic magnetite and/or pedogenic magnetite (e.g., Moskowitz et al., 1993; Egli, 2004a) in a magnetic mineralogy dominated by magnetite. For magnetite, the high ARM ratio is attributed to the SD particle size, giving rise to unusually strong ARMs (Maher, 1988). However, in the sediment of Laguna Potrok Aike, peak values of the ARM ratio are not related to an ARM maximum, but to an IRM minimum (Table 1; Figure 4). Therefore, and because not all intervals of facies type 2 display SD-like properties, finer magnetite particles alone do not account for the particular magnetic signature of facies 2 and magnetic minerals other than magnetite must be present.

The average IRM/SIRM values for facies 2 is lower than the average for the complete dataset and for the facies 1 (Table 1) pointing to a contribution of higher coercivity minerals such as hematite or goethite. This is supported by a systematically lower proportion of saturation acquired in forward fields of 0.3 T and 0.95 T (Table 1; Figure 4), and by higher values of high-field susceptibility in available discrete samples (Figure 4). For instance, the sample at 2537 cm cd (corresponding to feature *e* of facies 2) has a steeper high field slope in the raw hysteresis loop (Figure 3, light grey curve) relative to the typical pelagic, fine sediment, and tephra material. There is no significant dilution of the concentration-dependant rock-magnetic properties in facies 2 (Figure 4) as would be expected for an increase in para- or diamagnetic contributions. Hence, the steep slopes in facies 2 are attributed to unsaturated magnetic minerals in a 0.3 T field and could additionally reflect a contribution of ultrafine superparamagnetic particles. Finally, the

more open hysteresis loop and a FORC diagram covering a slightly larger range of coercivities than the typical pelagic sediment (Figure 3) is also consistent with a contribution of high coercivity minerals such as hematite and goethite to facies 2.

4.2.3 Stratigraphy of the rock-magnetic facies

Rock-magnetic results reveal that the higher proportion of magnetic minerals besides magnetite is found in relation to MMDs in the sediment of Laguna Potrok Aike. Iron sulfides (facies 1) are found within MMDs composed of sands and tephra (Figure 6). High coercivity minerals (facies 2) are found in sediment deposited immediately above MMDs (for example the features *i* and *j*; Figure 6). Weaker rock-magnetic signatures in facies 2 occur within MMDs, but with lower intensity (e.g., ARM ratio < 2.5 mmA^{-1}). We now focus on the 10 strongest signatures denoted as *a* to *j* (Figures 2 and 4). The L* values is a useful indicator of (white-colored) tephra layers, which are sometimes associated with iron sulfides at Laguna Potrok Aike (e.g., features *O* and *P*; Figure 6). While not all sand- and tephra-bearing MMD have rock-magnetic signatures of facies 1, iron sulfides are most frequently located directly at the base of MMD horizons, and a series of facies 1 features are sometimes observed within a MMD (for example features *N*, *O* and *P* in MMD52; Figure 6). Four MMDs are associated with both facies (1 and 2). However, most of the time the facies occur independently of each other, suggesting there is no link between their formations. Visual description of the rock-magnetic facies 2 sediment and associated MMDs are presented in Table 2. There is often plant macro remains of aquatic mosses visible in the sediment and the MMDs are either capped with sands, reworked tephra material (feature *b* is located above a tephra from Reclus volcano; Wastegård et al., 2013) or a grey mud layer. Feature *a* is the only one displaying yellow coloration. Interestingly, three grey mud layers (associated to features *c*, *h* and *j*) visibly overlay sediment containing clay aggregates (Figure 8) recently interpreted as indicators of permafrost melt (Jouve et al., submitted). In summary, facies 1 is characterized by iron sulfides inside MMDs composed of sand and tephra material, whereas facies 2 is characterized by high coercivity minerals deposited on the top of MMDs of various compositions.

Table 3. 2. Description of the sediment and mass movement deposits (MMDs) associated with the 10 labeled rock-magnetic facies 2.

Rock-magnetic facies 2		Depth[1]	Age[1]	Mass movement deposit	
Name	Sediment description	(cm cd)	(cal BP)	Thickness (cm)	Sediment description
a	Yellow color; vegetal debris	1184	9260 ± 715	22	Sands
b	Layer of vegetal debris	1648	16030 ± 560	174	Reworked tephra material including mud laminations
c	Grey mud overlaying clay balls in the MMD	1875	17320 ± 543	141	Mud
d	Layer of vegetal debris	2143	20250 ± 672	34	Sand at base , fining upward with plant debris on top
e	Grey mud	2533	24280 ± 1140	158	Mud
f	Mud	3678	30640 ± 1313	126	Mud and sands
g	Mud	4708	37290 ± 1316	12	Sand layers with mud clasts
h	Grey mud overlaying clay balls in the MMD	5753	46000 ± 4484	82	Sand at base , fining upward
i	Laminated mud	7403	49320 ± 7790	20	Sand and mud
j	Grey mud overlaying clay balls in the MMD	7600	49580 ± 8077	202	Mud, sand and tephra material, folded structure

[1]Depth and age as on the top of the MMD

5-Discussion

5.1 Gyroremanent magnetisation (GRM) and magnetic mineralogies

While the GRM acquisition during AF demagnetisation of the NRM (such as in facies 1) is frequently used as diagnostic of iron sulfides in sediments (Hu et al., 1998; 2002; Roberts et al., 2011; Snowball, 1997; Stephenson and Snowball, 2001), to our knowledge the acquisition of GRM during AF demagnetisation of the IRM (such as facies 2) was only reported by Thomson (1990) for pyrrhotite-bearing rocks from northern England. We interpret the acquisition of GRM in the facies 2 as indicative of field-dependant anisotropy in hematite and/or goethite particles. From Stephenson (1980), it is well known that the anisotropy of a sample is responsible for the GRM acquisition during AF demagnetisation. Consequently, only a magnetic mineral becoming magnetically anisotropic when subjected to an IRM can account for the acquisition of GRM *uniquely* during AF demagnetisation of the IRM (and not during AF demagnetisation of the NRM and ARM).The distinctive contribution of high coercivity minerals in rock-magnetic facies 2 (and the absence of iron sulfides such as greigite and pyrrhotite) hence suggests that pedogenic hematite and/or goethite must account for the observed GRM acquisition.

Both hematite and goethite minerals have crystal asymmetry due to structural defects and/or substitutions and as a result, display variable rock-magnetic properties (Dekkers, 1989; Liu et al., 2010; Rochette et al., 2005). The acquisition of GRM in facies 2 could be linked to a metastable domain state of pedogenic hematite as was hypothesized by Tauxe et al. (1990). This interpretation is supported by a simple model of realistic acicular SD particles by Potter and Stephenson (2006) revealing that hematite particles can display a range of variable stable orientations resulting in large field-impressed anisotropy and GRM acquisition during alternating field demagnetisation. In addition, a near anti-parallel orientation of the GRM in some of the facies 2 might also indicate grains prone to self-reversal as reported for oxidized iron oxides such as maghemite and ilmeno-hematite (Channell and Xuan, 2009; Roperch et al., 2012). If this is the case, the GRM acquired during AF demagnetisation of the NRM and ARM must have been swamped by the strong

normal component held by detrital magnetite and only detectable during AF demagnetisation of the IRM because of field-impressed anisotropy.

5.2 Origin of magnetic minerals

5.2.1 Authigenic formation of iron sulfides in facies 1

The production of magnetic iron sulfides such as greigite and pyrrhotite in sediments is well documented and requires sulfate-reducing conditions (Konhauser, 1998; Sagnotti, 2007). Early diagenetic pyrrhotite is unlikely to form at temperatures < 180°C (Horng and Roberts, 2006), however greigite is commonly preserved in marine or lacustrine sedimentary archives when the pyritisation process is interrupted (e.g., Fu et al., 2008; Blanchet et al., 2009; Brachfeld et al., 2009). The pyritisation process requires decomposable organic matter, dissolved sulfate and reactive detrital iron minerals (Berner, 1984). While there are abundant iron oxides in Laguna Potrok Aike (Gogorza et al., 2012; Lisé-Pronovost et al, 2013; submitted), the very low organic matter content in the sediment (average of 0.55% and 0.98% during the last Glacial period and since 17300 cal BP, respectively; Hahn et al., 2013) and the variable amount of dissolved sulfate (from 0 to 1500 ppm; Vuillemin et al., 2013) are the most likely factors limiting the pyritisation process. The low k_{LF} values of facies 1 (Table 1), the weak and unstable NRM as well as the sharp change in inclination (Figure 6) altogether point to dissolution of detrital magnetite, which in turn would have provided the required reactive Fe^{2+} for the formation of iron sulfides.

We infer that while diffusing upward, the Fe^{2+} reacted with available organic matter and dissolved sulfate in the pore water to form greigite. It is unclear whether organic matter or sulphates limited the pyritisation process in tephra layers. Nevertheless, precipitation of iron oxide coatings on minerogenic grains indicate excess Fe^{2+} reaching the oxic/anoxic boundary (Stumm and Morgan, 1996; Gobeil et al., 1997). The situation is different in sand layers, where abundant pore water sulfate suggests that organic matter most likely limited the process of pyritisation. A low-resolution study of site 1(position on Figure 1)

(Vuillemin et al., 2013) identified three intervals of significantly higher pore water sulfate interpreted as major mafic inputs to the lake. The depth correlation between sites 1 and 2 (Gehbardt, pers. comm.) indicates that these mafic inputs correspond to the cluster of facies 1 features *-I* to *-M*, and features 1-*H* and *-F* in reworked sand layers at site 2 (Figure 4). Hence, the preservation of greigite in these mafic sand layers was most likely promoted by higher sulfate availability and limited by low organic matter content. The high-resolution rock-magnetic identification of greigite in facies 1 provides support to the interpretation of Vuillemin et al. (2013) and additionally reveals 3 previously undetected sand layers with the same rock-magnetic signature (facies 1 features *-A*, *C*, and *R*). Despite minimal diagenetic processes in the sediment of Laguna Potrok Aike due to a well-oxygenated water column and a low organic content (Nuttin et al., 2013; Vuillemin et al., 2013; Hahn et al., submitted), our results reveal that adequate conditions for the authigenic formation of greigite were reached in some MMDs composed of sand and tephra material.

5.2.2 Input of pedogenic particles for facies 2

Rock-magnetic data reveal a series of 10 short intervals (facies 2) with a magnetically significant proportion of high coercivity minerals (hematite and/or goethite). We interpret these intervals as containing pedogenic particles transferred to the lake by extreme runoff events based on geological, limnological, stratigraphic and climatic evidences.

First, we consider the possible sources of high coercivity authigenic or detrital minerals in lake sediments. There is no paleolimnological evidence (since 51200 cal BP; Zolitschka et al., 2013, 2009) that Laguna Potrok Aike met the hypersaline and acidic lake conditions required for precipitation of authigenic hematite concretions, as documented for Lake Brown (Australia) and possibly also for planet Mars (Bowen et al., 2008), or for the precipitation of authigenic goethite as reported in acidic mining lakes (Blodau and Gatzek, 2006). In addition, the slow process of in-situ iron oxide oxidation at the sediment/water interface (e.g., Robinson, 2000) is unlikely for Laguna Potrok Aike because of high sedimentation rates (average of 90 cm/ka; Kliem et al., 2013). Stable values for magnetic grain size and concentration-dependant parameters (e.g., MDF_{NRM}, ARM) as well as the

maintained stability of NRM in facies 2 argues against diagenetic alteration of magnetic mineral assemblage. Therefore, the high coercivity minerals in facies 2 are interpreted as a detrital addition to the magnetic assemblage. Moreover, there are no hematite or goethite-bearing rocks in the Pali Aike volcanic field (Coronato et al., 2013; Ross et al., 2011), and consequently the most likely source of high coercivity minerals in our record is through oxidation of the abundant detrital magnetite in the lake catchment. The iron oxides maghemite, hematite and goethite are typically associated with soils and paleosols (Dunlop and Özdemir, 2007; Maher, 2011). In particular, paleosols in Argentina are precisely distinguished from loess deposits from their high coercivity minerals contribution (Orgeira et al., 1998). Maghemite (γFe_2O_3) is a cation-deficient spinel formed during pedogenesis, and is difficult to distinguish from magnetite based solely on room-temperature rock-magnetic properties. Further oxidation leads to hematite and goethite, which are "hard" antiferromagnetic minerals (e.g., Maher et al., 1999). Their strong resistance to magnetisation is the key magnetic property leading to the distinction of rock-magnetic facies 2 in Laguna Potrok Aike as well as further north in Argentinean paleosols (Orgeira et al., 1998). Soil formation in arid to semi-arid climates strongly depends on precipitations. In particular, when the mean annual precipitation is lower than ca. 200 mm/yr, bacterial activity (which releases the Fe^{2+} necessary for pedogenic magnetite precipitation) becomes limited, and as a result hematite and goethite accumulate (Maher, 2011). We note that goethite is more ubiquitous in soils than hematite, which is typically associated to tropical and sub-tropical climate (e.g., Maher, 2011). However, well-drained soils in a cooler climate can result in preferential accumulation of hematite when short periods of wetness alternate with long warm and dry periods (Schwertmann et al., 1982; Maher, 1998) and hematite was reported for Argentinean loess using rock magnetic, Mössbauer, and bulk geochemical measurements (Carter-Stiglitz et al., 2006). Regardless of the precise magnetic mineralogy, the high coercivity contribution in the PASADO record is interpreted as resulting from oxidation of detrital magnetite and the occasional SD-like properties of facies 2 possibly indicate a variable proportion of SP/SD magnetite and maghemite precipitated during wetter periods. In a biplot of MDF_{ARM} vs ARM ratio designed to

identify the provenance of magnetite particles (Egli, 2004a), rock-magnetic facies 2 clusters in a region between pedogenic/extracellular and biogenic magnetite. This further supports the presence of pedogenic particles in facies 2 and additionally reveals a possible contribution of biogenic magnetite in these intervals.

Second, we discuss the possible transport processes of pedogenic particles to the lake. Extreme precipitation events, snowfall and permafrost melt could generate runoff capable of carving gullies and canyons such as those visible around the lake today (Figure 1). Sudden water input can generate instabilities on the steep lake slopes and trigger a MMD above which the very fine pedogenic particles would settle. Today, extreme precipitation events are documented uniquely at times of weak SWW, when easterly and northern winds reach the region (Ohlendorf et al., 2013; Schäbitz et al., 2013) (Figure 1B). Figure 9 suggests that this relationship was probably maintained in the past for times of weaker winds (Lisé-Pronovost et al., submitted) associated with higher MMD frequency in Laguna Potrok Aike since 51,200 cal BP (Kliem et al., 2013). This interpretation builds on the idea of "event resistance" where in the presence of consistently strong winds from the same direction (e.g., the SWW during the Holocene), all the sediment able to be moved is moved after a certain period of time. As a result the number of MMD horizons decreases or cease, and there is a need for wind direction change and/or more extreme events to trigger the next MMD (Eden and Page, 1998). This is illustrated by absence of facies 2 in the PASADO record since the onset of strong SWW (Zolitschka et al., 2013; Lisé-Pronovost et al., submitted). In contrast, without persistent SWW over Laguna Potrok Aike during the last Glacial period (Zolitschka et al., 2013; Hahn et al., submitted; Lisé-Pronovost et al., submitted), the frequently changing wind directions and intensities (increased gustiness) could account for more frequent MMDs. This mechanism explains facies 2 and its relation to MMDs in the PASADO record. In addition, the presence of more humid air masses from the Atlantic could have favoured soil formation through more frequent precipitation and contribute to higher lake levels during the last Glacial (Zolitschka et al., 2013). Finally, the timing of rock-magnetic facies 2 validates the proposed transport mechanism because all

pedogenic runoff events occur during times of higher MMD frequency and gustiness (grey highlight on Figure 10).

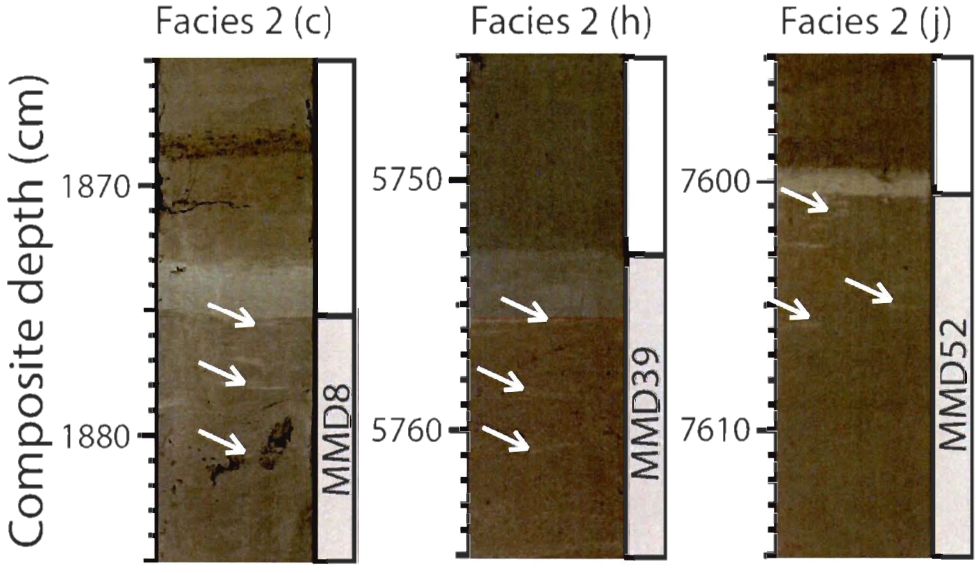

Figure 3. 8. Core photograph showing clay aggregates (some are pointed using white arrows) and mass movement deposits (MMDs) associated to facies 2 features *c*, *h* and *j*.

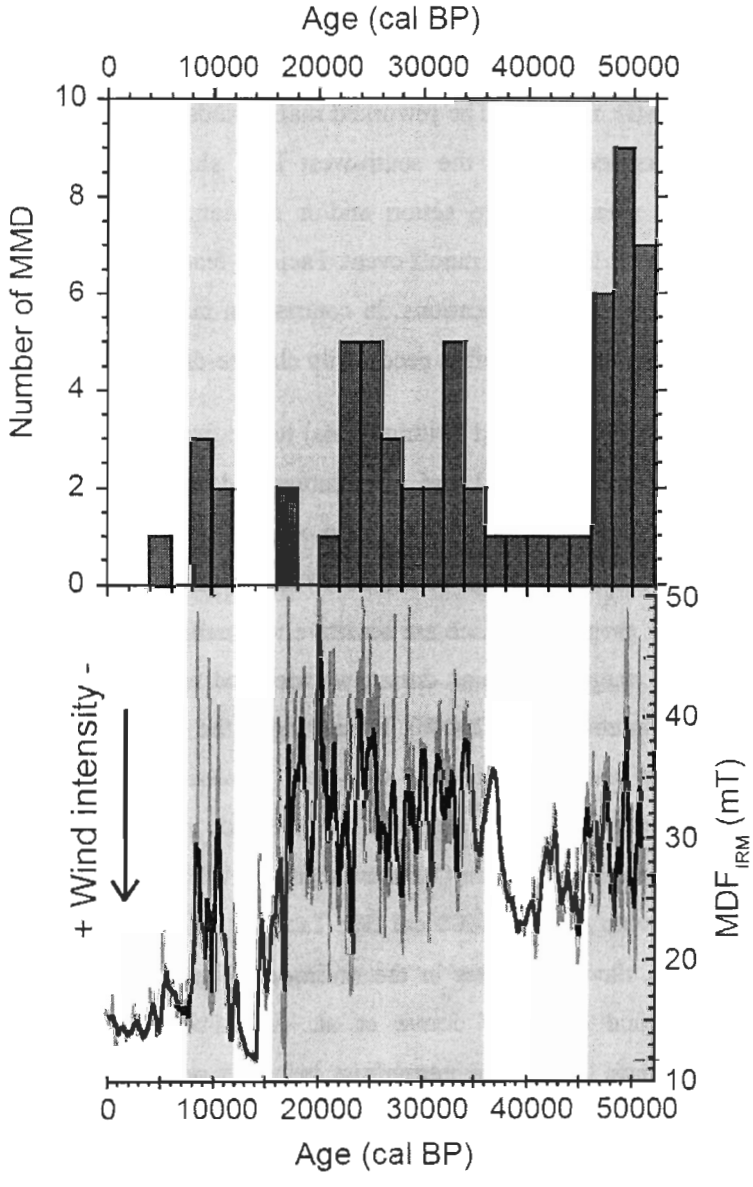

Figure 3. 9. Comparison of the frequency of mass movement deposits (MMDs) per 2000 years intervals and wind intensity proxy from Laguna Potrok Aike (MDF_{IRM}; Lisé-Pronovost et al., submitted).

5.3 Paleoclimatic implications

The formation of authigenic iron sulfides in the PASADO record indicate reducing conditions inside some MMD horizons. The reworked mafic sands of facies 1 were likely supplied from mafic rocks located on the south-west lake shore and could indicate increased erosion in this area by wave action and/or the temporary activation of a paleochannel visible on Figure 1 during a runoff event. Facies 1 features in reworked tephra material has no clear paleoclimatic implications. In contrast, in facies 2 the transport and deposition of pedogenic particles via runoff is necessarily climate-driven.

Events *g* and *h* (Table 2) correspond (within limits) to the two warmer periods of the last Glacial as recorded in Antarctica (A1 and A2, Blunier and Brooks, 2001; AIM8 and AIM12, EPICA community members, 2006). They also correspond to periods of increased productivity in Laguna Potrok Aike (Hahn et al., 2013) and to finer magnetite grains, as indicated by rock-magnetic properties which are sensitive to smaller grains (MDF_{ARM} and Mr/Ms) (Figure 10). Finer magnetite grains during warmer and more productive periods could indicate bacterial magnetite (Egli, 2004b). Interestingly, the degree of anisotropy of the magnetic susceptibility (although at only very low resolution) appears to follow changes in lake productivity and hence supports the presence of anisotropic biogenic magnetosomes typically occurring in chains (Moskovitz et al., 1993; Snowball et al., 2002). Event *h* likely associated with A2 (at 46000 cal BP; Table 2) is one of the three runoff events that corresponds to clay aggregates in the sediment (Figure 8). Building on the recent micro-sedimentological study of Jouve et al. (submitted), we interpret clay aggregates as direct evidence of melting permafrost bringing pedogenic iron minerals locked or formed within permafrost (e.g., Vogt and Larqué, 2002) to the lake.

Relict sand wedges attest to the presence of permafrost near Laguna Potrok Aike in the past (Bockheim et al., 2009) and Kliem et al. (2013b) recently dated a sand wedge from the last Glacial period near Laguna Potrok Aike using optically stimulated luminescence (OSL) dating.

The two other periods of higher lacustrine productivity in Laguna Potrok Aike are at ca. 50,000 cal BP and from the deglaciation to the Early Holocene (Hahn et al., 2013). Both are associated with input of pedogenic minerals. The event *j* corresponds to clay aggregates in the sediment (Figure 8) interpreted as permafrost melt. The closely following event *i* most likely results from a precipitation event because it is not associated with clay aggregates and overlays a MMD of muddy sands with plant macro remains of aquatic mosses suggesting erosive action at lower depths. The age uncertainty of the radiocarbon-based chronology is large in the older part of the record, but the events *i*, *j* and the coeval maximum productivity could correspond to the warming at ca. 54000 cal BP recorded in Antarctica (EPICA community members, 2006) (Table 2; Figure 10). Alternatively, the lake productivity could have been triggered by the input of nutrients by runoff and sediment remobilisation as also hypothesized by Hahn et al (2013). Events *b* and *c* correspond to the onset of deglaciation in the mid-latitudes of the Southern Hemisphere (17.3 ka cal BP; Schaefer, 2006) and to two sudden rise in temperature in southern South America (McCulloch et al., 2000). Event *c* at 17,320 cal BP corresponds (within the limit of the chronology) to the end of a major glacier advance of the southern Patagonian Ice Sheet (PIS) in the Magellanes Strait (Sugden et al., 2009) and to the retreat of the Seno Skyring Glacier (Kilian et al., 2007) only ca. 100 km south-west of Laguna Potrok Aike. It is also the youngest event characterized by clay aggregates (Figure 8) and interpreted as the result of permafrost melt. The following event *b* at 16,030 cal BP is interpreted as linked to extreme precipitation event(s) because it overlays a thick MMD (174 cm) composed of tephra material including mud laminations and layers of plant macro remains. Finally, the more recent event (*a* at 9260 cal BP; Table 2) is also associated with high lacustrine productivity and fine magnetite grains (Figure 10) and the yellow coloration (Table 2) of the sediment supports the presence of goethite for this interval (Schwertmann, 2008). Runoff event *a* is interpreted as triggered by an intense precipitation event at 9230 cal BP, which is consistent with a period of weak westerly flow in the southern Hemisphere (11,000-8000 cal BP; Fletcher and Moreno, 2012) as well as pollen-based

paleoprecipitation proxy from Laguna Potrok Aike (Schabitz et al., 2013) and the Magellan Strait region (McCulloch et al., 2000).

Three pedogenic layers, *d*, *e*, and *f*, were not deposited during the periods of higher lacustrine productivity. Yet, high values of the degree of anisotropy as well as local intermediate values of productivity are associated with pedogenic events *e* and *f* (Figure 10). This coincidence suggests that the crystalline or shape anisotropy of hematite/goethite particles might as well contribute to anisotropy together with biogenic magnetite.

Events *d* and *e* (Table 2) follow two major glacial advances of the PIS in the Magellanes Strait at 23,100-25,600 cal BP and 20,400-21,700 (Sudgen et al., 2009). While the runoff event *d* is the only pedogenic layer that is not associated with a previously documented warm period, the event *e* and *f* at 24,280 and 30,640 cal BP, respectively, are coeval with the warm period AIM2 and AIM4 in Dronning Maud Land, Antarctica (Figure 8; EPICA community members, 2006). Interestingly, a continental record from New Zealand similarly points to warmer temperatures during AIM2 as indicated by greater tree abundance (Callard et al., 2013).

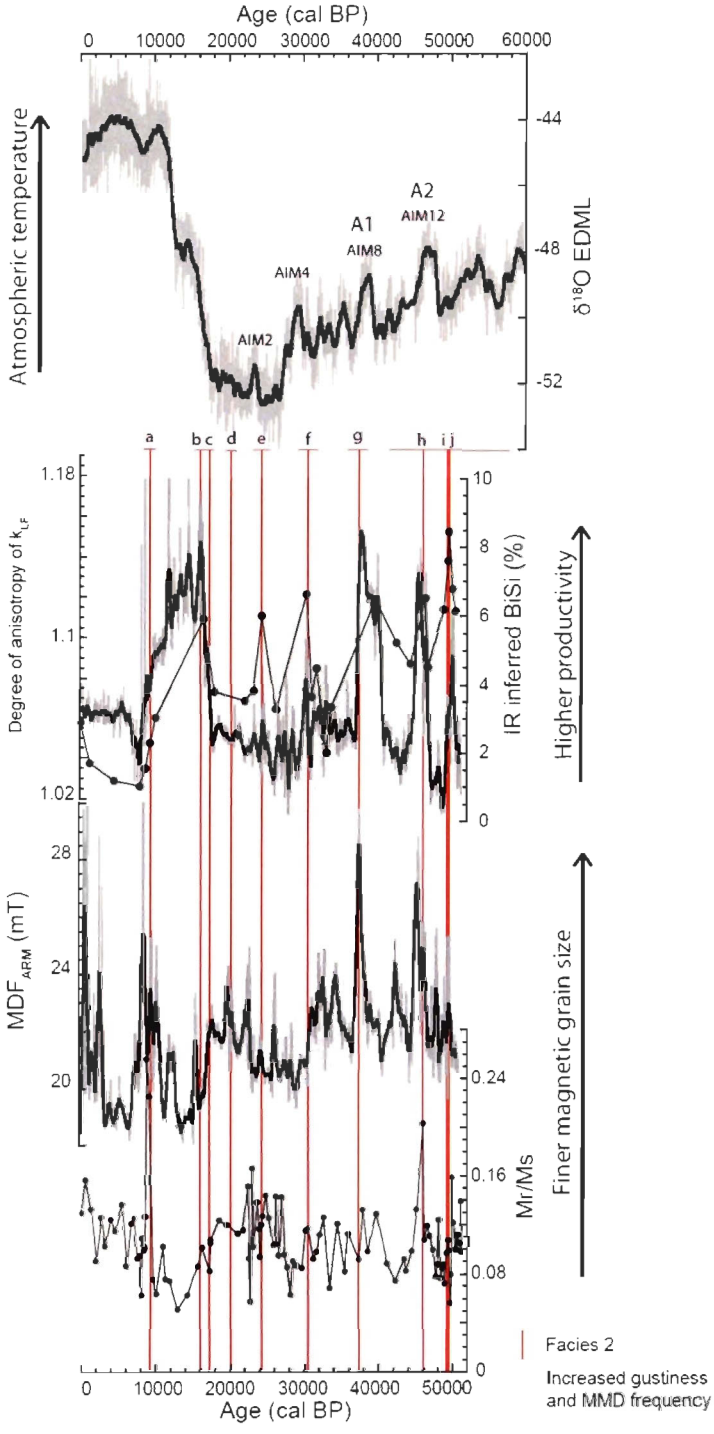
Age (cal BP)
0
10000
20000
30000
40000
50000
60000
Atmospheric temperature
-44
-48
-52
δ18O EDML
A2
AIM12
A1
AIM8
AIM4
AIM2
a
b c
d
e
f
g
h
i j
1.18
1.1
1.02
Degree of anisotropy of KLF
10
8
6
4
2
0
IR inferred BiSi (%)
Higher productivity
28
24
20
MDFARM (mT)
0.24
0.16
0.08
0
Mr/Ms
Finer magnetic grain size
Facies 2
Increased gustiness
and MMD frequency
Age (cal BP)

Figure 3. 10. Comparison of the paleotemperature proxy ($\delta^{18}O$) from Antarctica (EPICA community members, 2006), Laguna Potrok Aike productivity proxy (biogenic silica: BiSi; Hahn et al., 2013) and rock-magnetic properties including the degree of anisotropy of magnetic susceptibility, the median destructive field of anhysteretic remanent magnetisation (MDF_{ARM}), and the ratio Mr/Ms. MDF_{ARM} and Mr/Ms indicate changes in the smaller magnetic grain size fraction and are especially sensitive to SD magnetite (Maher, 1988; Dunlop and Özdemir, 2007). Thick black curves represent the millennial-scale variability and grey curves high-resolution data. The shading indicates periods with higher MMD frequency, generally lower wind intensity and increased gustiness (cf. Figure 8.). Red vertical lines indicate the timing of pedogenic minerals in the sediment record of Laguna Potrok Aike (facies 2 from *a* to *j*) and pink lines represent the age uncertainty of the radiocarbon-based chronology (Kliem et al., 2013). Antarctic isotope maxima (AIM; EPICA community members, 2006) and Antarctic warm events A1 and A2 (Blunier and Brook, 2001) are indicated.

6-Conclusions

The high-resolution rock-magnetic study of the sediments deposited in Laguna Potrok Aike since 51,200 cal BP indicates the presence of PSD magnetite with isolated intervals of iron sulfides (facies 1) and oxidized pedogenic particles (facies 2) representing a total of ca. 5% of the sedimentary sequence. The two distinct types of magnetic signatures are associated with MMDs in Laguna Potrok Aike and display contrasting rock-magnetic signatures compared to the rest of the record dominated by PSD magnetite (Gogorza et al., 2011; 2012; Recasens et al., 2012; Lisé-Pronovost et al., 2013).

This study reveals that changes in the magnetic mineralogy are useful for identifying MMD in hydrologically closed lake basins with a uniform sediment source such as in the case of Laguna Potrok Aike. In particular, we used spurious laboratory magnetisations as a useful means of identifying the sedimentary magnetic mineralogy. While GRM is well-documented for iron sulfides (as in facies 1), we have provided the first evidence of GRM acquisition during AF demagnetisation of IRM most likely attributed to pedogenic hematite (facies 2). In the rock-magnetic facies 1, iron sulfides are authigenically formed by sulfate reduction within MMD composed of mafic sand or tephra material. Facies 2 contains oxidized pedogenic iron minerals (hematite and goethite) formed in the lake catchment and transported to the lake by runoff events. Interestingly, a similar series of events characterized by high coercivity minerals and possibly attributed to pedogenized material during the last Glacial period was reported in the sediment sequence of the oligotrophic maar lake Massoko in Tasmania (Williamson et al., 1999), hinting at a possibly common formation and deposition process in volcanic field settings. In Laguna Potrok Aike, the pedogenic particles were deposited on top of a MMD horizons at times of increased lacustrine productivity, higher MMD frequency, and increased gustiness, which are nowadays climatic conditions associated to the enhanced influence of humid air masses from the Atlantic Ocean (Ohlendorf et al., 2013; Schäbitz et al., 2013). Such paleoclimatic conditions during the last Glacial period support the importance of gustiness (Mc Gee et al., 2010). The coincidence of these major precipitation/melt events with the warm periods

AIM-2, -4, -8 and -12 recorded in Antarctica (EPICA community members, 2006) reveals an Antarctic-like climate south-eastern Argentina. The rock-magnetic results also provide evidence for permafrost melt at ca. 50,000, 46,000 and 17,300 cal BP in the lake catchment of Laguna Potrok Aike. This work documents abrupt climate changes of regional and hemispheric significance.

Acknowledgements

We thank J. Labrie, F. Barletta, M.-P. St-Onge, A. Leclerc and D. Veres for their help in the laboratory at ISMER, J.J. Scagliotti and C. Ohlendorf for cube sampling at the University of Bremen, and M. Jackson for his help with anisotropy measurements at the Institute of Rock Magnetism of the University of Minnesota in Minneapolis. We thank Q. Simon for comments on an earlier version of this manuscript. This research is supported by the International Continental Scientific Drilling Program (ICDP) in the framework of the "Potrok Aike Maar Lake Sediment Archive Drilling Project" (PASADO). Funding for drilling was provided by the ICDP, the German Science Foundation (DFG), the Swiss National Funds (SNF), the Natural Sciences and Engineering Research Council of Canada (NSERC), the Swedish Vetenskapsradet (VR) and the University of Bremen. For their invaluable help in field logistics and drilling, we thank the staff of INTA Santa Cruz and Rio Dulce Catering as well as the Moreteau family and the DOSECC crew. This research was made possible through NSERC Special Research Opportunity and Discovery grants to P. Francus and G. St-Onge. We also acknowledge the Canadian Foundation for Innovation (CFI) for the acquisition and operation of the u-channel cryogenic magnetometer. C. Gogorza thanks the *Comisión Nacional de Investigaciones Científicas y Técnicas de la República Argentina* (CONICET) and the *Universidad Nacional del Centro de la Provincia de Buenos Aires* (UNCPBA). Finally, we acknowledge the support of NSERC and the Canadian Meteorological and Oceanographical Society (CMOS) for graduate scholarships to A. Lisé-Pronovost.

References

Anderson, R.F., Ali, S., Bradtmiller, L.I., Nielsen, S.H.H., Fleisher, M.Q., Anderson, B.E., Burckle, L.H., 2009. Wind-Driven Upwelling in the Southern Ocean and the Deglacial Rise in Atmospheric CO_2 , Science 323 (5920), 1443-1448.

Barrows, T.T., Juggins, S., De Deckker, P., Calvo, E., Pelejero, C., 2007. Long-term sea surface temperature and climate change in the Australian-New Zealand region: Australian-New Zealand climate change. Paleoceanography 22 (2) PA2215.

Basile, I., Grousset, F.E., Revel, M., Petit, J.R., Biscaye, P.E., Barkov, N.I., 1997. Patagonian origin of glacial dust deposited in East Antarctica (Vostok andDome C) during glacial stages 2, 4 and 6. Earth and Planet. Sci. Lett. 146, 573-589.

Berner, R.A., 1984. Sedimentary pyrite formation: an update. Geochimica et Cosmochimica Acta 48, 605–615.

Blanchet, C.L., Thouveny, N., Vidal, L., 2009. Formation and preservation of greigite (Fe_3S_4) in sediments from the Santa Barbara Basin: Implications for paleoenvironmental changes during the past 35 ka: greigite in Santa Barbara Basin. Paleoceanography 24, PA2224.

Blodau, C., Gatzek, C., 2006. Chemical controls on iron reduction in schwertmannite-rich sediments. Chem. Geol. 235, 366–376.

Blunier, T. and Brook, E.J., 2001. Timing of Millennial-Scale Climate Change in Antarctica and Greenland During the Last Glacial Period. Science 291, 109.

Bockheim, J., Coronato, A., Rabassa, J., Ercolano, B., Ponce, J., 2009. Relict sand wedges in southern Patagonia and their stratigraphic and paleo-environmental significance. Quat. Sci. Rev. 28, 1188–1199.

Bowen, B.B., Benison, K.C., Oboh-Ikuenobe, F.E., Story, S., Mormile, M.R., 2008. Active hematite concretion formation in modern acid saline lake sediments, Lake Brown, Western Australia. Earth Planet. Sci. Lett. 268, 52–63.

Brachfeld, S., Barletta, F., St-Onge, G., Darby, D., Ortiz, J.D., 2009. Impact of diagenesis on the environmental magnetic record from a Holocene sedimentary sequence from the Chukchi–Alaskan margin, Arctic Ocean. Glob. Planet. Change 68, 100–114.

Brachfeld, S.A., 2006. High-field magnetic susceptibility (χHF) as a proxy of biogenic sedimentation along the Antarctic Peninsula. Phys. Earth Planet. Inter. 156, 274–282.

Callard, S.L., Newnham, R.M., Vandergoes, M.J., Alloway, B.V., Smith, C., 2013. The vegetation and climate during the Last Glacial Cold Period, northern South Island, New Zealand. Quat. Sci. Rev. 74, 230–244.

Caniupán, M., Lamy, F., Lange, C.B., Kaiser, J., Arz, H., Kilian, R., Baeza Urrea, O., Aracena, C., Hebbeln, D., Kissel, C., Laj, C., Mollenhauer, G., Tiedemann, R., 2011. Millennial-scale sea surface temperature and Patagonian Ice Sheet changes off southernmost Chile (53°S) over the past ~60 kyr. Paleoceanography 26, PA3221.

Channell, J.E.T. and Xuan, C., 2009. Self-reversal and apparent magnetic excursions in Arctic sediments. Earth Planet. Sci. Lett. 284, 124–131.

Coronato, A., Ercolano, B., Corbella, H., Tiberi, P., 2013. Glacial, fluvial and volcanic landscape evolution in the Laguna Potrok Aike maar area, Southern Patagonia, Argentina. Quat. Sci. Rev. 71, 13–26.

D'Orazio, M., Agostini, S., Mazzarini, F., Innocenti, F., Manetti, P., Haller, M.J., Lahsen, A., 2000. The Pali Aike volcanic field, Patagonia: slab-window magmatism near the tip of South America. Tectonophysics 321, 407–427.

Day, R., Fuller, M., Schmidt, V.A., 1977. Hysteresis properties of titano-magnetite: grain size and compositional dependence. Phys. Earth Planet. Int. 13, 260-267.Dearing, 1999

Dearing, J.A., 1999. Environmental magnetic susceptibility: using the Bartington MS2 system. Chi Pub., Kenilworth.

Dekkers, M.J., 1989. Magnetic properties of natural pyrrhotite. II. High- and low-temperature behaviour of Jrs and TRM as a function of grain size. Phys. Earth Planet. Inter. 57, 266–283.

Dekkers, M.J., 1997. Environmental magnetism: an introduction. Geol. En Mijnb. 76, 163–182.

De Wall, H. and Worm, H.-U., 1993. Field dependence of magnetic anisotropy in pyrrhotite: effects of texture and grain shape, Phys. Earth Plan. Int. 76, 137-149.

Dunlop, D.J., 2002. Theory and application of the Day plot (Mrs/Ms versus Hcr/Hc) 1.Theoretical curves and tests using titanomagnetite data. J. Geophys. Res. 107 (B3), 1-22.

Dunlop, D.J., Özdemir, O., 2007. Magnetizations in rocks and minerals. In: Schubert, G. (Ed.), 2007. Geomagnetism, Treatise on Geophysics, vol. 5. Elsevier, pp. 277-336.

Eden, D.N., Page, M.J., 1998. Palaeoclimatic implications of a storm erosion record from late Holocene lake sediments, North Island, New Zealand. Palaeogeogr. Palaeoclim. Palaeoecol. 139, 37–58.

Egli, R., 2004a. Characterization of individual rock magnetic components by analysis of remanence curves. 1. Unmixing natural sediments. Studia Geophys. Geodaet. 48, 391–446.

Egli, R., 2004b. Characterization of individual rock magnetic components using the analysis of remanence curves, 3. Biogenic magnetite and natural processes in lakes, Physics and Chemistry of the Earth 29, 869-884.

EPICA community members, 2006. One-to-one coupling of glacial climate variability in Greenland and Antarctica. Nature 444, 195–198.

Evans, M.E. and Heller, F., 2003. Environmental magnetism: Principles and applications of enviromagnetics, international geophysics series vol. 86, Academic press, 299p

Frankel, R.B. and Bazylinski, D.A., 2003. Biologically induced mineralization by bacteria (in Biomineralization). Reviews in Mineralogy and Geochemistry 54, 95-114.

Fu, Y., von Dobeneck, T., Franke, C., Heslop, D., Kasten, S., 2008. Rock magnetic identification and geochemical process models of greigite formation in Quaternary marine sediments from the Gulf of Mexico (IODP Hole U1319A). Earth Planet. Sci. Lett. 275, 233–245.

Garreaud, R., P. Lopez, M. Minvielle, M. Rojas, 2013. Large Scale Control on the Patagonia Climate. J. of Climate 26, 215-230.

Gasse, F., Chalié, F., Vincens, A., Williams, A.J., Williamson, D., 2008. Climatic patterns in equatorial and southern Africa from 30,000 to 10,000 years ago reconstructed from terrestrial and near-shore proxy data. Quat. Sci. Rev. 27, 2316-2340.

Gobeil, C., Macdonald, R.W., Sundby, B., 1997. Diagenetic separation of cadmium and manganese in suboxic continental margin sediments. Geochim. Cosmochim. Acta 61, 4647–4654.

Gogorza, C.S.G., Irurzun, M.A., Sinito, A.M., Lisé-Pronovost, A., St-Onge, G., Haberzettl, T., Ohlendorf, C., Kastner, S., Zolitschka, B., 2012. High-resolution paleomagnetic records from Laguna Potrok Aike (Patagonia, Argentina) for the last 16,000 years. Geochem. Geophys. Geosystems 13, Q12Z37.

Gogorza, C.S.G., Sinito, A.M., Ohlendorf, C., Kastner, S., Zolitschka, B., 2011. Paleosecular variation and paleointensity records for the last millennium from southern South America (Laguna Potrok Aike, Santa Cruz, Argentina). Phys. Earth Planet. Inter. 184, 41–50.

Haberzettl, T., Anselmetti, F.S., Bowen, S.W., Fey, M., Mayr, C., Zolitschka, B., Ariztegui, D., Mauz, B., Ohlendorf, C., Kastner, S., Lücke, A., Schäbitz, F., Wille, M., 2009. Late Pleistocene dust deposition in the Patagonian steppe - extending and refining the paleoenvironmental and tephrochronological record from Laguna Potrok Aike back to 55ka. Quat. Sci. Rev. 28, 2927–2939.

Haberzettl, T., Kück, B., Wulf, S., Anselmetti, F., Ariztegui, D., Corbella, H., Fey, M., Janssen, S., Lücke, A., Mayr, C., Ohlendorf, C., Schäbitz, F., Schleser, G.H., Wille, M., Zolitschka, B., 2008. Hydrological variability in southeastern Patagonia and explosive volcanic activity in the southern Andean Cordillera during Oxygen Isotope Stage 3 and the Holocene inferred from lake sediments of Laguna Potrok Aike, Argentina. Palaeogeogr. Palaeoclim. Palaeoecol. 259, 213–229.

Haberzettl, T., Corbella, H., Fey, M., Janssen, S., Lucke, A., Mayr, C., Ohlendorf, C., Schabitz, F., Schleser, G.H., Wille, M., Wulf, S., Zolitschka, B., 2007. Lateglacial and Holocene wet-dry cycles in southern Patagonia: chronology, sedimentology and geochemistry of a lacustrine record from Laguna Potrok Aike, Argentina. The Holocene 17, 297–310.

Haberzettl, T., Fey, M., Lücke, A., Maidana, N., Mayr, C., Ohlendorf, C., Schäbitz, F., Schleser, G.H., Wille, M., Zolitschka, B., 2005. Climatically induced lake level changes during the last two millennia as reflected in sediments of Laguna Potrok Aike, southern Patagonia (Santa Cruz, Argentina). J. Paleolimnol. 33, 283–302.

Hahn, A., Kliem, P., Oehlerich, M., Ohlendorf, C., Zolitschka, B. and the PASADO Science Team, submitted. Elemental composition of Laguna Potrok Aike sediment sequence reveals paleoclimate change over the past 51 ka in southern Patagonia, Argentina.

Horng, C.-S., Roberts, A.P., 2006. Authigenic or detrital origin of pyrrhotite in sediments?: Resolving a paleomagnetic conundrum. Earth Planet. Sci. Lett. 241, 750–762.

Hu, S., Stephenson, A., Appel, E, 2002. A study of gyroremanent magnetisation (GRM) and rotational remanent magnetisation (RRM) carried by greigite from lake sediments, Geophys. J. Int. 151, 469-474.

Hu, S., Appel, E., Hoffmann, V., Schmahl, W.W., Wang, S., 1998. Gyromagnetic remanence acquired by greigite (Fe3S4) during static three-axis alternating field demagnetization. Geophys. J. Int. 134, 831–842.

Jouve, G., Francus, P., De Coninck, A.,Bouchard, F., Lamoureux, S.F. and the PASADO scvience team, submitted. microsedimentological investigations in lacustrine sediments from a maar lake: implications for paleoenvironmental reconstructions.

Jouve, G., Francus, P., Lamoureux, S., Provencher-Nolet, L., Hahn, A., Haberzettl, T., Fortin, D., Nuttin, L., 2013. Microsedimentological characterization using image analysis and μ-XRF as indicators of sedimentary processes and climate changes during Lateglacial at Laguna Potrok Aike, Santa Cruz, Argentina. Quat. Sci. Rev. 71, 191–204.

Kaiser, J., Lamy, F., Arz, H.W., Hebbeln, D., 2007. Dynamics of the millennial-scale sea surface temperature and Patagonian Ice Sheet fluctuations in southern Chile during the last 70kyr (ODP Site 1233). Quat. Int. 161, 77–89.

Kilian, R., Lamy, F., 2012. A review of Glacial and Holocene paleoclimate records from southernmost Patagonia (49–55°S). Quat. Sci. Rev. 53, 1–23.

Kilian, R., Schneider, C., Koch, J., Fesq-Martin, M., Biester, H., Casassa, G., Arévalo, M., Wendt, G., Baeza, O., Behrmann, J., 2007. Palaeoecological constraints on late Glacial and Holoceneice retreat in the Southern Andes (53°S). Global Planet. Change 59, 49-66.

Kliem, P., Enters, D., Hahn, A., Ohlendorf, C., Lisé-Pronovost, A., St-Onge, G., Wastegård, S., Zolitschka, B., 2013a. Lithology, radiocarbon chronology and sedimentological interpretation of the lacustrine record from Laguna Potrok Aike, southern Patagonia. Quat. Sci. Rev. 71, 54–69.

Kliem, P., Buylaert, J.P., Hahn, A., Mayr, C., Murray, A.S., Ohlendorf, C., Veres, D., Wastegård, S., Zolitschka, B., 2013b. Magnitude, geomorphologic response and climate links of lake level oscillations at Laguna Potrok Aike, Patagonian steppe (Argentina). Quat. Sci. Rev. 71, 131–146.

Knorr, G. and Lohmann, G., 2003. Southern Ocean origin for the resumption of Atlantic thermohaline circulation during deglaciation. Nature 424, 532–536.

Konhauser, K.O., 1998. Diversity of bacterial iron mineralization. Earth-Sci. Rev. 43, 91–121.

Larrasoaña, J.C., Roberts, A.P., Musgrave, R.J., Gràcia, E., Piñero, E., Vega, M., Martínez-Ruiz, F., 2007. Diagenetic formation of greigite and pyrrhotite in gas hydrate marine sedimentary systems. Earth Planet. Sci. Lett. 261, 350–366.

Lascu, I., Plank, C., in press. A new dimension to sediment magnetism: Charting the spatial variability of magnetic properties across lake basins. Glob. Planet. Change.

Lisé-Pronovost, A., St-Onge, G., Gogorza, C., Haberzettl, T., Jouve, G., Francus, P., Stoner, J., Zolitschka, B. and the PASADO science team, submitted. Rock-magnetic proxy of wind intensity since 51200 cal BP from the sediments of Laguna Potrok Aike in southern Patagonia.

Lisé-Pronovost, A., St-Onge, G., Gogorza, C., Haberzettl, T., Preda, M., Kliem, P., Francus, P., Zolitschka, B., 2013. High-resolution paleomagnetic secular variations and relative paleointensity since the Late Pleistocene in southern South America. Quat. Sci. Rev. 71, 91–108.

Liu, Q., Barrón, V., Torrent, J., Qin, H., Yu, Y., 2010. The magnetism of micro-sized hematite explained. Phys. Earth Planet. Inter. 183, 387–397.

Maher, B.A., 2011. The magnetic properties of Quaternary aeolian dusts and sediments, and their palaeoclimatic significance. Aeolian Res. 3, 87–144.

Maher, B.A., Alekseev, A., Alekseeva, T., 2003. Magnetic mineralogy of soils across the Russian Steppe: climatic dependence of pedogenic magnetite formation. Palaeogeogr. Palaeoclim. Palaeoecol. 201, 321–341.

Maher, B.A. and Thompson, R., 1999. Quaternary climates, environments, and magnetism. Cambridge University Press, Cambridge, UK; New York.

Maher, B.A., Thompson, R., Hounslow, M.W., 1999. In Maher and Thompson Quaternary climates, environments and magnetism. Cambridge University Press, 412 p.

Maher, B. A., and Taylor, R. M., 1988. Formation of ultrafine-grained magnetite in soils. Nature, 336, 368–370.

Maher, B.A, 1998. Magnetic properties of modern soils and Quaternary loessic paleosols: paleoclimatic implications. Palaeogeo. Palaeoclim. Palaeoeco. 137, 25-54.

Mayr, C., Lücke, A., Stichler, W., Trimborn, P., Ercolano, B., Oliva, G., Ohlendorf, C., Soto, J., Fey, M., Haberzettl, T., Janssen, S., Schäbitz, F., Schleser, G.H., Wille, M., Zolitschka, B., 2007. Precipitation origin and evaporation of lakes in semi-arid Patagonia (Argentina) inferred from stable isotopes (δ18O, δ2H). J. Hydrol. 334, 53–63.

McCulloch, R.D., Bentley, M.J., Purves, R.S., Hulton, N.R.J., Sudgen, D.E., Clapperton, C.M., 2000. Climatic inferences from glacial and palaeoecological evidence at the last glacial termination, southern South America. J. Quat. Sci. 15 (4), 409-417.

McGee, D., Broecker, W.S., Winckler, G., 2010. Gustiness: The driver of glacial dustiness? Quat. Sci. Rev. 29, 2340–2350.

Moskowitz, B.M., Frankel, R.B., Bazylinski, D.A., 1993. Rock magnetic criteria for the detection of biogenic magnetite. Earth Planet. Sci. Lett. 120, 283–300.

Muxworthy, A. R., and A. P. Roberts (2007), First-order reversal curve (FORC) diagrams, in Encyclopedia of Geomagnetism and Paleomagnetism, edited by D. Gubbins and E. Herrero-Bervera, pp. 266–272, Springer, Dordrecht, Netherlands.

Nuttin, L., Francus, P., Preda, M., Ghaleb, B., Hillaire-Marcel, C., 2013. Authigenic, detrital and diagenetic minerals in the Laguna Potrok Aike sediment sequence. Quat. Sci. Rev. 71, 109–118.

Ohlendorf, C., Fey, M., Gebhardt, C., Haberzettl, T., Lücke, A., Mayr, C., Schäbitz, F., Wille, M., Zolitschka, B., 2013. Mechanisms of lake-level change at Laguna Potrok Aike (Argentina) – insights from hydrological balance calculations. Quat. Sci. Rev. 71, 27–45.

Orgeira, M.J., Walther, A.M., Vasquez, C.A., Di Tommaso, I., Alonso, S., Sherwood, G., Yuguan, H., Vilas, J.F.A., 1998. Mineral magnetic record of paleoclimate variations in loess and paleosol from the Buenos Aires formation (Buenos Aires, Argentina). J. South Am. Earth Sci. 11 (6), 561-570.

Özdemir Ö. and Banerjee S.K., 1982. A preliminary magnetic study of soil samples from west central Minnesota. Earth Planet. Sci. Lett., 59, 393–403.

Pahnke, K., 2003. 340,000-Year Centennial-Scale Marine Record of Southern Hemisphere Climatic Oscillation. Science 301, 948–952.

Potter, D.K. and Stephenson, A., 2006. The stable orientations of the net magnetic moment within single-domain particles: Experimental evidence for a range of stable states and implications for rock magnetism and palaeomagnetism. Phys. Earth Plan. Int. 154, 337-349.

Pugh, R.S., McCave, I.N., Hillenbrand, C.-D., Kuhn, G., 2009. Circum-Antarctic age modelling of Quaternary marine cores under the Antarctic Circumpolar Current: Ice-core dust–magnetic correlation. Earth Planet. Sci. Lett. 284, 113–123.

Recasens, C., Ariztegui, D., Gebhardt, C., Gogorza, C., Haberzettl, T., Hahn, A., Kliem, P., Lisé-Pronovost, A., Lücke, A., Maidana, N., 2012. New insights into paleoenvironmental changes in Laguna Potrok Aike, southern Patagonia, since the Late Pleistocene: The PASADO multiproxy record. The Holocene 22, 1323–1335.

Roberts, A.P., 2006. High-resolution magnetic analysis of sediment cores: Strengths, limitations and strategies for maximizing the value of long-core magnetic data. Phys. Earth Planet. Inter. 156, 162–178.

Roberts, A.P., 1995. Magnetic properties of sedimentary greigite (Fe3S4). Earth Planet. Sci. Lett. 134, 227–236.

Roberts, A.P., Chang, L., Rowan, C.J., Horng, C.-S., Florindo, F., 2011. Magnetic properties of sedimentary greigite (Fe_3S_4): An update. Rev. Geophys. 49.

Roberts, A., Pike, C.R., Verosub, K.L, 2000. First-order reversal curve diagrams: A new tool for characterizing the magnetic properties of natural samples. Jour. Geophys. Res. 105(B12), 28,461-28,475.

Roberts, A.P., Liu, Q., Rowan, C.J., Chang, L., Carvallo, C., Torrent, J., Horng, C.-S., 2006. Characterization of hematite (α–Fe_2O_3), goethite (α-FeOOH), greigite (Fe_3S_4), and pyrrhotite (Fe_7S_8) using first-order reversal curve diagrams. J. Geophys. Res. 111.

Rochette, P., Mathé, P.-E., Esteban, L., Rakoto, H., Bouchez, J.-L., Liu, Q., Torrent, J., 2005. Non-saturation of the defect moment of goethite and fine-grained hematite up to 57 Teslas. Geophys. Res. Lett. 32.

Roperch, P., Chauvin, A., Valdez, F., 2012. Partial self-reversal of TRM in baked soils and ceramics from Ecuador. Phys. Earth Planet. Inter. 210-211, 8–20.

Ross, P.-S., Delpit, S., Haller, M.J., Németh, K., Corbella, H., 2011. Influence of the substrate on maar–diatreme volcanoes — An example of a mixed setting from the Pali Aike volcanic field, Argentina. J. Volcanol. Geotherm. Res. 201, 253–271.

Sagnotti, L., 2007. Iron Sulphides, in Gubbins and Herrero-Bervera, 2007. Encyclopedia of Geomagnetism and Paleomagnetism.

Sagnotti, L., Winkler, A., 1999. Rock magnetism and palaeomagnetism of greigite-bearing mudstones in the Italian peninsula. Earth Planet. Sci. Lett. 165, 67–80.

Schäbitz, F., Wille, M., Francois, J.-P., Haberzettl, T., Quintana, F., Mayr, C., Lücke, A., Ohlendorf, C., Mancini, V., Paez, M.M., Prieto, A.R., Zolitschka, B., 2013. Reconstruction of palaeoprecipitation based on pollen transfer functions – the record of the last 16 ka from Laguna Potrok Aike, southern Patagonia. Quat. Sci. Rev.

Schaefer, J.M., 2006. Near-Synchronous Interhemispheric Termination of the Last Glacial Maximum in Mid-Latitudes. Science 312, 1510–1513.

Schwertmann, U., Murad, E., Schulze, D.G., 1982. Is there Holocene reddening (hematite formation) in soils of axeric temperature climates? Geoderma 27, 209-223.

Schwertmann, U., 2008. Iron oxides, In: (Ed.) W. Chesworth, Encyclopedia of soil science, 902 p.

Snowball, I., 1991. Magnetic hysteresis properties of greigite (Fe3S4) and a new occurrence in Holocene sediments from Swedish Lappland. Physics of the Earth and Planetary Interiors 68 (1991), 32– 40.

Snowball, I.F., 1997. Gyroremanent magnetization and the magnetic properties of greigite-bearing clays in southern Sweden. Geophys. J. Int. 129, 624–636.

Snowball, I.F. and Thompson, R., 1990. A stable chemical remanence in Holocene sediments, J. Geophys. Res. 95, 4471–4479.

Snowball, I., Zillen, L., Sandgren, P., 2002. Bacterial magnetite in Swedish varved lake-sediments: a potential bio-marker of environmental change. Quaternary International 88, 13-19.

Stephenson, A., 1980. A gyroremanent magnetization in anisotropic magnetic material, Nature 284, 49-51.

Stephenson, A. and Snowball, I.F., 2001. A large gyromagnetic effect in greigite. Geophys. J. Int. 145, 570–575.

Stoner, J.S., St-Onge, G., 2007. Chapter Three Magnetic Stratigraphy in Paleoceanography: Reversals, Excursions, Paleointensity, and Secular Variation, in: Developments in Marine Geology. Elsevier, pp. 99–138.

Stoner, J.S., Channell, J.E.T., Hillaire-Marcel, C., 1996. The magnetic signature of rapidly deposited detrital layers from the deep Labrador Sea: Relationship to North Atlantic Heinrich layers, Paleoceanography 11 (3), 309-325.

Stumm, W. and Morgan, J.J., 1996. Aquatic Chemistry, Chemical Equilibria and Rates in Natural Waters, 3rd ed. John Wiley & Sons, Inc., New York, 1022p.

Sugden, D.E., McCulloch, R.D., Bory, A.J.-M., Hein, A.S., 2009. Influence of Patagonian glaciers on Antarctic dust deposition during the last glacial period. Nat. Geosci. 2, 281–285.

Tauxe, L., 2010. Essentials of Paleomagnetism, Univ. Of Calif. Press, San Diego. 513 p.

Tauxe, L., Constable, C.G., Stokking, L.B., Badgley, C., 1990. The use of anisotropy to determine the origin of characteristic remanence in the Siwalik red beds of northern Pakistan, J. Geophys. Res. 95, 4391-4404.

Tauxe, L., Mullender, T.A.T., Pick, T., 1996. Potbellies, wasp-waists, and superparamagnetism in magnetic hysteresis. J. Geophys. Res. 101 (B1), 571e583.

Thompson, R., Oldfield, F., 1986. Environmental Magnetism. Allen & Unwin, London.

Thomson, G.F., 1990. The anomalous demagnetization of pyrrhotite. Geophys. J. Int. 103, 425-430.

Verosub, K.L. and Roberts, A.P., 1995. Environmental magnetism: Past, present, and future, J. Geophys. Res. 100 (B2), 2175-2192.

Vogt, T. and Larqué, P., 2002. Clays and secondary minerals as permafrost indicators: examples from the circum-Baikal region. Quat. Int. 95, 175–187.

Vuillemin, A., Ariztegui, D., De Coninck, A.S., Lucke, A, Mayr, C., Schubert, C.J. and the PASADO Scientific Team, 2013. Origin and significance of diagenetic concretions in sediments of Laguna Potrok Aike, southern Argentina. J. Paleolimnol 50, 275-291.

Wastegård, S., Veres, D., Kliem, P., Hahn, A., Ohlendorf, C., Zolitschka, B., 2013. Towards a late Quaternary tephrochronological framework for the southernmost part of South America – the Laguna Potrok Aike tephra record. Quat. Sci. Rev. 71, 81–90.

Weber, M.E., Kuhn, G., Sprenk, D., Rolf, C., Ohlwein, C., Ricken, W., 2012. Dust transport from Patagonia to Antarctica – A new stratigraphic approach from the Scotia Sea and its implications for the last glacial cycle. Quat. Sci. Rev. 36, 177–188.

Wehland, F., Stancu, A., Rochette, P., Dekkers, M.J., Appel, E., 2005. Experimental evaluation of magnetic interaction in pyrrhotite bearing samples. Phys. Earth Planet. Inter. 153, 181–190.

Wille, M., Maidana, N.I., Schäbitz, F., Fey, M., Haberzettl, T., Janssen, S., Lücke, A., Mayr, C., Ohlendorf, C., Schleser, G.H., Zolitschka, B., 2007. Vegetation and climate dynamics in southern South America: The microfossil record of Laguna Potrok Aike, Santa Cruz, Argentina. Rev. Palaeobot. Palynol. 146, 234–246.

Williams, M., Cook, E., van der Kaars, S., Barrows, T., Shulmeister, J., Kershaw, P., 2009. Glacial and deglacial climatic patterns in Australia and surrounding regions from 35 000 to 10 000 years ago reconstructed from terrestrial and near-shore proxy data. Quat. Sci. Rev. 28, 2398–2419.

Williamson, D., Jackson, M.J., Banerjee, S.K., Marvin, J., Merdaci, O, Thouveny, N., Decobert, M., Gibert-Massault, E., Massault, M., Mazaudier, D., Taieb, M., 1999. Magnetic signatures of hydrological change in a tropical Maar-Lake (Lake Massoko, Tanzania): Preliminary results. Phys. Chem. Earth (A) 24 (9), 799-803.

Zolitschka, B., Anselmetti, F., Ariztegui, D., Corbella, H., Francus, P., Lücke, A., Maidana, N., Ohlendorf, C., Schäbitz, F., Wastegård, S., 2013. Environment and climate of the last 51,000 years – new insights from the Potrok Aike maar lake Sediment Archive Drilling prOject (PASADO). Quat. Sci. Rev. 71, 1-12.

Zolitschka, B., Anselmetti, F., Ariztegui, D., Corbella, H., Francus, P., Ohlendorf, C., Schäbitz, the P.S.D.T., 2009. The Laguna Potrok Aike Scinetific Drilling Project PASADO (ICDP Expedition 5022). Sci. Drill. 8, 29-34.

Zolitschka, B., Schäbitz, F., Lücke, A., Corbella, H., Ercolano, B., Fey, M., Haberzettl, T., Janssen, S., Maidana, N., Mayr, C., Ohlendorf, C., Oliva, G., Paez, M.M., Schleser, G.H., Soto, J., Tiberi, P., Wille, M., 2006. Crater lakes of the Pali Aike Volcanic Field as key sites for paleoclimatic and paleoecological reconstructions in southern Patagonia, Argentina. J. South Am. Earth Sci. 21, 294–309.

DISCUSSION ET CONCLUSIONS GÉNÉRALES

L'étude à haute résolution des propriétés magnétiques des sédiments du lac *Laguna Potrok Aike* a permis de répondre aux deux objectifs de cette thèse, soit 1) reconstituer la variabilité du champ magnétique terrestre à haute résolution dans le sud de l'Amérique du Sud, et 2) établir des indicateurs magnétiques de changements climatiques. Ainsi les résultats ont permis de reconstituer la variabilité du champ magnétique dans une région précédemment peu documentée, d'établir un nouvel indicateur magnétique de l'intensité des vents et de documenter une série de 10 évènements d'inondation extrême dans le sud-est de la Patagonie depuis 51200 cal BP. Cette thèse a donc exploré les diverses applications du magnétisme sédimentaire en révélant à la fois un enregistrement paléomagnétique et un enregistrement paléoclimatique.

L'ensemble des données obtenues dans la cadre de cette thèse a permis de mettre en évidence quatre populations de grains magnétiques associées à différents processus: la magnétite détritique à domaines pseudo-uniques (*pseudo-single domain*, PSD; ca. 0,1-20 µm; Moskowitz, 1991) associée à l'aimantation naturelle rémanente (chapitre 1), une fraction légèrement plus grossière (ca. 10-30 µm) de magnétite détritique associé au transport par suspension sur de courtes distances indiquant l'intensité des vents (chapitre 2), la greigite authigène associée à des conditions suboxiques à l'intérieur de couches de sables et de cendres volcaniques remobilisés (chapitre 3), et des minéraux magnétiques de haute coercivité d'origine pédogénique déposés au-dessus de certains mouvements de masse et indiquant des évènements d'inondation (chapitre 3). La figure 1 illustre les processus de formation et de transport associés aux différents minéraux magnétiques (magnétite, hématite/goethite et greigite) présents dans les sédiments du lac Laguna Potrok Aike. L'enregistrement géomagnétique n'est pas compromis par la formation authigène de

greigite, ni par la dissolution de la magnétite puisque ces intervalles (faciès magnétique 1; chapitre 3) sont exclusivement associés à des couches de sédiments redéposés qui sont exclus de la séquence composite pélagique (Kliem et al., 2013). La propriété des grains de magnétite plus grossiers à acquérir davantage de IRM (e.g., Peters and Dekkers, 2003) s'est révélée particulièrement utile dans l'étude des sédiments du lac *Laguna Potrok Aike*. Elle a permis d'une part l'établissement de la MDF_{IRM} comme indicateur de l'intensité des vents dans le sud-est de la Patagonie et d'autre part la sélection du ratio NRM/ARM comme meilleure estimation de la RPI (puisque la coercivité de la NRM ressemble davantage à celle de la ARM qu'à celle de la IRM). La paléointensité relative (RPI) a été corrigée afin de soustraire l'influence de la taille des grains magnétiques. L'influence de la MDF_{NRM} sur le ratio NRM/ARM est fort probablement le résultat des nombreux dépôts millimétriques de silts grossiers et de sables fins intercalés dans le sédiment pélagique (Kliem et al., 2013), et de manière générale à la taille variable des grains de magnétite transportés par le vent.

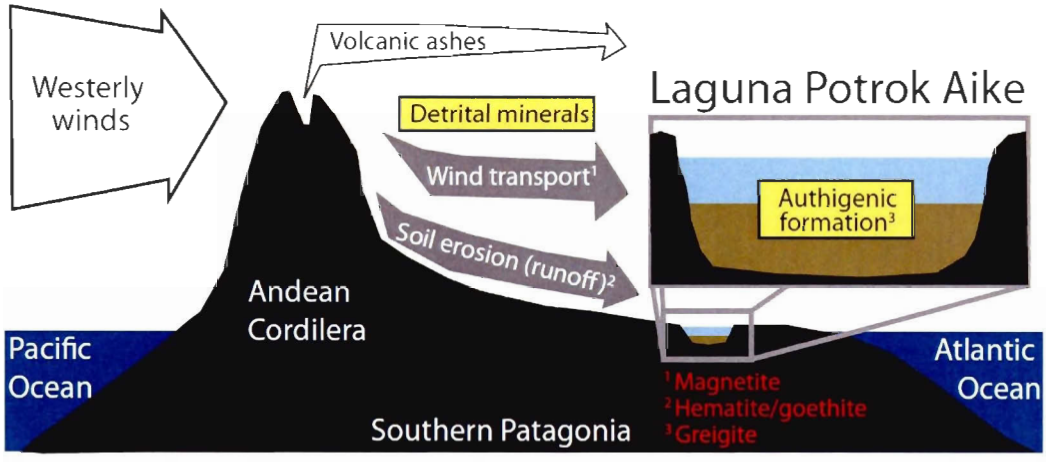

Figure 1. Schéma synthèse des sources et des processus de transport des différents minéraux magnétiques présents dans les sédiments du lac Laguna Potrok Aike.

Dans l'ensemble, l'étude du magnétisme environnemental des sédiments du lac *Laguna Potrok Aike* démontre que les changements de concentration et de granulométrie magnétique (chapitre 2) ainsi que de minéralogie magnétique (chapitre 3) sont des

indicateurs paléoclimatiques sensibles dans la région source des poussières atmosphériques déposées en Antarctique durant la dernière période glaciaire. Ces résultats démontrent qu'un enregistrement géomagnétique peut être préservée malgré un clair signal environnemental en autant que des populations magnétiques distinctes soient associées à différents processus. Des résultats similaires ont été obtenus dans la mer du Labrador (Stoner et al., 2000) et dans la baie de Baffin (Simon et al., 2012) où les sédiments reflètent à la fois un signal géomagnétique de qualité et des séries de couches sédimentaires redéposées liées entres autres aux évènements de Heinrich et à la dynamique des glaciers. En milieu lacustre, d'autres exemples où les grains magnétiques ont enregistré la variabilité géomagnétique et climatique sont le Lac du Bouchet en France (Williams et al., 1996; 1998), le lac Baikal en Sibérie (Demory et al., 2005a; b) et le lac Summer au États-Unis (Negrini et al., 2000).

Dans le chapitre 1, un nouvel enregistrement paléomagnétique (inclinaison, déclinaison et paléointensité relative) à haute résolution depuis 51200 cal BP a été reconstitué à partir des sédiments du lac *Laguna Potrok Aike*. Les analyses magnétiques indiquent clairement que la magnétite PSD domine l'assemblage magnétique de la séquence sédimentaire complète, supportant les précédentes études à basse résolution (Recasens et al., 2012) et à partir des sédiments déposés depuis 16000 cal BP (Gogorza et al., 2011; 2012). La comparaison du nouvel enregistrement avec les archives sédimentaires marines et lacustres les plus proches dans le sud de l'Amérique du Sud, ailleurs dans l'hémisphère Sud, ainsi qu'avec des courbes de références et modèles dipolaires globaux révèle une variabilité similaire au moins à l'échelle millénaire. Dans l'enregistrement PASADO, les excursions géomagnétiques de Laschamp et Mono Lake (ca. 41000 et 32000 cal BP, respectivement; Singer, sous presse) sont caractérisées par de larges et rapides changements d'inclinaison et de déclinaison paléomagnétiques associées à des périodes de faibles paléointensité relative. De plus, les changements rapides de l'inclinaison et de la déclinaison à ca. 20000 cal BP pourraient vraisemblablement être associé à l'excursion géomagnétique enregistrée en détail dans des laves volcaniques d'Hawaii (Hilina Pali; Laj et al., 2002; Teanby et al., 2002) et en Chine (Changbaishan; Singer, sous presse). Si

l'évènement géomagnétique en Patagonie est effectivement lié à l'excursion Hilina Pali/Changbaishan, cela implique une structure du champ de part et d'autre de l'océan Pacifique et entre les latitudes moyennes nord et sud, indiquant possiblement une structure globale de la géodynamo. Un autre résultat important de cette thèse concerne une diminution marquée de la paléointensité relative et un changement rapide des directions paléomagnétiques à ca. 46000 cal BP. Ces changements sont comparables à ce qui est observé pendant l'excursion géomagnétique de Laschamp dans les sédiments de *Laguna Potrok Aike* et les enregistrements les plus proches présentent aussi de tels changements (i.e., compilation SAPIS dans l'océan Atlantique sud, Stoner et al., 2002; ODP-1233 au large du Chili; Lund et al., 2006). Un minimum d'intensité à ce moment est aussi observé à différents degrés ailleurs dans l'hémisphère Sud, mais absent de l'autre côté du globe aux lacs Baikal (Sibérie; Peck et al., 1996) et Biwa (Japon; Hayashida et al., 2007). Ainsi, les changements rapides à ca. 46000 cal BP sont un signal apparemment régional et d'origine non-dipolaire qui pourrait être un analogue de l'anomalie magnétique de l'Atlantique sud (SAA) observé à la surface de la Terre depuis ca. 400 ans. Finalement, les changements géomagnétiques à ca. 46000 cal BP constituent un nouveau marqueur chronostratigraphique régional. Bien que l'incertitude de la chronologie basée sur des datations radiocarbones soit grande dans cette partie de l'enregistrement au site 2 (ca. +/- 5000 ans; Klem et al., 2013), la corrélation prochaine avec le site 1 qui possède une chronologie par luminescence (Buylaert et al., 2013) permettra sans doute de mieux définir l'âge du nouveau marqueur paléomagnétique.

Dans le chapitre 2, des indicateurs magnétiques de l'activité éolienne à 52°S dans le sud-est de la Patagonie ont été présentés. Les indicateurs de l'activité éolienne sont liés à la concentration et à la taille des grains magnétiques. La combinaison des propriétés magnétiques et des analyses granulométriques à haute résolution a permis d'établir que 1) le signal de susceptibilité magnétique des sédiments du lac *Laguna Potrok Aike* est un indicateur de la poussière atmosphérique à l'échelle multi-millénaire comme supposé par Haberzettl et al. (2009), et 2) le MDF_{IRM} des sédiments de *Laguna Potrok Aike* est un indicateur de l'intensité des vents puisqu'il reflète majoritairement la taille des grains de

magnétite transportés sur de courtes distances par suspension. La taille des grains est communément utilisée pour reconstituer l'activité éolienne dans les dépôts de loess (Vandenbergue, 2013) et peut aussi être utile dans des sédiments lacustres (e.g. Muhs et al., 2003; An et al., 2012). L'aspect novateur du MDF_{IRM} comme indicateur de l'intensité des vents réside dans le fait qu'il représente uniquement les grains magnétiques d'une fraction granulométrique précise. Donc à l'instar des mesures de taille de grain du sédiment total, MDF_{IRM} n'est pas influencée par une composition sédimentaire complexe et/ou changeante, en autant que l'assemblage magnétique soit dominé par de la magnétite d'origine détritique. Un biais introduit par des micropumices sur les ratios élémentaires Fe/Mn, Fe/Ti and Mn/Ti dans certains intervalles (Jouve et al., 2013; Hahn et al., soumis) n'a pas permis de comparer le MDF_{IRM} avec d'autres indicateurs de l'apport détritiques sur la séquence complète PASADO. Ainsi de futures études dédiées au développement d'autres types d'indicateurs de l'activité éolienne à partir des sédiments du lac *Laguna Potrok Aike* seraient pertinentes pour valider plus avant l'indicateur magnétique. En ce sens, Ohlendorf and Gehbardt (2013) explorent actuellement la possibilité de caractériser le sédiment d'origine éolienne par statistiques multivariées des données de granulométrie, de minéralogie et de propriétés physiques et géochimiques sur un petit nombre d'échantillons. Alternativement, une étude de la concentration de quartz comme l'ont fait Xiao et al. (1997) à partir des sédiments du lac Biwa au Japon pourrait également être appropriée. Finalement, un autre avantage de la MDF_{IRM} comme indicateur de l'intensité des vents est sont acquisition rapide, non-destructive et de manière continue, à l'inverse des autres méthodes proposées ci-dessus.

L'enregistrement lacustro-éolien présenté dans le chapitre 2 pourra être utile notamment pour évaluer le rôle du vent dans le sud-est de la Patagonie par rapport au rôle de la surface érodable (Sugden et al., 2009) dans la zone source des poussières atmosphériques déposées en Antarctique, ou encore pour investiguer la variabilité des vents d'ouest de l'hémisphère Sud en Patagonie au cours du temps. En effet, l'importance présumée des vents d'ouest pour la ventilation de l'océan Austral durant la dernière transition climatique (e.g., Anderson et al., 2009) a motivé un nombre croissant d'études

dédiées à reconstituer la dynamique passée (i.e., déplacement, contraction/extension) des vents d'ouest en Patagonie (e.g., Lamy et al., 2010; Fletcher and Moreno, 2011; Heinman, 2011; Montade et al., 2013). Toutefois, il n'y a pas à ce jour de consensus sur l'évolution des vents depuis la dernière période Glaciaire (Kohfeld et al., 2013). Le nouveau traceur à haute résolution présenté ici pourra donc permettre, en association avec d'autres enregistrements et des modèles climatiques, d'adresser l'importante question du rôle des vents d'ouest de l'hémisphère Sud sur le climat depuis la dernière période glaciaire.

Dans le chapitre 3, des indicateurs magnétiques de changements climatiques dans le sud-est de la Patagonie ont été présentés. Deux signatures magnétiques distinctes (faciès magnétiques 1 et 2) indiquent la présence d'autres minéraux magnétiques que la magnétite (i.e., greigite et hématite et/ou goethite) dans des intervalles précis qui représentent au total moins de 5% de la séquence sédimentaire composite. Malgré leur rareté, ces minéraux magnétiques sont de sensibles indicateurs paléoclimatiques et constituent de clairs marqueurs stratigraphiques qui pourront être utilisés dans le processus de corrélation des deux sites de forage PASADO. En outre, l'approche analytique en continu sur la longue séquence sédimentaire a permis de démontrer que la formation de sulfides de fer (greigite; faciès 1) précédemment identifiée de manière ponctuelle à certaines profondeurs (Vuillemin et al., 2013; Jouve et al., 2013) est exclusive aux couches de sable et de cendres volcaniques redéposées. Il a été démontré, basé sur des évidences géologiques, limnologiques, stratigraphiques et climatiques que le faciès 2 (hématite et/ou goethite) résulte d'évènements d'inondation liés à des précipitations intenses et à la fonte de pergélisol. Les évènements d'inondation sont aussi associées à des périodes de productivité plus intense dans le lac *Laguna Potrok Aike* (Hahn et al., 2013), à la dynamique des glaciers dans la région (e.g., Kilian et al., 2007; Sudgen et al., 2009) et à chaque période chaude de la dernière période glaciaire tel qu'enregistré dans les carottes de glace en Antarctique depuis 51200 cal BP (Blunier and Brooks, 2001; EPICA community members, 2006). Ainsi, le magnétisme des sédiments du lac *Laguna Potrok Aike* indique que le climat de la Patagonie est lié à la variabilité climatique en Antarctique, incluant les deux plus chaudes périodes de la dernière période glaciaire (AIM8 et AIM12; EPICA community

members, 2006) et la transition climatique, tel qu'indiqué aussi par des analyses sédimentologiques (Hahn et al., 2013). De plus, les propriétés magnétiques documentent pour la première fois des changements climatiques en Patagonie associés aux périodes chaudes AIM2 et AIM4 (EPICA community members, 2006).

Les signatures magnétiques présentées dans le chapitre 3 fournissent aussi des informations importantes sur l'utilisation de certaines propriétés magnétiques. Premièrement, la coïncidence de valeurs extrêmement élevées du ratio interparamagnétique kARM/IRM avec le faciès 2 suggère que des minéraux de forte coercivité peuvent influencer ce ratio de façon significative. Il apparait donc recommandable d'utiliser kARM/IRM en combinaison avec des indicateurs de la minéralogie magnétique si l'on veut l'utiliser comme indicateur de la taille des grains ou de l'interaction magnétostatique. Deuxièmement, alors que l'acquisition de gyrorémanence (GRM) durant la démagnétisation par champ alternatif de l'aimantation rémanente naturelle (NRM) est communément utilisée pour identifier la greigite (e.g., faciès 1; Roberts et al., 2011), nous avons documenté pour la première fois l'acquisition de GRM pendant la démagnétisation de l'aimantation isothermale rémanente (IRM). Ce résultat semble être associé aux grains d'hématite d'origine pédogénique.

Finalement, l'enregistrement paléomagnétique et paléoclimatique de *Laguna Potrok Aike* pourra être utilisé pour 1) contribuer à corréler les sites de forage PASADO 1 et 2, 2) préciser la chronologie PASADO dans certains intervalles où les changements paléomagnétiques sont clairement d'origine globale ou régionale, 3) investiguer le rôle des vents d'ouest de l'hémisphère Sud sur le climat depuis la dernière période glaciaire, 4) développer une courbe paléomagnétique de référence dans le sud de l'Amérique du Sud, notamment pour la période Holocène où d'autres enregistrements lacustres sont disponibles (e.g., Gogorza et al., 2002; 2004; 2006; Irurzun et al., 2006; 2008; 2009; Heirman, 2011) et d'autres seront éventuellement disponibles (e.g., paléointensité du forage ODP-1233; séquences sédimentaires du projet IMAGES-PACHIDERME le long de la côte chilienne), 5) calibrer les futurs modèles du champ magnétique de la Terre afin de mieux comprendre

la géodynamique interne (e.g., Constable, 2011) et en particulier l'évolution des structures récurrentes du champ dans l'hémisphère Sud (Korte and Holme, 2010), et 6) investiguer l'influence de l'intensité du champ magnétique sur la production des isotopes cosmogéniques à l'échelle sub-millénaire (St-Onge et al., 2003; Snowball and Sandgren, 2002) en comparant notamment avec des enregistrement à haute résolution du ^{10}Be et ^{36}Cl contenus dans les carottes de glace en Antarctique (Raisbeck et al., 2007) et au Groenland (Muscheler et al., 2005).

RÉFÉRENCES BIBLIOGRAPHIQUES

An, F., Ma, H., Wei, H., Lai, Z., 2012. Distinguishing aeolian signature from lacustrine sediments of the Qaidam Basin in northeastern Qinghai-Tibetan Plateau and its palaeoclimatic implications. Aeolian Res. 4, 17–30.

Anderson, R.F., Ali, S., Bradtmiller, L.I., Nielsen, S.H.H., Fleisher, M.Q., Anderson, B.E., Burckle, L.H., 2009. Wind-Driven Upwelling in the Southern Ocean and the Deglacial Rise in Atmospheric CO_2 , Science 323 (5920), 1443-1448.

Blunier, T. and Brook, E.J., 2001. Timing of Millennial-Scale Climate Change in Antarctica and Greenland During the Last Glacial Period. Science 291, 109.

Brachfeld, S., Banerjee, S.K., 2000. A new high-resolution geomagnetic paleointensity record for the North American Holocene: a comparison of sedimentary and absolute intensity data. J. Geophys. Res. 105 (B1), 821-834.

Buylaert, J.-P., Murray, A.S., Gebhardt, A.C., Sohbati, R., Ohlendorf, C., Thiel, C., Wastegård, S., Zolitschka, B., 2013. Luminescence dating of the PASADO core 5022-1D from Laguna Potrok Aike (Argentina) using IRSL signals from feldspar. Quat. Sci. Rev. 71, 70–80.

Constable, C.G., 2011. Modelling the geomagnetic field from syntheses of paleomagnetic data. Phys. Earth Planet. Inter. 187, 109–117.

Demory, F., Nowaczyk, N.R., Witt, A., Oberhänsli, H., 2005a. High-resolution magnetostratigraphy of late quaternary sediments from Lake Baikal, Siberia: timing of intracontinental paleoclimatic responses. Glob. Planet. Change 46, 167–186.

Demory, F., Oberhänsli, H., Nowaczyk, N.R., Gottschalk, M., Wirth, R., Naumann, R., 2005b. Detrital input and early diagenesis in sediments from Lake Baikal revealed by rock magnetism. Glob. Planet. Change 46, 145–166.

EPICA community members, 2006. One-to-one coupling of glacial climate variability in Greenland and Antarctica. Nature 444, 195–198.

Fletcher, M.-S., Moreno, P.I., 2012. Have the Southern Westerlies changed in a zonally symmetric manner over the last 14,000 years? A hemisphere-wide take on a controversial problem. Quat. Int. 253, 32–46.

Gogorza, C.S.G., Sinito, A.M., Lirio, J.M., Nuñez, H., Chaparro, M., Vilas, J.F., 2002. Paleosecular variations 0–19,000 years recorded by sediments from Escondido Lake (Argentina). Phys. Earth Planet. Inter. 133, 35–55.

Gogorza, C.S.., Lirio, J.., Nuñez, H., Chaparro, M., Bertorello, H.., Sinito, A.., 2004. Paleointensity studies on Holocene–Pleistocene sediments from lake Escondido, Argentina. Phys. Earth Planet. Inter. 145, 219–238.

Gogorza, C.S.G., Irurzun, M.A., Chaparro, M.A.E., Lirio, J.M., Nuñez, H., Bercoff, P.G., Sinito, A.M., 2006. Relative paleointensity of the geomagnetic field over the last 21,000 years BP from sediment cores, Lake El Trébol (Patagonia, Argentina). Earth Planets Space 58, 1323–1332.

Gogorza, C.S.G., Sinito, A.M., Ohlendorf, C., Kastner, S., Zolitschka, B., 2011. Paleosecular variation and paleointensity records for the last millennium from southern South America (Laguna Potrok Aike, Santa Cruz, Argentina). Phys. Earth Planet. Inter. 184, 41–50.

Gogorza, C.S.G., Irurzun, M.A., Sinito, A.M., Lisé-Pronovost, A., St-Onge, G., Haberzettl, T., Ohlendorf, C., Kastner, S., Zolitschka, B., 2012. High-resolution paleomagnetic records from Laguna Potrok Aike (Patagonia, Argentina) for the last 16,000 years. Geochem. Geophys. Geosystems 13(12), Q12Z37.

Haberzettl, T., Anselmetti, F.S., Bowen, S.W., Fey, M., Mayr, C., Zolitschka, B., Ariztegui, D., Mauz, B., Ohlendorf, C., Kastner, S., Lücke, A., Schäbitz, F., Wille, M., 2009. Late Pleistocene dust deposition in the Patagonian steppe - extending and refining the paleoenvironmental and tephrochronological record from Laguna Potrok Aike back to 55ka. Quat. Sci. Rev. 28, 2927–2939.

Hahn, A., Kliem, P., Oehlerich, M., Ohlendorf, C., Zolitschka, B. and the PASADO Science Team, submitted. Elemental composition of Laguna Potrok Aike sediment sequence reveals paleoclimate change over the past 51 ka in southern Patagonia, Argentina.

Hahn, A., Kliem, P., Ohlendorf, C., Zolitschka, B., Rosén, P., 2013. Climate induced changes as registered in inorganic and organic sediment components from Laguna Potrok Aike (Argentina) during the past 51 ka. Quat. Sci. Rev. 71, 154–166.

Hayashida, A., Ali, M., Kuniko, Y., Kitagawa, H., Torii, M., Takemura, K., 2007. Environmental magnetic record and paleosecular variation data for the last 40 kyrs from the Lake Biwa sediments, Central Japan. Earth Planets Space 59, 807–814.

Heirman, 2011.'A wind of change': changes in position and intensity of the southern hemisphere westerlies during oxygen isotope stages 3, 2 and 1. PhD thesis, Ghent University, Ghent, Germany.

Hofmann, D.I., Fabian, K., 2009. Correcting relative paleointensity records for variations in sediment composition: Results from a South Atlantic stratigraphic network. Earth Planet. Sci. Lett. 284, 34–43.

Irurzun, M.A., Gogorza, C.S.G., Chaparro, M.A.E., Lirio, J.M., Nuñez, H., Vilas, J.F., Sinito, A.M., 2006. Paleosecular variations recorded by Holocene-Pleistocene sediments from Lake El Trébol (Patagonia, Argentina). Phys. Earth Planet. Inter. 154, 1–17.

Irurzun, M.A., Gogorza, C.S.G., Sinito, A.M., Chaparro, M.A.E., Nuñez, H., Lirio, J.M., 2008. Paleosecular variations 12–20 Kyr as recorded by sediments from Lake Moreno (southern Argentina). Stud. Geophys. Geod. 52, 157–172.

Irurzun, M.A., Gogorza, C.S.G., Torcida, S., Lirio, J.M., Nuñez, H., Bercoff, P.G., Chaparro, M.A.E., Sinito, A.M., 2009. Rock magnetic properties and relative paleointensity stack between 13 and 24kyr BP calibrated ages from sediment cores, Lake Moreno (Patagonia, Argentina). Phys. Earth Planet. Inter. 172, 157–168.

Jouve, G., 2013. Caractérisation microsédimentologique et géochimique des sédiments lacustres de la Laguna Potrok Aike, dans la province de Santa Cruz en Patagonie argentine : implications paléoenvironnementales et paléoclimatiques. PhD Thesis INRS-ETE Quebec, Canada

Jouve, G., Francus, P., Lamoureux, S., Provencher-Nolet, L., Hahn, A., Haberzettl, T., Fortin, D., Nuttin, L., 2013. Microsedimentological characterization using image analysis and μ-XRF as indicators of sedimentary processes and climate changes during Lateglacial at Laguna Potrok Aike, Santa Cruz, Argentina. Quat. Sci. Rev. 71, 191–204.

Kilian, R., Schneider, C., Koch, J., Fesq-Martin, M., Biester, H., Casassa, G., Arévalo, M., Wendt, G., Baeza, O., Behrmann, J., 2007. Palaeoecological constraints on late Glacial and Holoceneice retreat in the Southern Andes (53°S). Global Planet. Change 59, 49-66.

King, J.W., Benerjee, S.K., Marvin, J., 1983. A new rock-magnetic approach to selecting sediments for geomagnetic paleointensity studies: application to paleointensity for the last 4000 years. J. Geophys. Res. 88 (B7), 5911-5921.

Kliem, P., Enters, D., Hahn, A., Ohlendorf, C., Lisé-Pronovost, A., St-Onge, G., Wastegård, S., Zolitschka, B., 2013. Lithology, radiocarbon chronology and sedimentological interpretation of the lacustrine record from Laguna Potrok Aike, southern Patagonia. Quat. Sci. Rev. 71, 54–69.

Kohfeld, K.E., Graham, R.M., de Boer, A.M., Sime, L.C., Wolff, E.W., Le Quéré, C., Bopp, L., 2013. Southern Hemisphere westerly wind changes during the Last Glacial Maximum: paleo-data synthesis. Quat. Sci. Rev. 68, 76–95.

Korte, M., Holme, R., 2010. On the persistence of geomagnetic flux lobes in global Holocene field models. Phys. Earth Planet. Inter. 182, 179–186.

Lamy, F., Kilian, R., Arz, H.W., Francois, J.-P., Kaiser, J., Prange, M., Steinke, T., 2010. Holocene changes in the position and intensity of the southern westerly wind belt. Nat. Geosci. 3, 695–699.

Laj, C., Kissel, C., Scao, V., Beer, J., Thomas, D.M., Guillou, H., Muscheler, R., Wagner, G., 2002. Geomagnetic intensity and inclination variations at Hawaii for the past 98kyr from core SOH-4 (Big Island): a new study and a comparison with existing contemporary data. Phys. Earth Planet. Inter. 129, 205–243.

Lund, S.P., Stoner, J., Lamy, F., 2006. Late Quaternary paleomagnetic secular variation and chronostratigraphy from ODP sites 1233 and 1234. In: Tiedemann, R., Mix, A.C., Richter, C., Ruddiman, W.F. (Eds.), Proceedings of the Ocean Drilling Program, Scientific Results, vol. 202.

Montade, V., Combourieu Nebout, N., Kissel, C., Haberle, S.G., Siani, G., Michel, E., 2013. Vegetation and climate changes during the last 22,000yr from a marine core near Taitao Peninsula, southern Chile. Palaeogeogr. Palaeoclimatol. Palaeoecol. 369, 335–348.

Moskowitz, B.M., 1991. Hitchhiker's Guide to Magnetism, Enviromental Magnetism Workshop, 48p.

Muhs, D.R., Ager, T.A., Been, J., Bradbury, J.P., Dean, W.E., 2003. A late quaternary record of eolian silt deposition in a maar lake, St. Michael Island, western Alaska. Quat. Res. 60, 110–122.

Muscheler, R., Beer, J., Kubik, P.W., Synal, H.-A., 2005. Geomagnetic field intensity during the last 60,000 years based on 10Be and 36Cl from the Summit ice cores and 14C. Quat. Sci. Rev. 24, 1849–1860.

Negrini, R., Erbes, D., Faber, K., Herrera, A., Roberts, A., Cohen, A., Wigand, P., Foit, F., 2000. A paleoclimate record for the past 250,000 years from Summer Lake, Oregon, USA. 1. chronology and magnetic proxies for lake level. J. Paleolimnol. 24, 125–149.

Nowaczyk, N.R., Harwart, S., Melles, M., 2001. Impact of early diagenesis and bulk particle grain size distribution on estimates of relative geomagnetic palaeointensity variations in sediments from Lama Lake, northern Central Siberia, Geophys. J. Int. 145, 300-306.

Ohlendorf, C., Gebhardt, C., 2013. Characterizing the eolian sediment component in the lacustrine record of Laguna Potrok Aike (southeastern Patagonia). AGU Fall meeting abstract.

Peck, J.A., King, J.W., Colman, S.M., Kravchinsky, V.A., 1996. An 84-kyr paleomagnetic record from the sediments of Lake Baikal Siberia. J. Geophys. Res. 101 (B5), 11365-11385.

Peters, C., Dekkers, M.J., 2003. Selected room temperature magnetic parameters as a function of mineralogy, concentration and grain size. Phys. Chem. Earth Parts ABC 28, 659–667.

Raisbeck, G., Yiou, F., Jouzel, J., Stocker, T.F., 2007. Direct north-south synchronization of abrupt climate change record in ice cores using Beryllium 10. Clim. Past 3, 541–547.

Recasens, C., Ariztegui, D., Gebhardt, C., Gogorza, C., Haberzettl, T., Hahn, A., Kliem, P., Lisé-Pronovost, A., Lücke, A., Maidana, N., 2012. New insights into paleoenvironmental changes in Laguna Potrok Aike, southern Patagonia, since the Late Pleistocene: The PASADO multiproxy record. The Holocene 22, 1323–1335.

Roberts, A.P., Chang, L., Rowan, C.J., Horng, C.-S., Florindo, F., 2011. Magnetic properties of sedimentary greigite (Fe_3S_4): An update. Rev. Geophys. 49.

Singer, B.S., sous presse. A Quaternary Geomagnetic Instability Time Scale, Quaternary Geochronology, Available online 31 October 2013, http://dx.doi.org/10.1016/j.quageo.2013.10.003.

Simon, Q., St-Onge, G., Hillaire-Marcel, C., 2012. Late Quaternary chronostratigraphic framework of deep Baffin Bay glaciomarine sediments from high-resolution paleomagnetic data: BAFFIN BAY LATE QUATERNARY STRATIGRAPHY. Geochem. Geophys. Geosystems 13(1), Q0AO03.

Snowball, I., Sandgren, P., 2002.Geomagnetic field variations in northern Sweden during the Holocene quantified from varved lake sediments and their implications for cosmogenic nuclide production rates, The Holocene 12(5), 517-530.

Stoner, J.S., Channell, J.E.T., Hillaire-Marcel, C., Kissel, C., 2000. Geomagnetic paleointensity and environmental record from Labrador Sea core MD95-2024: global marine sediment and ice core chronostratigraphy for the last 110 kyr. Earth Planet. Sci. Lett. 183, 161–177.

Stoner, J.S., Laj, C., Channell, J.E.T., Kissel, C., 2002. South Atlantic and North Atlantic geomagnetic paleointensity stacks (0–80ka): implications for inter-hemispheric correlation. Quat. Sci. Rev. 21, 1141–1151.

St-Onge, G., Stoner, J.S., Hillaire-Marcel, C., 2003. Holocene paleomagnetic records from the St. Lawrence Estuary, eastern Canada: centennial- to millennial-scale geomagnetic modulation of cosmogenic isotopes. Earth Planet. Sci. Lett. 209, 113–130.

Sugden, D.E., McCulloch, R.D., Bory, A.J.-M., Hein, A.S., 2009. Influence of Patagonian glaciers on Antarctic dust deposition during the last glacial period. Nat. Geosci. 2, 281–285.

Tauxe, L., 1993. Sedimentary records of relative paleointensity of the geomagnetic field: theory and practice. Rev. Geophys. 31 (3), 319-354.

Teanby, N., Laj, C., Gubbins, D., Pringle, M., 2002. A detailed palaeointensity and inclination record from drill core SOH1 on Hawaii. Phys. Earth Planet. Inter. 131, 101–140.

Vuillemin, A., Ariztegui, D., Coninck, A.S., Lücke, A., Mayr, C., Schubert, C.J., 2013. Origin and significance of diagenetic concretions in sediments of Laguna Potrok Aike, southern Argentina. J. Paleolimnol. 50, 275–291.

Vandenberghe, J., 2013. Grain size of fine-grained windblown sediment: A powerful proxy for process identification. Earth-Sci. Rev. 121, 18–30.

Williams, T., Thouveny, N., Creer, K.M., 1996. Palaeoclimatic significance of the 300 ka mineral magnetic record from the sediments of lac du Bouchet, France, Quat. Sci. Rev. 15, 223-235.

Williams, T., Thouveny, N., Creer, K.M., 1998. A normalized intensity record from lac du Bouchet: geomagnetic palaeointensity for the last 300 kyr? Earth and Planet. Sci. Lett. 156, 33-46.

Xiao, J., Inouchi, Y., Kumai, H., Yoshikawa, S., Kondo, Y., Liu, T., An, Z., 1997. Eolian quartz flux to Lake Biwa, Japan, over the past 145,000 years. Quaternary Research 48, 48–57.

Zolitschka, B., Anselmetti, F., Ariztegui, D., Corbella, H., Francus, P., Lücke, A., Maidana, N.I., Ohlendorf, C., Schäbitz, F., Wastegård, S., 2013. Environment and climate of the last 51,000 years – new insights from the Potrok Aike maar lake Sediment Archive Drilling prOject (PASADO). Quat. Sci. Rev. 71, 1–12.